TURKISH SOCIETY OF CARDIOLOGY

October 2026
Volume 30, Issue 10

THE ANATOLIAN JOURNAL OF CARDIOLOGY

Original Investigations

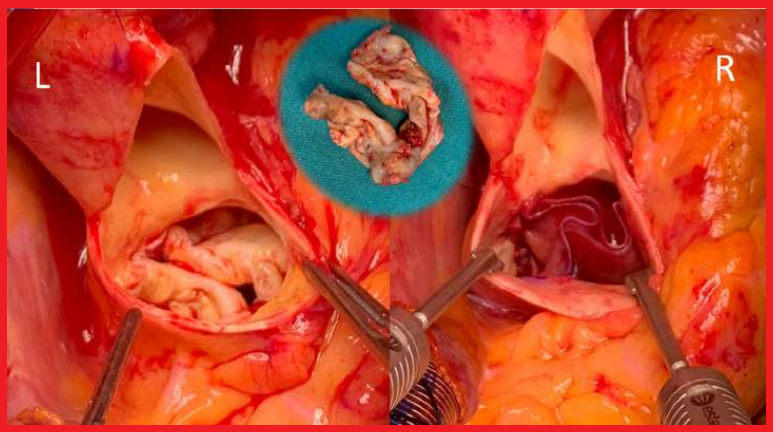

KARE

ISSN - 2149-2263 eISSN 2149-2271
www.anatoljcardiol.com

THE ANATOLIAN JOURNAL OF CARDIOLOGY

Editor-in-Chief

Prof. Dr. Çetin Erol, Ankara, Türkiye

Editors

Cem Barçın, Ankara, Türkiye
Asife Şahinarslan, Ankara, Türkiye

Previous Editor-in-Chief

Bilgin Timuralp, Eskişehir, Türkiye

Associate Editors

Nihal Akar Bayram, Ankara, Türkiye
Hasan Arı, Bursa, Türkiye
Serdal Arslan, Mersin, Türkiye
Oben Baysan, Ankara, Türkiye
Ahmet Kaya Bilge, İstanbul, Türkiye
Muzaffer Değertekin, İstanbul, Türkiye
Recep Demirbağ, Şanlıurfa, Türkiye
Ş. Remzi Erdem, Ankara, Türkiye
İlkay Erdoğan, Ankara, Türkiye
Faruk Ertaş, Diyarbakır, Türkiye
Ali Serdar Fak, İstanbul, Türkiye
Deniz Göksedef, İstanbul, Türkiye
Sadi Güleç, Ankara, Türkiye
Can Yücel Karabay, İstanbul, Türkiye
Hande Kaymakçalan Çelebiler, New Haven, CT, USA
Alper Kepez, İstanbul, Türkiye
Nurgül Keser, İstanbul, Türkiye
Teoman Kılıç, Kocaeli, Türkiye
Tarık Kıvrak, Elazığ, Türkiye
Ece Konaç, Ankara, Türkiye
Serdar Kula, Ankara, Türkiye
Selma Metintaş, Eskişehir, Türkiye
Levent Oktar, Ankara, Türkiye
Necla Özer, Ankara, Türkiye
Murat Özeren, Mersin, Türkiye
Leyla Elif Sade, Pittsburgh, PA, USA
Belma Turan, Ankara, Türkiye
Ercan Tutar, Ankara, Türkiye
Omaç Tüfekçioğlu, Ankara, Türkiye
F. Ajlan Tükün, Ankara, Türkiye
Erol Tülümen, İstanbul, Türkiye
Canan Uluoğlu, Ankara, Türkiye
Taner Ulus, Eskişehir, Türkiye
Mehmet Uzun, İstanbul, Türkiye
Özlem Yıldırımtürk, İstanbul, Türkiye
Aylin Yıldırır, Ankara, Türkiye
Mehmet Birhan Yılmaz, İzmir, Türkiye
Dilek Çiçek Yılmaz, Mersin, Türkiye
Uygar Çağdaş Yüksel, Ankara, Türkiye

Senior Biostatistics Editor

Kazım Özdamar, Eskişehir, Türkiye

Biostatistics Editor

Fezan Mutlu, Eskişehir, Türkiye

Social Media Editor

Ümit Yaşar Sinan, İstanbul, Türkiye

Editorial Board

Selçuk Adabağ, Minneapolis, MN, USA
Rüçhan Akar, Ankara, Türkiye
Yasemin Alanay, İstanbul, Türkiye
Bülent Behlül Altunkeser, Konya, Türkiye
Emre Aslanger, İstanbul, Türkiye
Yasin Ay, İstanbul, Türkiye
Saide Aytekin, İstanbul, Türkiye
Gamze Babur Güler, İstanbul, Türkiye
Luiggi P. Badano, Udine, Italy
Anzel Bahadır, Düzce, Türkiye
Yücel Balbay, Ankara, Türkiye
Adrian Baranchuk, Kingston, Ontario, Canada
Nico Bruining, Rotterdam, The Netherlands
Raffaele Bugiardini, Bologna, Italy
Stephane Carlier, Mons, Belgium
Anthony De Maria, San Diego, CA, USA
Ali Emin Denktaş, Houston, TX, USA
Polychronis Dilaveris, Athens, Greece
Mohaned Egred, Newcastle upon Tyne, UK
Ertuğrul Ercan, İzmir, Türkiye
Okan Erdoğan, İstanbul, Türkiye
Ali Gholamrezanezhad, Tahran, İran
Michael Gibson, Boston, MA, USA
Barış Güngör, İstanbul, Türkiye
Bülent Görenek, Eskişehir, Türkiye
Ali Gürbüz, İzmir, Türkiye
Yekta Gürlertop, Edirne, Türkiye
Suzan Hatipoğlu, Canterbury, UK
Cemil İzgi, London, UK
Serkan Kahraman, İstanbul, Türkiye
Arzu Kalaycı, Boston, MA, USA
Ergün Barış Kaya, Ankara, Türkiye
Cihangir Kaymaz, İstanbul, Türkiye
Mustafa Kılıçkap, Ankara, Türkiye
Derya Kocakaya, İstanbul, Türkiye
Serdar Küçükoğlu, İstanbul, Türkiye
Pedro Lemos, São Paulo, SP, Brazil
Thomas F. Lüscher, Zurich, Switzerland
Peter Macfarlane, Renfrewshire, Scotland
Orhan Maden, Ankara, Türkiye
Robert W. Mahley, San Francisco, CA, USA
Giuseppe Mancia, Milan, Italy
G.B. John Mancini, Vancouver BC, Canada
Kambis Mashayekhi Krozingen, Germany
Pascal Meier, London, UK
Franz H. Messerli, New York, USA
Sanem Nalbantgil, İzmir, Türkiye
Zeki Öngen, İstanbul, Türkiye
Mehmet Özkan, İstanbul, Türkiye
Fausto J. Pinto, Lisbon, Portugal
Sotirios N. Prapas, Athens, Greece
Francesco Saia, Bologna, Italy
M. Raşit Sayın, Trabzon, Türkiye
Mark V. Sherrid, New York, USA
Horst Sievert, Frankfurt, Germany
Richard Sutton, Monaco, Monaco
Gülten Taçoy, Ankara, Türkiye
S. Lale Tokgözoğlu, Ankara, Türkiye
Murat Tuzcu, Cleveland, OH, USA
Dilek Ural, İstanbul, Türkiye
Hadley Wilson, Charlotte, NC, USA
Bedrettin Yıldızeli, İstanbul, Türkiye
Hikmet Yorgun, Ankara, Türkiye
Jose L. Zamorano, Madrid, Spain
Wojciech Zareba, New York, USA
Yuqing Zhang, Beijing, China

TURKISH SOCIETY OF CARDIOLOGY

The Owner on behalf of the Turkish Society of Cardiology / Türk Kardiyoloji Derneği adına İmtiyaz Sahibi: Ertuğrul Okuyan
Address: Nish İstanbul A Blok Kat: 8, No: 47-48 Çobançeşme Sanayi Cad. No: 11 Yenibosna, Bahçelievler 34196 İstanbul, Türkiye
Phone: +90 212 221 1730-38 Fax: +90 212 221 1754 E-mail: tkd@tkd.org.tr Web: www.tkd.org.tr Editor-in-Chief Office: Editorial Office Assistant: Ebru Boz Sandıkçı, Phone: +90 (535) 461 41 62, E-mail: info@anatoljcardiol.com

KARE

KARE PUBLISHING
Address: Göztepe Mah. Fahrettin Kerim Gökay Cad. No: 200, da: 2, Kadıköy, İstanbul, Türkiye
Phone: +90 216 550 61 11
Web: www.karepb.com
E-mail: kare@karepb.com

THE ANATOLIAN JOURNAL OF CARDIOLOGY

AIMS AND SCOPE

The Anatolian Journal of Cardiology is an international monthly periodical on cardiology published on independent, unbiased, double-blinded and peerreview principles. The journal's publication language is English however titles of articles, abstracts and Keywords are also published in Turkish on the journal's web site.

The Anatolian Journal of Cardiology aims to publish qualified and original clinical, experimental and basic research on cardiology at the international level. The journal's scope also covers editorial comments, reviews of innovations in medical education and practice, case reports, original images, scientific letters, educational articles, letters to the editor, articles on publication ethics, diagnostic puzzles, and issues in social cardiology.

The target readership includes academic members, specialists, residents, and general practitioners working in the fields of adult cardiology, pediatric cardiology, cardiovascular surgery and internal medicine.

The editorial and publication processes of the journal are conducted in accordance with the guidelines of the International Committee of Medical Journal Editors (ICMJE), the World Association of Medical Editors (WAME), the Council of Science Editors (CSE), the European Association of Science Editors (EASE), the Committee on Publication Ethics (COPE) and the HEART Group.

The Anatolian Journal of Cardiology is indexed in Science Citation Index Expanded, PubMed/MEDLINE, EMBASE, Scopus, EMCare, CINAHL, Gale/Cengage Learning, EBSCO, DOAJ, ProQuest, Index Copernicus and TÜBİTAK ULAKBİM TR Index.

The requirements for submission of manuscripts and detailed information about the evaluation process are available in the published journal and also as 'Instructions for Authors' on the web site (http://www.anatoljcardiol.com).

Statements and opinions expressed in the Anatolian Journal of Cardiology reflect the views of the author(s). All liability for the advertisements rests with the appropriate organization(s). The Turkish Society of Cardiology, the editor-in-chief and KARE do not accept any responsibility for these articles and advertisements.

Subscriptions
The Anatolian Journal of Cardiology is printed on acid-free paper. Applications for subscriptions should be made to the Editorial Office. The abstracts and full texts of published articles can be accessed free of charge at http://www.anatoljcardiol.com.

Financial support and advertising
The revenue of the Anatolian Journal of Cardiology is derived from subscription charges and advertisements. Institutions wishing to place an advertisement in the printed version of the journal or on the web page should contact KARE.

Owner : Turkish Society of Cardiology
Address : Çobançeşme Sanayi Cad., No: 11, Nish İstanbul, A Blok, No: 47-48, 34196, Yenibosna, Bahçelievler, İstanbul, Türkiye
Phone : +90 212 221 17 30 / +90 0212 221 17 38
Fax : +90 212 221 17 54
E-mail : tkd@tkd.org.tr

Editor-in-Chief : Prof. Dr. Çetin Erol
Address : Çobançeşme Sanayi Cad., No: 11, Nish İstanbul, A Blok, No: 47-48, 34196, Yenibosna, Bahçelievler, İstanbul, Türkiye
Phone : +90 (535) 461 41 62
Fax : +90 (212) 221 17 54
E-mail : info@anatoljcardiol.com

Publisher : KARE PUBLISHING
Address : Göztepe Mah. Fahrettin Kerim Gökay Cad. No: 200, da: 2, Kadıköy, İstanbul, Türkiye
Phone : +90 216 550 61 11
E-mail : kare@karepb.com
Web page : www.karepb.com

INSTRUCTIONS FOR AUTHORS

The Anatolian Journal of Cardiology is published in accordance with the principles of independent, unbiased, and double-blinded peer review. It publishes original research related to clinical, experimental and basic sciences on cardiology, editorial comments, reviews covering current issues, educational articles, scientific letters, case reports, letters to the editor, original images, articles on history of medicine and publication ethics, diagnostic puzzles, and interviews deemed appropriate for the purposes and scope of the journal.

The journal evaluates only the manuscripts submitted through its online submission system on the web site http://www.anatoljcardiol.com. Manuscripts sent by other means will not be accepted.

The primary conditions for the acceptance of manuscripts for publication are originality, scientific value and citation potential.

STATEMENTS AND GUIDELINES

Statements

- All statements and opinions expressed in the manuscripts published in the Anatolian Journal of Cardiology reflect the views of the author(s). All liability for the advertisements rests with the appropriate organization(s). The Turkish Society of Cardiology, the Editor-in-Chief and KARE do not accept any responsibility for articles and advertisements.
- The manuscripts submitted to the journal, except abstracts, presentations, reviews and parts of theses, should not have been accepted and published previously elsewhere in electronic or printed format. Manuscripts evaluated and rejected by other journals must mention any previous submissions and supply reviewer's reports. This will help to accelerate the evaluation process. If the submitted manuscript has been previously presented at a meeting, the name, date, city and country must be specified.
- The authors transfer all copyrights of the manuscript in the framework of national and international regulations to the Turkish Society of Cardiology as of evaluation process. A Copyright Transfer Form signed by corresponding author in order must be submitted to the journal with manuscript. After acceptance of manuscript, all of authors must fill and sign Copyright Transfer form. A separate form for each manuscript should be submitted. Manuscripts submitted without a Copyright Transfer Form will not be accepted. In the case of rejection, all copyrights transfer to the authors again. Authors must confirm that they will not submit the work to another journal, publish it in the original or another language and or allow a third party to use the manuscript without the written permission of the Turkish Society of Cardiology.
- All contents are the authors' responsibility. All financial liability and legal responsibility associated with the copyright of submitted tables, figures and other visual materials protected by national and international laws rest with the authors. The authors take responsibility for any legal proceedings issued against the journal.
- Rejected manuscripts will not be returned except for artwork.
- To clarify scientific contributions and responsibilities and any conflict of interest issues relevant to the manuscript, all parts of the 'Authors' Contribution' form must be completed by the corresponding author and the 'ICMJE Uniform Disclosure Form for Potential Conflicts of Interest' must be completed online by all authors. Both forms should be included in the manuscript at the time of original submission.

Guidelines

- The format of the manuscripts must be in accordance with the ICMJE Recommendations for the Conduct, Reporting, Editing and Publication of Scholarly Work in Medical Journals (updated in December 2014: http://www.icmje.org/icmje-recommendations.pdf).
- The presentation of the manuscripts must be in accordance with international guidelines. CONSORT should be used for randomized trials, STROBE for observational studies, STARD for diagnostic studies, PRISMA for systematic reviews and meta-analyses, ARRIVE for animal studies, and TREND for non-randomized behavior and public health studies.

Ethics

- All manuscripts will be vetted by the Editor-in-Chief's Office for possible plagiarism and duplication. Sanctions will be imposed in accordance with the guidelines of the Committee on Publication Ethics (COPE) and with the principles of the HEART Group when non-ethical issues arise. The authors must obtain the permission of the copyright holder for non-original tables, figures, graphs, images and other visuals.
- The authors should acknowledge and provide detailed information on any contributions in kind and financial support given by any foundations, institutions and firms.
- An ethics committee report prepared in conformity with the WMA Declaration of Helsinki - Ethical Principles for Medical Research Involving Human Subjects and the Guide for the Care and Use of Laboratory Animals is required to be submitted with experimental and clinical studies, drug trial studies and some case reports. Authors may be asked by the Editor-in-Chief's Office for an ethics committee report or similar in other circumstances also. Manuscripts reporting the results of experimental studies must explain in detail all procedures which volunteer subjects and patients have undergone and a statement indicating that consent for the study has been obtained from all subjects should be included in the text. Animal studies should clearly specify how pain or discomfort has been relieved.

Artificial Intelligence (AI)–Assisted Technology

At submission, the journal should require authors to disclose whether they used artificial intelligence (AI)– assisted technologies (such as Large Language Models [LLMs], chatbots, or image creators) in the production of submitted work. Authors who use such technology should describe, in both the cover letter and the submitted work, how they used it. Use of AI for writing assistance should be reported in the acknowledgment section. Authors who used AI technology to conduct the study should describe its use in the methods section in sufficient detail to enable replication to the approach, including the tool used, version, and prompts where applicable. Chatbots (such as ChatGPT) should not be listed as authors because they cannot be responsible for the accuracy, integrity, and originality of the work, and these responsibilities are required for authorship. Therefore, humans are responsible for any submitted material that included the use of AI-assisted technologies. Authors should carefully review and edit the result because AI can generate authoritative-sounding output that can be incorrect, incomplete, or biased. Authors should not list AI and AIassisted technologies as an author or co-author, nor cite AI as an author. Authors should be able to assert that there is no plagiarism in their paper, including in text and images produced by the AI. Humans must ensure there is appropriate attribution of all quoted material, including full citations.

PREPARATION AND SUBMISSION OF MANUSCRIPTS

Manuscript files should be prepared with Microsoft Office Word. The online submission system will direct authors during all stages of submission and provide necessary support for accelerating the submission process. A list of the files that should be supplied through the online submission system is provided below.

1. Title Page
2. Main Text
3. Tables, Graphs and Figures
4. Copyright Transfer Form
5. Author Contribution Form
6. ICMJE Uniform Disclosure Form for Potential Conflicts of Interest

1. Title Page

Information about the authors and their institutions should not be included in the main text, tables, figures and video documents. Since submitted manuscripts are evaluated by the reviewers through the online system, personal identification is excluded in the interests of unbiased interpretation. Thus, only information about the manuscript as specified below should be included on the title page. For each type of manuscript, it is mandatory to upload a title page as a separate Microsoft Word document through the online submission system. The title page should include the names of the authors with their latest academic degrees, and the name of the department and institution, city and country where the study was conducted. If the study was conducted in several institutions, the affiliation of each author must be specified with symbols. The correspondence address should contain the full name of the corresponding author, postal and e-mail addresses, phone and fax numbers. If the content of the manuscript has been presented before, the name, date and place of the meeting must be noted. Disclosure of conflict of interest, institutional and financial support, author contributions, acknowledgments, and ORCID iDs of the authors should be included on the title page.

2. Main Text

The manuscripts submitted to our journal are classified and evaluated according to the manuscript types stated below. During preliminary evaluation, the editors assess whether a manuscript's format and sub-headings are prepared in accordance with the journal's guidelines. Therefore, it is important that authors check the accuracy of the main text in terms of the following.

A. Manuscript types
- **Original investigation**
- **Editorial comment**
- **Review**
- **Education**
- **Scientific letter**
- **Case report**
- **Original image**
- **Letter to the editor**
- **Publication ethics**
- **Scientific puzzle**
- **Miscellaneous articles**

B. References

C. Special Terms and Conditions

A. Manuscript types

- **Original Research**
- Title
- Highlights: Each submission should be accompanied by 3 to 5 "highlight points" which should emphasize the most striking results of the study and highlight the message that is intended to be conveyed to the readers. It should be limited to 70 words.
- Structured Abstract: It should be structured with Objective, Methods, Results and Conclusion subheadings and should be limited to 250 words.
- Keywords: This section should contain a minimum of three and a maximum of six items in accordance with Medical Subject Headings (MeSH) terms prepared by the National Library of Medicine (NLM) and should be placed just below the abstract.
- Main Text: It should consist of Introduction, Methods, Results, Discussion, Limitations of the Study and Conclusion sections and should not exceed 5000 words excluding the references.
- References: The reference list should be provided following the Main Text. Limiting the number of references to 50 is usually sufficient.
- Tables, Figures and Images: They should be placed below the reference list and numbered according to their consecutive order in the main text.
- Title, Structured Abstract and Keywords should also be provided in Turkish for manuscripts submitted by Turkish authors or from Türkiye. However, translations of these sections for manuscripts submitted by foreign authors outside Türkiye will be the responsibility of the publisher.

Statistical Analysis: Statistical analysis should be conducted in accordance with the guidelines on reporting statistical data in medical journals [Altman DG, Gore SM, Gardner MJ, Pocock SJ. Statistical guidelines for contributors to medical journals. Br Med J 1983: 7; 1489-93 and Lang T, Altman D. Basic statistical reporting for articles published in clinical medical journals: the SAMPL Guidelines. In: Smart P, Maisonneuve H, Polderman A (editors). Science Editors' Handbook, European Association of Science Editors, 2013.]. The software used for statistical analysis must be described. Data must be expressed as mean ± standard deviation when parametric tests are used to compare continuous variables. For nonparametric tests, data must be expressed as median (minimum-maximum) or percentiles (25th and 75th percentiles). In advanced and complex statistical analyses, relative risk (RR), odds ratio (OR) and hazard ratio (HR) must be supported by confidence intervals and p values. The outcomes of statistical analyses and interpretation of the results must be in evidence-based scientific language (Editors of Heart Group journals. Statement on matching language to the type of evidence used in describing outcomes data. Anatolian Journal of Cardiology 2012;12:709).

- **Editorial Comment**

Authors are selected and invited by the Editor-in-Chief. This type of manuscript aims at providing a brief commentary on an article published in the journal by a researcher who is an authority in the relevant field or by the reviewer of the article.

- Title
- Main Text: It should not include subheadings and should be limited to 500 words.
- References: The reference list should follow the main text and the number of references should be limited by 15.
- Abstract, Keywords, Tables, Figures, Images and other visuals are not included in editorial comments.
- The title should also be provided in Turkish for works submitted by Turkish authors or from Türkiye. The title of the manuscripts submitted by foreign authors outside Türkiye will be translated into Turkish by the Editor-in-Chief's Office.

- **Review**

Reviews prepared by authors with extensive knowledge on a particular field, which has been reflected in international literature by a high number of publications and citations, are evaluated. The authors may be invited by the Editor-in-Chief. A review should be prepared in the format describing, discussing and evaluating the current level of knowledge or topic that is to be used in the clinical practice and it should guide further studies.

- Title
- Highlights: Each submission should be accompanied by 3 to 5 "highlight points" which should emphasize the most striking results of the study and highlight the message that is intended to be conveyed to the readers. It should be limited to 70 words.
- Abstract: It should not include subheadings and should be limited to 250 words.
- Keywords: This section should contain a minimum of three and a maximum of six items in accordance with Medical Subject Headings (MeSH) terms prepared by the National Library of Medicine (NLM) and should be provided just below the abstract.
- Main Text: It should include Introduction, other subheadings and Conclusion sections and should be limited to 5000 words excluding the references.

- References: The reference list should be placed just below the main text and the number of references should not exceed 50.
- Tables, Figures and Images: They should be provided after the reference list according to their order of appearance in the text.
- For reviews submitted by Turkish authors or from Türkiye, Title, Abstract and Keywords should also be provided in Turkish. For reviews submitted by foreign authors outside Türkiye, translations of these sections will be the responsibility of the publisher.

NOTE: The originality of the visuals included in the reviews should be assured by submission of an accompanying letter by the authors. Appropriate citation should be done for the visuals adapted from previously published sources, in accordance with the original versions of the printed or electronic copies. The written permission obtained from the copyright holder (publisher, journal or authors) should be sent to the Editor-in-Chief's Office.

- **Education**
  Knowledge confirmed by the results of recent research studies, involved in education at academic level and used in clinical practices should be presented in detail in this type of manuscript.
- Title
- Abstract: It should not include subheadings and it should be limited to 250 words.
- Keywords: This section should contain a minimum of three and a maximum of six items in accordance with Medical Subject Headings (MeSH) terms prepared by the National Library of Medicine (NLM) and should be provided just below the abstract.
- Main Text: It should include Introduction, other subheadings and Conclusion sections and should not exceed 5000 words excluding the references.
- References: The reference list should be provided just below the main text and the number of references should be limited to 50.
- Tables, Figures and Images: They should be provided after the reference list according to their order of appearance in the main text.
- For educational articles submitted by Turkish authors or from Türkiye, Title, Abstract and Keywords should also be provided in Turkish. For articles submitted by foreign authors outside Türkiye, the translation of these sections will be carried out by the Editor-in-Chief's Office.

- **Scientific Letter**
  Manuscripts which announce a new scientific invention, are clinically significant, and are in the form of a preliminary report are accepted for publication as scientific letters.
- Title
- Main Text: It should include Introduction, other subheadings and Conclusion sections and should not exceed 900 words excluding the references.
- References: The reference list should be provided just below the main text and the number of references should be limited to 10.
- Tables, Figures and Images: They should be provided below the reference list according to their order of appearance in the text and should be limited to two.
- Abstract and Keywords should not be included.
- For scientific letters submitted by Turkish authors or from Türkiye, the Title should also be provided in Turkish. For letters submitted by foreign authors outside Türkiye, the translation of these sections will be carried out by Editor-in-Chief's Office.

- **Case Report**
  Since a limited number of case reports is published, only reports which are related to rare cases and conditions that constitute challenges in diagnosis and treatment, offer new methods or suggest knowledge not included in books, and are interesting and educational are accepted for publication.
- Title
- Main Text: It should include Introduction, Case Report, Discussion and Conclusion sections and should not exceed 700 words excluding the references.
- References: The reference list should follow the main text and the number of references should be limited to 10.
- Tables, Figures and Images: They should be provided after the reference list according to their order of appearance in the text and should be limited to two.
- Abstract and Keywords are not included.
- For case reports submitted by Turkish authors or from Türkiye, the Title should also be provided in Turkish. For case reports submitted by foreign authors outside Türkiye, the translation of these sections will be carried out by the Editor-in-Chief's Office.

NOTE 1: Case reports that include video images have a better chance of publication.

- **Original Image**
  Impressive and rare images that reflect significant findings based on clinical science,
  shed light on fundamental mechanisms of diseases, emphasize abnormalities or
  introduce new treatment methods are accepted for publication.
- Title
- Main Text: It should not include subheadings and it should be limited to 250 words.
- Tables, Figures and Images: They should be provided after the main text according to their order of appearance in the text and should be limited to two.
- Abstract, Keywords and References are not included.
- For original images submitted by Turkish authors or from Türkiye, the Title should also be written in Turkish. For images submitted by foreign authors outside Türkiye, the translation of this section into Turkish will be carried out by the publisher.

NOTE 1: Those manuscripts with video images have a better chance of publication.

NOTE 2: Manuscripts prepared in accordance with original image criteria are published only as an e-page at the journal's website http://www.anatoljcardiol.com.

- **Letter to the Editor**
  Letters to the Editor aim to discuss the importance of a manuscript previously published in the journal. This type of manuscripts should also include a comment on the published manuscript. Moreover, articles on topics of interest to readers within the scope of the journal, especially on educational issues, can be published in the format of a Letter to the Editor.
- Title
- Main Text: It should not include subheadings and it should be limited to 500 words.
- References: The reference list should follow the main text and the number of references should be limited to five. The volume, year, issue, page numbers, authors' names and title of the manuscript should be clearly stated, included in the list of references and cited within the text.
- Abstract, Keywords, Tables, Figures and Images, and other visuals are not included.
- For manuscripts submitted by Turkish authors or from Türkiye, the Title should also be written in Turkish. For manuscripts submitted by foreign authors outside Türkiye, the translation of this section into Turkish will be carried out by the publisher.

- **Publication Ethics**
  These articles include current information on research and publication ethics and also cases of ethical violation.
- Title
- Main Text: It should not exceed 900 words.
- References: The reference list should follow the main text and the number of references should be limited to 10.
- Tables, Figures and Images: They should be placed after the reference list according to their order of appearance in the text and limited to two.

- Abstract and Keywords are not included.
- For articles submitted by Turkish authors or from Türkiye, the Title should also be written in Turkish. For articles submitted by foreign authors outside Türkiye, the translation of this section into Turkish will be carried out by the publisher.

- **Scientific Puzzle**

Images obtained directly or on operation, visuals revealed through EKG and/or imaging methods, and macroscopic-microscopic anatomical, pathological findings of attentiongrabbing and rare cases can be published. Unlike original images, the diagnosis and outcome of the case and image are hidden at the beginning in diagnostic puzzles. Four multiple-choice questions are prepared. In the following pages of the journal, the correct answer in terms of precise diagnosis and outcome is given with an explanation and didactic images and then discussed. The Editor-in-Chief will convert suitable images into the format of a diagnostic puzzle with the authors' permission.

- Title
- Main Text: It should not exceed 500 words.
- References: The reference list should follow the main text and be limited to a maximum of three.
- Tables, Figures and Images: They should be placed after the reference list according to their order of appearance in the text and should be limited to five.
- Abstract and Keywords should not be included
- For diagnostic puzzles submitted by Turkish authors or from Türkiye, the Title should also be provided in Turkish. For diagnostic puzzles submitted by foreign authors outside Türkiye, the translation of this section into Turkish will be carried out by the publisher.

- **Miscellaneous**
  This type of manuscript covers important events and obituaries.
- Title
- Main Text: It should not exceed 1000 words.
- References: The reference list should follow the main text and the number of references should be limited to 10.
- Tables, Figures and Images: They should be placed after the reference list according to their order of appearance in the text and should be limited to five.
- Abstract and Keywords should not be included.
- For manuscripts submitted by Turkish authors or from Türkiye, the Title should also be provided in Turkish. For manuscripts submitted by foreign authors outside Türkiye, the translation of this section into Turkish will be carried out by the publisher.

B. References

- References should be numbered in the order in which they are cited within the main text.
- Only manuscripts published or accepted for publication should be cited.
- Recent publications related to the topic of the manuscript should be reviewed.
- References that are inaccessible and not indexed in any database should not be cited.
- The titles of journals should be abbreviated in accordance with (Patrias K. Citing medicine: the NLM style guide for authors, editors, and publishers [Internet]. 2nd ed. Wendling DL, technical editor. Bethesda (MD): National Library of Medicine (US); 2007 - [updated 2011 Sep 15; cited Year Month Day].

When there are six or fewer authors, all authors should be listed. If there are seven or more authors, the first three authors should be listed followed by "et al." In the main text of the manuscript, references should be cited in superscript after punctuation.Both in-text citations and the references must be prepared according to the AMA Manual of style.The style and punctuation of the references should be formatted as in the following examples.

Journal: Muller C, Buttner HJ, Peterson J, Roskomun H. A randomized comparison of clopidogrel and aspirin versus ticlopidine and aspirin after placement of coronary artery stents. *Circulation*. 2000;101(6):590-593.

Book Chapter: Sherry S. Detection of thrombi. In: Strauss HE, Pitt B, James AE, eds. *Cardiovascular Medicine*. St Louis: Mosby; 1974:273-285.

Book with Single Author: Cohn PF. *Silent Myocardial Ischemia and Infarction*. 3rd ed. New York: Marcel Dekker; 1993.

Editor(s) as author: Norman IJ, Redfern SJ, eds. *Mental Health Care for Elderly People*. New York: Churchill Livingstone; 1996.

Conference Paper: Bengisson S. Sothemin BG. Enforcement of data protection, privacy and security in medical informatics. In: Lun KC, Degoulet P, Piemme TE, Rienhoff O, eds. MEDINFO 92. Paper presented at the 7th World Congress on Medical Informatics; September 6-10 1992; Geneva, Switzerland. Amsterdam: North-Holland; 1992:1561-1565.

Scientific or Technical Report: Smith P. Golladay K. Payment for durable medical equipment billed during skilled nursing facility stays. Final report. Dallas (TX) Dept. of Health and Human Services (US). Office of Evaluation and Inspections: October 1994. Report No: HHSIGOE 169200860.

Thesis: Kaplan SI. *Post-hospital Home Health Care: Elderly Access and Utilization*. Dissertation. Washington University; 1995.

Manuscripts accepted for publication but not published yet: Leshner AI. *Molecular Mechanisms of Cocaine Addiction. N Engl J Med*. Forthcoming 1997.

Epub ahead of print articles: Aksu HU, Ertürk M, Gül M, Uslu N. Successful treatment of a patient with pulmonary embolism and biatrial thrombus. *Anatolian J Cardiol*. December 26, 2012. doi: 10.5152/akd.2013.062. [Epub ahead of print].

Manuscript published in electronic format: Morse SS. Factors in the emergence of infectious diseases. *Emerg Infect Dis (serial online)*. l995 Jan-Mar (cited 1996 June 5): 1(1): (24 screens). Available from: http:/ www.cdc.gov/ncidodlEID/cid.htm.

C. Special Terms and Conditions

- For double-blinded peer-review process, the names of the corresponding author and other authors, their affiliations and any information on the study centres should not be included in any part of the submitted manuscripts and images, except the Title Page.
  This information should be added to the relevant section of the online submission system and included in the Title Page.
- Pharmaceutical products should be written with their generic names and brand and company names, city and country should be specified for medical equipment and devices.

3. Tables, Graphs and Figures

- Tables, Graphs, Figures and other visuals should be numbered in the order of their citation within the text and names of patients, doctors and institutions should not be disclosed.
- Tables should be prepared in a Microsoft Office Word document using the command 'Insert Table' and inserted at the end of the references in the main text.
- Tables should not be submitted in JPEG, TIFF or other visual formats. For microscopic images, the magnification ratio and staining technique used should be specified in addition to figure legends.
- All visuals should have a high resolution (minimum 300 dpi).
- The thickness of the lines in graphs should be sufficient to minimize loss of quality if size reduction is needed during the printing process. The width of the graphs should be 9 cm or 18 cm.

Drawings should be performed by professionals. No grey colours should be used.
- Abbreviations should be explained in alphabetical order at the bottom of the tables, graphs and figures
- Roman numbers should be avoided in tables and figures within the text and their titles.
- Decimal numbers used in text, tables and figures should be separated by commas in Turkish sections and by dots in English sections.
- Tables should be easily understandable and should not repeat the data in the main text.
- In addition to the pictures included in case reports and original images, video and movie images are published on the journal's website. These images should be prepared in MPEG format with a maximum size of 2 MB. They should be submitted to the journal with the manuscript documents. The names of patients, doctors, institutions and places should be omitted from all documents.

NOTE: All visuals in the manuscripts are printed in black and white without charge. If color printing is required, Turkish authors must pay 300 TL, while foreign authors must pay 300 USD. For payment methods, please contact the Editor-in-Chief's Office of the Anatolian Journal of Cardiology.

EVALUATION AND PUBLICATION

- The main text submitted to the journal must be in English. Manuscripts written in other languages are not accepted. Citation potential is higher for manuscripts in English.
- The Editor-in-Chief's Office checks the conformity of the manuscript with the journal's general guidelines before sending it to associate editors and reviewers. Any manuscripts not prepared in accordance with the journal's guidelines will be returned for revision. The evaluation period is limited to 21 days. If revision is requested, authors should submit their revised manuscripts within 24 days. Manuscripts and revisions should be submitted through the online manuscript submission system at the website http://www.anatoljcardiol.com. Manuscripts sent by e-mail will not be accepted.
- Manuscripts are evaluated in accordance with the principles of double-blinded peer review. Of the submitted manuscripts, those considered to be suitable are subjected to preliminary evaluation by the Editor-in-Chief's assistants in terms of style, format, etc. and by the Editor-in-Chief in terms of their content. Manuscripts considered to be scientifically adequate are assigned to four reviewers. These reviewers are independent experts and members of the editorial board who have published internationally on the topic of the manuscript. Research articles, systematic reviews and meta-analyses are also evaluated by the Editor-in-Chief's statistician counsellors in addition to peer review. When needed, the manuscripts are scanned by the Editor-in-Chief's Office using the iThenticate program for determination of plagiarism and non-ethical situations. Also, all manuscripts are reviewed and edited for compliance with the rules of English grammar. All contributing authors of a manuscript accepted for publication are deemed to have accepted the right of editors to make corrections provided that no fundamental change is made to the basic meaning of the original text. Manuscripts not accorded priority for publication by the Editor-in-Chief, Editor, Associate Editors and Referees are rejected.
- Reviewers who seek assistance from a trainee or colleague in the performance of a review should acknowledge these individuals' contributions in the written comments submitted to the editor. Reviewers must maintain the confidentiality of the manuscript, which may prohibit the uploading of the manuscript to software or other AI technologies where confidentiality cannot be assured. Reviewers must request permission from the journal prior to using AI technology to facilitate their review.
- The retraction requests of the manuscripts close to the final decision in evaluation process, without any reasonable explanation (not contrary to the Publication Ethics) is considered in the scope of rejection decision. Manuscripts that are not revised and resubmitted within the specified time and fail to notify the journal accordingly will be rejected.
- Once a manuscript is accepted for publication, addition to the author list, removal from the author list and order change cannot be effected.
- Manuscripts accepted for publication are prepared as 'Epub ahead of print articles' and published with an assigned DOI on the journal website http://www.anatoljcardiol.com.
- Information on the latest status of manuscripts submitted for evaluation and other information about the journal are available on the website http://www.anatoljcardiol.com. Contact details for the Editor-in-Chief's Office and the publisher are given below.

ARTICLE PROCESSING CHARGE

As of March 1, 2026, the Anatolian Journal of Cardiology will request an article processing charge (APC) for newly submitted manuscripts accepted for publication.

APC rates are determined by article type and the corresponding author's membership status in the Turkish Society of Cardiology.

1. Research Articles, Review Articles, and Meta-Analyses

- USD 1,000 + 20% VAT for non-member foreign authors
- USD 600 + 20% VAT for the Turkish Society of Cardiology members

2. Case Reports

- USD 500 + 20% VAT for non-member foreign authors
- USD 300 + 20% VAT for the Turkish Society of Cardiology members

APCs finance the publishing services offered by the journal, such as managing peer reviews, handling administrative expenses, producing articles in PDF and other formats, distributing articles to different platforms, and other publishing-related activities.

Owner : **Turkish Society of Cardiology**
Address : Çobançeşme Sanayi Cad., No: 11, Nish İstanbul, A Blok, No: 47-48, 34196, Yenibosna, Bahçelievler, İstanbul, Türkiye
Phone : +90 212 221 17 30 / +90 0212 221 17 38
Fax : +90 212 221 17 54
E-mail : tkd@tkd.org.tr

Editor-in-Chief : **Prof. Dr. Çetin Erol**
Address : Çobançeşme Sanayi Cad., No: 11, Nish İstanbul, A Blok, No: 47-48, 34196, Yenibosna, Bahçelievler, İstanbul, Türkiye
Phone : +90 (535) 461 41 62
Fax : +90 (212) 221 17 54
E-mail : info@anatoljcardiol.com

Publisher : **KARE PUBLISHING**
Address : Göztepe Mah. Fahrettin Kerim Gökay Cad. No: 200, da: 2, Kadıköy, İstanbul, Türkiye
Phone : +90 216 550 61 11
E-mail : kare@karepb.com
Web page : www.karepb.com

THE ANATOLIAN JOURNAL OF CARDIOLOGY

CONTENTS

THE ANATOLIAN JOURNAL OF CARDIOLOGY

Official journal of the TURKISH SOCIETY OF CARDIOLOGY

Becker Muscular Dystrophy, Biomarkers and Risk Scores

EDITORIAL

Becker muscular dystrophy (BMD) is a primary myopathy caused by mutations in the dystrophin gene on chromosome Xq21.2, which often affects the myocardium and cardiac conduction system. However, there is limited experience with cardiac disease in BMD. This review by Finsterer J from Austria aims to summarize and discuss recent advances and future perspectives regarding the clinical presentation, diagnosis, treatment, and outcome of cardiac involvement in BMD.

Demirkıran et al from Türkiye assessed the mid-term clinical and echocardiographic outcomes of the Ozaki (aortic valve neocuspidization, AVNeo) procedure performed at a single center. What did they find?

Coronary artery perforation (CAP) is a rare life-threatening complication of percutaneous coronary intervention (PCI). Although several risk factors for CAP have been described, real-world multicenter studies analysing the clinical outcomes remain limited. Turna et al from Türkiye presents a comprehensive two-center evaluation of CAP, focusing on angiographic severity, management strategies, and short- and long-term outcomes.

The uric acid-to-HDL cholesterol ratio (UHR) has recently emerged as a novel composite biomarker reflecting both pro-oxidant and anti-inflammatory balance. Astan et al from Türkiye evaluated the relationship between UHR and coronary slow flow.

Atıcı et al from Türkiye performed a simulation to compare CVD risk scores using the widely applied Framingham and Reynolds systems, as well as more recently developed PREVENT system. Which one is the best?

Primary (non-ischemic) cardiomyopathy poses diagnostic challenges due to phenotypic heterogeneity and non-specific clinical presentation, and commonly used circulating biomarkers have limited disease specificity. He et al from China aimed to prioritize mechanism-informed plasma biomarkers and evaluate their diagnostic discrimination in a clinical cohort. New findings?

A recently proposed uric acid index combining fasting glucose, triglycerides, and uric acid has shown promise in cardiovascular risk stratification. Çamkıran et al from Türkiye assessed whether the index could predict significant coronary artery stenosis (≥50%) on coronary CT angiography and compared its diagnostic performance with serum uric acid.

The cardiovascular effects of sodium–glucose cotransporter-2 inhibitors and dipeptidyl peptidase-4 inhibitors (DPP-4i) have attracted increasing interest in patients with type 2 diabetes mellitus. Kaya and Köker from Türkiye compared the time-dependent effects of empagliflozin and linagliptin on left ventricular diastolic function and global longitudinal strain in these patients.

And a case report, letters, e-page original...

I hope this new issue of our journal will be interest of our readers.

Çetin Erol

Editor-in-Chief, Ankara, Türkiye

DOI: 10.14744/AnatolJCardiol.2026.10

Copyright@Author(s) - Available online at anatoljcardiol.com.
Content of this journal is licensed under a Creative Commons Attribution-NonCommercial 4.0 International License.

THE ANATOLIAN JOURNAL OF CARDIOLOGY

Official journal of the TURKISH SOCIETY OF CARDIOLOGY

Clinical Presentation, Diagnosis, Treatment, and Outcome of Heart Disease in Becker Muscular Dystrophy

ABSTRACT

Becker muscular dystrophy (BMD) is a primary myopathy caused by mutations in the dystrophin gene on chromosome Xq21.2, which often affects the myocardium and cardiac conduction system. However, there is limited experience with cardiac disease in BMD. This review aims to summarize and discuss recent advances and future perspectives regarding the clinical presentation, diagnosis, treatment, and outcome of cardiac involvement in BMD. Data were retrieved by searching for relevant articles in the PubMed and Google Scholar databases. Cardiac disease in BMD is characterized by myocardial fibrosis, can be subclinical or clinical, and manifests as left or right ventricular systolic dysfunction with/without heart failure due to dilated or hypertrophic cardiomyopathy, diastolic dysfunction with preserved/decreased systolic function, conduction disturbances and supraventricular/ventricular arrhythmias, thrombus formation, arterial hypertension, pulmonary hypertension, left ventricular hypertrabeculation, coronary artery disease, and valve defects. Cardiac involvement in BMD must be detected and treated at an early stage, because it progresses over time and has a significant impact on the course of the disease. Established treatment methods include non-invasive therapies with small molecules and catheter-based invasive therapies (stent implantation, endocardial and epicardial ablation), device-related treatments (pacemaker, implantable cardioverter–defibrillator, cardiac resynchronization therapy, left ventricular assist device), and heart surgery. Cardiac involvement in BMD occurs in about two-thirds of patients, is subclinical in the early stages but becomes symptomatic as the heart disease progresses, requires early diagnosis, and can be treated with non-invasive and invasive therapies, with prognosis improving with early detection and adequate treatment.

Keywords: Arrhythmias, Becker muscular dystrophy, cardiomyopathy, dystrophin, noncompaction

REVIEW

INTRODUCTION

Becker muscular dystrophy (BMD) is a rare primary myopathy that is usually caused by large in-frame duplications or deletions affecting one or more exons, and rarely by small deletions/duplications/insertions, splice site variants that maintain the reading frame, or point mutations, including nonsense mutations that generate a stop codon and missense mutations that disrupt the reading frame in the *dystrophin* gene on chromosome Xq21.2.[1] Becker muscular dystrophy manifests phenotypically as skeletal muscle myopathy,[1] significant cardiovascular complications,[2] occasional epilepsy,[3] and occasional cognitive impairment.[4,5] Joints, ligaments, and bones may be secondarily affected due to skeletal muscle weakness, joint dislocations, and contractures.[6] Becker muscular dystrophy differs from allelic Duchenne muscular dystrophy (DMD) by the presence of dystrophin in Western blot or immunohistochemistry. Becker muscular dystrophy is an X-linked recessive disorder that is either transmitted via female carriers of a dystrophin mutation in one of their X-chromosomes or occurs spontaneously in males due to germline mutations in the X-chromosome.[1] Not only males but also female carriers show phenotypic symptoms if the major part of the chromosome carrying the mutation is not inactivated according to the Lyon hypothesis.[7] The prevalence of BMD is estimated at 1 in 18 000 male births.[8] This narrative review aims to summarize and discuss recent advances and future perspectives regarding the clinical

Copyright@Author(s) - Available online at anatoljcardiol.com.
Content of this journal is licensed under a Creative Commons Attribution-NonCommercial 4.0 International License.

Josef Finsterer

Department of Neurology, Neurology & Neurophysiology Center, Vienna, Austria

Corresponding author:
Josef Finsterer
✉ fifigs1@yahoo.de

Available Online Date: August 19, 2026

Cite this article as: Finsterer J. Clinical presentation, diagnosis, treatment, and outcome of heart disease in Becker muscular dystrophy. *Anatol J Cardiol.* 2026;30(10):631-643.

DOI: 10.14744/AnatolJCardiol.2026.6700

presentation, diagnosis, treatment, and outcome of cardiac involvement in BMD.

METHODS

Data for this review were obtained through a literature search in the PubMed, Embase, and Google Scholar databases using the search terms "Becker muscular dystrophy," "dystrophinopathy," "dystrophin," and "X-linked myopathy" in combination with "heart," "myocardium," "arrhythmias," "heart failure," "systolic dysfunction," "diastolic dysfunction," "thrombus," "heart valve," "cardiac conduction," "treatment," and "therapy." In addition, reference lists were searched for articles that met the search criteria. Articles containing original data on the occurrence, diagnosis, treatment, and course of heart disease in BMD were included. Articles that did not contain original data, were not available as full articles, were not written in English, or were duplicates were excluded (Figure 1).

RESULTS

Clinical Manifestations

A total of 86 articles meeting the inclusion criteria were identified (Figure 1). Heart disease within the BMD encompasses not just a single disease, but several different clinical entities.

Types of Cardiac Involvement

The most common manifestation of cardiac involvement in BMD is dilated cardiomyopathy (dCMP), which results from the replacement of cardiomyocytes by fibrous tissue, leading to impaired contractility and thus dilation of the left and right ventricles (Table 1).[9,10] In rare cases, BMD can also manifest as hypertrophic cardiomyopathy.[11,12] If systolic dysfunction exceeds a certain level, patients develop heart failure, which is clinically characterized by jugular vein enlargement, exertional dyspnea, and leg edema. Liver congestion may also cause pain in the upper abdomen. Reduced myocardial contractility can lead not only to left ventricular systolic dysfunction, but also to left ventricular diastolic dysfunction, which is classified into four degrees of severity: 1. impaired relaxation (E/A ratio <1), 2. pseudonormal filling, 3. reversible restrictive filling pattern (E/A ratio >2), and 4. irreversible restrictive filling pattern.[13] Patients with BMD often also show cardiac conduction disorders (atrial, Hissian, and infra-Hissian)[14] or supraventricular and ventricular arrhythmias,[13] including sinus tachycardia, atrial fibrillation (AFIB),[15] atrial flutter (AFLU), ventricular extrasystoles, non-sustained or sustained ventricular tachycardia, or cardiac arrest.[16] Depending on the stage of the disease, ECG abnormalities can be detected in up to 77% of patients.[14] The classic pattern of ECG abnormalities in patients with BMD includes high R-waves, Q-waves in the left precordial leads, right axis deviation, and complete right bundle branch block.[17] These ECG abnormalities correlate with a predilection for myocardial fibrosis in the posterobasal wall.[17,18] Rare manifestations of cardiac involvement include arterial hypertension,[19] pulmonary hypertension,[3] coronary artery disease,[20] valvular heart disease (mitral regurgitation),[21] left ventricular hypertrabeculation (LVHT) (Figure 2),[22-24] congenital heart disease (bicuspid aortic valve),[25] coronary artery dissection,[19] or Takotsubo syndrome (broken heart syndrome) (Table 1).[26] Early-onset cardiomyopathy is associated with mutations that disrupt the spectrin repeat in the rod domain region, as well as with mutations in exons 12, 14-17, or 31-42, whereas late-onset cardiomyopathy is associated with a deletion of exons 2-9 and 45-49.[27]

Prevalence of Cardiac Involvement

The frequency of cardiac involvement in BMD is between 60% and 75%.[19] In the vast majority of cases, heart disease develops after the onset of muscular symptoms,[20] but there are rare cases in which cardiomyopathy preceded the muscular manifestations.[22,28,29] In a recent study of 163 patients with BMD, heart disease occurred before the onset of muscle symptoms in only 5 patients with an average age of 33 years.[29] Another case of heart disease occurring before muscle disease has also been reported.[30] The prevalence of heart disease increases with age.[31]

Symptoms and Signs

Symptoms that patients with CMP and BMD may experience include fatigue, exercise intolerance, shortness of breath at rest or during exertion, edema, palpitations, chest pain, fainting, headache, dizziness, polyuria, or nocturia. Cardiologic signs may include arrhythmias, ventricular extrasystoles, tachycardia, bradycardia, abnormal heart sounds, crackles, crepitus, leg edema, liver enlargement, or jugular venous distension.

Diagnosis

The diagnosis of heart disease in BMD is usually made by a cardiologist based on medical history, clinical examination, standard ECG, long-term ECG, loop recording, stress testing, transthoracic or transesophageal echocardiography, stress echocardiography, cardiac MRI (cMRI), coronary angiography, or scintigraphy (e.g., TC-99m single photon emission computed tomography (SPECT) or methoxyisobutylisonitrile (MIBI) SPECT. Cardiac MRI is preferable to echocardiography, as echocardiography can be difficult in patients with scoliosis, chest deformities, ventilation disorders, and contractures. In addition, cMRI can detect late gadolinium enhancement (LGE), which occurs predominantly in the postero-basal region in a subendocardial distribution. Late gadolinium enhancement correlates with myocardial fibrosis, increases with age, and correlates with the decline in ejection fraction (EF).[31]

Treatment

The treatment of heart disease in BMD can be classified as approved (established) or in development/experimental/

HIGHLIGHTS

- Cardiac involvement in Becker muscular dystrophy (BMD) occurs in about two-thirds of patients.
- Cardiac involvement is subclinical in the early stages but becomes symptomatic as the heart disease progresses.
- Cardiac involvement requires early diagnosis.
- Cardiac disease in BMD can be treated with non-invasive and invasive therapies, with prognosis improving with early detection and adequate treatment.

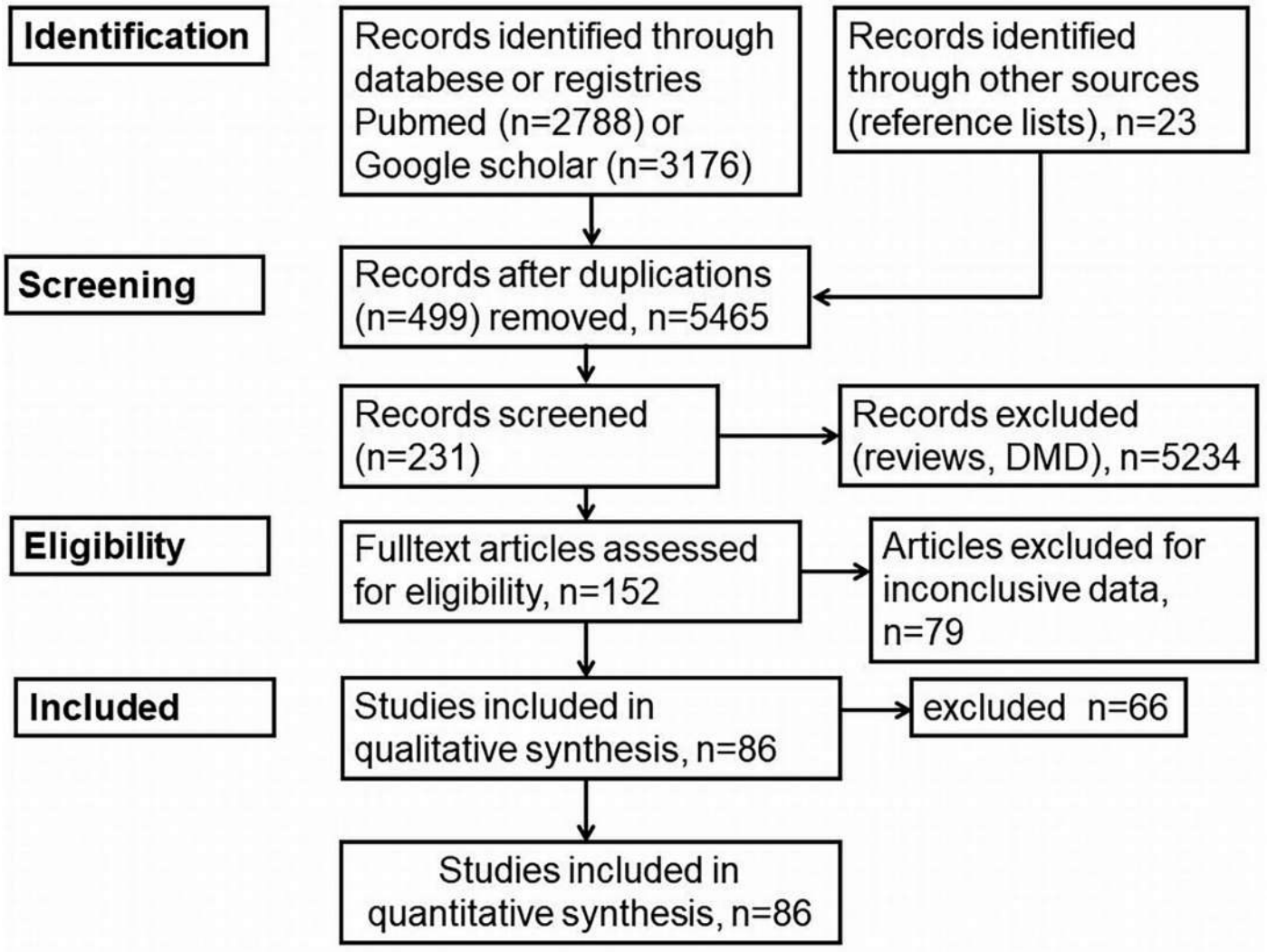

Figure 1. Flow chart of literature search results and study selection process.

innovative (Table 2). Approved therapies can be further subdivided into non-invasive or invasive, as well as prophylactic (presymptomatic) or symptomatic therapies. Established non-invasive therapies include physical therapy, pharmacological treatment, avoidance of cardiotoxic drugs, and partially gene therapies (read-through, exon skipping, gene editing, and gene replacement) (Table 2). Invasive treatments can be classified as catheter-based (minimally invasive), device-related, or surgical (HTX, aortocoronary bypass, left atrial appendage resection, trabecular resection in LVHT, valve replacement, thoracic or spinal stabilization). Future therapies can be classified as pharmacological, cell-based, or gene therapies. The question of who should treat heart disease in BMD can be answered clearly. The cardiologist should treat symptomatic patients, while prophylaxis can also be prescribed by the treating neurologist.

Standard (Established) Therapies

There is evidence that several medications can have a positive effect on heart function in patients with BMD and carriers. However, drug therapy for heart disease is often only effective to a limited extent, as heart disease can progress rapidly and require a switch to invasive therapy. In advanced stages of cardiac involvement, only a combination of different therapies is often beneficial.

Non-invasive Therapies

Pre-symptomatic Treatment

The question of whether asymptomatic patients with BMD with normal systolic function should receive drugs that prevent or delay the development of myocardial fibrosis has not yet been investigated in large-scale studies. However, there is evidence from studies with patients with DMD that angiotensin-converting enzyme inhibitors (ACEIs), angiotensin receptor blockers (ARBs), mineralocorticoid receptor antagonists (MRAs), and glucocorticoids delay the development of fibrosis and dCMP.[32,33] Angiotensin-converting enzyme inhibitors and ARBs are known to not only reduce cardiac afterload but also mitigate myocardial fibrosis by interfering with the renin–angiotensin system (RAS) and blocking angiotensin II,[34] transforming growth factor-beta

Table 1. Cardiac Abnormalities in Becker Muscle Dystrophy and Their Treatment

Abnormality	Treatment
Hypertrophic cardiomyopathy	GDMT
Dilated cardiomyopathy	GDMT
Systolic dysfunction	GDMT
Diastolic dysfunction	GDMT
Conduction defects	GDMT
Supra-ventricular arrhythmias	GDMT
Ventricular arrhythmias	GDMT
Thrombus formation	OAC
Coronary heart disease	GDMT
Arterial hypertension	GDMT
Pulmonary hypertension	GDMT
Mitral valve insufficiency	Valve replacement
Congenital heart disease	GDMT
LVHT	Depends on type of complications
Takotsubo syndrome	Beta-blockers

GDMT, guideline-directed medical treatment; LVHT, left ventricular hypertrabeculation; OAC, oral anticoagulation.

Table 2. Classification of Established and Experimental Therapies for Cardiac Disease in Becker Muscular Dystrophy

- Approved Standard Therapies
  - Non-invasive therapies
    - Drug (pharmaceutical)
      - Pre-symptomatic
      - Symptomatic
        - Systolic dysfunction
        - Diastolic dysfunction
        - Arrhythmias and conduction disturbances
        - Thrombus formation
        - Other cardiac abnormalities
    - Avoidance of cardiotoxic compounds
    - Resistance training
  - Invasive therapy
    - Catheter-based
    - Implants
    - Surgery
- Upcoming therapies
  - Pharmacological
  - Cell-based therapies
  - Genetic therapy
    - Targeting the disease causing gene
      - Correction of the genetic defect
        - Read through therapies
        - Exon skipping
        - Gene editing
          - DNA editng
          - RNA editing
      - Gene replacement therapy (mini-/micro-dystrophin)
    - Targeting non-disease-causing genes (SERCA2a, Trum63, S100A1, ARC)

(TGF1b), an important mediator of fibrosis, fibroblast proliferation, collagen synthesis, and the overall development of fibrotic tissue.[35] Similarly, ARBs reduce myocardial fibrosis by counteracting the pro-fibrotic effects of the RAS by reducing inflammation, myofibroblast differentiation, and the production of extracellular matrix proteins involved in the fibrotic process.[36] Mineralocorticoid receptor antagonists are known to counteract fibrosis and improve ventricular function by blocking the action of aldosterone, which stimulates the transcription of collagen genes.[37] Angiotensin-converting enzyme inhibitor, ARBs, and MRAs are typically used when myocardial fibrosis is documented on cardiac magentic resonance tomography (cMRT) but systolic function is preserved, there is an asymptomatic decrease in ejection fraction (EF), EF is <55%, or asymptomatic arrhythmias occur. Whether glucocorticoids (e.g., deflazacort, prednisone, and prednisolone) can delay myocardial fibrosis in asymptomatic patients with BMD has not yet been systematically investigated. However, studies in patients with DMD have shown that glucocorticoids can delay the decline in cardiac function by suppressing TGF1b and the inflammatory immune response following fibrosis.[38] In a study of 21 patients with DMD treated with deflazacort for 3 years, the prevalence of dCMP was lower compared to the control group.[39] In a study of 48 patients with DMD who received either deflazacort or prednisone, the patients treated with steroids had higher fractional shortening (FS) than the untreated patients.[40] In a study of 14 patients with DMD who received steroids over a period of 4.5 years, the patients treated with steroids had less ventricular dilation and systolic dysfunction than the untreated patients.[41] In a study involving 462 patients with DMD, the onset of dCMP was delayed by 2.1 years in patients treated with steroids.[42] The limitations of all these studies are that they are retrospective and that the steroid doses administered varied considerably.[31] As a rule, only a few patients with BMD are treated with prednisone in the long term (9 in a study involving 163 cases).[29]

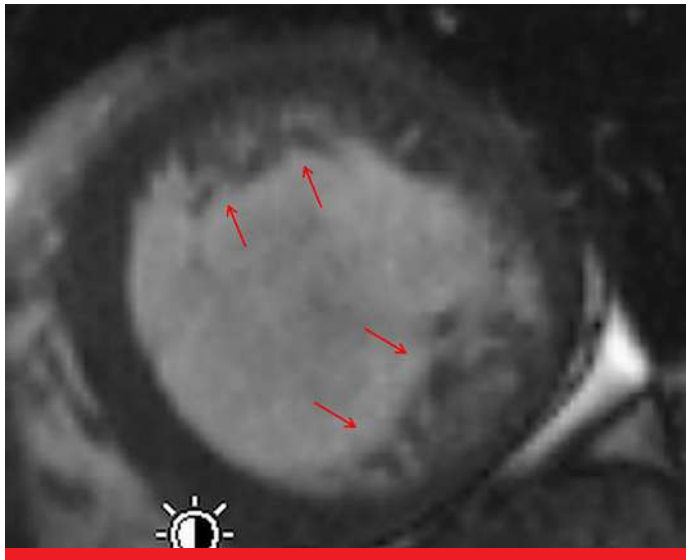

Figure 2. cMRI of a female carrier of a dystrophin deletion showing extensive left ventricular hypertrabeculation in the short axis view. cMRI, cardiac MRI.

Symptomatic Treatment

Pharmacological

Systolic Dysfunction

The treatment of systolic dysfunction (EF <50%, FS <28%) with/without heart failure in patients with BMD is carried out according to the established American Heart Association/American College of Cardiology/Heart Failure Society of America (AHA/ACC/HFSA) guidelines from 2022.[43] This guideline-directed drug therapy (GDMT) is based on the administration of a combination of 4drug classes (quad therapy): 1. A neprilysin inhibitor (e.g., sacubitril) together with an ARB (e.g., valsartan) or an ACEI, 2. Beta-blockers (e.g., bisoprolol), 3. MRAs (e.g., eplerenone, spironolactone, vamorolone), and 4. Sodium-glucose cotransporter 2 inhibitors (SGLT-2) (e.g., sitagliptin, dapagliflozin).[43] Additionally, loop diuretics (e.g., furosemide) and fibrates (e.g., fenofibrate) may be administered. Beta-blockers are known to reduce heart rate and myocardial oxygen demand. However, there is also evidence that perindopril and bisoprolol do not improve ventricular function in patients with DMD.[44] Arterial hypotension may limit the use of beta-blockers. Mineralocorticoid receptor antagonists are usually administered to patients with New York Heart Association class III or IV who are already optimally controlled with ACEI and beta-blockers.[45] In a study of 20 patients with DMD with preserved EF, eplerenone resulted in a smaller reduction in left ventricular circumferential strain compared to 20 controls.[46] In a single patient with BMD, heart failure was treated with sacubitril/valsartan (2×50 mg/day), furosemide (2×20 mg/day), spironolactone (25 mg/day), dapagliflozin (10 mg/day), fenofibrate (160 mg/day), and bisoprolol (2.5 mg/day).[47]

Whether steroids (e.g., deflazacort, prednisone, and prednisolone), which are used to inhibit the progression of fibrosis and dystrophy in skeletal muscle, are also beneficial in symptomatic heart disease, particularly dCMP, has not been systematically investigated in patients with BMD. However, there is evidence from studies in patients with DMD that steroids, especially deflazacort (0.9 mg/kg/day) and prednisone (0.75 mg/kg/day or 10 days of treatment, 10 days off), can improve systolic function and increase cardiac output.[38] Steroids are known to modulate gene expression by activating/suppressing transcription, inhibit or delay secondary inflammation after muscular dystrophy by inhibiting TGF-β, and modulate metabolic stress even in symptomatic patients.[34] Givinostat, a histone deacetylase inhibitor approved by the FDA and EMA for the treatment of patients with DMD aged 6 years and older with all genetic variants of DMD, has not been studied for a potential effect on heart disease in BMD.

Diastolic Dysfunction

Treatment of stage I diastolic dysfunction focuses on treating the underlying causes, such as high blood pressure, diabetes, and coronary heart disease, as well as lifestyle changes (e.g., healthy diet, regular exercise, avoiding nicotine, balanced nutrition, aerobic exercise, reducing saturated fats, sugar, and sodium intake, stress reduction, and adequate sleep). In pseudonormalization (stage II), medications such as ACEI, calcium channel blockers, and diuretics may be helpful, whereas other medications may control blood pressure or heart rate. In severe cases (stages III and IV), treatments may include advanced options such as left ventricular assist devices (LVADs) or, in rare cases, heart transplantation (HTX).

Arrhythmias and Conduction Disturbances

Arrhythmias and conduction disturbances are thought to be caused by fibrosis of the cardiac conduction system (Purkinje fibers).[48] Beta-blockers are usually administered to reduce the heart rate in cases of sinus tachycardia. If beta-blockers are ineffective or cause side effects, amiodarone is usually tried.[49] If amiodarone is ineffective, ivabradine, a selective I(f) current blocker in sinus node cells, is an option.[50] Unlike beta-blockers, ivabradine does not cause hypotension. In a 22-year-old patient with BMD, dCMP, systolic dysfunction, and sinus tachycardia, ramipril was successfully replaced with candesartan, ivabradine, and furosemide.[50] Discontinuation of ivabradine led to recurrence of sinus tachycardia and arterial hypotension.[50] In a DMD rat model, ivabradine reduced the progression of cardiomyopathy and lowered the heart rate to normal values.[51] Premature ventricular complexes (beats) usually do not require treatment, but if they cause syncope or non-sustained ventricular tachycardia, or if they are associated with a positive family history of sudden cardiac death (SCD), treatment with beta-blockers, calcium channel blockers, or ablation is indicated. Non-sustained ventricular tachycardias are treated with beta-blockers and, if these are ineffective, with an implantable cardioverter defibrillator (ICD) according to the 2017 AHA/ACC guidelines for ventricular arrhythmias.[52] QT dispersion has been shown to be increased in BMD, which is associated with an increased risk of SCD.[53] Wolff-Parkinson-White (WPW) syndrome has been shown to be the first manifestation of BMD, but no accessory pathways could be identified during attempted radiofrequency ablation.[54] Atrial fibrillation or AFLU should be treated according to the established AHA/ACC guidelines from 2023.[55] Atrial, Hissian, or infra-Hissian conduction disturbances are a domain of invasive therapy.

Thrombus Formation

The question of whether and when patients with BMD should receive oral anticoagulants (OAC) has not yet been clarified. However, according to the 2024 AHA/ACC guidelines, patients with AFIB or AFLU should receive OAC if the CHA2DS2-VASc score is >1 in men and >2 in women[56] and if the HAS-BLED score is below 3. However, the decision should be made on an individual basis, using the HAS-BLED score to assess bleeding risk, not to deny treatment, but to identify and treat modifiable bleeding factors. The AHA/ACC guidelines also recommend OAC for patients with severe systolic dysfunction, especially shortly after diagnosis of heart fialure (HF) or if there is a history of thromboembolism or AFIB.[43] A case of cardioembolic thromboembolism with ischemic stroke has been reported in a 65-year-old BMD patient who was treated with OAC in addition to diuretics and dopamine.[15] The question of whether patients with BMD and LVHT should receive OAC due to the risk of cardioembolic thromboembolism remains unresolved. However,

if thrombi are documented in the intertrabecular spaces on cMRI, experts recommend the administration of OAC.[57,58] Medications used as OACs include vitamin-K antagonists (e.g., phenprocoumon and warfarin), direct thrombin antagonists (e.g., dabigatran, argatroban, bivalirudin, and lepirudin), thrombin receptor antagonists (e.g., vorapaxar), and factor-X-inhibitors (e.g., rivaroxaban, apixaban, and edoxaban). Only vitamin K antagonists should be used in patients with mechanical heart valves.

Other Cardiac Abnormalities

Pulmonary hypertension is treated in accordance with established guidelines using endothelin receptor antagonists (e.g., ambrisentan and bosentan), phosphodiesterase inhibitors (e.g., sildenafil), and OAC.[16,59] Heart transplants should only be considered in cases of treatment-resistant disease. If patients with BMD also suffer from coronary heart disease, valve stenosis, or valve insufficiency, GDMT should be used. The use of statins or PCSK-9 inhibitors for hyperlipidemia and elevated low density lipoprotein (LDL) or elevated Lp(a) should be considered.[60] However, statins and fibrates should be administered with caution as they can trigger rhabdomyolysis, cause cardiomyopathy, and lead to HF.

Avoidance of Cardiotoxic Compounds: Side effects of cardiac therapy may include myopathies caused by beta-blockers or statins. There is evidence that statins can also cause cardiomyopathy and heart failure.[61] Amiodarone is known to cause thyroid dysfunction and visual disturbances. Volatile halogenated anesthetics and succinylcholine can cause malignant hyperthermia with tachycardia, ventricular arrhythmias, and disseminated intravascular coagulation. Therefore, beta-blockers (e.g., propranolol, labetalol), statins, amiodarone, succinylcholine, and volatile anesthetics should be administered with caution.[19,62,63] It is also recommended to avoid QT-prolonging drugs (e.g., amiodarone, sotalol, haloperidol, ziprasidone, macrolides, fluoroquinolones, citalopram, and tricyclics). Nonsteroidal anti-inflammatory drugs have been shown to exacerbate heart failure in patients with isolated BMD.[64] Certain chemotherapeutic agents can cause heart failure, and local anesthetics and proton pump inhibitors can trigger ventricular arrhythmias.

Resistance Training: Although resistance training can improve muscle strength, functional ability, and quality of life in patients with BMD, its effects on cardiac function are less clear. This is because no systematic studies have been conducted on the effect of resistance training on cardiac function in patients with BMD. A study involving a single patient with BMD who completed 12 weeks of resistance training failed to demonstrate any positive effect on cardiac function.[65] In a study involving 5 patients with BMD who completed a 12-week resistance training program, the mean maximum voluntary contraction increased, and the time taken to move from sitting to standing and to climb and descend stairs became significantly faster, but the effects on the myocardium were not investigated.[66] In a study involving 11 patients with BMD, 12 weeks of training improved VO_2max by 47% and maximum work capacity by 80%.[67] However, systolic function did not change.[67]

Invasive Therapy

There are no systematic studies on the benefits of catheter-based intervention, device-based treatment, or surgical treatment of heart disease in patients with BMD, but case reports and case studies provide promising results. There is also evidence from patients with DMD that invasive therapies are becoming increasingly important for the treatment of heart disease in patients with BMD.

Catheter Based

In cases of non-valvular AFIB or AFLU where OAC is not possible, ablation of the left atrium may be attempted.[16,68] If patients with non-valvular AFIB have a high risk of stroke but also a high risk of bleeding or other reasons that prevent long-term OAC, closure of the left atrial appendage (LAA) is a therapeutic option.[69] However, it must be considered that the LAA is an actuator in a control loop for intravascular volume regulation and may lose this function upon closure. Closure of the LAA aims to prevent embolization of clots from the LAA into the general circulation. However, this goal cannot be achieved if the closure leaks.[70] In patients with BMD presenting with acute symptomatic or asymptomatic coronary artery disease, a stent should be inserted in accordance with established guidelines.[71] In chronic coronary artery disease, aortocoronary bypass surgery (ACBP) is indicated.[71] In cases of concomitant congenital heart disease (e.g., tetralogy of Fallot),[72] closure of an atrial septal defect (ASD) or ventricular septal defect (VSD) using catheter-based implants may be considered. If, despite the indication for valve reconstruction, thoracotomy and the use of a heart-lung machine or general anesthesia are contraindicated, this can be performed by transcatheter valve implantation (e.g., TAWI).

Implants

In cases of sick sinus syndrome, atrioventricular-block, or symptomatic sinoatrial-block, implantation of a pacemaker (PM) should be considered.[73] In cases of survived cardiac arrest or persistent ventricular tachycardia, an ICD should be implanted in accordance with the AHA/ACC guidelines.[73] Cardiac resynchronization therapy (CRT) with or without a defibrillator (CRT-D) is indicated if heart failure is present together with asynchrony between the innervation of the right and left ventricles.[22,73] Left ventricular assist devices may be indicated for mechanical circulatory support when conventional drug therapies or CRT/CRT-D systems are ineffective for treating heart failure and patients with BMD are not eligible for HTX.[74] Left ventricular assist devices can be implanted in patients on the waiting list for HTX to bridge the time until surgery. In a female BMD carrier with dCMP as the only symptom of the disease, heart failure progressed so rapidly that she required an LVAD prior to HTX.[74]

Surgery

Heart transplant is an established alternative to drug and device-based cardiac therapy when these prove unsuccessful in BMD presenting with heart failure (refractory systolic dysfunction). It is indicated for patients with end-stage heart failure who cannot be treated with other means, especially in cases of refractory heart failure or life-threatening

ventricular arrhythmias.[75] In a study of 29 patients with muscular dystrophy (52% had BMD), the results in terms of infection rates, rejection, and allograft vasculopathy were similar to those of 275 controls.[76] Aortocoronary bypass surgery is indicated when stent implantation is no longer indicated for coronary artery disease or when chronic coronary artery stenosis is present. Valve replacement is indicated for severe secondary mitral regurgitation, but can also be performed transcutaneously. Resection of the left atrial appendage in AFIB has been proposed, but its effectiveness is controversial. Whether patients with LVHT could benefit from trabecular resection, as has been suggested,[77] is also controversial, as such procedures do not guarantee that the trabeculae will not recur. If valve replacement cannot be performed transcutaneously, thoracotomy with open-heart surgery remains an option. All cardiac surgery can only be performed if respiratory function is not impaired and the overall survival rate is considered sufficient. Since all cardiac surgeries are usually performed under general anesthesia, there is a risk of malignant hyperthermia, which is why individual patients may need to be tested for susceptibility to malignant hyperthermia before surgery. It should also be noted that some of the immunosuppressants administered to prevent transplant rejection after heart transplantation may be cardiotoxic and may impair not only cardiac function but also the function of striated skeletal muscle.[78] Because scoliosis or thoracic deformities can also be a feature of BMD, especially in patients who are wheelchair-bound, the scoliosis can become so severe that it impairs heart and lung function. In this case, patients can benefit cardiologically from surgical correction of scoliosis using Harrington rods.[79] Overall, there is currently only limited experience with applicable invasive cardiac therapies in patients with BMD. In a study of 163 patients with BMD, 8 patients had a PM implanted, 11 had an ICD implanted, 4 had an LVAD implanted, and 7 had undergone HTX.[29] Left-sided cardiac sympathetic denervation is a surgical technique that could be used to prevent malignant arrhythmias.

Upcoming (Experimental) Therapies

Pharmacological

To counteract the loss of sarcolemmal integrity, synthetic amphiphilic copolymers, in particular poloxamer-188, have been investigated as membrane-stabilizing therapy in preclinical animal models for DMD (mdx mice and dystrophic dogs) and have shown promising results.[80] Poloxamer-188 works by selectively attaching itself to sites of membrane damage where mechanical stress or micro-tears expose the hydrophobic interior of the lipid bilayer.[81] It is unknown whether this effect also applies to BMD animal models (dmd del 52-55 mice, dmd del exon 3-16 rats, and del 45-47 bmx mice[82]). Poloxamer-188 localizes and seals membrane disturbances and effectively reduces membrane permeability. Treated animals showed improved cardiac output and better structural preservation, underscoring the potential for membrane repair.[80] An initial clinical trial with patients with DMD is currently underway to investigate the safety and efficacy of the approach, but no results are available yet. However, there are also reports that demonstrate a positive effect on the heart muscle but a harmful effect on skeletal muscle.[83]

Cell Based

CAP-1002 [Deramiocel®] is derived from mesenchymal stem cells from the heart and is a cell-based therapy based on the ability of stem cells to secrete regulatory, regenerative, and anti-inflammatory factors that support muscle repair. CAP-1002 aims to improve regenerative capacity to reduce inflammation, promote tissue healing, and potentially regenerate damaged cardiomyocytes. CAP-1002 was evaluated in a phase-2 study of 26 patients with DMD who received either CAP-1002 or placebo quarterly for 1 year.[84] The primary endpoint was the change in Performance of Upper Limb version 1.2 (PUL 1.2) scores for the mid-elbow after 12 months.[84] The mean change in PUL 1.2 score in the mid-elbow region after 12 months compared to baseline favored CAP-1002 over placebo.[84] It was concluded that CAP-1002 is safe and effective in reducing the deterioration of upper limb function in patients with late-stage DMD. Under CAP-1002, various measures of cardiac function and structure (e.g., FS, EF, wall thickness, and LVEDD) determined by cMRI improved.[84] In a study of 13 patients with DMD who received 75 million mesenchymal stem cells (MSCs) injected into the right circumflex artery, areas of fibrosis decreased visibly on cMRI and regional wall motion abnormalities improved.

Genetic Therapy

Gene therapy aims to restore the production of functional dystrophin protein in affected muscle and heart muscle tissue.[81] Gene therapy is necessary because sustained dystrophin expression is essential for the continuous protection of cardiomyocytes.[85] Gene therapy can be divided into therapies that target the disease-causing gene and therapies that target non-disease-causing genes (e.g., *S100A1, SERCA2a,* and *ARC*).

Targeting Disease-Causing Gene

Gene therapy targeting the disease-causing gene is performed either by correcting the underlying mutation in the dystrophin gene (e.g., exon skipping, read-through approach, and gene editing) or by introducing a new functional copy of the gene into the patient's cells.[86]

Correction of the Genetic Defect:

Read-through Therapies

In patients with a nonsense mutation (10%-20% of BMD cases), in which premature stop codons interrupt dystrophin production, read-through therapy with agents that enable the ribosome to bypass the faulty stop signal and continue translation, thereby potentially restoring functional dystrophin, is justified.[81] One drug that showed promising results in mice in bypassing stop codons was gentamicin.[81] However, gentamicin failed in human trials.[87] It is unknown whether read-through therapies can also be beneficial for the myocardium in BMD, but data from a few patients with DMD show that ataluren, an oxadiazole for which the EMA did not extend approval in 2024, has shown not only motor improvement but also a positive effect on the myocardium.[88] In a study of 7 ambulatory patients with DMD who received ataluren for an average of 4 years at an average age of 7.5 years, only 1 of them developed dCMP at the age of 11 and suffered acute myocardial injury.[88] In a study of 4 patients with DMD

who received ataluren over a period of 4 years, FS improved in 3 patients. Only 1 patient developed dCMP.[89]

Exon Skipping

Exon skipping is another promising approach to restore the disrupted reading frame and generate a truncated but functional dystrophin protein. Exon skipping utilizes antisense oligonucleotides (AONs) such as phosphodiamidate morpholino oligomers (PMOs), the 2'OMe modification, or tricycloDNA oligomers. These bind to specific splice sites and mask certain exons during the splicing process, thereby promoting the exclusion of the target exons.[90] The application of AONs led to an improved EF in mdx mice.[91] However, FDA-approved AONs such as eteplirsen, golodirsen, viltolarsen, brogidirsen, and casimersen showed only a moderate improvement in muscle performance and a limited effect on the heart.[90] In a retrospective study of 122 patients with DMD who received eteplirsen (targets exon 51), the annual decline in EF was −0.66% in the eteplirsen-treated patients compared to −1.38% in the control group.[90] Patients treated with eteplirsen had a lower risk of developing heart failure.[90] Golodirsen and viltolarsen target exon 53, casimersen targets exon 45, and brogirdisen targets exon 44, but so far none have shown benefit for cardiac function or the prevention of myocardial fibrosis in patients with DMD. Drisapersen, a 2'OMe-based ASO targeting exon 51 in DMD, also failed to demonstrate clinical benefit in a phase-3 trial despite promising initial results.[92] Its effect on the heart has not been investigated. To overcome the challenges of administering AONs to myocardial tissue, peptide-conjugated PMOs (PPMOs) represent a promising alternative to single AONs. In a study in dystrophic dogs, intracoronary administration of PPMOs for multiexon skipping resulted in a reduction of Q-amplitude and Q/R ratio, as well as restoration of dystrophin expression in the Purkinje fibers of the heart, leading to improvement or prevention of cardiac conduction abnormalities.[93] Another new generation of AONs is tricyclo-DNA, which improved cardiorespiratory function in mdx mice.[91]

Gene Editing

DNA Editing

CRISPR/Cas9 gene editing technologies are used to repair specific mutations, either by knock-in of deleted exons or knock-out of mutated exons, and have shown promising results in preclinical models and hold potential for personalized mutation-specific interventions.[94] In mdx mice, removal of the mutated exon 23 from the dystrophin gene by administration of the CRISPR/Cas9 system via adeno-associated viruses (AAV) for expression of the modified dystrophin gene led to partial restoration of functional dystrophin protein in myofibers and heart muscles and improved muscle function.[95] Delivery of the CRISPR/Cas9 system via AAV to express the modified *dystrophin* gene resulted in partial restoration of functional dystrophin protein in myofibers and heart muscles, improvement in muscle biochemistry, and increased muscle strength.[94] In a DMD mouse model with deletion of exons 52-54 that develops an early-onset cardiac phenotype, CRISPR/Cas9 administered intravenously via AAV restored functional dystrophin expression by excision or skipping of exon 55.[95] Transcript editing and dystrophin restoration were primarily limited to cardiac tissue.[95] In a mouse model with a deletion of exon 44 in the *dystrophin* gene, single-swap editing, in which an adenine base editor edits a single base pair at a splice donor site or splice acceptor site to enable exon skipping, restored dystrophin protein expression in cardiomyocytes derived from induced pluripotent stem cells (iPSCs) by restoring the 3 most therapeutically relevant exons, 45, 51, and 53.[96]

By applying this knock-in approach to correct all mutations downstream of exon 44 in DMD-specific iPSC lines harboring mutations in exons 45 and 51, the expression of mini-dystrophin was confirmed by Western blot and immunofluorescence staining.[97] Transplantation of gene-edited myogenic progenitor cells derived from DMD iPSCs into NSG/mdx4Cv mice resulted in the formation of donor-derived myofibers, as evidenced by the dual expression of human dystrophin and lamin A/C. This provided proof-of-concept for the use of programmable nucleases to develop an autologous iPSC-based therapy for muscular dystrophies.[97] In a study of DMD iPSCs with deletion of exon 50, full-length dystrophin expression and membrane localization in cardiomyocytes were restored by targeted addition of exon 50 at the junction of exon 49 and intron 49 using homologous recombination (HDR).[98]

RNA Editing

Using a mini-dCas13X-mediated RNA adenine base editing strategy (mxABE) for the treatment of the nonsense point mutation c.4174CYT in the dystrophin gene, robust expression of the dystrophin protein was achieved at over 50% of the wild-type (WT) level by enabling premature termination codon (PTC) read-through in muscle tissue and by 54% in the myocardium.[99]

Gene Replacement Therapy

Gene replacement therapies can be classified as in vivo gene therapy, in which genetic material is introduced directly into the patient's body, often via infusion or targeted treatment of a specific organ, whereas in ex vivo gene therapy, the patient's cells are isolated, modified in the laboratory, and then reinfused to the body. In vivo therapy is used for organs that are difficult to access, whereas ex vivo therapy is used for diseases that affect accessible tissues such as blood. Both methods use a vector, often derived from a modified virus, to transport the therapeutic genes to the cells.

Gene replacement therapy involves the administration of a mini-dystrophin or micro-dystrophin gene (μ-dys) that is engineered to fit within the packaging limits of the most commonly used AAV.[100,101] In mini-dystrophins, part of the rod domain is removed, whereas in μ-dys, a significant portion of the rod domain and C-terminus is removed. These truncated versions of the gene encode truncated forms of dystrophin that retain essential functional domains of full-length dystrophin and may offer significant clinical benefit.[81] Gene therapy using AAV to deliver mini-/μ-dys is currently the most promising strategy for DMD.[102] Mini-dystrophin transferred into a DMD mouse model resulted in normalization of the ECG, reduction of fibrosis, and improvement in EF. Similarly, μ-dys normalized heart rate, PR- and QT-intervals,

and cardiomyocyte integrity.[103] In a study of a site-specific gene addition strategy in iPSCs derived from a DMD patient with exon 50 deletion, a mini-dystrophin cassette was precisely targeted to the ribosomal RNA gene locus by homologous recombination using transcription activator-like effector nickases (TALENickases).[104] After differentiation of the target clone into cardiomyocytes, dystrophin expression and membrane localization were restored, and increased spontaneous contraction was observed in the modified cardiomyocytes.[104] Howard et al[105] recently developed the first DMD mouse model (Fiona mice) that reproducibly led to heart failure. This model shows that heart inflammation and fibrosis occur before functional decline. Fibrosis does not progress further, but inflammation persists after functional loss. The model was also used to test the efficacy of µ-dys therapy for the prevention of heart failure.[105] µ-dys therapy prevented a decline in heart function and suppressed the occurrence of inflammation and fibrosis.[105]

Another gene replacement therapy is the intravenous administration of delandistrogen moxeparvovec [Elevidys®] from Sarepta Therapeutics, which has been approved by the FDA.[81] However, there are still some challenges regarding the immune response, efficient administration, long-term expression, and safety.[81] Reports of myocarditis-like reactions due to immune responses targeting either the AAV vector or the µ-dys have emerged in ongoing studies. In addition, a recently published report showed that a Phase 3 study with Elevidys failed to demonstrate a significant therapeutic effect. There have also been 3 deaths of patients who suffered acute liver failure after receiving experimental gene therapy for DMD.[81] The severe hepatotoxicity underscores the need for a better understanding of dose thresholds for vectors, patient susceptibility, and long-term safety. Rigorous evaluation of these side effects, particularly immune-related complications, is essential. The combination of AAV therapy with PPMO resulted in a significant improvement in myocardial structure.[106] Several other µ-dys-based gene replacement therapies are currently in clinical trials to evaluate safety and efficacy.[81]

Numerous other microgen configurations and different AAV serotypes have been investigated in animal models in many laboratories. Bottlenecks in gene therapy for DMD/BMD using mini/µ-dys administration include the fact that most of these approaches are only suitable for infants with strong muscle cell regeneration and immature immune systems and require a high dose of rAAV.[102] However, a high dose of rAAV can cause an immune response and acute liver toxicity.[102]

Targeting Non-disease Genes

Gene therapy targeting non-disease-causing genes is based on the upregulation and expression of non-dystrophin genes whose gene products have a positive effect on cardiac function.[86] Increasing calcium concentration in the endoplasmatic reticulum through *SERCA2q* expression restores calcium homeostasis and prevents cell death. Gene therapy through *SERCA2a* gene expression is based on pumping calcium from the cytoplasm into the sarcoplasmic reticulum.[86] Increasing the expression of *SERCA2a* in mice using AAV serotype-9 led to normalization of the ECG.[86] In a phase-2 study, *SERCA2a* gene therapy improved heart failure, systolic function, and diastolic volume.[107] Dual overexpression of *S100A1* and *ARC* in mdx mice improved diastolic dysfunction, long-term cardiac outcome, and heart failure caused by µ-dys expression.[108]

Monitoring

Patients with heart disease in BMD must be monitored regularly in order to start, adjust, or intensify cardiac therapy. Patients with BMD should be examined regularly (at least once/year) for heart disease from the age of 10 years [https://www.mda.org/disease/becker-muscular-dystrophy/medical-management]. If cardiac involvement in BMD progresses rapidly during the course of the disease,[109] follow-up intervals may need to be shortened to 6 months or less. During follow-up examinations, patients should undergo long-term ECG and echocardiography. In patients with non-compaction, it is advisable to perform repeated cMRT with contrast medium to determine whether intraventricular or intertrabecular thrombus formation is present, so that the appropriate time for OAC to prevent cardiac embolism is not missed. If patients develop ventricular arrhythmias, a decision must be made as to whether they require implantation of a pacemaker or an ICD to prevent SCD. If the heart disease cannot be treated with medication or devices, HTX should be considered, as the survival rate without severe COI is usually quite good.[110]

Outcome

The course of heart disease in BMD depends heavily on the quality of diagnostic and therapeutic treatment of heart defects. Although there are few systematic studies on the optimal treatment of heart disease in BMD, it can be assumed that early detection, the use of prophylaxis, and optimized symptomatic treatment could be factors that determine the course of heart disease in these patients. Despite improved cardiac therapies for heart disease in BMD, these patients still die mainly from difficult-to-treat systolic dysfunction or difficult-to-treat malignant arrhythmias.[45] In addition, some patients die of SCD despite having an implanted ICD.[110] In a study of 163 patients with BMD, no association was found between heart disease and loss of walking ability.[29] There may also be deterioration of systolic and diastolic dysfunction similar to patients with DMD.[111]

CONCLUSIONS

Cardiac involvement is now a well-established phenotypic feature of male patients with BMD, female carriers, and animal models of BMD, and has been extensively described and discussed in the literature. Patients with BMD must be prospectively evaluated for cardiac disease, as it may be subclinical at onset and early treatment may prevent or delay potentially difficult-to-treat complications of the myocardium and intracardiac conduction system. Symptomatic cardiac therapy should remain in the hands of cardiologists and cardiac surgeons, as specialists are required to adequately treat the complex abnormalities that can occur during the course of the disease. There is growing evidence that steroids, read-through approaches, exon skipping, or

gene replacement therapies may be beneficial not only for muscle impairment but also for cardiac involvement in BMD. Various approaches to gene therapy are promising for the future, and some of them have already found their way into clinical application. There is also evidence that early treatment leads to better outcomes than late initiation of cardiac therapy. Much work remains to be done in the future to clarify open questions regarding the optimal and most effective therapeutic treatment of cardiac disease in BMD. Overall, the hearts of patients with BMD require proactive treatment within the framework of a multidisciplinary care model.

Ethics Committee Approval: Ethical approval was not reuqired, as no patients were exmained.

Peer-review: Externally peer-reviewed.

Author Contributions: Concept – J.F.; Design – J.F.; Supervision – J.F.; Data Collection and/or Processing – J.F.; Analysis and/or Interpretation – J.F.; Literature Search – J.F.; Writing – J.F.; Critical Review – J.F.

Declaration of Interests: The author has no conflicts of interest to declare.

Funding: The author declare that this study received no financial support.

REFERENCES

1. Straub V, Guglieri M. An update on Becker muscular dystrophy. *Curr Opin Neurol*. 2023;36(5):450-454. [CrossRef]
2. Finsterer J, Stöllberger C. Cardiac involvement in Becker muscular dystrophy. *Can J Cardiol*. 2008;24(10):786-792. [CrossRef]
3. Armijo Gómez JA, Fernandez-Garcia MA, Camacho A, et al. Epilepsy in Duchenne and Becker muscular dystrophies. *Ann Clin Transl Neurol*. 2024;11(6):1456-1464. [CrossRef]
4. Cumbo F, Tosi M, Catteruccia M, et al. Evolution of neuropsychological and behavioral profile in a cohort of pediatric patients with Becker muscular dystrophy in a longitudinal study. *Neuromuscul Disord*. 2024;36:33-37. [CrossRef]
5. Koeks Z, Hellebrekers DMJ, van de Velde NM, et al. The neurocognitive profile of adults with Becker muscular dystrophy in the Netherlands. *J Neuromuscul Dis*. 2022;9(4):543-553. [CrossRef]
6. Kaneda RR. Becker's muscular dystrophy: orthopedic implications. *J Am Osteopath Assoc*. 1980;79(5):332-335.
7. Carrel L, Brown CJ. When the Lyon(ized chromosome) roars: ongoing expression from an inactive X chromosome. *Philos Trans R Soc Lond B Biol Sci*. 2017;372(1733):20160355. [CrossRef]
8. Magot A, Wahbi K, Leturcq F, et al. Diagnosis and management of Becker muscular dystrophy: the French guidelines. *J Neurol*. 2023;270(10):4763-4781. [CrossRef]
9. Chen Y, Zhu Y, Zhou Y, Zeng J. Becker muscular dystrophy with dilated cardiomyopathy: a case report. *Clin Case Rep*. 2021;9(9):e04777. [CrossRef]
10. Mavrogeni S, Markousis-Mavrogenis G, Papavasiliou A, et al. Cardiac involvement in Duchenne and Becker muscular dystrophy. *World J Cardiol*. 2015;7(7):410-414. [CrossRef]
11. Dolader P, Field E, Sarkozy A, et al. Becker muscular dystrophy associated with sarcomeric hypertrophic cardiomyopathy in a paediatric patient: a case report. *Eur Heart J Case Rep*. 2019;3(3):ytz117. [CrossRef]
12. Park OY, Ahn Y, Park WS, et al. Rapid progression from hypertrophic cardiomyopathy to heart failure in a patient with Becker's muscular dystrophy. *Eur J Heart Fail*. 2005;7(4):684-688. [CrossRef]
13. Daubert MA. Diastolic function in heart failure with reduced ejection fraction: the overlooked prognosticator? *JACC Heart Fail*. 2019;7(9):818-820. [CrossRef]
14. Al-Raqad MK, Alwahsh S, Hejazi IS, et al. Electrocardiographic changes in Jordanian patients with Becker muscular dystrophy. *Cureus*. 2023;15(10):e47553. [CrossRef]
15. Atsumi M, Tanaka A, Kawarabayashi T, et al. Cerebral embolism associated with Becker muscular dystrophy-related dilated cardiomyopathy. *No To Shinkei*. 2004;56(2):163-167.
16. Mohan Krothapalli S, Demetroulis E, Sigurdsson G, et al. Epicardial ablation of ventricular tachycardia in a patient with Becker muscular dystrophy. *HeartRhythm Case Rep*. 2016;2(2):183-186. [CrossRef]
17. Steare SE, Dubowitz V, Benatar A. Subclinical cardiomyopathy in Becker muscular dystrophy. *Br Heart J*. 1992;68(3):304-308. [CrossRef]
18. Melacini P, Fanin M, Danieli GA, et al. Myocardial involvement is very frequent among patients affected with subclinical Becker's muscular dystrophy. *Circulation*. 1996;94(12):3168-3175. [CrossRef]
19. Zhou SY, Wang D, Liu C, et al. Laparoscopic gynecological surgery in an adult woman with Becker muscular dystrophy performed with sevoflurane with cisatracurium anesthesia: a case report. *Med (Baltim)*. 2020;99(16):e19733. [CrossRef]
20. Amore L, Lamendola P, Buffon A, et al. Beyond cardiomyopathy: a case of coronary artery disease in Becker muscular dystrophy. *Eur Heart J Suppl*. 2025;27:suaf076.238. [CrossRef]
21. Yamazaki K, Minakata K, Nakane T, et al. Thyroid storm after mitral valve repair in a patient with Becker muscular dystrophy. *J Card Surg*. 2021;36(2):739-742. [CrossRef]
22. Andrikopoulos G, Kourouklis S, Trika C, et al. Cardiac resynchronization therapy in Becker muscular dystrophy. *Hellenic J Cardiol*. 2013;54(3):227-229.
23. Stöllberger C, Finsterer J, Blazek G, et al. Left ventricular noncompaction in a patient with Becker's muscular dystrophy. *Heart*. 1996;76(4):380. [CrossRef]
24. Shah L, Tam I, Nosib S. Non-compaction cardiomyopathy, Becker muscular dystrophy, neuropathy and recurrent syncope. *BMJ Case Rep*. 2021;14(11):e244745. [CrossRef]
25. Feeley C, Rasbridge S. Cardiomyopathy with a unique finding of bicuspid aortic valve in Becker's muscular dystrophy. *Cardiovasc Pathol*. 2006;15(6):347-351. [CrossRef]
26. Saprungruang A, Vithessonthi K, Vorasettakarnkij Y, et al. Recurrent takotsubo syndrome in a boy with Duchenne muscular dystrophy: a case report. *J Cardiol Cases*. 2019;20(1):14-19. [CrossRef]
27. Kaspar RW, Allen HD, Ray WC, et al. Analysis of dystrophin deletion mutations predicts age of cardiomyopathy onset in Becker muscular dystrophy. *Circ Cardiovasc Genet*. 2009;2(6):544-551. [CrossRef]
28. Ruiz-Cano MJ, Delgado JF, Jiménez C, et al. Successful heart transplantation in patients with inherited myopathies associated with end-stage cardiomyopathy. *Transplant Proc*. 2003;35(4):1513-1515. [CrossRef]
29. Riguzzi P, Borland H, James MK, et al. Characterisation of a large, single-centre cohort of patients with Becker muscular dystrophy to inform standardised care guidelines. *J Neurol*. 2025;272(7):448. [CrossRef]
30. Finsterer J, Bittner RE, Grimm M. Cardiac involvement in Becker's muscular dystrophy, necessitating heart transplantation, 6 years before apparent skeletal muscle involvement. *Neuromuscul Disord*. 1999;9(8):598-600. [CrossRef]

31. Kameda S, Higo S, Shiba M, et al. Modeling reduced contractility and stiffness using iPSC-derived cardiomyocytes generated from female Becker muscular dystrophy carrier. *JACC Basic Transl Sci*. 2023;8(6):599-613. [CrossRef]
32. Conway KM, Thomas S, Ciafaloni E, et al. Prophylactic use of cardiac medications for delay of left ventricular dysfunction in Duchenne muscular dystrophy. *Birth Defects Res*. 2024;116(1):e2260. [CrossRef]
33. Conway KM, Thomas S, Neyaz T, et al. Prophylactic use of cardiac medications and survival in Duchenne muscular dystrophy. *Muscle Nerve*. 2025;71(4):574-582. [CrossRef]
34. Silva MC, Magalhães TA, Meira ZMA, et al. Myocardial fibrosis progression in Duchenne and Becker muscular dystrophy: a randomized clinical trial. *JAMA Cardiol*. 2017;2(2):190-199. [CrossRef]
35. Brooks WW, Bing OH, Robinson KG, et al. Effect of angiotensin-converting enzyme inhibition on myocardial fibrosis and function in hypertrophied and failing myocardium from the spontaneously hypertensive rat. *Circulation*. 1997;96(11):4002-4010. [CrossRef]
36. Kaschina E, Lauer D, Lange C, et al. Angiotensin AT^2 receptors reduce inflammation and fibrosis in cardiovascular remodeling. *Biochem Pharmacol*. 2024;222:116062. [CrossRef]
37. Ibarrola J, Garaikoetxea M, Garcia-Peña A, et al. Beneficial effects of mineralocorticoid receptor antagonism on myocardial fibrosis in an experimental model of the myxomatous degeneration of the mitral valve. *Int J Mol Sci*. 2020;21(15):5372. [CrossRef]
38. Cui Y, Shao S, Zhang L, et al. The effects of glucocorticoids on cardiac function of patients with Duchenne muscular dystrophy: benefit or not? *Eur J Pediatr*. 2025;184(5):313. [CrossRef]
39. Silversides CK, Webb GD, Harris VA, et al. Effects of deflazacort on left ventricular function in patients with Duchenne muscular dystrophy. *Am J Cardiol*. 2003;91(6):769-772. [CrossRef]
40. Markham LW, Spicer RL, Khoury PR, et al. Steroid therapy and cardiac function in Duchenne muscular dystrophy. *Pediatr Cardiol*. 2005;26(6):768-771. [CrossRef]
41. Markham LW, Kinnett K, Wong BL, et al. Corticosteroid treatment retards development of ventricular dysfunction in Duchenne muscular dystrophy. *Neuromuscul Disord*. 2008;18(5):365-370. [CrossRef]
42. Barber BJ, Andrews JG, Lu Z, et al. Oral corticosteroids and onset of cardiomyopathy in Duchenne muscular dystrophy. *J Pediatr*. 2013;163(4):1080-4.e1. [CrossRef]
43. Heidenreich PA, Bozkurt B, Aguilar D, et al. 2022 AHA/ACC/HFSA guideline for the management of heart failure: executive summary: a report of the American College of Cardiology/American Heart Association joint committee on clinical practice guidelines. *Circulation*. 2022;145(18):e876-e894. [CrossRef]
44. Bourke JP, Bryant A, Landon G, et al. Preventing cardiomyopathy in Duchenne muscular dystrophy: long-term follow-up of patients in the randomised, placebo-controlled drug-trial of perindopril and bisoprolol. *Eur J Neurol*. 2025;32(3):e70097. [CrossRef]
45. Ho R, Nguyen ML, Mather P. Cardiomyopathy in Becker muscular dystrophy: overview. *World J Cardiol*. 2016;8(6):356-361. [CrossRef]
46. Raman SV, Hor KN, Mazur W, et al. Eplerenone for early cardiomyopathy in Duchenne muscular dystrophy: a randomised, double-blind, placebo-controlled trial. *Lancet Neurol*. 2015;14(2):153-161. [CrossRef]
47. Gishto T Sr, Methoxha S, Shuka N, et al. Management of cardiac involvement in Becker muscular dystrophy: a case report. *Cureus*. 2024;16(11):e73029. [CrossRef]
48. Nomura H, Hizawa K. Histopathological study of the conduction system of the heart in Duchenne progressive muscular dystrophy. *Acta Pathol Jpn*. 1982;32(6):1027-1033. [CrossRef]
49. Finsterer J, Gelpi E, Stöllberger C. Left ventricular hypertrabeculation/noncompaction as a cardiac manifestation of Duchenne muscular dystrophy under non-invasive positive-pressure ventilation. *Acta Cardiol*. 2005;60(4):445-448. [CrossRef]
50. Finsterer J, Stöllberger C, Berger E. Beneficial effect of ivabradine in dilated cardiomyopathy from Becker muscular dystrophy. *Herz*. 2012;37(6):702-705. [CrossRef]
51. Tochinai R, Kimura K, Saika T, et al. Ivabradine ameliorates cardiomyopathy progression in a Duchenne muscular dystrophy model rat. *Exp Anim*. 2024;73(2):145-153. [CrossRef]
52. Al-Khatib SM, Stevenson WG, Ackerman MJ, et al. 2017 AHA/ACC/HRS guideline for management of patients with ventricular arrhythmias and the prevention of sudden cardiac death: executive summary: a report of the American College of Cardiology/American Heart Association Task Force on Clinical Practice guidelines and the Heart Rhythm Society. *Circulation*. 2018;138(13):e210-e271. [CrossRef]
53. Nigro G, Nigro G, Politano L, et al. Is the value of QT dispersion a valid method to foresee the risk of sudden death? A study in Becker patients. *Heart*. 2002;87(2):156-157. [CrossRef]
54. Finsterer J, Stöllberger C, Quasthoff S. Wolff-Parkinson-White syndrome as initial manifestation of Becker muscular dystrophy. *Herz*. 2008;33(4):307-310. [CrossRef]
55. Joglar JA, Chung MK, Armbruster AL, et al. 2023 ACC/AHA/ACCP/HRS guideline for the diagnosis and management of atrial fibrillation: a report of the American College of Cardiology/American Heart Association joint committee on clinical practice guidelines. *Circulation*. 2023;149(1):e1-e156. [CrossRef]
56. Katritsis DG, Gersh BJ, Camm AJ. Anticoagulation in atrial fibrillation - current concepts. *Arrhythm Electrophysiol Rev*. 2015;4(2):100-107. [CrossRef]
57. Chimenti C, Lavalle C, Magnocavallo M, et al. A proposed strategy for anticoagulation therapy in noncompaction cardiomyopathy. *ESC Heart Fail*. 2022;9(1):241-250. [CrossRef]
58. Stöllberger C, Wegner C, Finsterer J. CHADS2- and CHA2DS-2VASc scores and embolic risk in left ventricular hypertrabeculation/noncompaction. *J Stroke Cerebrovasc Dis*. 2013;22(6):709-712. [CrossRef]
59. Ruopp NF, Cockrill BA. Diagnosis and treatment of pulmonary arterial hypertension: a review. *JAMA*. 2022;327(14):1379-1391. [CrossRef]
60. Enkhmaa B, Berglund L. Statins and Lp(a): the plot thickens. *Atherosclerosis*. 2019;289:173-175. [CrossRef]
61. Langsjoen PH, Langsjoen JO, Langsjoen AM, et al. Statin-associated cardiomyopathy responds to statin withdrawal and administration of coenzyme Q^{10}. *Perm J*. 2019;23:18-257. [CrossRef]
62. Shi H, Chen R, Li M, et al. Acute hepatotoxicity of intravenous amiodarone in a Becker muscular dystrophy patient with decompensated heart failing and ABCB4 gene mutation: as assessed for causality using the updated RUCAM. *J Cardiothorac Surg*. 2024;19(1):464. [CrossRef]
63. Kim YJ, Kim HR, Jeon HJ, et al. Rhabdomyolysis in a patient taking nebivolol. *Kidney Res Clin Pract*. 2016;35(3):182-186. [CrossRef]
64. Stöllberger C, Finsterer J. Worsening of heart failure in Becker muscular dystrophy after nonsteroidal anti-inflammatory drugs. *South Med J*. 2005;98(4):478-480. [CrossRef]
65. Roque JM, Carvalho VO, Pascoalino LN, et al. Physical training in Becker muscular dystrophy associated with heart failure. *Arq Bras Cardiol*. 2011;97(6):e128-e131. [CrossRef]
66. Bostock EL, O'Dowd DN, Payton CJ, et al. The effects of resistance exercise training on strength and functional tasks in adults

with limb-girdle, Becker, and facioscapulohumeral dystrophies. *Front Neurol*. 2019;10:1216. [CrossRef]
67. Sveen ML, Jeppesen TD, Hauerslev S, et al. Endurance training improves fitness and strength in patients with Becker muscular dystrophy. *Brain*. 2008;131(11):2824-2831. [CrossRef]
68. Esteve-Ruiz I, Moraleda-Salas MT, Amigo-Otero E, et al. Epicardial ablation of ventricular tachycardia in a patient with dilated cardiomyopathy due to Becker muscular dystrophy: a case report. *Eur Heart J Case Rep*. 2025;9(9):ytaf406. [CrossRef]
69. Pison L, Potpara TS, Chen J, et al. Left atrial appendage closure-indications, techniques, and outcomes: results of the European Heart Rhythm Association Survey. *Europace*. 2015;17(4):642-646. [CrossRef]
70. Stöllberger C, Finsterer J, Schneider B. Haemodynamic changes after interventional closure of the left atrial appendage may facilitate peri-device leaks. *Eur Heart J*. 2024;45(41):4443-4444. [CrossRef]
71. Lawton JS, Tamis-Holland JE, Bangalore S, et al. 2021 ACC/AHA/SCAI guideline for coronary artery revascularization: a report of the American College of Cardiology/American Heart Association joint committee on clinical practice guidelines. *Circulation*. 2021;145(3):e18-e114. [CrossRef]
72. Kocabas S, Yedicocuklu D, Askar F, et al. Anesthetic management of a child with Duchenne muscular dystrophy undergoing correction of Fallot's tetralogy. *Paediatr Anaesth*. 2008;18(5):448-450. [CrossRef]
73. Stöllberger C, Finsterer J. Left ventricular synchronization by biventricular pacing in Becker muscular dystrophy as assessed by tissue Doppler imaging. *Heart Lung*. 2005;34(5):317-320. [CrossRef]
74. Komoriyama H, Fukushima A, Takahashi Y, et al. Rapidly progressive heart failure in a female carrier of Becker muscular dystrophy with no skeletal muscle symptoms. *Intern Med*. 2019;58(17):2545-2549. [CrossRef]
75. Lim HS, Gustafsson F. Heart transplantation: risks and success. *Circ Heart Fail*. 2023;16(5):e010623. [CrossRef]
76. Wu RS, Gupta S, Brown RN, et al. Clinical outcomes after cardiac transplantation in muscular dystrophy patients. *J Heart Lung Transplant*. 2010;29(4):432-438. [CrossRef]
77. Takamatsu M, Kamohara K, Sato M, et al. Effect of noncompacted myocardial resection on isolated left ventricular noncompaction. *Ann Thorac Surg*. 2020;110(5):e387-e389. [CrossRef]
78. Elezaby A, Dexheimer R, Sallam K. Cardiovascular effects of immunosuppression agents. *Front Cardiovasc Med*. 2022;9:981838. [CrossRef]
79. Thada PK, Bhandari J, Forshaw KC, et al. Becker muscular dystrophy. In: *StatPearls* [Internet]; Updated 2024 January 30. Treasure Island (FL): StatPearls Publishing. Accessed 2025 Jan-. https://www.ncbi.nlm.nih.gov/books/NBK556092/.
80. Townsend D, Turner I, Yasuda S, et al. Chronic administration of membrane sealant prevents severe cardiac injury and ventricular dilatation in dystrophic dogs. *J Clin Invest*. 2010;120(4):1140-1150. [CrossRef]
81. Muchir A. Fighting for every beat: cardiac therapies in Duchenne muscular dystrophy. *Skelet Muscle*. 2025;15(1):25. [CrossRef]
82. Heier CR, McCormack NM, Tully CB, et al. The X-linked Becker muscular dystrophy (bmx) mouse models Becker muscular dystrophy via deletion of murine dystrophin exons 45-47. *J Cachexia Sarcopenia Muscle*. 2023;14(2):940-954. [CrossRef]
83. Terry RL, Kaneb HM, Wells DJ. Poloxamer [corrected] 188 has a deleterious effect on dystrophic skeletal muscle function. *PLOS One*. 2014;9(3):e91221. [CrossRef]
84. McDonald CM, Marbán E, Hendrix S, et al. Repeated intravenous cardiosphere-derived cell therapy in late-stage Duchenne muscular dystrophy (HOPE-2): a multicentre, randomised, double-blind, placebo-controlled, phase 2 trial. *Lancet*. 2022;399(10329):1049-1058. [CrossRef]
85. Wasala NB, Lai Y, Shin JH, et al. Genomic removal of a therapeutic mini-dystrophin gene from adult mice elicits a Duchenne muscular dystrophy-like phenotype. *Hum Mol Genet*. 2016;25(13):2633-2644. [CrossRef]
86. Shin JH, Bostick B, Yue Y, et al. SERCA2a gene transfer improves electrocardiographic performance in aged mdx mice. *J Transl Med*. 2011;9:132. [CrossRef]
87. Wagner KR, Hamed S, Hadley DW, et al. Gentamicin treatment of Duchenne and Becker muscular dystrophy due to nonsense mutations. *Ann Neurol*. 2001;49(6):706-711. [CrossRef]
88. Ahmad M, ElRasoul A, Sedayou R, et al. Safety and effectiveness of ataluren in patients with Duchenne muscular dystrophy: single-center experience from Saudi Arabia. *J Int Med Res*. 2024;52(12):3000605241305252. [CrossRef]
89. Ebrahimi-Fakhari D, Dillmann U, Flotats-Bastardas M, et al. Off-label use of ataluren in four non-ambulatory patients with nonsense mutation Duchenne muscular dystrophy: effects on cardiac and pulmonary function and muscle strength. *Front Pediatr*. 2018;6:316. [CrossRef]
90. Iff J, Desguerre I, Liu Y, et al. Association between exon-skipping therapy with eteplirsen and cardiac outcomes in Duchenne muscular dystrophy. *J Neuromuscul Dis*. 2025;13(2):179-189. [CrossRef]
91. Goyenvalle A, Griffith G, Babbs A, et al. Functional correction in mouse models of muscular dystrophy using exon-skipping tricyclo-DNA oligomers. *Nat Med*. 2015;21(3):270-275. [CrossRef]
92. Goemans NM, Tulinius M, van den Akker JT, et al. Systemic administration of PRO051 in Duchenne's muscular dystrophy. *N Engl J Med*. 2011;364(16):1513-1522. [CrossRef]
93. Echigoya Y, Nakamura A, Nagata T, et al. Effects of systemic multiexon skipping with peptide-conjugated morpholinos in the heart of a dog model of Duchenne muscular dystrophy. *Proc Natl Acad Sci U S A*. 2017;114(16):4213-4218. [CrossRef]
94. Nelson CE, Hakim CH, Ousterout DG, et al. In vivo genome editing improves muscle function in a mouse model of Duchenne muscular dystrophy. *Science*. 2016;351(6271):403-407. [CrossRef]
95. Rok M, Wong TWY, Maino E, et al. Prevention of early-onset cardiomyopathy in *Dmd* exon 52-54 deletion mice by CRISPR-Cas9-mediated exon skipping. *Mol Ther Methods Clin Dev*. 2023;30:246-258. [CrossRef]
96. Chai AC, Chemello F, Li H, et al. Single-swap editing for the correction of common Duchenne muscular dystrophy mutations. *Mol Ther Nucleic Acids*. 2023;32:522-535. [CrossRef]
97. Dhoke NR, Kim H, Azzag K, et al. A novel CRISPR-Cas9 strategy to target DYSTROPHIN mutations downstream of Exon 44 in patient-specific DMD iPSCs. In: *Cells*. 2024;13(11):972. [CrossRef]
98. Xiao R, Zhou M, Wang P, et al. Full-length dystrophin restoration via targeted exon addition in DMD-patient specific iPSCs and cardiomyocytes. *Int J Mol Sci*. 2022;23(16):9176. [CrossRef]
99. Li G, Jin M, Li Z, et al. Mini-dCas13X-mediated RNA editing restores dystrophin expression in a humanized mouse model of Duchenne muscular dystrophy. *J Clin Invest*. 2023;133(3):e162809. [CrossRef]
100. Duan D. Systemic AAV Micro-dystrophin gene therapy for Duchenne muscular dystrophy. *Mol Ther*. 2018;26(10):2337-2356. [CrossRef]
101. Gregorevic P, Allen JM, Minami E, et al. rAAV6-microdystrophin preserves muscle function and extends lifespan in severely dystrophic mice. *Nat Med*. 2006;12(7):787-789. [CrossRef]

102. Li N, Song Y. Strategies for bottlenecks of rAAV-mediated expression in skeletal and cardiac muscle of Duchenne muscular dystrophy. *Genes (Basel)*. 2022;13(11):2021. [CrossRef]
103. Lai Y, Duan D. Progress in gene therapy of dystrophic heart disease. *Gene Ther*. 2012;19(6):678-685. [CrossRef]
104. Zeng B, Zhou M, Liu B, et al. Targeted addition of mini-dystrophin into rDNA locus of Duchenne muscular dystrophy patient-derived iPSCs. *Biochem Biophys Res Commun*. 2021;545:40-45. [CrossRef]
105. Howard ZM, Dorn LE, Lowe J, et al. Micro-dystrophin gene therapy prevents heart failure in an improved Duchenne muscular dystrophy cardiomyopathy mouse model. *JCI Insight*. 2021;6(7):e146511. [CrossRef]
106. Forand A, Muchir A, Mougenot N, et al. Combined treatment with peptide-conjugated Phosphorodiamidate morpholino oligomer-PPMO and AAV-U7 rescues the severe DMD phenotype in mice. *Mol Ther Methods Clin Dev*. 2020;17:695-708. [CrossRef]
107. Jessup M, Greenberg B, Mancini D, et al. Calcium Upregulation by Percutaneous Administration of Gene Therapy in Cardiac Disease (CUPID): a phase 2 trial of intracoronary gene therapy of sarcoplasmic reticulum Ca2+-ATPase in patients with advanced heart failure. *Circulation*. 2011;124(3):304-313. [CrossRef]
108. Hammers DW, Hart CC, Lee YI, et al. 100A1 and ARC gene therapy as a treatment for DMD cardiomyopathy. *bioRxiv*. 2025. [CrossRef]
109. Finsterer J, Stöllberger C, Blazek G, et al. Cardiac involvement over 10 years in myotonic and Becker muscular dystrophy and mitochondrial disorder. *Int J Cardiol*. 2007;119(2):176-184. [CrossRef]
110. Ammendola E, Russo V, Politano L, et al. Is heart rate variability a valid parameter to predict sudden death in patients with Becker's muscular dystrophy? *Heart*. 2006;92(11):1686-1687. [CrossRef]
111. Turan Ö, Kocabaş A. Disturbed atrial conduction in patients with Duchenne muscular dystrophy. *Anatol J Cardiol*. 2024;28(10):493-498. [CrossRef]

THE ANATOLIAN JOURNAL OF CARDIOLOGY

Official journal of the TURKISH SOCIETY OF CARDIOLOGY

Mid-Term Outcomes of the Ozaki Procedure: A Single-Center Experience

ABSTRACT

Background: To assess the mid-term clinical and echocardiographic outcomes of the Ozaki (aortic valve neocuspidization (AVNeo)) procedure performed at a single center.

Methods: A total of 258 patients who underwent the AVNeo procedure between February 2019 and February 2025 were retrospectively analyzed. Demographic, operative, and echocardiographic data were evaluated. Patients were followed up with clinical examinations and transthoracic echocardiography at discharge, 3 months, 6 months, and annually thereafter.

Results: The mean follow-up duration was 36 ± 17.5 months. The average age was 56.4 ± 15.1 years, and 31.6% were female. The mean peak pressure gradient across the aortic valve was 17.0 (11.8-20.2) mm Hg immediately after surgery, then 14.0 (11.0-19.0) mm Hg at 1 year and 17.0 (12.0-23.0) mm Hg at 3 years. The Friedman analysis demonstrated a statistically significant change in peak pressure gradient over time ($\chi^2 = 68.103$, $P < .001$). Preoperatively, ejection fraction was 58.0 (52.0–64.0) %, increasing to 60.0 (56.0–62.0) % at 1 year and 61.0 (59.0–62.0) % at 3 years. Mild aortic regurgitation was seen in 2.7% of patients, and the reoperation rate was 0.38%. There were 3 in-hospital deaths (1.1%). Minimally invasive approaches (5 patients via a right anterior thoracotomy, 7 patients via an upper J sternotomy) were successfully performed in selected patients without needing to convert to full sternotomy.

Conclusion: The AVNeo procedure provides excellent mid-term outcomes with low complication and reoperation rates. Its compatibility with minimally invasive approaches and avoidance of anticoagulation make it a promising, durable alternative to conventional aortic valve replacement.

Keywords: Aortic valve neocuspidization, aortic valve reconstruction, autologous pericardium, minimally invasive cardiac surgery, Ozaki procedure

ORIGINAL INVESTIGATION

Tuna Demirkıran[1]
Yiğit Tokgöz[1]
Veli Can Özdemir[1]
Tayfun Özdem[1]
Emre Kubat[2]
Gökhan Erol[1]
Murat Kadan[3]
Serdar Fırtına[4]
Salim Yaşar[4]
Kubilay Karabacak[1]

[1]*Department of Cardiovascular Surgery, Gülhane Training and Research Hospital, University of Health Sciences, Ankara, Türkiye*
[2]*Department of Cardiovascular Surgery, İskenderun Gelişim Hospital, Hatay, Türkiye*
[3]*Department of Cardiovascular Surgery, Memorial Ankara Hospital, Ankara, Türkiye*
[4]*Department of Cardiology, Gülhane Training and Research Hospital, University of Health Sciences, Ankara, Türkiye*

Corresponding author:
Kubilay Karabacak
✉ kubilaykarabacak@yahoo.com

Received: November 25, 2025
Accepted: March 3, 2026
Available Online Date: May 20, 2026

Cite this article as: Demirkıran T, Tokgöz Y, Özdemir VC, et al. Mid-term outcomes of the ozaki procedure: A single-center experience. *Anatol J Cardiol.* 2026;30(10):644-650.

DOI: 10.14744/AnatolJCardiol.2026.6045

INTRODUCTION

Since Dr. Dwight Harken performed the first successful aortic valve replacement (AVR) in 1960, it has remained the standard treatment for aortic valve disease (AVD) and is now the most common heart valve surgery worldwide. Despite advances in prosthetic valve technology, an ideal prosthetic valve has not yet been developed. Mechanical heart valve prostheses require lifelong anticoagulation, which carries an estimated 2% annual risk of major bleeding after AVR.[1] On the other hand, bioprosthetic valves are mainly limited by structural valve degeneration, which often requires reoperation.[2] The growing popularity and standardization of repair techniques for atrioventricular valves, combined with the limitations of prosthetic valves, have increased interest in aortic valve repair for AVD.[3] However, few centers perform this procedure, which is mostly used for aortic valve insufficiency, and few surgeons specialize in it.

The first documented aortic valve reconstruction using glutaraldehyde-treated autologous pericardium was reported by Duran et al.[4,5] Building on this method, Ozaki et al standardized aortic valve reconstruction—now called the "Ozaki procedure"—by tailoring 3 different cusp sizes, usually based on the distance between the commissures, while accounting for the different hemodynamic stresses on each cusp.[6,7] The Ozaki procedure has become a valuable treatment option for

Copyright@Author(s) - Available online at anatoljcardiol.com.
Content of this journal is licensed under a Creative Commons Attribution-NonCommercial 4.0 International License.

various aortic valve conditions, including aortic stenosis (AS), aortic regurgitation (AR), and infective endocarditis, and its use is growing globally.[8]

The aortic valve neocuspidization (AVNeo) procedure was introduced at the center in February 2019. This study aims to evaluate the mid-term clinical outcomes of patients who underwent the AVNeo procedure at the institution.

METHODS

Study Design and Patient Population

The Institutional Ethics Committee approved the study protocol (Approval date: October 9, 2025, No: 2025/176). The first consecutive 258 patients who underwent the AVNeo procedure at the center between February 2019 and February 2025 were included in the study. Data were collected and analyzed retrospectively to evaluate the mid-term clinical outcomes of the procedure after receiving ethics committee approval. Throughout the study period, the institution routinely performed both conventional AVR and the AVNeo procedure. The AVNeo procedure was offered to patients with suitable valve anatomy who declined prosthetic valves, had a small aortic annulus with a risk of patient–prosthesis mismatch, or were deemed good candidates based on the heart team's assessment. Patients requiring redo aortic valve surgery were excluded from the study. Additionally, the AVNeo procedure was avoided at the institution when usable autologous pericardium was unavailable (e.g., due to prior pericarditis or prior thoracic radiation). All patients provided informed consent before surgery. They underwent routine postoperative follow-up with clinical evaluations and transthoracic echocardiography at 3 months, 6 months, and annually afterward. The study was conducted in accordance with the Declaration of Helsinki.

Surgical Technique

The surgical procedure was performed through a median sternotomy in 244 patients. As the expertise in the AVNeo technique and minimally invasive cardiac surgery increased, alternative approaches in select cases with isolated aortic valve issues were used: 5 patients underwent surgery via a right anterior thoracotomy, and 7 patients were treated through an upper J sternotomy. All cases employed standard cannulation techniques and routine myocardial protection with antegrade cold blood cardioplegia. Autologous pericardium was harvested and prepared to at least 7 × 8 cm. Proper sizing was emphasized as a key factor for procedural success. After excising and customizing the native aortic valve cusps, new pericardial cusps were implanted using the standardized AVNeo procedure (Figure 1).[6,7,9] In patients with bicuspid or unicuspid morphology, tricuspidization was performed (Figure 2).[9,25]

Statistics

Continuous variables were assessed for normal distribution using the Shapiro–Wilk test and visual inspection of Q-Q plots. Data that followed a normal distribution were reported as mean ± standard deviation, while non-normally distributed variables were presented as median [interquartile range (IQR)]. Categorical data were summarized with frequencies and percentages. Since the study included multiple surgical groups with repeated echocardiographic measurements across follow-up periods (preoperative, 1st month, 3-12 months, and beyond 12 months), a repeated-measures analysis was applied. As continuous echocardiographic variables were predominantly non-normally distributed, within-group changes over time were analyzed using the Friedman non-parametric 2-way ANOVA. Post-hoc pairwise comparisons between time points were performed using the Wilcoxon signed-rank test with Bonferroni correction (adjusted significance threshold: $\alpha = 0.05/6 = 0.0083$). Between-group comparisons at each time point were performed using the Kruskal–Wallis test. For significant Kruskal–Wallis results, post-hoc pairwise comparisons were conducted using the Mann–Whitney *U*-test with Bonferroni correction ($\alpha = 0.05/3 = 0.017$). All statistical analyses were conducted using IBM SPSS Statistics, version 26 (Armonk, NY, USA).

RESULTS

Preoperative Characteristics

The study cohort had a mean age of 56.4 ± 15.1 years (range 17-80), with females comprising 31.6% (n = 79). Detailed clinical and preoperative echocardiographic baseline characteristics are shown in Tables 1 and 2. Valve morphology was bicuspid in 17% (n = 44), unicuspid in 0.003% (n = 1), and tricuspid in the remaining 82.5% (n = 213). The median logistic EuroSCORE was 3.0 (1.0-4.0).

Operative Data

Concomitant surgical interventions included coronary artery bypass grafting (CABG) in 18 patients, mitral valve replacement (MVR) in 21, and ascending aortic surgery in 36 patients (comprising 19 Florida sleeve procedures and 17 supracoronary ascending aortic replacements). Additionally, 1 patient underwent combined MVR and ascending aortic surgery, 3 had combined MVR and CABG, one had CABG with ascending aortic surgery, and 1 had simultaneous CABG and carotid endarterectomy. The mean durations for cardiopulmonary bypass and aortic cross-clamp were 166.6 ± 47.8 minutes and 122.5 ± 30.9 minutes, respectively. For isolated AVNeo procedures, these times were shorter, averaging 132.6 ±

HIGHLIGHTS

- The Ozaki procedure showed excellent mid-term hemodynamic performance and valve durability in 258 patients.
- The technique demonstrated low reoperation rates (0.38%) and minimal postoperative complications, with no need for prosthetic conversion.
- The technique was feasible in complex combined cardiac surgeries and through minimally invasive approaches, including right anterior thoracotomy and upper J sternotomy, and was safely implemented.
- The Ozaki procedure maintained natural aortic annular dynamics, showed good hemodynamic performance even in patients with small aortic annuli, and eliminated the need for lifelong anticoagulation therapy.

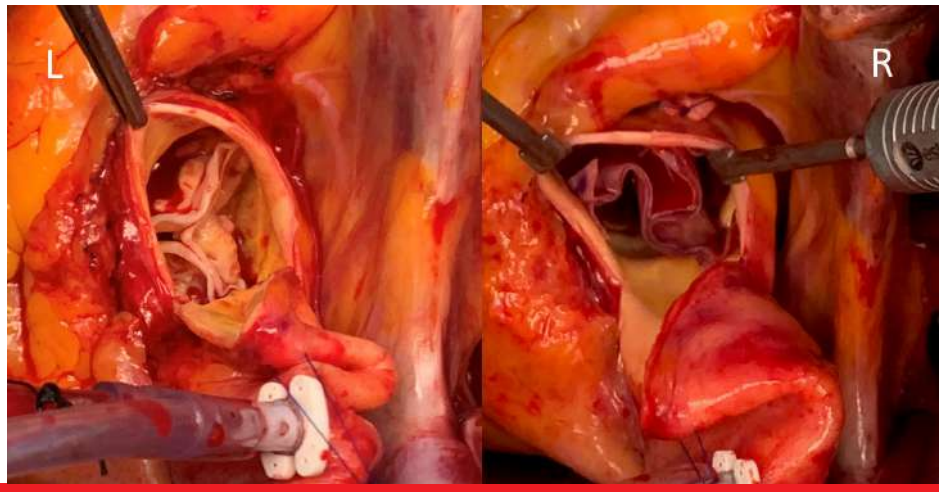

Figure 1. Intraoperative images before and after the AVNeo (Ozaki) aortic valve reconstruction. The image on the left displays the native aortic valve with calcified cusps before removal, while the image on the right shows the reconstructed valve with autologous pericardial leaflets after the procedure.

36.9 minutes for cardiopulmonary bypass and 101.7 ± 24.3 minutes for cross-clamping. None of the minimally invasive approaches required conversion to full median sternotomy. Intraoperative transesophageal echocardiography confirmed satisfactory hemodynamic function of all reconstructed aortic valves, with no cases needing conversion to prosthetic valve replacement.

Postoperative Outcomes

Hospitalization and ICU stay: The average length of stay in the intensive care unit was 1.2 ± 0.8 days, while the total hospital stay averaged 6.5 ± 2.1 days.

Echocardiographic findings: The mean follow-up period was 36 ± 17.5 months. Predischarge transthoracic echocardiography showed a mean peak pressure gradient of 17.0 (11.8-20.2) mm Hg, with mild AR identified in 7 patients. At 1-year and 3-year follow-ups, mean peak gradients were 14.0 (11.0-19.0) mm Hg and 17.0 (12.0-23.0), respectively. The Friedman analysis showed a statistically significant change in peak pressure gradient over time ($\chi^2 = 68.103$, $P < .001$). Post hoc Wilcoxon analysis with a Bonferroni correction confirmed that the gradient decreased significantly from preoperative values at all postoperative time points (all $P < .001$), with no significant differences between postoperative time points (all $P > .0083$), indicating stable, sustained hemodynamic improvement. One patient who underwent an isolated AVNeo procedure required reoperation due to grade 2 AR at 2 months postoperatively. A significant improvement in left ventricular function was observed in patients after the Ozaki procedure. Preoperatively, ejection fraction was 58.0 (52.0–64.0)%, increasing to 60.0 (56.0–62.0)% at 1 year and 61.0 (59.0–62.0)% at 3 years. A Friedman test showed a statistically significant change over time ($\chi^2 = 30.314$, $P < .001$). Post hoc pairwise comparisons indicated that the

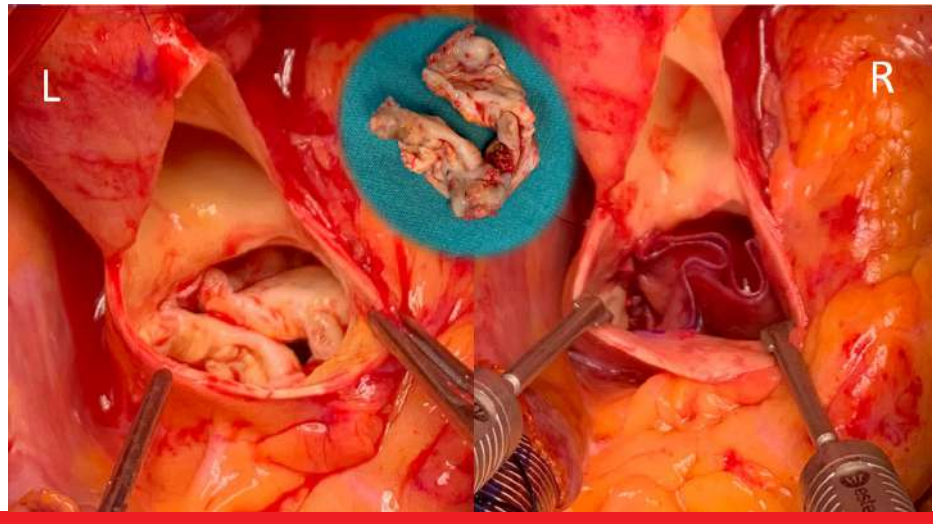

Figure 2. Intraoperative images showing the morphology of a bicuspid native aortic valve before removal (left), the excised native valve leaflets (center), and the reconstructed aortic valve with autologous pericardial cusps after completing the tricuspidization procedure (right).

Table 1. Preoperative Clinical Characteristics of the Patients

	Number of Patients	Percentage (%)
Diabetes mellitus	73	28.29
Hypertension	154	59.68
Hyperlipidemia	36	13.95
Coronary artery disease	59	22.86
Previous cerebrovascular accident	6	2.32
Glomerular filtration rate		
<30	6	2.32
30-60	18	6.97
>60	234	90.69

Table 2. Preoperative Echocardiographic Characteristics of Patients

Parameters	Values
Ejection fraction, (IQR) (%)	58.0 (52.0-64.0)
≥55	190 (73.64)
45–54	29 (11.24)
36–44	24 (9.3)
≤35	15 (5.81)
Left atrium (mm)	42.2 ± 7.1
Left ventricular end-diastolic diameter, (IQR) (mm)	60.0 (57.0-62.0)
Aortic annulus (mm)	23.3 ± 2.6
Patology (%)	
Aortic stenosis (AS)	127 (49.22)
Aortic regurgitation (AR)	88 (34.1)
Mixed lesion (AS + AR)	43 (16.66)

improvement became significant at 1 year and was maintained at 3 years ($P < .001$ for both comparisons vs. baseline). The median left ventricular end-diastolic diameter was 60.0 (57.0–62.0) mm preoperatively and decreased significantly to 52.0 (49.0–55.0) mm at 1 year, further declining to 49.0 (46.0–52.0) mm at 3-year follow-up. A Friedman test showed a statistically significant change over time ($\chi^2 = 52.751$, $P < .001$). Post hoc pairwise comparisons confirmed significant reductions at both 1 year and 3 years compared with baseline ($P < .001$), consistent with progressive and sustained ventricular reverse remodeling. Within-group temporal changes in echocardiographic parameters for the surgical subgroups (isolated AVNeo, AVNeo + CABG, AVNeo + MVR, ascending aortic procedures) and between-group comparisons at corresponding follow-up time points are presented in Table 3.

Anticoagulation strategy: Routine anticoagulation was not given after isolated AVNeo procedures. Patients without other reasons for anticoagulation received 100 mg of aspirin

Table 3. Echocardiographic Parameters in the Preoperative and Postoperative Follow-up Periods According to Concomitant Surgical Procedure Groups

Variables	Time	Group 1 Isolated AVNeo	Group 2 AVNeo + CABG	Group 3 AVNeo + MVR	Group 4 AVNeo + AAS	*P* (Between Groups) Kruskal–Wallis	*P* (Over time) Friedman G1 / G2 / G3 / G4
Ejection fraction (%)	Preoperative	60.0 (60.0-65.0)	60.0 (60.0-65.0)	60.0 (50.0-60.0)	60.0 (60.0-65.0)	**<.001***	**G1: <.001*** G2: .024* G3:** .201 NS **G4: .002****
	Predischarge	60.0 (60.0-60.0)	60.0 (55.0-60.0)	55.0 (50.0-60.0)	60.0 (55.0-60.0)	.082	
	1st year	60.0 (60.0-60.0)	60.0 (52.5-60.0)	58.0 (50.0-60.0)	60.0 (60.0-65.0)	**<.001***	
	3rd year	60.0 (60.0-61.2)	60.0 (60.0-65.0)	60.0 (55.0-60.0)	60.0 (60.0-60.0)	**.032***	
Maximum gradient (mm Hg)	Preoperative (Aortic stenosis)	73.0 (65.8-96.0)	74.0 (54.0-90.0)	75.0 (40.8-83.0)	65.5 (26.0-76.2)	**.043***	**G1: <.001*** G2: .004** G3:** .710 NS **G4: .005****
	Predischarge	16.5 (12.0-20.0)	17.0 (14.0-21.0)	10.5 (10.0-21.0)	17.0 (12.0-20.0)	.410	
	1st year	16.5 (12.0-23.0)	13.0 (11.2-18.5)	13.0 (11.0-14.0)	12.0 (10.0-18.0)	.127	
	3rd year	17.0 (12.0-21.0)	19.5 (16.5-23.2)	22.0 (13.0-24.0)	12.0 (9.0-14.8)	**.039***	
Mean gradient (mm Hg)	Preoperative (Aortic stenosis)	46.0 (41.0-58.0)	43.0 (37.2-60.0)	48.0 (36.8-55.8)	41.0 (30.0-52.0)	.053	**G1: <.001*** G2:** .670 NS **G3:** .740 NS **G4: .002****
	Predischarge	11.0 (9.0-15.8)	9.0 (5.5-11.8)	5.0 (3.0-12.0)	8.0 (7.5-10.0)	.122	
	1st year	10.0 (8.2-14.5)	8.5 (6.5-10.2)	7.0 (4.0-8.0)	8.0 (5.0-11.0)	.074	
	3rd year	8.5 (5.0-13.0)	11.0 (10.2-14.8)	10.0 (6.0-14.0)	4.0 (4.0-10.5)	.263	

Data are presented as median (IQR). *P* (between groups): Kruskal–Wallis test. *P* (Over time): For each group, a separate Friedman non-parametric 2-way ANOVA (G1-G4) was performed. Post-hoc comparisons were conducted using the Wilcoxon signed-rank test with Bonferroni correction ($\alpha = 0.0083$).
AAS, ascending aortic surgery; CABG, coronary artery bypass graft; MVR, mitral valve replacement; NS, not significant.
*$P < .05$, **$P < .01$, ***$P < .001$.

daily for 1 month after surgery. One patient had an ischemic stroke on postoperative day 7; no other thromboembolic events were reported.

Early postoperative complications: Eight patients (3.1%) required surgical re-exploration for bleeding in the early postoperative period, including 2 who underwent isolated AVNeo procedures. There were 3 in-hospital deaths: 1 from low cardiac output syndrome on postoperative day 1 (combined AVNeo and bioprosthetic MVR operation), 1 due to mesenteric ischemia on day 3 (isolated AVNeo procedure), and 1 from ischemic stroke on day 7 (isolated AVNeo procedure). A permanent pacemaker was implanted in 1 patient with severe annular calcification.

DISCUSSION

This study reinforces the AVNeo procedure as a safe, effective, and reproducible option for aortic valve reconstruction, showing excellent mid-term clinical and echocardiographic outcomes. The procedure's adaptability to minimally invasive approaches and complex concomitant surgeries further expands its applicability. The results are consistent with and add to the growing evidence supporting the AVNeo technique as a valuable alternative to traditional prosthetic valve replacement.

The cohort included the first consecutive 258 patients who underwent the AVNeo procedure at the center over 6 years. The average cardiopulmonary bypass and cross-clamp times are consistent with previous reports, despite a significant number of patients undergoing additional procedures such as CABG, MVR, and ascending aortic surgery.[7,8] This indicates that the AVNeo technique can be safely incorporated into complex cardiac surgeries without substantially increasing operative time.

While most procedures were performed via median sternotomy, the use of minimally invasive approaches—including right anterior thoracotomy and upper J sternotomy—in selected cases without converting to full sternotomy or prosthetic valve replacement highlights the growing versatility and safety of the AVNeo procedure. These findings complement recent literature showing the feasibility of minimally invasive AVNeo surgery, which may reduce surgical trauma and promote faster recovery.[10,11] To the best of the knowledge, this is the first report in the literature describing the performance of the Ozaki procedure through a right anterior thoracotomy using a direct vision approach.

Hemodynamic performance was excellent, with mean peak pressure gradients remaining low and stable over a mean follow-up of 36 months. Only a small subset of patients exhibited mild AR, and the reoperation rate was low (0.38%). Additionally, there was a gradual decrease in left ventricular dimensions during the first postoperative year, which may reflect favorable reverse remodeling following valve reconstruction. These outcomes align with prior studies showing durable valve function and favorable hemodynamics of glutaraldehyde-treated autologous pericardial cusps.[8,12] The low rate of significant regurgitation and reoperation indicates good mid-term valve function.

Although aortic valve repair avoids the disadvantages of prosthetic valves, it is still performed in a limited set of conditions, mainly aortic insufficiency, and only by a few surgeons.[13] Bioprosthetic valves, which eliminate the need for lifelong anticoagulation, have durability limitations, whereas mechanical valves require lifelong anticoagulation with associated risks. Additionally, neither type of prosthesis can achieve hemodynamics as favorable as those of the native aortic valve. In a healthy aortic valve, opening begins with systolic dilation of the annulus, creating a maximal effective orifice area that reduces stress on the aortic cusps. As a result, even if the healthy native aortic valve has a small annulus, it maintains a low gradient. Conversely, prosthetic valves restrict annular motion throughout the cardiac cycle because they are fixed with a rigid ring. The most significant advantage of the AVNeo procedure is the preservation of this dynamic function.[14,15] Additionally, full systolic opening of each cusp in a reconstructed valve helps achieve the maximum effective orifice area. It also maintains coordination between the left ventricle and the aortic root during the cardiac cycle, leading to excellent hemodynamic results, as shown in the study.

The incidence of calcific AS has increased approximately fourfold over the past 3 decades, and aortic valve stenosis is now the most common valvular pathology in developed countries.[16,17] The increasing prevalence of AS has led to more patients with small aortic annuli, requiring advanced surgical techniques such as annular enlargement or complete root replacement to prevent patient-prosthesis mismatch. These procedures pose risks, including perioperative mortality, readmission, reoperation, and impacts on long-term survival.[18,19] The AVNeo procedure eliminates these risks by maintaining native annular dynamics and offering better hemodynamic performance without requiring annular enlargement or root replacement, especially in older patients.

Durability in aortic valve repair largely depends on the effective height between the free edges of the cusps and their attachment points, which should be at least 8-9 mm. In the AVNeo procedure, the free edges of the cusps are raised to the level of the sinotubular junction, ensuring an effective height of at least 10 mm.[20] Also, glutaraldehyde-treated autologous pericardium has superior mechanical strength—4 times greater than non-calcified native valves and 10 times greater than calcified valves—and shows a low tendency for calcification.[21] Additionally, using autologous tissue lowers the risk of infection by avoiding foreign materials. These factors together support the long-term durability and function of the reconstructed valve. Furthermore, autologous pericardium is easily accessible and cost-effective for all patients.

Valve-in-valve transcatheter aortic valve replacement (ViV TAVR) offers a less invasive option than redo surgery for high-risk patients with failing bioprosthetic valves, but it is

limited by patient-prosthesis mismatch, elevated residual gradients, and the risk of coronary obstruction.[22] Although not part of this cohort, the AVNeo procedure's preservation of native annular dynamics may support future transcatheter interventions without the limitations seen in ViV TAVR, providing a clear advantage.[23]

Our study also highlights low thromboembolic complication rates and the avoidance of routine anticoagulation in isolated AVNeo cases, providing quality-of-life benefits over mechanical prostheses, especially for younger patients.

The AVNeo technique is feasible and applicable to various aortic valve pathologies, including AS, AR, and infective endocarditis. It can also be adapted for bicuspid, unicuspid, and quadricuspid morphologies.[9,24,25] Additionally, it is compatible with root reimplantation procedures for annuloaortic ectasia.[12] In this series, 36 patients underwent the AVNeo procedure along with ascending aortic surgery, including the Florida sleeve technique and supracoronary ascending aortic replacement. The previous study introduced a novel combination of the Florida sleeve with AVNeo reconstruction for patients with concomitant AVD and sinus of Valsalva aneurysm.[26] This novel approach has been used for the simultaneous treatment of sinus of Valsalva aneurysms with aortic valve abnormalities, providing a comprehensive surgical strategy that combines the benefits of both procedures.

This study presents a large series of 258 patients undergoing the AVNeo procedure at a single center. The sizable sample and systematic follow-up enhance the reliability and generalizability of the findings, providing one of the most comprehensive mid-term evaluations of this surgical technique to date. By including not only the standard median sternotomy but also minimally invasive approaches like right anterior thoracotomy and upper J sternotomy, the study demonstrates the versatility and adaptability of the AVNeo procedure in real-world clinical settings. Additionally, the inclusion of patients undergoing complex combined surgeries (e.g., CABG, MVR, ascending aortic surgery) highlights the procedure's feasibility and safety in complex cardiac interventions. This research adds to the growing global evidence supporting the AVNeo procedure as a viable alternative to traditional valve replacement.

CONCLUSION

The AVNeo procedure is a safe, effective, and feasible option for aortic valve reconstruction, especially advantageous for patients with small aortic roots or those seeking alternatives to prosthetic valves. Its compatibility with minimally invasive approaches and simultaneous surgeries broadens surgical choices, potentially enhancing recovery and minimizing trauma. The low thromboembolic risk and the avoidance of lifelong anticoagulation further increase its attractiveness, particularly for younger patients. These promising mid-term results justify further long-term and multicenter studies to determine durability and compare its effectiveness with traditional valve replacement methods.

Study Limitations

Although the study offers valuable mid-term clinical and echocardiographic outcomes with an average follow-up of about 36 months, longer-term data are needed. The results are based on a single-center cohort, which could limit how widely the findings apply. Differences in surgical skills, patient selection, and perioperative care across centers can affect outcomes. Multi-center studies would help confirm reproducibility and wider applicability. Without a randomized comparison to traditional prosthetic valve replacement or other surgical methods, it's hard to definitively determine superiority or equivalence. The study includes relatively few patients with unicuspid, bicuspid, and quadricuspid valve morphologies, as well as those undergoing minimally invasive approaches, which may restrict conclusions about these groups. Additionally, the influence of concomitant procedures on long-term valve function needs further investigation.

Ethics Committee Approval: This study was approved by Gülhane Training and Research Hospital Non-Interventional Research Ethics Committee (Approval date: October 9, 2025, No: 2025/176).

Informed Consent: Informed consent was obtained from all participants.

Peer-review: Externally peer-reviewed.

Availability of data and materials: The datasets used and/or analyzed during the current study are available from the corresponding author on reasonable request.

AI-Assisted Technologies Statement: Artificial intelligence–assisted technologies were not used in the production of the submitted study.

Author Contributions: Concept – T.D., Y.T., T.Ö., K.K.; Design – T.D., T.Ö., G.E., K.K.; Supervision – K.K., M.K., S.F.; Resources – M.K., S.F., S.Y., K.K.; Materials – V.C.Ö., T.Ö., E.K., S.Y., K.K.; Data Collection and/or Processing – V.C.Ö., E.K., Y.T., G.E.; Analysis and/or Interpretation – T.D., S.Y., Y.T., V.C.Ö.; Literature Search – T.D., S.F., E.K., T.Ö., K.K.; Writing – T.D., K.K., G.E.; Critical Review – K.K., M.K., S.F.

Declaration of Interests: The authors have no conflicts of interest to declare.

Funding: The authors declare that this study received no financial support.

REFERENCES

1. Otto CM, Nishimura RA, Bonow RO, et al. 2020 ACC/AHA guideline for the management of patients with valvular heart disease: a report of the American College of Cardiology/American Heart Association joint committee on clinical practice guidelines. *Circulation*. 2020;143(5):e72-e227. [CrossRef]
2. Chiang YP, Chikwe J, Moskowitz AJ, Itagaki S, Adams DH, Egorova NN. Survival and long-term outcomes following bioprosthetic vs mechanical aortic valve replacement in patients aged 50 to 69 years. *JAMA*. 2014;312(13):1323-1329. [CrossRef]
3. De Paulis R, Chirichilli I, De Kerchove L, et al. Current status of aortic valve repair surgery. *Eur Heart J*. 2025;46(15):1394-1411. [CrossRef]

4. Duran CMG, Gometza B, Kumar N, Gallo R, Martin-Duran R. Aortic valve replacement with freehand autologous pericardium. *J Thorac Cardiovasc Surg*. 1995;110(2):511-516. [CrossRef]
5. Al Halees Z, Al Shahid M, Al Sanei A, Sallehuddin A, Duran C. Up to 16 years follow-up of aortic valve reconstruction with pericardium: a stentless readily available cheap valve? *Eur J Cardiothorac Surg*. 2005;28(2):200-5; discussion 205. [CrossRef]
6. Ozaki S, Kawase I, Yamashita H, et al. Aortic valve reconstruction using self-developed aortic valve plasty system in aortic valve disease. *Interact Cardiovasc Thorac Surg*. 2011;12(4):550-553. [CrossRef]
7. Ozaki S, Kawase I, Yamashita H, et al. A total of 404 cases of aortic valve reconstruction with glutaraldehyde-treated autologous pericardium. *J Thorac Cardiovasc Surg*. 2014;147(1):301-306. [CrossRef]
8. Badalyan SS, Markosyan SV, Ismailbaev AM, Asghar A, Ur Rehman AU. Outcomes of Ozaki procedure/aortic valve neocuspidization for aortic valve diseases: a systematic review. *Anatol J Cardiol*. 2023;27(11):619-627. [CrossRef]
9. Ozaki S, Kawase I, Yamashita H, et al. Reconstruction of bicuspid aortic valve with autologous pericardium: usefulness of tricuspidization. *Circ J*. 2014;78(5):1144-1151. [CrossRef]
10. Nguyen DH, Vo AT, Le KM, et al. Minimally invasive Ozaki procedure in aortic valve disease: the preliminary results. *Innovations (Phila)*. 2018;13(5):332-337. [CrossRef]
11. Rosseĭkin EV, Kobzev EE, Bazylev VV. Minimally invasive Ozaki technique. *Angiol Sosud Khir*. 2019;25(3):142-155. [CrossRef]
12. Ozaki S, Kawase I, Yamashita H, Uchida S, Takatoh M, Kiyohara N. Midterm outcomes after aortic valve neocuspidization with glutaraldehyde-treated autologous pericardium. *J Thorac Cardiovasc Surg*. 2018;155(6):2379-2387. [CrossRef]
13. Saczkowski R, Malas T, De Kerchove L, El Khoury G, Boodhwani M. Systematic review of aortic valve preservation and repair. *Ann Cardiothorac Surg*. 2013;2(1):3-9. [CrossRef]
14. Prinzing A, Böhm J, Sideris K, Vitanova K, Lange R, Krane M. AVNeo improves early haemodynamics in regurgitant bicuspid aortic valves compared to aortic valve repair. *Interact Cardiovasc Thorac Surg*. 2022;35(5):ivac226. [CrossRef]
15. Yamamoto N, Ito H, Inoue K, et al. Impact of valvuloarterial impedance on left ventricular reverse remodeling after aortic valve neocuspidization. *J Cardiothorac Surg*. 2022;17(1):13. [CrossRef]
16. Carabello BA, Paulus WJ. Aortic stenosis. *Lancet*. 2009;373(9667):956-966. [CrossRef]
17. Yi B, Zeng W, Lv L, Hua P. Changing epidemiology of calcific aortic valve disease: 30-year trends of incidence, prevalence, and deaths across 204 countries and territories. *Aging (Albany NY)*. 2021;13(9):12710-12732. [CrossRef]
18. Fallon JM, DeSimone JP, Brennan JM, et al. The incidence and consequence of prosthesis–patient mismatch after surgical aortic valve replacement. *Ann Thorac Surg*. 2018;106(1):14-22. [CrossRef]
19. Sá MPBO, Carvalho MMB, Sobral Filho DC, et al. Impact of surgical aortic root enlargement on the outcomes of aortic valve replacement: a meta-analysis of 13 174 patients. *Interact Cardiovasc Thorac Surg*. 2019;29(1):74-82. [CrossRef]
20. Yaku H. Aortic valve reconstruction with autologous glutaraldehyde-treated pericardium: a new paradigm for aortic valve surgery. *Circ J*. 2014;78(5):1063-1065. [CrossRef]
21. Yamashita H, Ozaki S, Iwasaki K, Kawase I, Nozawa Y, Umezu M. Tensile strength of human pericardium treated with glutaraldehyde. *Ann Thorac Cardiovasc Surg*. 2012;18(5):434-437. [CrossRef]
22. Hahn RT, Webb J, Pibarot P, et al. 5-year follow-up from the PARTNER 2 aortic valve-in-valve registry for degenerated aortic surgical bioprostheses. *JACC Cardiovasc Interv*. 2022;15(7):698-708. [CrossRef]
23. Satomi N, Miyasaka M, Enta Y, et al. Transcatheter aortic valve replacement for structural valve deterioration after aortic valve neocuspidization. *Catheter Cardiovasc Interv*. 2025;106(1):610-620. [CrossRef]
24. Kawase I, Ozaki S, Yamashita H, et al. Original aortic valve plasty with autologous pericardium for quadricuspid valve. *Ann Thorac Surg*. 2011;91(5):1598-1599. [CrossRef]
25. Kawase I, Ozaki S, Yamashita H, et al. Aortic valve reconstruction of unicuspid aortic valve by tricuspidization using autologous pericardium. *Ann Thorac Surg*. 2012;94(4):1180-1184. [CrossRef]
26. Karabacak K. A new alternative to the Bentall procedure: aortic valve neocuspidization (Ozaki procedure) with the Florida sleeve aortic root reconstruction. *Multimed Man Cardiothorac Surg*. 2023;2023:mmcts.2023.020. [CrossRef]

THE ANATOLIAN JOURNAL OF CARDIOLOGY

Official journal of the TURKISH SOCIETY OF CARDIOLOGY

Coronary Artery Perforation During Percutaneous Coronary Intervention: A Two-Center Real-World Case Series and Review of Management Strategies

ABSTRACT

Background: Coronary artery perforation (CAP) is a rare life-threatening complication of percutaneous coronary intervention (PCI). Although several risk factors for CAP have been described, real-world multicenter studies analyzing the clinical outcomes remain limited. This study presents a comprehensive 2-center evaluation of CAP, focusing on angiographic severity, management strategies, and short- and long-term outcomes.

Methods: In this study, patients of CAP were included and perforations were classified according to the Ellis system. Primary outcomes were procedural success, cardiac tamponade, pericardiocentesis, cardiogenic shock, and 30-day mortality. Secondary outcomes were late mortality and ejection fraction at the end of first month.

Results: Totally, 53 cases of CAP were identified. Ten patients had Ellis grade I, 30 patients had grade II, and 13 patients had grade III perforations. The rate of successful procedure was 100% in grade I, 90% in grade II, and 30.8% in grade III ($P < .001$). Hemodynamic compromise was observed predominantly in grade III perforations. Early mortality occurred in 7 patients (13.2%) and was strongly associated with severe Ellis grades ($P < .001$). Late mortality occurred in 5 patients (9.4%), and chronic renal insufficiency was identified as a significant predictor of mortality ($P = .018$). Ejection fraction was significantly lower in grade III perforations at the end of first month ($P = .005$).

Conclusion: Increasing Ellis grade was strongly associated with procedural failure, hemodynamic instability, and early mortality, whereas late outcomes were predominantly influenced by systemic comorbidities rather than the severity of perforation. These findings underscore the importance of prompt intraprocedural management and comprehensive post-discharge care in patients with CAP.

Keywords: Complications, coronary artery disease, coronary artery perforation, Ellis classification, percutaneous coronary intervention, tamponade

INTRODUCTION

Coronary artery perforation (CAP) is one of the most feared complications of percutaneous coronary intervention (PCI). Although it is a rare event, it can lead to catastrophic outcomes, rapidly progressing to cardiac tamponade, hemodynamic collapse, the need for emergency surgery, and even death. The reported incidence of CAP in contemporary practice ranges from 0.1% to 0.6%. However, its occurrence is significantly more common in complex PCI scenarios, such as interventions involving heavily calcified lesions, bifurcations, and chronic total occlusions (CTOs).[1-3] With the increase in high-risk PCI procedures globally and a growing number of elderly and comorbid patients undergoing revascularization, the absolute number of CAP cases has risen, despite the overall incidence remaining stable.[4] These trends highlight the importance of understanding the mechanisms, risk factors, and evidence-based management strategies related to CAP in real-world practice.

The mechanisms that lead to CAP are diverse and closely related to factors such as lesion morphology, wire behavior, balloon or stent over-sizing, and the use of

Copyright@Author(s) - Available online at anatoljcardiol.com.
Content of this journal is licensed under a Creative Commons Attribution-NonCommercial 4.0 International License.

ORIGINAL INVESTIGATION

Fahrettin Turna[1]
Asım Enhoş[2]
Oğuzhan Abanoz[3]
Mehmet Şirin Yıldız[4]
Mahmut Uluganyan[3]

[1]*Department of Cardiology, Sakarya Training and Research Hospital, Sakarya, Türkiye*
[2]*Department of Cardiology, İstanbul Medipol University, İstanbul, Türkiye*
[3]*Department of Cardiology, Bezmialem Vakıf University, İstanbul, Türkiye*
[4]*Department of Cardiology, Tunceli State Hospital, Tunceli, Türkiye*

Corresponding author:
Fahrettin Turna
✉ fturna_53@hotmail.com

Received: January 16, 2026
Accepted: March 10, 2026
Available Online Date: May 12, 2026

Cite this article as: Turna F, Enhoş A, Abanoz O, Yıldız MŞ, Uluganyan M. Coronary artery perforation during percutaneous coronary intervention: A two-center real-world case series and review of management strategies. *Anatol J Cardiol.* 2026;30(10):651-660.

DOI: 10.14744/AnatolJCardiol.2026.6160

plaque-modifying technologies. Guide-wire related injuries—particularly those caused by hydrophilic or stiff CTO wires—are the leading cause of distal perforations. In contrast, oversized balloons, high-pressure post-dilatation, rotational or orbital atherectomy, and intravascular lithotripsy (IVL) can increase the risk of proximal or main-vessel perforations in patients.[5-8] Coronary artery perforation severity is commonly graded using the Ellis classification, introduced in 1994. This system categorizes perforations from mild extraluminal crater formation (Grade I) to frank contrast extravasation (Grade III).[1] This classification not only predicts the likelihood of hemodynamic compromise but also guides clinical management. Grades I and II lesions generally respond to prolonged balloon inflation or conservative therapy; however, Grade III perforations often require covered stent implantation, coil or balloon embolization, and may necessitate emergency surgery.[5-6,9-10] Notably, Ellis Grade III perforations have been associated with mortality rates as high as 20%-44%, primarily due to rapid progression to tamponade and cardiogenic shock.[6,11]

Despite these risks, real-world multicenter data evaluating the characteristics, mechanisms, and outcomes of CAP remain limited.[4] Previous studies are often single-center or confined to specific PCI subgroups, such as CTO interventions. Furthermore, many contemporary analyses lack detailed stratification of outcomes based on Ellis grades or do not differentiate between determinants of acute versus late mortality. Therefore, a combined case series with an integrated review can provide meaningful clinical insights by contextualizing experiences from individual centers within a broader evidence base.

Management of CAP necessitates immediate recognition and rapid escalation through a structured therapeutic algorithm. Prolonged balloon inflation is the first-line approach for achieving hemostasis; however, many cases—particularly those classified as Ellis Grade II or III—require additional therapies. Covered stents are preferred for large proximal perforations, while coil or microcoil embolization is often employed for distal vessel injuries and small-caliber branches.[12-14] In severe cases involving evolving tamponade or failed percutaneous strategies, emergency pericardiocentesis and surgical intervention may be life-saving. Despite these established principles, real-world outcomes exhibit variability influenced by perforation severity, lesion complexity, and the presence of shock or renal dysfunction at the time of presentation.

HIGHLIGHTS

- Coronary artery perforation occurred in approximately 0.25% of percutaneous coronary intervention procedures in this real-world 2-center cohort.
- Increasing Ellis grade was strongly associated with procedural failure, hemodynamic instability, and early mortality, with Ellis grade III representing the highest-risk subgroup.
- Ellis grade III perforations were characterized by high rates of cardiac tamponade, cardiogenic shock, emergency surgery, and markedly reduced procedural success.
- Early mortality was primarily driven by acute hemodynamic collapse and unsuccessful hemostasis, whereas late mortality was predominantly related to systemic comorbidities, particularly chronic renal insufficiency.

The present study offers a comprehensive 7-year, 2-center retrospective analysis of CAP. A total of 53 cases with complete clinical and procedural data were included in the final evaluation. This dataset represents one of the more detailed real-world cohorts of CAP from the region, encompassing both early and late clinical outcomes while providing insights into the interplay between Ellis classification, procedural strategies, hemodynamic deterioration, and mortality. By integrating detailed angiographic characteristics with contemporary management approaches, this study aims to enhance understanding of CAP prognosis in modern PCI practice and identify potential avenues for prevention, early recognition, and more effective intervention.

METHODS

This retrospective, observational study encompassed all patients who underwent coronary angiography or PCI at 2 high-volume centers from January 2018 to January 2025. Within this time interval, a total of 44 428 coronary angiograms and 21515 PCI procedures were conducted across the participating institutions. All cases of CAP identified during or immediately following PCI were screened for inclusion. The diagnosis of CAP was based on angiographic visualization and was classified according to the Ellis classification system. Initially, 53 perforation cases were identified, and detailed procedural images, angiography recordings, and operator reports were subsequently reviewed for each specific case.

Data collection was conducted in multiple stages. Initially, imaging archives from the catheterization laboratories were reviewed to extract procedural characteristics, including lesion morphology, types of guidewires used, balloon and stent parameters, inflation pressures, timing of perforation, and treatment modalities employed. Subsequently, electronic hospital databases were searched to gather demographic information, comorbidities, laboratory values, echocardiographic findings, and in-hospital outcomes.

For cases with missing or incomplete clinical follow-up data—such as late mortality, re-hospitalization, or clinical status within the 1- to 12-month period—patients or their first-degree relatives were contacted via telephone. If follow-up data could not be verified through database review or patient contact, those cases were excluded from the final analysis. As a result, the dataset reflects a fully validated cohort in which both procedural and clinical details were reliably obtained.

Management strategies following perforation were categorized into 5 distinct approaches: (1) prolonged balloon inflation, (2) covered stent implantation, (3) coil or wire-induced embolization, (4) balloon embolization, and (5)

emergency surgical repair. Hemodynamic complications, including hypotension, cardiac tamponade, pericardiocentesis requirement, and cardiogenic shock, were documented systematically. Early mortality was defined as any death occurring within 30 days after the index procedure, while late mortality referred to death occurring between 1 and 12 months post-procedure. The left ventricular ejection fraction at the 1-month mark was obtained from transthoracic echocardiography reports.

Statistical analysis was conducted using SPSS software (IBM SPSS Statistics, Version 26.0; IBM Corp., Armonk, NY, USA). Normality of continuous variables was assessed using the Shapiro–Wilk test. Continuous variables are reported as mean ± standard deviation for those with a normal distribution or as median (interquartile range) for non-normally distributed variables. Categorical variables are presented as counts and percentages. Group comparisons involved the use of the Student's *t*-test or Mann–Whitney *U*-test for continuous variables, and the chi-square test or Fisher's exact test for categorical variables. For comparisons among Ellis groups, analysis of variance (ANOVA) or Kruskal–Wallis testing was employed. A *P* value of less than .05 was regarded as statistically significant. This study was approved by the Local Ethics Committee (decision date: 17 June 2025, decision number: E-43012747-050.04-481619/351). The study was conducted in accordance with the principles of the Declaration of Helsinki.

RESULTS

A total of 53 patients with complete clinical and procedural data were included in the final analysis. The mean age of the population was 66 years, with 69.8% of the population being male. According to the Ellis classification, 10 patients (18.9%) were categorized as Ellis grade I, 30 patients (56.6%) as Ellis grade II, and 13 patients (24.5%) as Ellis grade III.

Baseline Characteristics According to Ellis Classification

Baseline demographic and clinical variables did not show significant differences among the 3 Ellis groups (Table 1).

The Ellis-III group exhibited a higher mean age (70.2 ± 6.3 years) compared to the Ellis-I (61.6 ± 10.9 years) and Ellis-II (65.6 ± 11.9 years) groups, although this difference was not statistically significant ($P = .159$). Key cardiovascular risk factors—including hypertension, diabetes mellitus, hyperlipidemia, chronic renal insufficiency, and prior coronary artery disease—were consistently distributed among the groups ($P > .05$ for all). Furthermore, no significant variations were observed concerning multivessel disease, the presence of CTO, calcification grade, or the rates of pre- and post-dilatation across the groups. These results highlight the uniformity of the patient population, ensuring a more reliable analysis of outcomes based on Ellis classification.

Procedural Findings

Perforation timing exhibited significant differences among the Ellis groups ($P = .005$). Patients classified as Ellis-I and Ellis-II experienced coronary perforations primarily following balloon predilatation and stent implantation, while wire-induced and post-dilatation perforations were more prevalent in the Ellis-III group. Although inflation pressures were numerically higher in the Ellis-I group (15.6 ± 2.8 atm), these did not reach statistical significance across groups ($P = .130$). Additionally, the use of hydrophilic wires was noted in 23.3% of Ellis-II patients and 15.4% of Ellis-III patients, with no significant difference observed ($P = .282$).

The treatment strategy for perforation varied significantly between the groups ($P = .001$). Balloon tamponade was the most commonly employed approach in Ellis-I (90.0%) and Ellis-II (63.3%) patients, while covered stent implantation (61.5%) and emergency surgery (38.5%) were more frequently necessary in the Ellis-III group.

Clinical Outcomes and Complications by Ellis Group

An increasing Ellis grade was strongly associated with worse clinical outcomes (Table 1). Procedural success was achieved in 100% of Ellis-I, 90% of Ellis-II, but only 30.8% of Ellis-III patients ($P < .001$). Hemodynamic complications, including cardiogenic shock (69.2%), hypotension (92.3%), cardiac tamponade (69.2%), and the need for pericardiocentesis (38.5%), were overwhelmingly concentrated in the Ellis-III group ($P < .001$ for each). Additionally, early mortality significantly increased with the severity of perforation, reaching 38.5% in Ellis-III patients compared to 0% in Ellis-I and 6.7% in Ellis-II ($P = .012$).

Left ventricular ejection fraction at 1 month also decreased progressively with Ellis severity, showing values of 57.5 ± 5.9% for Ellis-I, 52.1 ± 7.9% for Ellis-II, and 45.0 ± 8.9% for Ellis-III ($P = .005$).

Early Mortality (First 30 Days)

Among the 53 patients in the study, 7 experienced early mortality, resulting in a rate of 13.2% (Table 2).

Age, sex, and most cardiovascular risk factors did not significantly differ between survivors and non-survivors. However, hypertension was more prevalent among survivors (71.7% vs. 28.6%; $P = .038$). Additionally, procedural variables such as stent implantation, inflation pressure, the use of hydrophilic wires, and the prevalence of CTOs showed no significant association with early mortality.

Several intra-procedural and post-procedural factors were significantly associated with early mortality. Perforation timing was notably different ($P = .033$), with non-survivors often experiencing perforations during the mid-procedure period (after stent implantation). Unsuccessful interventions were more frequent in non-survivors (28.6% vs. 84.8% success in survivors; $P = .004$). Cardiogenic shock (85.7% vs. 8.7%; $P < .001$), tamponade (71.4% vs. 10.9%; $P = .002$), hypotension (85.7% vs. 34.8%; $P = .016$), and the need for pericardiocentesis (57.1% vs. 8.7%; $P = .007$) were significantly associated with early mortality. Ellis-III lesions were also disproportionately represented among early mortality cases ($P = .013$). Thrombolysis in myocardial infarction (TIMI) flow grade scores differed markedly, with lower TIMI flow observed in non-survivors ($P < .001$).

Late Mortality (1-12 Months)

Late mortality was observed in 5 patients (9.4%) (Table 3).

Table 1. Distribution of Clinical and Procedural Variables Across Ellis Groups

Variables	Ellis Groups			P
	Group 1 (n = 10)	Group 2 (n = 30)	Group 3 (n = 13)	
Age	61.6 ± 10.9	65.6 ± 11.9	70.2 ± 6.3	.159*
Gender (F/M)	2/8	11/19	4/9	.671£
HT (%)	7 (70.0)	21 (70.0)	7 (53.8)	.580 £
HL (%)	3 (30.0)	22 (73.3)	8 (61.5)	.053 £
DM (%)	6 (60.0)	19 (63.3)	8 (61.5)	1.000 £
Chronic renal insufficiency (%)	3 (30.0)	11 (36.7)	3 (23.1)	.785 £
History of CAD (%)	6 (60.0)	18 (60.0)	9 (69.2)	.861 £
History of past percutaneous coronary artery intervention (%)	4 (40.0)	15 (50.0)	6 (46.2)	.930 ¥
Multivessel (%)	6 (60.0)	23 (76.7)	11 (84.6)	.383 £
Calcification Grade (0/I/II/III)	0/2/3/5	2/4/18/6	0/1/5/7	.225 £
CTO (%)	2 (20.0)	7 (23.3)	2 (15.4)	.899 £
Pre-dilatation (%)	10 (100.0)	27 (90.0)	13 (84.6)	.573 £
Stent (%)	8 (80.0)	22 (73.3)	11 (15.4)	.902 £
Post-dilatation (%)	5 (50.0)	17 (56.6)	5 (38.5)	.546 ¥
Perforation time (1/2/3/4)	4/2/0/4	9/4/12/5	2/5/0/6	.005 £
Inflation pressure	15.6 ± 2.8	13.7 ± 2.9	13.5 ± 1.7	.130*
Guidewire tip stiffness (operator-reported)	1 (1-3)	1 (0.8-4.5)	1 (0.8-4.5)	.454 #
Hydrophilic wire (%)	0 (0.0)	7 (23.3)	2 (15.4)	.282 £
Technique for the treatment of perforation (1/2/3/4/5)	9/1/0/0/0	19/8/2/1/0	2/8/0/0/3	**.001** £
Successful intervention (%)	10 (100.0)	27 (90.0)	4 (30.8)	**<.001** £
Pericardiocentesis (%)	0 (0.0)	3 (10.0)	5 (38.5)	**.018** £
Prompt surgery (%)	0 (0.0)	0 (0.0)	5 (38.5)	**<.001** £
Cardiogenic shock (%)	0 (0.0)	1 (3.3)	9 (69.2)	**<.001** £
Hypotension (%)	3 (30.0%	7 (23.3)	12 (92.3)	**<.001** ¥
Cardiac tamponade (%)	0 (0.0)	1 (3.3)	9 (69.2)	**<.001** £
Anticoagulant usage (%)	0 (0.0)	2 (6.6)	3 (23.1)	.166 £
Anti-aggregant usage (%)	5 (50.0)	24 (80.0)	9 (69.2)	.182 £
Mortality in the first month (%)	0 (0.0)	2 (6.7)	5 (38.5)	**.012** £
Mortality between 1 and 12th months (%)	1 (10.0)	5 (16.7)	6 (46.2)	.999 £
EF at the end of the first month	57.5 ± 5.9	52.1 ± 7.9	45.0 ± 8.9	**.005***
Effusion during discharge (%)	0 (0.0)	4 (13.2)	3 (23.1)	.085 £
TIMI flow grade (0/1/2/3)	0/0/1/9	1/3/3/22	4/0/0/4	**.029** £

TIMI flow grade: 0 = no perfusion; 1 = penetration without perfusion; 2 = partial perfusion; 3 = normal perfusion. Guidewire tip stiffness was recorded based on operator assessment and manufacturer-reported characteristics.Technique for the treatment of perforation: (1) prolonged balloon inflation, (2) covered stent implantation, (3) coil or wire-induced embolization, (4) balloon embolization, and (5) emergency surgical repair. Perforation time: (1) predilatation, (2) stent implantation, (3) wire-induced, (4) postdilatation with non-compliant balloon.
CAD, coronary artery disease; CTO, chronic total occlusion of coronary arteries; DM, diabetes mellitus; EF, ejection fraction (echocardiography); Ellis, Ellis classification of coronary artery perforation during angiography; HL, hyperlipidemia; HT, hypertension.
*ANOVA [mean S.D].
¥X^2 test [number (percentage)]
£Fisher Exact test [number (percentage)].
#Kruskal-Wallis H test [median (min.-max.].

No significant differences were noted with respect to age, sex, multivessel disease, the presence of CTOs, calcification grade, or procedural characteristics. Unlike early mortality, the timing of perforation and the Ellis grade did not show a correlation with late mortality rates.

Chronic renal insufficiency was identified as the primary predictor of late mortality, being significantly more prevalent among patients who died within 1-12 months (80.0% vs. 22.0%; *P* = .018). Notably, there were no significant differences in the incidence of cardiac tamponade, pericardiocentesis, or shock during the index hospitalization, suggesting that late mortality was predominantly driven by underlying comorbidities rather than the acute severity of the procedural event. Furthermore, the use of anticoagulants showed a borderline association with outcomes (*P* = .053), suggesting

Table 2. Distribution of Study Variables According to Early Mortality

Variables	Mortality Within the First Month		P
	Survivors (n = 46)	Exitus (n = 7)	
Age	66 (44-85)	72 (44-85)	.269 ℧
Gender (F/M)	13/33	4/3	.192 £
HT (%)	33 (71.7)	2 (28.6)	**.038** £
HL (%)	30 (65.2)	3 (42.9)	.405 £
DM (%)	29 (63.0)	4 (57.1)	1.000 £
Chronic renal insufficiency (%)	13 (28.3)	4 (57.1)	.192 £
History of CAD (%)	29 (63.0)	4 (57.1)	1.000 £
History of past percutaneous coronary artery intervention (%)	21 (45.7)	4 (57.1)	.694 £
Multivessel (%)	34 (73.9)	6 (85.7)	.667 £
Calcification Grade (0/I/II/III)	1/7/24/14	1/0/2/4	.162 £
CTO (%)	11 (23.9)	0 (0.0)	.667 £
Pre-dilatation (%)	43 (93.5)	7 (100.0)	1.000 £
Stent (%)	35 (76.1)	6 (85.7)	.679 £
Post-dilatation (%)	24 (52.2)	3 (42.9)	.704 ¥
Perforation time (1/2/3/4)	14/7/10/15	1/4/2/0	**.033** £
Inflation pressure	14 (10-22)	12 (12-16)	.384 ℧
Guidewire tip stiffness (operator-reported)	1 (0.8-4.5)	1 (0.8-4.5)	.953 ℧
Hydrophilic wire (%)	7 (15.2)	2 (28.6)	.587 £
Technique for the treatment of perforation (1/2/3/4/5)	29/11/2/1/3	1/6/0/0/0	**.036** £
Successful intervention (%	39 (84.8)	2 (28.6)	**.004** £
Pericardiocentesis (%)	4 (8.7)	4 (57.1)	**.007** £
Prompt surgery (%)	4 (8.7)	1 (14.3)	1.000 £
Cardiogenic shock (%)	4 (8.7)	6 (85.7)	**<.001** £
Hypotension (%)	16 (34.8)	6 (85.7)	**.016** £
Cardiac tamponade (%)	5 (10.9)	5 (71.4)	**.002** £
Anticoagulant usage (%)	4 (8.7)	1 (14.3)	1.000 £
Anti-aggregant usage (%)	35 (76.1)	3 (42.9)	.090 £
ELLIS Score (1/2/3)	0/3/9	10/27/4	**.013** £
TIMI flow grade (0/1/2/3)	1/3/3/34	4/0/1/1	**<.001** £

TIMI flow grade: 0 = no perfusion; 1 = penetration without perfusion; 2 = partial perfusion; 3 = normal perfusion. Guidewire tip stiffness was recorded based on operator assessment and manufacturer-reported characteristics.Technique for the treatment of perforation: (1) prolonged balloon inflation, (2) covered stent implantation, (3) coil or wire-induced embolization, (4) balloon embolization, and (5) emergency surgical repair. Perforation time: (1) predilatation, (2) stent implantation, (3) wire-induced, (4) postdilatation with non-compliant balloon.
CAD, coronary artery disease; CTO, chronic total occlusion of coronary arteries; DM, diabetes mellitus; EF, ejection fraction (echocardiography); Ellis, Ellis classification of coronary artery perforation during angiography; HL, hyperlipidemia; HT, hypertension.
℧Mann–Whitney *U*-test [median (min.*max)].
¥X^2 test [number (percentage)].
£Fisher Exact test [number (percentage)].

that pharmacological management may play a significant role in influencing long-term survival among this patient cohort.

Factors Associated With Procedural Failure

A total of 12 patients (22.6%) experienced an unsuccessful intervention (Table 4).

Baseline characteristics—including age, sex, diabetes, hypertension, hyperlipidemia, and renal insufficiency—were comparable between successful and unsuccessful intervention groups. In contrast, procedural variables exhibited significant differences, suggesting that the factors associated with the intervention's success may be more closely tied to the specific management strategies employed rather than the demographic or clinical baseline features of the patients.

Successful cases are more likely to involve stent implantation (82.9% vs. 58.3%; $P = .007$) and post-dilation (61.0% vs. 16.7%; $P = .007$). Additionally, inflation pressures were significantly higher in successful interventions ($P = .045$), indicating that optimized stent deployment may play a crucial role in effectively sealing perforations.

Severe complications were significantly more prevalent in unsuccessful interventions, including cardiac tamponade (75.0% vs. 2.4%), cardiogenic shock (75.0% vs. 2.4%), hypotension (75.0% vs. 31.7%), and the need for pericardiocentesis (33.3% vs. 9.8%; $P < .01$ for all). Emergency surgery was

Table 3. Distribution of Study Variables According to Late Mortality

Variables	Mortality Between 1st and 12th Months		P
	Survivors (n = 41)	Exitus (n = 5)	
Age	66 (44-85)	66 (64-82)	.437 ℧
Gender (F/M)	11/30	2/3	.612 £
HT (%)	29 (70.7)	4 (80.0)	1.000 £
HL (%)	27 (65.9)	3 (60.0)	1.000 £
DM (%)	25 (61.0)	4 (80.0)	.637 £
Chronic renal insufficiency (%)	9 (22.0)	4 (80.0)	**.018** £
History of CAD (%)	26 (63.4)	3 (60.0)	1.000 £
History of past percutaneous coronary artery intervention (%)	20 (48.9)	1 (20.0)	.356 £
Multivessel (%)	34 (73.9)	6 (85.7)	.594 £
Calcification Grade (0/I/II/III)	1/6/21/13	0/1/3/1	1.000 £
CTO (%)	11 (26.8)	0 (0.0)	.317 £
Pre-dilatation (%)	38 (92.7)	5 (100.0)	.317 £
Stent (%)	30 (73.2)	5 (100.0)	.317 £
Post-dilatation (%)	22 (53.7)	2 (40.0)	.659 £
Perforation time (1/2/3/4)	13/5/10/13	1/2/0/2	.311 £
Inflation pressure	14 (10-22)	15 (14-16)	.218 ℧
Guidewire tip stiffness (operator-reported)	1 (0.8-4.5)	1 (1-1)	.328 ℧
Hydrophilic wire (%)	7 (17.1)	0 (0.0)	.580 £
Technique for the treatment of perforation (1/2/3/4/5)	26/9/2/1/3	3/2/0/0/0	.809£
Successful intervention (%)	34 (82.9)	5 (100.0)	.580 £
Pericardiocentesis (%)	4 (9.8)	0 (0.0)	1.000 £
Prompt surgery (%)	4 (9.8)	0 (0.0)	1.000 £
Cardiogenic shock (%)	4 (9.8)	0 (0.0)	1.000 £
Hypotension (%)	13 (31.7)	3 (60.0)	.325 £
Cardiac tamponade (%)	5 (12.2)	0 (0.0)	1.000 £
Anticoagulant usage (%)	2 (4.9)	2 (40.0)	.053 £
Anti-aggregant usage (%)	31 (75.6)	4 (80.0)	1.000 £
ELLIS Score (1/2/3)	0/3/9	10/27/4	**.999** £
TIMI flow grade (0/1/2/3)	1/2/3/30	0/1/0/4	.443 £

TIMI flow grade: 0 = no perfusion; 1 = penetration without perfusion; 2 = partial perfusion; 3 = normal perfusion. Guidewire tip stiffness was recorded based on operator assessment and manufacturer-reported characteristics.Technique for the treatment of perforation: (1) prolonged balloon inflation, (2) covered stent implantation, (3) coil or wire-induced embolization, (4) balloon embolization, and (5) emergency surgical repair. Perforation time: (1) predilatation, (2) stent implantation, (3) wire-induced, (4) postdilatation with non-compliant balloon.
CAD, coronary artery disease; CTO, chronic total occlusion of coronary arteries; DM, diabetes mellitus; EF, ejection fraction (echocardiography); Ellis, Ellis classification of coronary artery perforation during angiography; HL, hyperlipidemia; HT, hypertension.
℧Mann–Whitney *U*-test [median (min.*max)].
¥X^2 test [number (percentage)].
£Fisher Exact test [number (percentage)].

required exclusively in the failed-intervention group (41.7%; $P < .001$). Furthermore, the majority of unsuccessful cases were categorized as Ellis grade III ($P < .001$). The TIMI flow grade was also significantly lower in the unsuccessful group, with most patients exhibiting TIMI 0-1 flow ($P < .001$), underscoring the correlation between procedural failure and adverse clinical outcomes.

Overall Mortality and Follow-Up

At the 12-month follow-up, total mortality reached 22.6% (12 patients), including 7 early deaths and 5 late deaths. The distribution of outcomes aligns with the established bimodal risk pattern associated with coronary perforation, characterized by an initial phase primarily marked by acute hemodynamic collapse, followed by a later phase influenced by underlying systemic comorbidities. The observed survival trends are consistent with findings from previous high-volume registries and multicenter studies on CAP, which similarly report early mortality rates and associated risk profiles.[2,12]

DISCUSSION

This 2-center, 7-year analysis provides a detailed real-world assessment of CAP in contemporary PCI practice. Although CAP remains an infrequent complication, the findings confirm that it is associated with substantial mortality both in the early and late stages. In this cohort, CAP occurred in approximately 0.25% of PCI procedures, with early and late mortality rates of 13.2% and 9.4%, respectively. These results

Table 4. Distribution of Study Variables Between Groups Based on Intervention Success

Variables	Success of Intervention		P
	Unsuccessful (n = 12)	Successful (n = 41)	
Age	67 (57-85)	66 (44-85)	.509 ʊ
Gender (F/M)	5/7	12/29	.418 ¥
Mortality within the first month (%)	5 (41.7)	2 (4.9)	<.001¥
Mortality between 1st and 12th months (%)	0 (0.0)	5 (12.2)	.331 £
HT (%)	6 (50.0)	29 (70.7)	.182 ¥
HL (%)	7 (58.3)	26 (63.4)	.749 ¥
DM (%)	7 (58.3)	26 (63.4)	.749 ¥
Chronic renal insufficiency (%)	3 (25.0)	14 (34.2)	.551 ¥
History of CAD (%)	6 (50.0)	27 (65.9)	.319 ¥
History of past percutaneous coronary artery intervention (%)	6 (50.0)	19 (46.3)	.823 ¥
Multivessel (%)	9 (75.0)	31 (75.6)	.966 ¥
Calcification Grade (0/I/II/III)	0/0/5/7	2/7/21/11	.173 £
CTO (%)	2 (16.7)	9 (22.0)	.691 ¥
Application of pre-dilatation (%)	11 (91.7)	39 (95.1)	1.000 £
Stent usage (%)	7 (58.3)	34 (82.9)	**0.007** ¥
Application of post-dilatation (%)	2 (16.7)	25 (61.0)	**0.007** ¥
Perforation time (1/2/3/4)	2/5/2/3	13/6/10/12	0.279 £
Inflation pressure	12 (10-16)	14 (10-22)	.045 ʊ
Guidewire tip stiffness (operator-reported)	1 (1-4.5)	1 (0.8-4.5)	.786 ʊ
Hydrophilic wire	1 (8.3)	8 (19.5)	.364 ¥
Technique for the treatment of perforation (1/2/3/4/5)	4/5/0/0/3	26/12/2/1/0	**.017** £
Pericardiocentesis (%)	4 (33.3)	4 (9.8)	**.044** ¥
Prompt surgery (%)	5 (41.7)	0 (0.0)	**<.001** £
Cardiogenic shock (%)	9 (75.0)	1 (2.4)	**<.001** ¥
Hypotension (%)	9 (75.0)	13 (31.7)	**.007** ¥
Cardiac tamponade (%)	9 (75.0)	1 (2.4)	**<.001** ¥
Anticoagulant usage (%)	2 (4.9)	2 (40.0)	.576 £
Anti-aggregant usage (%)	8 (66.7)	30 (73.2)	.660 £
ELLIS Score (1/2/3)	0/3/9	10/27/4	**<.001** £
TIMI flow grade (0/1/2/3)	5/1/0/0	0/2/4/35	**<.001** £

TIMI flow grade: 0 = no perfusion; 1 = penetration without perfusion; 2 = partial perfusion; 3 = normal perfusion. Guidewire tip stiffness was recorded based on operator assessment and manufacturer-reported characteristics.Technique for the treatment of perforation: (1) prolonged balloon inflation, (2) covered stent implantation, (3) coil or wire-induced embolization, (4) balloon embolization, and (5) emergency surgical repair. Perforation time: (1) predilatation, (2) stent implantation, (3) wire-induced, (4) postdilatation with non-compliant balloon.
CAD, coronary artery disease; CTO, chronic total occlusion of coronary arteries; DM, diabetes mellitus; EF, ejection fraction (echocardiography); Ellis, Ellis classification of coronary artery perforation during angiography; HL, hyperlipidemia; HT, hypertension.
ʊMann–Whitney *U*-test [median (min.*max)].
¥X^2 test [number (percentage)].
£Fisher Exact test [number (percentage)].

are consistent with prior registry data and meta-analyses, reinforcing the clinical relevance of CAP despite its low incidence.[1,12] A clear association was observed between perforation severity, as defined by the Ellis classification, and adverse procedural and clinical outcomes. An increasing Ellis grade was associated with higher rates of procedural failure, hemodynamic instability, and mortality, underscoring the continued relevance of this classification for risk stratification and management guidance in patients with CAP.[1,7]

The most compelling observation derived from this cohort is the pronounced risk gradient across Ellis grades. Ellis grade III perforations were found to be correlated with significantly higher rates of cardiogenic shock, cardiac tamponade, pericardiocentesis, emergency surgical interventions, and procedural failure, culminating in an early mortality rate approaching 40%. These findings substantiate the foundational observations articulated by Ellis and colleagues.[1] They are consistent with subsequent large-scale analyses that reinforce the association between Ellis grade III perforation and adverse clinical outcomes.[2-3] In contrast to earlier registries that reported early mortality rates ranging from approximately 10% to 20% for Ellis grade III lesions, the higher mortality observed in the cohort is likely reflective of the

modern PCI landscape. This landscape is characterized by more complex lesion subsets, an aging patient demographic, and a greater prevalence of comorbid conditions, which collectively contribute to the increased risk associated with these perforations.[3,6]

In this study, nearly all patients with Ellis grade III perforations exhibited profound hemodynamic instability, with hypotension and cardiac tamponade observed in the majority of cases. These rates significantly exceed those reported in various studies focusing on CTOs and registry data, where the frequency of cardiac tamponade typically ranges from 30% to 40%.[2,3,6] This observation implies that, within the context of contemporary clinical practice, Ellis grade III perforation may represent not solely a mechanical complication but also a surrogate marker for extreme procedural and physiological stress. Upon the occurrence of rapid contrast extravasation, the subsequent cascade of acute blood loss, elevated pericardial pressure, myocardial compression, and cardiogenic shock may become self-perpetuating, even when successful angiographic sealing of the vessel is technically accomplished.[2,6,12]

The present study elucidates significant distinctions in the mechanisms underlying CAP and corresponding therapeutic responses. In line with established management algorithms, balloon tamponade was generally effective in Ellis grade I and many grade II perforations.[7,12,15] In contrast, Ellis grade III lesions frequently required the implantation of a covered stent or surgical intervention.[11,13] Although covered stents were promptly deployed in most severe cases, procedural success remained limited, suggesting that mechanical vessel sealing alone may be insufficient once profound hemodynamic deterioration has developed.[10,16]

Distal, wire-related perforations exhibit a distinct clinical profile that warrants specific consideration in the management of CAP. In alignment with existing literature, these injuries—predominantly attributed to hydrophilic or stiff guidewires—demonstrate a favorable response to intervention techniques such as coil or wire-tip embolization. Furthermore, they are infrequently associated with severe complications, including cardiac tamponade, cardiogenic shock, or the necessity for surgical intervention.[5,9,14,17] These findings reinforce the importance of tailoring treatment strategies to both perforation location and mechanism, supporting algorithmic, mechanism-driven management approaches rather than a uniform therapeutic response for all CAP types.[15]

A significant contribution of this study is the precise distinction established between the determinants of early and late mortality related to CAP. Early mortality was predominantly influenced by acute hemodynamic compromise, specifically manifesting as cardiogenic shock, cardiac tamponade, and failure to achieve immediate hemostasis. Notably, cardiogenic shock was identified as the most significant predictor of mortality, corroborating findings from previous registry and observational studies.[2,6,12] These results underscore the premise that early survival following CAP is contingent mainly upon operator skill and procedural dynamics, necessitating swift recognition of complications, prompt and decisive intervention, and effective coordination within the catheterization laboratory team. Such insights are critical for refining clinical strategies and improving patient outcomes in the context of CAP.

In contrast, the patterns of late mortality observed between 1 and 12 months post-procedure exhibited a fundamentally distinct trajectory. Notably, neither the Ellis grade nor specific procedural characteristics demonstrated a significant association with late mortality outcomes. Instead, chronic renal insufficiency emerged as the predominant predictor of late mortality, underscoring the critical influence of systemic disease burden on long-term prognoses following PCI.[18,19] This temporal dissociation between immediate and delayed mortality outcomes supports the conceptualization of a bimodal risk model in the context of CAP. Specifically, the acute phase is characterized by risks that are predominantly driven by the severity of the procedure and the ensuing hemodynamic instability. In contrast, the chronic phase appears to be governed by patient vulnerability as well as the burden of comorbid conditions. Patients who survive the initial perforation event transition away from a risk profile that is directly influenced by the perforation incident, towards a broader cardiovascular risk continuum that is shaped predominantly by renal function and overall systemic health.

Procedural characteristics that correlate with successful intervention underscore the critical importance of technical optimization in PCI. Higher rates of stent implantation, appropriate post-dilation, and adequate inflation pressures were associated with improved procedural success. These results suggest that meticulous attention to vessel sealing and stent expansion might effectively mitigate persistent extravasation and prevent subsequent hemodynamic deterioration.· Conversely, unsuccessful interventions predominantly cluster within the category of Ellis grade III perforations, which are characterized by severe complications, poor TIMI flow, and an increased requirement for emergency surgical intervention.[10]

Collectively, these findings suggest that CAP should not be viewed merely as an unpredictable technical mishap; instead, it should be recognized as an operator-dependent complication whose outcomes are significantly influenced by procedural decision-making, the readiness of devices, and established pathways for the rapid escalation of care. While prevention remains paramount, the data emphasize that once perforation occurs, patient survival hinges on the operator's technical expertise within the catheterization laboratory, alongside a systematic and protocol-driven approach to managing hemodynamic compromise.[12,15]

Ultimately, this study offers a comprehensive and contemporary examination of CAP within the context of real-world PCI practice. It substantiates the premise that the severity of perforation serves as a pivotal element in the early risk stratification of affected patients. At the same time, the long-term prognosis is predominantly determined by the presence of systemic comorbidities, rather than the perforation event itself. Conceptualizing CAP as a 2-stage clinical

syndrome—encompassing both acute and chronic phases—may facilitate the optimization of immediate management strategies and the development of structured post-discharge follow-up protocols. This approach aims to enhance clinical outcomes in patients experiencing this rare but clinically significant complication.

In the present study, no statistically significant association was observed between traditionally recognized high-risk lesion or device characteristics—such as CTOs, severe calcification, or hydrophilic guidewire use—and early mortality. At first glance, this finding may appear inconsistent with prior registry-based studies that have identified lesion complexity and device-related factors as important contributors to coronary perforation and adverse outcomes.[1-3] However, several considerations may help explain this observation. Contemporary PCI practice has evolved substantially, with improved operator experience, more meticulous procedural planning, and broader application of refined interventional techniques, particularly in high-volume centers. In addition, advances in device technology—including improvements in guidewire design, plaque-modifying systems, and covered stent performance—may attenuate the clinical impact of anatomical complexity once perforation occurs.[3,6] Furthermore, careful patient selection and procedural strategy in modern practice may limit the translation of lesion-related risk into early mortality. Finally, the relatively modest sample size of the cohort may have reduced the statistical power to detect smaller effect sizes. Therefore, the absence of statistical significance in the analysis should not be interpreted as the absence of clinical relevance, but rather as a reflection of evolving PCI practice and improvements in the contemporary management of coronary perforation. Taken together, these findings support the concept that, in contemporary PCI, outcomes following coronary perforation are influenced not only by lesion complexity but also by operator-dependent factors and advances in procedural management.[1,6]

CONCLUSION

In this contemporary 2-center cohort, CAP remained a rare but clinically serious complication of PCI. Perforation severity, as defined by the Ellis classification, was the primary determinant of procedural failure, hemodynamic instability, and early mortality. Ellis grade III perforations represented a true interventional emergency, frequently leading to tamponade, cardiogenic shock, and the need for surgical intervention despite prompt percutaneous management.

Importantly, this study demonstrates a temporal dissociation in prognostic determinants following CAP. While procedural factors and acute hemodynamic stabilization primarily influenced early survival, late mortality was driven predominantly by systemic comorbidities, particularly chronic renal insufficiency. These findings underscore the importance of both optimized intraprocedural management and comprehensive post-discharge care in enhancing outcomes for patients with CAP.

Collectively, these real-world data underscore the imperative of enhancing outcomes following coronary perforation through excellence in 2 interrelated domains: executing decisive and technically optimized interventions in the acute phase and implementing meticulous, longitudinal management strategies for high-risk patients during the chronic phase.

Strengths and Limitations

Strengths

This study represents one of the most enormous real-world, 2-center datasets on CAP in the region, offering a detailed and contemporary profile of this life-threatening complication.

There is a granular analysis of early versus late mortality: unlike most prior studies, the cohort clearly differentiates between acute, perforation-driven mortality and late, comorbidity-driven mortality, providing a more nuanced understanding of patient risk trajectories.

The study provides detailed therapeutic stratification, offering precise comparisons of outcomes based on management strategies, including balloon tamponade, covered stenting, coil/guidewire embolization, balloon embolization, and surgical intervention. These findings deliver insights directly applicable to clinical practice.

A comprehensive hemodynamic assessment is included, which involves the systematic evaluation of conditions such as shock, tamponade, hypotension, and TIMI flow, yielding a multidimensional perspective on clinical instability.

The comparison of Ellis subgroups facilitates a precise characterization of perforation severity, its clinical consequences, and procedural responses, enhancing the understanding of CAP management.

Limitations

Retrospective design: While reflective of real-world practice, the retrospective methodology introduces inherent limitations related to data completeness and potential selection bias, which may affect the findings.

Absence of a uniform imaging strategy: The lack of standardized use of intravascular ultrasound or optical coherence tomography restricts the ability to evaluate lesion morphology as a predictor of perforation risk or outcomes.

Detailed procedural device selection: Specific details regarding device choices, such as the types of atherectomy systems or IVL used, were not uniformly recorded, limiting the ability to interpret the mechanistic aspects of these interventions.

Limited long-term follow-up: The absence of follow-up data beyond 1 year prevents a comprehensive assessment of very late outcomes, which could provide valuable insights into the long-term effects of CAP management.

Clinical Implications

Coronary artery perforation is a rare but life-threatening complication of PCI, especially concerning Ellis grade III lesions.

Rapid recognition and immediate hemostasis are crucial for improving early survival rates; therefore, catheterization laboratories performing complex PCI should have easy access to covered stents and embolization tools.

Treatment strategies should be tailored to the mechanism and location of the perforation, with embolization techniques preferred for distal wire-related injuries.

Early mortality primarily results from hemodynamic collapse, while late mortality is more closely related to systemic comorbidities, notably renal dysfunction.

Survivors of acute perforation require structured post-discharge follow-up that emphasizes optimizing comorbidities rather than focusing solely on perforation-specific issues.

Ethics Committee Approval: This study was approved by the Sakarya University Faculty of Medicine Scientific Research Ethics Committee (decision date: June 17, 2025, decision number: E-43012747-050.04-481619/351). It was conducted in accordance with the principles of the Declaration of Helsinki.

Informed Consent: Informed consent was waived due to the retrospective nature of the study.

Peer-review: Externally peer-reviewed.

Artificial Intelligence: The authors declare that artificial intelligence–assisted technologies (such as large language models) were used only for language editing and grammar improvement. The authors take full responsibility for the scientific content, data interpretation, and conclusions of the manuscript.

Author Contributions: Concept – F.T.; Design – F.T.; Supervision – M.U., A.E.; Resource – M.U., A.E., F.T.; Materials – M.U., A.E., F.T, M.Ş.Y., O.A.; Data Collection and/or Processing – F.T., M.Ş.Y., O.A.; Analysis and/or Interpretation – F.T.; Literature Review – M.U., A.E., F.T, M.Ş.Y., O.A.; Writer – F.T.; Critical Review – F.T., M.U., A.E.

Declaration of Interests: The authors have no conflict of interest to declare.

Funding: The authors declared that this study has received no financial support.

REFERENCES

1. Ellis SG, Ajluni S, Arnold AZ, et al. Increased coronary perforation in the new device era. Incidence, classification, management, and outcome. *Circulation*. 1994;90(6):2725-2730. [CrossRef]
2. Shimony A, Joseph L, Mottillo S, Eisenberg MJ. Coronary artery perforation during percutaneous coronary intervention: a systematic review and meta-analysis. *Can J Cardiol*. 2011;27(6):843-850. [CrossRef]
3. Azzalini L, Poletti E, Ayoub M, et al. Coronary artery perforation during chronic total occlusion percutaneous coronary intervention: epidemiology, mechanisms, management, and outcomes. *EuroIntervention*. 2019;15(9):e804-e811. [CrossRef]
4. Akkuş O, Yadsıbaş R, Demirkıran RF, et al. Changes in acute coronary syndrome clinic after the devastating earthquake in Türkiye. *Anatol J Cardiol*. 2024;28(9):446-453. [CrossRef]
5. Brilakis ES, Karmpaliotis D, Patel V, Banerjee S. Complications of chronic total occlusion angioplasty. *Interv Cardiol Clin*. 2012;1(3):373-389. [CrossRef]
6. Kinnaird T, Kwok CS, Davies R, et al. Coronary perforation complicating percutaneous coronary intervention in patients presenting with an acute coronary syndrome: an analysis of 1013 perforation cases from the British Cardiovascular Intervention Society database. *Int J Cardiol*. 2020;299:37-42. [CrossRef]
7. Lee MS, Shamouelian A, Dahodwala MQ. Coronary artery perforation following percutaneous coronary intervention. *J Invasive Cardiol*. 2016;28(3):122-131.
8. Megaly M, Brilakis ES, Sedhom R, et al. Outcomes with orbital and rotational atherectomy for inpatient percutaneous coronary intervention. *Cardiol Ther*. 2021;10(1):229-239. [CrossRef]
9. Mahmud E, Douglas JS Jr. Coil embolization for successful treatment of perforation of chronically occluded proximal coronary artery. *Catheter Cardiovasc Interv*. 2001;53(4):549-552. [CrossRef]
10. Totsugawa T, Kuinose M, Yoshitaka H, et al. Surgical treatment for Ellis type 3 coronary perforation during percutaneous catheter intervention. *Circ J*. 2012;76(2):377-381. [CrossRef].
11. Al-Lamee R, Ielasi A, Latib A et al. Incidence, predictors, management, immediate and long-term outcomes following grade III coronary perforation. *JACC Cardiovasc Interv*. 2011;4(1):87-95. [CrossRef].
12. Dippel EJ, Kereiakes DJ, Tramuta DA, et al. Coronary perforation during percutaneous coronary intervention in the era of abciximab platelet glycoprotein IIb/IIIa blockade: an algorithm for percutaneous management. *Catheter Cardiovasc Interv*. 2001;52(3):279-286. [CrossRef]
13. Kilic ID, Fabris E, Serdoz R, et al. Coronary covered stents. *EuroIntervention*. 2016;12(10):1288-1295. [CrossRef].
14. Hachinohe D, Kashima Y, Okada Y, et al. Coil embolization for coronary artery perforation: A retrospective analysis of 110 patients. *J Interv Cardiol*. 2021;2021:9022326. [CrossRef]
15. Giannini F, Candilio L, Mitomo S, et al. A Practical Approach to the Management of Complications During Percutaneous Coronary Intervention. *JACC Cardiovasc Interv*. 2018;11(18):1797-1810. [CrossRef]
16. Patel VG, Michael TT, Mogabgab O, et al. Clinical, angiographic, and procedural predictors of periprocedural complications during chronic total occlusion percutaneous coronary intervention. *J Invasive Cardiol*. 2014;26(3):100-105.
17. Wong CM, Kwong Mak GY, Chung DT. Distal coronary artery perforation resulting from the use of hydrophilic coated guidewire in tortuous vessels. *Cathet Cardiovasc Diagn*. 1998;44(1):93-96. doi:10.1002/(sici)1097-0304(199805)44:1<93::aid-ccd22>3.0.co;2-p
18. Gunning MG, Williams IL, Jewitt DE, Shah AM, Wainwright RJ, Thomas MR. Coronary artery perforation during percutaneous intervention: incidence and outcome. *Heart*. 2002;88(5):495-498. [CrossRef]
19. Stankovic G, Orlic D, Corvaja N, et al. Incidence, predictors, in-hospital, and late outcomes of coronary artery perforations. *Am J Cardiol*. 2004;93(2):213-216. [CrossRef]

THE ANATOLIAN JOURNAL OF CARDIOLOGY

Official journal of the TURKISH SOCIETY OF CARDIOLOGY

Uric Acid-to-High-Density Lipoprotein Cholesterol Ratio and Coronary Slow Flow: An Integrative Marker of Microvascular Dysfunction

ABSTRACT

Background: Coronary slow flow (CSF) is an angiographic finding characterized by delayed distal vessel opacification despite normal epicardial coronary arteries. Its pathophysiology is multifactorial and involves microvascular dysfunction, endothelial impairment, and chronic inflammation. The uric acid-to-high-density lipoprotein (HDL) cholesterol ratio (UHR) has recently emerged as a novel composite biomarker reflecting both pro-oxidant and anti-inflammatory balance. This study aimed to evaluate the relationship between UHR and CSF.

Methods: In this retrospective cross-sectional study, 218 patients with normal or near-normal coronary arteries on angiography were analyzed. Patients were divided into 2 groups according to the presence of CSF based on thrombolysis in myocardial infarction (TIMI) frame count. Demographic, clinical, and laboratory parameters were compared between groups. Receiver operating characteristic (ROC) analysis was used to determine the discriminatory performance of UHR, and multiple logistic regression was performed to identify independent predictors of CSF.

Results: The mean UHR value was significantly higher in the CSF group compared with the control group (0.13 ± 0.04 vs. 0.09 ± 0.04, $P < .001$). Receiver operating characteristic analysis demonstrated that a UHR cut-off >0.107 predicted CSF with moderate discriminatory ability (area under the curve (AUC) = 0.733, 95% CI: 0.66-0.79, $P < .001$), with 73.5% sensitivity and 76.2% specificity. Multiple analyses suggested that UHR was independently associated with CSF (OR 1.20 per 0.01-unit increase, 95% CI 1.09-1.31, $P < .001$).

Conclusion: Elevated UHR was independently associated with CSF and may represent a readily available biomarker reflecting the metabolic-inflammatory balance contributing to coronary microvascular dysfunction. These findings should be interpreted as associative and hypothesis-generating.

Keywords: Coronary slow flow, endothelial dysfunction, inflammation, microcirculation, uric acid-to-HDL ratio

ORIGINAL INVESTIGATION

INTRODUCTION

Coronary slow flow (CSF) is an angiographic phenomenon characterized by delayed contrast opacification of the distal coronary vasculature in the absence of obstructive epicardial coronary artery disease. It is reported in 1%-7% of patients undergoing coronary angiography and is now considered a form of coronary microvascular dysfunction (CMD).[1-3] CSF has been associated with recurrent angina, arrhythmias, and sudden cardiac death, emphasizing its clinical relevance.[4,5]

Although the exact mechanisms underlying CSF are not fully understood, studies suggest that endothelial dysfunction, increased inflammatory burden, oxidative stress, and microvascular autoregulatory abnormalities contribute to its pathophysiology.[6-9]

Serum uric acid, the final product of purine metabolism, reflects both oxidative and inflammatory status and is considered a mediator of endothelial injury.[10,11] Conversely, high-density lipoprotein cholesterol (HDL-C) exerts vasculoprotective effects through its antioxidant and anti-inflammatory properties.[12,13] A reduction

Ramazan Astan[1]
Eyyüp Erkiz[1]
Erdoğan İlkay[2]

[1]*Department of Cardiology, Batman Training and Research Hospital, Batman, Türkiye*
[2]*Department of Cardiology, Medicana International Ankara Hospital, Ankara, Türkiye*

Corresponding author:
Ramazan Astan
✉ drastan80@gmail.com

Received: December 31, 2025
Accepted: March 17, 2026
Available Online Date: May 11, 2026

Cite this article as: Astan R, Erkiz E, İlkay E. Uric acid-to-high-density lipoprotein cholesterol ratio and coronary slow flow: an integrative marker of microvascular dysfunction. *Anatol J Cardiol.* 2026;30(10):661-667.

DOI: 10.14744/AnatolJCardiol.2026.6173

Copyright@Author(s) - Available online at anatoljcardiol.com.
Content of this journal is licensed under a Creative Commons Attribution-NonCommercial 4.0 International License.

in HDL-C levels has been linked to impaired endothelial function and atherosclerosis progression.[14]

The uric acid-to-HDL-C ratio (UHR) has emerged as a novel and integrated biomarker, capturing the detrimental influence of uric acid and the protective role of HDL-C. Uric acid-to-HDL-C ratio represents a balance between pro-oxidant uric acid and anti-inflammatory HDL-C, providing a composite index of vascular homeostasis. Recent literature has shown that UHR is associated with several conditions, including inflammation, insulin resistance, metabolic syndrome, and cardiovascular disease.[15,16]

However, the potential relationship between UHR and CSF has not been previously studied. Considering the pathophysiological overlap between the determinants of UHR and the mechanisms underlying CSF, it was hypothesized that an elevated UHR would be associated with the presence of CSF. Therefore, this study aimed to investigate the clinical utility of UHR as a potential biomarker in patients with CSF.

METHODS

Study Design and Population

This retrospective cross-sectional study included 218 consecutive patients who underwent coronary angiography between January 2023 and January 2025 at a tertiary referral center due to typical angina or positive noninvasive ischemia tests. Patients with angiographically normal or near normal epicardial coronary arteries were eligible. Exclusion criteria were significant coronary artery stenosis (>50%), prior myocardial infarction, valvular heart disease, left ventricular systolic dysfunction (LVEF <50%), cardiomyopathy, chronic kidney disease (defined as estimated glomerular filtration rate (eGFR) <60 mL/min/1.73 m^2), liver disease, active infection, systemic inflammatory or autoimmune disease, malignancy, and use of drugs known to affect uric acid or lipid metabolism, including uric acid–lowering therapies (e.g., allopurinol), diuretics known to increase uric acid levels, or lipid-lowering therapy initiated within the last 3 months. Estimated glomerular filtration rate was calculated using the MDRD equation based on serum creatinine, age, and sex.

HIGHLIGHTS

- Coronary slow flow (CSF) represents a manifestation of coronary microvascular dysfunction and low-grade inflammation.
- The uric acid-to-HDL cholesterol ratio (UHR) integrates pro-oxidant burden and reduced vasoprotective capacity.
- Uric acid-to-HDL cholesterol ratio levels were significantly higher in patients with CSF compared with controls.
- Uric acid-to-HDL cholesterol ratio remained independently associated with CSF after multiple logistic regression adjustment.
- Uric acid-to-HDL cholesterol ratio may serve as a simple, low-cost biomarker reflecting microvascular dysfunction.

Angiographic Assessment

Coronary angiography was performed via the femoral or radial approach using the standard Judkins technique. Angiograms were acquired using the Siemens Artis Zee angiography system (Siemens Healthineers, Germany) at 15 frames per second. Coronary slow flow (CSF) was defined using the corrected thrombolysis in myocardial infarction (TIMI) frame count (cTFC) method. The angiographic system in the laboratory recorded at 15 frames per second (fps); therefore, all measured TIMI frame counts were multiplied by 2 to ensure comparability with the conventional 30 fps reference values, consistent with the original definitions of Gibson et al. Patients were classified as CSF if cTFC exceeded 27.6 for LAD, 22.6 for LCx, and 20.4 for RCA. Coronary contrast was administered manually with an iodinated contrast agent at an estimated rate of 3-4 mL/s, in line with previous reports emphasizing the importance of injection speed and volume standardization for reliable TIMI frame count assessment. Thrombolysis in myocardial infarction frame counts were evaluated by 2 experienced interventional cardiologists who were blinded to the patients' clinical data and group allocation. In cases of uncertainty, consensus was reached by the 2 observers. Because independent duplicate measurements were not performed, intra- and inter-observer variability could not be formally assessed.

Biochemical Analysis

Blood samples were obtained after at least 12 hours of fasting. Serum uric acid, HDL cholesterol, and other routine biochemical parameters were measured using standard enzymatic methods (Roche Diagnostics, Germany). The UHR was calculated by dividing the serum uric acid level (mg/dL) by the HDL cholesterol level (mg/dL).

Statistical Analysis

Continuous variables were tested for normality using the Kolmogorov–Smirnov test. Data were presented as mean ± standard deviation (SD) or median (interquartile range, IQR) for continuous variables, and as numbers (percentages) for categorical variables. Comparisons between groups were performed using Student's *t*-test or Mann–Whitney *U*-test for continuous variables and chi-square test for categorical variables. Receiver operating characteristic (ROC) curve analysis was performed to evaluate the predictive ability of UHR for CSF, and the area under the curve (AUC) with 95% CI was calculated using the bootstrap method (2000 resamples). Logistic regression analyses were performed to identify predictors of CSF. Variables with $P < .10$ in univariate analysis were included in the multiple logistic regression model. The multiple logistic regression model was adjusted for age, sex, smoking status, triglyceride levels, and hypertension. A 2-tailed *P* value <.05 was considered statistically significant. A post-hoc power analysis was performed based on the observed discriminative performance of UHR (AUC = 0.733). At a 2-sided α level of .05, the sample size of the present study provided greater than 85% statistical power to detect significant differences between groups. Multicollinearity was assessed using variance inflation factors (VIF). Analyses were performed using SPSS version 29.0 (IBM Corp., Armonk, NY, USA).

Ethical Considerations

This study was conducted as a retrospective analysis under an existing ethics approval obtained for a broader investigation of coronary slow flow and related clinical and laboratory parameters. The present analysis represents a predefined secondary evaluation focusing on the UHR as a metabolic–inflammatory marker. All data were collected retrospectively from anonymized clinical records and handled in accordance with the principles of the Declaration of Helsinki. The requirement for informed consent was waived by the Institutional Ethics Committee due to the retrospective design of the study (Decision No: 280118606,429; Date: June 25, 2025).

RESULTS

Patient Characteristics

A total of 218 patients were included, of whom 113 (51.8%) had CSF and 105 (48.2%) had normal coronary flow. There were no significant differences in diabetes mellitus or hyperlipidemia between the 2 groups, whereas hypertension was less frequent among patients with CSF (30.5% vs. 15.9%, $P = .034$) (Table 1). This finding likely reflects the younger age and male predominance of the CSF group rather than a true protective effect of hypertension. Age was significantly lower in the CSF group (49.1 ± 11.2 vs. 55.1 ± 11.0, $P < .001$) in univariate comparisons; however, in the multivariate model it showed only a borderline association with CSF ($P = .091$). Male sex and smoking were significantly more prevalent among patients with CSF (71.7% vs. 47.6%, $P < .001$; and 41.6% vs. 25.7%, $P = .001$, respectively). Regarding laboratory parameters, patients with CSF had significantly higher serum uric acid levels and lower HDL-C concentrations (both $P < .001$). Consequently, the UHR was markedly elevated in the CSF group ($P < .001$) (Table 2).

Table 1. Baseline Demographic and Clinical Characteristics of the Study Population

Variables	CSF (−)	CSF (+)	*P*
Age (years)	55.1 ± 11.0	49.1 ± 11.2	<.001
Male, n (%)	50 (47.6)	81 (71.7)	<.001
Hypertension, n (%)	32 (30.5)	18 (15.9)	.034
Diabetes Mellitus, n (%)	27 (25.7)	22 (19.5)	.308
Hyperlipidemia, n (%)	42 (40.0)	54 (47.8)	.275
Smoking, n (%)	27 (25.7)	47 (41.6)	.001
Glucose (mg/dL)	114.08 ± 41.38	108.96 ± 33.48	.022
Creatinine (mg/dL)	0.86 ± 0.34	0.86 ± 0.23	.251
Uric Acid (mg/dL)	4.8 ± 1.63	5.46 ± 1.42	<.001
CRP (mg/L)	3.94 ± 3.14	3.70 ± 2.85	.570
Total Cholesterol (mg/dL)	186.83 ± 38.78	178.5 ± 38.56	.036
HDL-C (mg/dL)	58.6 ± 14.2	46.4 ± 11.4	<.001
LDL-C (mg/dL)	104.4 ± 32.97	98.3 ± 30	.152
Triglyceride (mg/dL)	140.6 ± 78.1	177.1 ± 101.7	.007
AST (U/L)	25 ± 10.1	30.1 ± 33.1	.188
ALT (U/L)	23.74 ± 11.88	33.23 ± 44.31	.033
Sodium (mmol/L)	136.72 ± 11.95	138.76 ± 2.52	.019
Potassium (mmol/L)	4.38 ± 0.44	4.25 ± 0.42	.034
WBC (10^3/μL)	7.85 ± 2.22	8.36 ± 2.43	.104
Hemoglobin (g/dL)	14.1 ± 1.54	14.7 ± 1.79	.006
Platelets (10^3/μL)	255.54 ± 72.35	243.98 ± 65.96	.630
eGFR (mL/min/1.73 m^2)	86.99 ± 22.48	92.99 ± 25.90	.069

ALT, alanine aminotransferase; AST, aspartate aminotransferase; CSF, coronary slow flow; CRP, C-reactive protein; eGFR, estimated glomerular filtration rate; HDL-C, high-density lipoprotein cholesterol; LDL-C, low-density lipoprotein cholesterol; WBC, white blood cell.

Thrombolysis in Myocardial Infarction Frame Count Standardization

Because the angiography system used in the study recorded at 15 frames per second, TIMI frame counts were multiplied by 2 to standardize them to the conventional 30 fps reference values. Using the standard diagnostic thresholds defined by Gibson et al[13] (LAD > 27.6, Cx > 22.6, and RCA > 20.4), 52 patients (23.9%) had LAD-CSF, 36 (16.5%) had Cx-CSF, and 50 (22.9%) had RCA-CSF (Table 3). These findings confirm that the CSF classification remained consistent after technical standardization.

Receiver Operating Characteristic Analysis

Receiver operating characteristic curve analysis demonstrated that UHR had a moderate discriminatory power for predicting CSF (AUC = 0.733, 95% CI: 0.66-0.79, $P < .001$). The optimal cutoff value of 0.107 yielded 73.5% sensitivity and 76.2% specificity (Figure 1). Boxplot analysis further confirmed that UHR values were significantly higher in the CSF group compared with controls (Figure 2).

Regression Analyses

In univariate logistic regression analysis, UHR was significantly associated with the presence of CSF ($P < .001$). In the multiple logistic regression model (Table 4), adjusted for age, sex, smoking status, triglyceride levels, and hypertension, UHR remained an independent predictor of CSF (OR = 1.20 per 0.01-unit increase; 95% CI: 1.09-1.31; $P < .001$). Model calibration was evaluated using the Hosmer–Lemeshow goodness-of-fit test, which indicated good calibration of the multiple logistic regression model ($P > .05$). Age showed a borderline association with the presence of CSF (OR = 0.97; 95% CI: 0.93-1.00; $P = .091$), while sex, smoking, triglyceride levels, and hypertension were not independently associated with CSF. Sensitivity analyses were performed after excluding patients with diabetes mellitus and current smokers to assess the robustness of the findings. In these analyses, UHR remained independently associated with CSF.

Table 2. Comparison of UHR and Coronary TIMI Frame Counts Between Groups

Variables	CSF (−) (n = 105)	CSF (+) (n = 113)	*P*
Uric acid to HDL cholesterol ratio (UHR)	0.09 ± 0.04	0.13 ± 0.05	<.001
LAD TIMI frame count	16.45 ± 3.46	27.56 ± 13.56	<.001
Cx TIMI frame count	9.30 ± 1.68	14.54 ± 7.36	<.001
RCA TIMI frame count	9.97 ± 1.73	20.12 ± 8.03	<.001

Cx, circumflex artery; LAD, left anterior descending artery; RCA, right coronary artery; TIMI, thrombolysis in myocardial infarction; UHR, uric acid-to-HDL cholesterol ratio.

Table 3. Adjusted TIMI Frame Count Values (Standardized to 30 fps) and CSF Positivity Rates

TIMI Variables	Threshold (30 fps)	Mean ± SD	CSF Positive (n, %)
LAD TIMI (adjusted)	>27.6	44.41 ± 22.94	52 (23.9)
Cx TIMI (adjusted)	>22.6	24.03 ± 12.03	36 (16.5)
RCA TIMI (adjusted)	>20.4	30.37 ± 15.53	50 (22.9)

As the angiography system operates at 15 frames per second, all measured TIMI frame counts were multiplied by 2 to align with the standard 30 fps-based thresholds. Coronary slow flow (CSF) was defined using the classical thresholds proposed by Gibson et al[13]: LAD > 27.6, Cx > 22.6, and RCA > 20.4 (all in 30 fps terms).

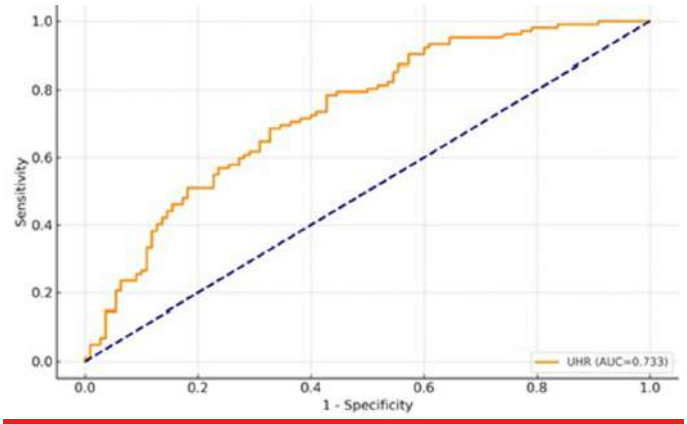

Figure 1. Receiver operating characteristic (ROC) curve of the uric acid-to-HDL cholesterol ratio (UHR) for predicting coronary slow flow (CSF). The area under the curve (AUC) was 0.733 (95% CI: 0.66-0.79). UHR, uric acid-to-HDL cholesterol ratio; CSF, coronary slow flow.

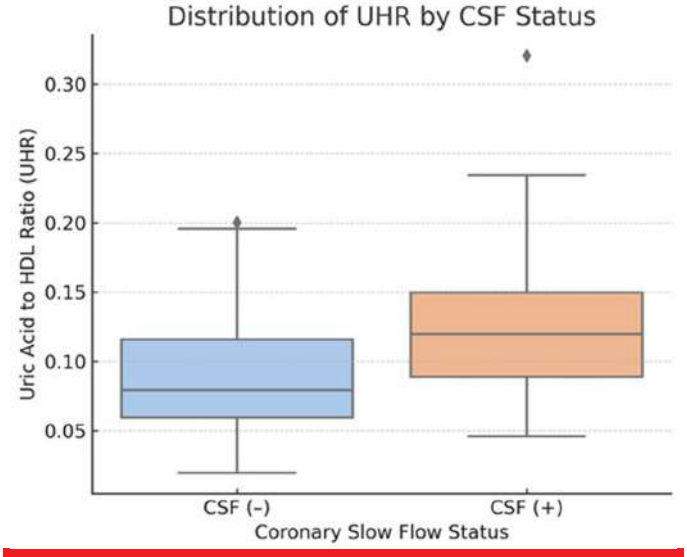

Figure 2. Boxplot showing the distribution of UHR in patients with CSF and in controls with normal coronary flow. UHR was significantly higher in the CSF group ($P < .001$).

DISCUSSION

In this study, the relationship between UHR and CSF were investigated, an angiographic phenomenon characterized by delayed opacification of the distal coronary vasculature in the absence of obstructive epicardial coronary artery disease. The findings showed that UHR levels were significantly higher in patients with CSF compared with those with normal coronary flow. Furthermore, UHR demonstrated a moderate discriminatory ability for predicting CSF in ROC analysis (AUC = 0.733, 95% CI: 0.66-0.79, $P < .001$) and remained independently associated with CSF in multiple logistic regression analysis after adjustment for age, sex, smoking status, triglyceride levels, and hypertension. These findings suggest a statistically significant but modest association between UHR and CSF.

Table 4. Multiple Logistic Regression for Predictors of Coronary Slow Flow

Variables	OR	95% CI (Lower)	95% CI (Upper)	*P*
UHR (per 0.01 unit)	1.20	1.09	1.31	<.001
Age (per year)	0.97	0.93	1.00	.091
Sex: male vs. female (reference)	1.55	0.75	3.21	.239
Smoking: yes vs. no (reference)	0.79	0.35	1.75	.554
Triglycerides (per mg/dL)	1.00	1.00	1.00	.825
Hypertension: yes vs. no (reference)	0.64	0.30	1.37	.250

The multiple logistic regression model was adjusted for age, sex, smoking status, triglyceride levels, and hypertension. Odds ratios are presented with 95% CI. The UHR odds ratio is expressed per 0.01-unit increase to provide clinically interpretable effect sizes given the relatively small numerical range of UHR. UHR, uric acid-to-HDL cholesterol ratio

Coronary slow flow is a manifestation of microvascular dysfunction, low-grade inflammation, and endothelial impairment. Although first described by Tambe et al in 1972, its pathophysiological mechanisms remain incompletely understood.[14] Inflammation, increased oxidative stress, and altered rheological properties of blood have been implicated. In particular, studies have demonstrated that impaired endothelial nitric oxide production and microvascular constriction significantly contribute to CSF development. Furthermore, inflammatory cytokines such as CRP and IL-6 are frequently elevated in patients with CSF.[15-18]

Elevated uric acid levels can promote endothelial dysfunction, vascular smooth muscle proliferation, and oxidative stress, whereas low HDL cholesterol levels are known to impair reverse cholesterol transport and antioxidant defense.[19-22] Thus, UHR may provide a composite measure of pro-inflammatory and atherogenic burden. Previous studies have linked hyperuricemia[19] and low HDL-C[20] to CSF separately, but the combined use of these parameters as a ratio may provide additional pathophysiological insight into the metabolic–inflammatory milieu underlying microvascular dysfunction. UHR may serve as a pragmatic integrative biomarker reflecting both pro-oxidant burden and reduced vasoprotective capacity. However, the present study did not formally evaluate whether UHR provides incremental predictive value beyond its individual

components, and UHR should therefore be interpreted as a pragmatic composite index rather than a statistically validated superior marker.

In addition to biochemical markers, the findings also revealed that male sex and smoking were significantly more prevalent among patients with CSF. These demographic and behavioral patterns are consistent with previous reports, which have identified the male sex as a predisposing factor due to sex-related differences in endothelial function and vascular reactivity.[5,14]Similarly, cigarette smoking has been shown to promote oxidative stress, impair nitric oxide bioavailability, and induce microvascular dysfunction, all of which are central to the pathogenesis of CSF.[6,18] The additive impact of smoking on uric acid levels and HDL metabolism may further potentiate the pro-inflammatory milieu captured by UHR, amplifying microvascular compromise.

Recently, UHR has gained attention as a novel biomarker for cardiovascular risk stratification. Studies have shown its association with metabolic syndrome, atherosclerotic cardiovascular disease, arterial stiffness, and adverse outcomes in patients with acute coronary syndrome. Furthermore, elevated UHR levels are associated with increased coronary artery calcium scores and subclinical atherosclerosis in asymptomatic individuals. [23-27]

The optimal cut-off value for UHR in predicting CSF was determined to be 0.107 in the study, with a sensitivity of 73.5% and specificity of 76.2%. This supports the notion that UHR may be a useful non-invasive biomarker for identifying patients at risk for CSF, although further studies are needed to compare its performance with its individual components. The association of UHR with CSF may reflect the dual contribution of uric acid–induced oxidative stress and impaired HDL-mediated vasoprotection in microcirculation.

A corrected TIMI frame count methodology was applied because the angiographic acquisition rate in the catheterization laboratory was 15 frames per second (fps), which differs from the standard 30 fps used in most prior studies. To ensure compatibility with published diagnostic thresholds, the measured TIMI frame counts were adjusted by multiplying them by 2. This allowed a direct comparison with the standard reference values reported in the literature, namely >27.6 for LAD, >22.6 for CX, and >20.4 for RCA.[13] Importantly, the threshold values themselves were not altered, as they were already established based on a 30 fps acquisition rate. This methodological correction enhanced the precision of the CSF classification and ensured the validity and comparability of the results with those of previous research.

The study included a relatively modest but comparable sample size to previous investigations of CSF, together with detailed laboratory profiling. The higher uric acid levels and lower HDL-C concentrations observed in the CSF group are consistent with previous findings and support the use of UHR as a synthesized inflammatory/metabolic marker. Moreover, the ROC and regression analyses confirmed a statistically significant association between UHR and CSF.

The multiple logistic regression analysis suggested that UHR was independently associated with CSF, even after adjustment for age, sex, smoking, triglycerides, and hypertension (Table 4). An OR of approximately 1.20 per 0.01-unit increase underscores the potential clinical relevance of UHR, warranting further prospective investigation in the context of microvascular dysfunction. This effect size represents a statistically significant but modest association, suggesting that small variations in UHR within the observed clinical range may be associated with differences in the likelihood of CSF. The absence of significant multicollinearity (all VIF values <10) supports the robustness of this association.

In the cohort, hyperlipidemia tended to be more frequent in patients with CSF, consistent with previous reports, although without reaching statistical significance. Conversely, hypertension and diabetes mellitus were less common among CSF patients, likely reflecting the younger age and male predominance of this group rather than a true protective effect. These findings indicate that CSF can occur even in patients with relatively few conventional cardiovascular risk factors, underscoring the role of alternative mechanisms such as inflammation and microvascular dysfunction. Interestingly, UHR remained associated with CSF even among patients with fewer traditional cardiovascular risk factors, supporting its potential role as a non-traditional metabolic indicator of microvascular dysfunction.

Despite these contributions, several limitations should be acknowledged. This study had a retrospective, observational, cross-sectional, and single-center design, which inherently limits causal inference and the generalizability of the findings. The relatively modest sample size may have limited the statistical power of the study, although it was comparable to previous CSF investigations. Waist circumference data were unavailable; therefore, formal diagnosis of metabolic syndrome could not be established. Although several metabolic components (fasting glucose, triglycerides, HDL-C, and hypertension) were available and considered in the analyses, residual confounding related to metabolic syndrome cannot be fully excluded. Potential confounders such as dietary habits, serum insulin, or medication use (e.g., diuretics, statins) that could influence uric acid or HDL levels were not assessed. Although recently initiated lipid-lowering therapy was an exclusion criterion, long-term stable statin use was allowed and may represent a potential residual confounder. A single measurement of laboratory parameters was relied on, and did not evaluate longitudinal outcomes such as recurrent angina or cardiovascular events. Thrombolysis in myocardial infarction frame counts were assessed by 2 blinded interventional cardiologists in consensus; since independent duplicate measurements were not performed, intra- and inter-observer variability could not be calculated. Furthermore, mechanistic assays to directly evaluate oxidative stress and endothelial dysfunction were not performed, and the observed associations remain observational. Finally, although the cohort was homogeneous and carefully selected, the results may not be generalizable to other populations without external validation.

From a mechanistic standpoint, the findings are consistent with contemporary evidence indicating that CSF represents a state of increased microvascular resistance, reflected by elevated cTFC, and is closely linked to systemic inflammation and endothelial dysfunction. Although recent analyses have shown that angiographic CSF is an imperfect surrogate for invasively measured CMD, the application of standardized imaging protocols and validated cTFC thresholds continues to support its role as a clinically relevant phenotype of microvascular disease.[28-31]Consistent with the findings, Lu et al demonstrated that endothelial dysfunction–related biomarkers are closely associated with coronary heart disease, supporting the biological plausibility of integrative indices such as the uric acid–to–HDL cholesterol ratio in coronary microvascular disorders.[32]

From a clinical perspective, UHR constitutes a readily available, low-cost composite biomarker integrating the prooxidant burden (uric acid) with diminished vasoprotective function (HDL-C). Large-scale, population-based cohorts have consistently demonstrated that higher UHR levels are associated with an increased incidence of cardiovascular disease, as well as with both all-cause and cardiovascular mortality, particularly among individuals with diabetes or prediabetes.[33,34] These converging data reinforce the observation that elevated UHR parallels the presence of CSF. They also provide a rationale for prospective investigations to determine whether UHR-guided risk stratification or longitudinal surveillance could improve outcomes in patients with suspected microvascular angina.

CONCLUSION

This study introduces UHR as a novel, simple, and easily accessible biomarker that is significantly associated with CSF. The moderate association between UHR and CSF highlights the intertwined role of low-grade inflammation and metabolic imbalance in the pathophysiology of slow coronary flow. Future multicenter and prospective studies are needed to validate these findings and to determine whether UHR may complement existing clinical risk models for risk stratification and treatment monitoring in patients with CSF.

Ethics Committee Approval: This study was approved by the Local Ethics Committee of Batman Training and Research Hospital (Approval No: 280118606,429; Date: June 26, 2025).

Informed Consent: Informed consent was waived by the institutional ethics committee due to the retrospective design of the study.

Peer-review: Externally peer-reviewed.

Data Availability: The data supporting the findings of this study are available from the corresponding author upon reasonable request.

Artificial Intelligence Disclosure: The authors declare that no artificial intelligence–assisted technologies were used in the preparation of this manuscript.

Author Contributions: Concept – R.A., E.E.; Design – R.A., E.E.; Supervision – R.A., E.İ.; Resources – R.A., E.E.; Materials – R.A., E.E.; Data Collection and/or Processing – R.A., E.E., Analysis and/or Interpretation – R.A., E.E.; Literature Search – R.A., E.E.; Writing – R.A.; Critical Review – R.A., E.İ.

Declaration of Interests: The authors have no conflicts of interest to declare.

Funding: The authors declare that this study received no financial support.

REFERENCES

1. Beltrame JF, Limaye SB, Horowitz JD. The coronary slow flow phenomenon: a new coronary microvascular disorder. *Cardiology*. 2002;97(4):197-202.[CrossRef].
2. Hawkins BM, Stavrakis S, Rousan TA, Abu-Fadel M, Schechter E. Coronary slow flow—prevalence and clinical correlations. *Circ J*. 2012;76(4):936-942. [CrossRef].
3. Wen ZG, Long JJ, Wang Y. Association between inflammatory burden index and coronary slow flow phenomenon in patients with chest pain and no obstructive coronary arteries. *BMC Cardiovasc Disord*. 2024;24(1):595.[CrossRef] .
4. Aparicio A, Cuevas J, Morís C, Martín M. Slow coronary blood flow: pathogenesis and clinical implications. *Eur Cardiol*. 2022;17:e08. [CrossRef].
5. Wang X, Nie SP. The coronary slow flow phenomenon: characteristics, mechanisms and implications. *Cardiovasc Diagn Ther*. 2011;1(1):37-43. [CrossRef].
6. Zhu Q, Wang S, Huang X, et al. Understanding the pathogenesis of coronary slow flow: recent advances. *Trends Cardiovasc Med*. 2024;34(3):137-144. [CrossRef].
7. Camsarl A, Pekdemir H, Cicek D, et al. Endothelin-1 and nitric oxide concentrations and their response to exercise in patients with slow coronary flow. *Circ J*. 2003;67(12):1022-1028. [CrossRef].
8. Feig DI, Kang DH, Johnson RJ. Uric acid and cardiovascular risk. *N Engl J Med*. 2008;359(17):1811-1821.[CrossRef].
9. Borghi C, Verardi FM, Pareo I, Bentivenga C, Cicero AFG. Hyperuricemia and cardiovascular disease risk. *Expert Rev Cardiovasc Ther*. 2014;12(10):1219-1225. [CrossRef].
10. Mineo C, Shaul PW. Novel biological functions of high-density lipoprotein cholesterol. *Circ Res*. 2012;111(8):1079-1090. [CrossRef].
11. Zhu X, Yin H, Han J, et al. Association between uric acid to HDL-C ratio and metabolic dysfunction–associated steatotic liver disease in type 2 diabetes mellitus: a cross-sectional study. *Diabetes Metab Syndr Obes*. 2025;18:1459-1466. [CrossRef].
12. Lai X, Chen T. Association of serum uric acid to high-density lipoprotein cholesterol ratio with all-cause and cardiovascular mortality in patients with diabetes or prediabetes: a prospective cohort study. *Front Endocrinol (Lausanne)*. 2024 ;15:1476336.[CrossRef].
13. Gibson CM, Cannon CP, Daley WL, et al. TIMI frame count: a quantitative method of assessing coronary artery flow. *Circulation*. 1996;93(5):879-888. [CrossRef].
14. Tambe AA, Demany MA, Zimmerman HA, Mascarenhas E. Angina pectoris and slow flow velocity of dye in coronary arteries: a new angiographic finding. *Am Heart J*. 1972;84(1):66-71. [CrossRef].
15. Li JJ, Qin XW, Li ZC, et al. Increased plasma C-reactive protein and interleukin-6 concentrations in patients with slow coronary flow. *Clin Chim Acta*. 2007;385(1-2):43-47. [CrossRef].
16. Pekdemir H, Cicek D, Camsari A, et al. The relationship between plasma endothelin-1, nitric oxide levels, and heart rate variability in patients with coronary slow flow. *Ann Noninvasive Electrocardiol*. 2004;9(1):24-33. [CrossRef].
17. Mangieri E, Macchiarelli G, Ciavolella M, et al. Slow coronary flow: clinical and histopathological features in patients with

otherwise normal epicardial coronary arteries. *Cathet Cardiovasc Diagn*. 1996;37(4):375-381. (doi:10.1002/(SICI)1097-0304(199604)37:4<375::AID-CCD7>3.0.CO;2-8).
18. Li JJ, Xu B, Li ZC, Qian J, Wei BQ. Is slow coronary flow associated with inflammation? *Med Hypotheses*. 2006;66(3):504-508. [CrossRef].
19. Kanbay M, Segal M, Afsar B, Kang DH, Rodriguez-Iturbe B, Johnson RJ. The role of uric acid in the pathogenesis of human cardiovascular disease. *Heart*. 2013;99(11):759-766. [CrossRef].
20. Barter PJ, Nicholls S, Rye KA, Anantharamaiah GM, Navab M, Fogelman AM. Antiinflammatory properties of HDL. *Circ Res*. 2004;95(8):764-772. [CrossRef].
21. Kalay N, Aytekin M, Kaya MG, et al. The relationship between inflammation and slow coronary flow: increased red cell distribution width and serum uric acid levels. *Turk Kardiyol Dern Ars*. 2011;39(6):463-468. [CrossRef].
22. Vairaperumal T, Tsai ZY, Liu PY. Emerging predictors by non-HDL-C/HDL-C ratio and novel biomarkers for coronary slow flow phenomenon. *Acta Cardiol Sin*. 2024;40(4):367-372. [CrossRef]
23. Zhou X, Xu J. Association between serum uric acid-to-high-density lipoprotein cholesterol ratio and insulin resistance in patients with type 2 diabetes mellitus. *J Diabetes Investig*. 2024;15(1):113-120. [CrossRef]
24. Yi Y, Luo Q, Chen J, et al. Association between the uric acid-to–HDL-cholesterol ratio (UHR) and the risk of cardiovascular disease and dyslipidemia: a population-based study. *Lipids Health Dis*. 2025;24(1):143. [CrossRef].
25. Wang H, Ba Y, Gao X, et al. Association between serum uric acid to high density lipoprotein-cholesterol ratio and arterial stiffness in a Japanese population. *Med (Baltim)*. 2023;102(31):e34182. [CrossRef].
26. Bayraktar MF. Correlation between uric acid/HDL ratio and total calcium score in coronary CT angiography. *Northwestern Med J*. 2024;4(1):22-26. [CrossRef].
27. Cui Y, Zhang W. Long-term cardiovascular risk and mortality associated with uric acid to HDL-C ratio: a 20-year cohort study in adults over 40. *Sci Rep*. 2025;15(1):14242. [CrossRef]
28. Sezgin AT, Sigirci A, Barutcu I, et al. Vascular endothelial function in patients with slow coronary flow. *Coron Artery Dis*. 2003;14(2):155-161. [CrossRef]
29. Fineschi M, Bravi A, Gori T. The "slow coronary flow" phenomenon: evidence of preserved coronary flow reserve despite increased resting microvascular resistances. *Int J Cardiol*. 2008 July 21;127(3):358-361. [CrossRef]
30. Taqueti VR, Di Carli MF. Coronary microvascular disease pathogenic mechanisms and therapeutic options: JACC state-of-the-art review. *J Am Coll Cardiol*. 2018;72(21):2625-2641. [CrossRef].
31. Ong P, Camici PG, Beltrame JF, et al. International standardization of diagnostic criteria for microvascular angina. *Int J Cardiol*. 2018;250:16-20. [CrossRef].
32. Lu H, Xu L, Chen H, et al. Correlation between serum microRNA-18a level and endothelial function and prognosis in female coronary heart disease patients. *Anatol J Cardiol*. 2024;28(7):345-352. [CrossRef].
33. Huang X, Hu L, Li J, Wang X. U-shaped association of uric acid to HDL cholesterol ratio (UHR) with ALL-cause and cardiovascular mortality in diabetic patients: NHANES 1999-2018. *BMC Cardiovasc Disord*. 2024;24(1):744. [CrossRef] .
34. Kuwabara M, Borghi C, Cicero AFG, et al. Elevated serum uric acid increases risks for developing high LDL cholesterol and hypertriglyceridemia: A five-year cohort study in Japan . *Int J Cardiol*. 2018;261:183-188. [CrossRef]

THE ANATOLIAN JOURNAL OF CARDIOLOGY

Official journal of the TURKISH SOCIETY OF CARDIOLOGY

A Comparative Study of Cardiovascular Risk Calculation Systems and the New PREVENT Model

ABSTRACT

Background: Cardiovascular diseases (CVD) are a largely preventable cause of death worldwide. There are many risk factors that influence CVD, some of which are modifiable and others non-modifiable. Several systems, such as the widely used Framingham, Reynolds, and the most recently developed Predicting Risk of Cardiovascular Disease EVENTs (PREVENT), are used to calculate an individual's CVD risk based on the effects of these risk factors.

Methods: This study compared CVD risk scores calculated using the Framingham, Reynolds, and PREVENT systems. The risk factors common to these 3 systems were determined to be age, gender, smoking status, high-density lipoprotein cholesterol, total cholesterol, and systolic blood pressure, and the effects of these risk factors on CVD risk were evaluated. The numerical risk scores obtained because of the effects of risk factors were presented comparatively in tables created based on gender and smoking status.

Results: According to the results obtained, it was observed that the PREVENT system provides more individualized results by including renal, metabolic, and social markers in the calculation and provides a more detailed assessment by also considering the age of risk.

Conclusion: These features may enable PREVENT to classify both low- and high-risk patients more clearly. This classification of patients may contribute to changing the course of CVD, a major global disease, by enabling appropriate interventions and treatments.

Keywords: Cardiovascular disease, Framingham heart study, PREVENT model, Reynolds risk score, risk assessment

ORIGINAL INVESTIGATION

INTRODUCTION

According to the World Health Organization, non-communicable diseases (NCDs) cause 74% of deaths globally. The majority of NCDs are caused by a group of diseases called cardiovascular diseases (CVDs).[1] Cardiovascular diseases include rheumatic heart disease, myocarditis, endocarditis, hypertensive heart disease, pulmonary arterial hypertension, aortic aneurysm, and many other conditions in which the heart and blood vessels are damaged.[2,3]

Cardiovascular disease is largely preventable, and modifiable risk factors include smoking, alcohol consumption, obesity, low physical activity, and high body mass index (BMI). Non-modifiable factors include environmental factors such as air pollution, metal exposure, and genetic factors. In addition, metabolic and behavioral risk factors such as high systolic blood pressure (SBP) and secondhand smoke exposure also play important roles in the development of CVD.[2,4] Considering the global morbidity and mortality rates of CVD, interventions targeting risk factors are critically important for preventing the development of the disease (primary prevention) and for preventing recurrence by improving risk factors in existing patients (secondary prevention). These interventions also play a major role in prolonging survival time and improving quality of life.[5,6]

For the identification of risk factors and the resulting CVD due to their combination, disease risk can be estimated based on age, gender, and the number and

Copyright@Author(s) - Available online at anatoljcardiol.com.
Content of this journal is licensed under a Creative Commons Attribution-NonCommercial 4.0 International License.

Yasemin Atıcı[1]
Makbule Beyza Şen[2]
Doğan Yücel[1]

[1]*Department of Medical Biochemistry, Faculty of Medicine, Lokman Hekim University, Ankara, Türkiye*
[2]*Department of Biochemistry, Faculty of Pharmacy, Lokman Hekim University, Ankara, Türkiye*

Corresponding author:
Yasemin Atıcı
✉ yasemin.atici@lokmanhekim.edu.tr

Received: November 28, 2025
Accepted: March 27, 2026
Available Online Date: July 21, 2026

Cite this article as: Atıcı Y, Şen MB, Yücel D. A comparative study of cardiovascular risk calculation systems and the new PREVENT model. *Anatol J Cardiol.* 2026;30(10):668-683.

DOI: 10.14744/AnatolJCardiol.2026.6049

severity of risk factors. These estimations enable the development of preventive treatment strategies for low-risk individuals, early diagnosis, appropriate treatment, and urgent interventions for high-risk individuals. In this way, more targeted and effective measures can be taken to protect individual health.[7]

To calculate CVD risk, various risk prediction models are available that assess the combined effect of one or more modifiable and/or non-modifiable risk factors. Examples of these systems include the Framingham Heart Study, PROCAM, SCORE,[8] ASSIGN,[9] Reynolds,[10,11] QRISK,[12] PREVENT.[13] These systems are used to predict an individual's risk of CVD. Age, gender, and smoking status are among the common risk factors included in these systems. These factors are considered fundamental elements for calculating and predicting CVD risk. Over time, additional factors such as SBP, total cholesterol (TC), high-density lipoprotein cholesterol (HDL-C), BMI, left ventricular hypertrophy, diabetes mellitus (DM), family history (FH), use of antihypertensive medications, use of lipid-lowering medications, low-density lipoprotein cholesterol (LDL-C), hemoglobin A1c (HbA1c) levels, high-sensitivity C-reactive protein (hsCRP), a FH of premature coronary heart disease, and social deprivation have also been incorporated. These additional factors contribute to predicting the CVD risk score.[14,15]

The first cohort of the Framingham study was initiated in 1948 with 5209 participants aged 30-62 years, and it was later followed by 5 additional cohorts.[16] This study identified risk factors contributing to CVD, investigated their effects, and introduced the term "risk factors for CVD."[17] As a result of the Framingham study, major cardiovascular risk factors were identified, and their effects on the disease were extensively investigated.[16,18]

The Reynolds system was developed in 2007 to estimate the risk of CVD, diabetes, and cancer in women, with approximately 24 500 female participants over 45 years of age, initially without health problems.[10] The system was also used to calculate the risk score in US male participants aged 50 years and older who were free of CVD, diabetes, and cancer.[11]

The most recently developed PREVENT study, conducted between 1992 and 2017, included approximately 6.6 million individuals aged 30-79 without known CVD and 46 different data sets. The PREVENT study is gender-specific and race-independent, offering high discrimination power and calibration ability across various patient groups. Additionally, it allows the predicted risk score for CVD subtypes to be estimated based on specified parameters and simulation scenarios.[13]

The aim of this study is to calculate CVD risk using the widely applied Framingham and Reynolds risk prediction systems, as well as the most recently developed PREVENT system. The study also aims to compare the output and classifications of estimated risk score results for different patient populations, taking into account the effects of modifiable and non-modifiable risk factors for each system. Calculations were performed taking into account risk factors common to all 3 systems.

HIGHLIGHTS

- Systems like Framingham, Reynolds, and Predicting Risk of Cardiovascular Disease EVENTs are available to calculate cardiovascular diseases (CVD) risk.
- Predicting Risk of Cardiovascular Disease EVENTs offers detailed assessment and classification capabilities for 10- and 30-year periods.
- Predicting Risk of Cardiovascular Disease EVENTs also evaluates the calculated "risk age," offering more individualized results.
- Predicting Risk of Cardiovascular Disease EVENTs can contribute to altering the course of CVD through clear classification.

METHODS

This study was designed as a simulation to evaluate CVD risk score results. First, common and non-common risk factors used to calculate CVD risk in all 3 systems were identified. Based on these factors, scenarios representing different risk levels were created, and the final impact of these risk factors on CVD risk was systematically analyzed. In this study, CVD risk was calculated using the Framingham, Reynolds, and PREVENT risk prediction systems, and the results obtained by each system were compared. To compare the 3 systems, 2 separate tables containing common values for women and men were prepared, and each table was organized to include 2 sub-tables covering smokers and non-smokers.

The risk factors common to all 3 CVD risk calculation systems (gender, age, smoking status, SBP, TC, and HDL-C) have been identified, and the following ranges have been established for these parameters: age (30-75 years), SBP (90-160 mmHg), TC (130-320 mg/dL), and HDL-C (20-100 mg/dL) have been defined for these parameters. In addition to the risk factors common to the Framingham, Reynolds, and PREVENT systems, each system also includes non-common risk factors that affect the calculation results. The non-common risk factors are: vascular disease (VD), DM, and antihypertensive medication use (AntiHT) in the Framingham system; hsCRP factor in the Reynolds system, and BMI, estimated glomerular filtration rate (eGFR), DM, AntiHT, lipid-lowering drugs, urine albumin/creatinine ratio (uACR), and HbA1c in the PREVENT system, which is the most comprehensive system. To prevent these factors from affecting the risk score results in different systems and to enable a more transparent comparison, reference values for healthy individuals were taken into account. In the Reynolds system, the hsCRP level (0.7 mg/L) was entered, while in the PREVENT system, BMI (22 kg/m^2) and eGFR (95 mL/min/1.73 m^2) values were entered, and other non-common risk factors were not included in the calculations.

To calculate your 10-year CVD/ASCVD risk, use the Framingham risk score calculator https://reference.medscape.com/calculator/252/framingham-risk-score-2008, the Reynolds risk score calculator https://www.scymed.com/

en/smnxph/phqgg440.htm and the PREVENT risk score calculator https://professional.heart.org/en/guidelines-and-statements/prevent-calculator.

The risk score was obtained by simulating the 6 jointly determined risk factor values, where the numerical values assigned to each relevant field in each system were entered individually. Each risk score result in the tables has different risk factor values. The systems used are automated systems, and the results obtained by entering each risk factor (parameter) value individually into the systems in the form of numerical values determined for that factor in the tables were used to create the tables. The systems automatically calculate risk scores, provide a numerical risk score result, and interpret these results. The risk score result in each cell of the tables and the total risk profile emerging according to that system are presented, enabling comparison between systems. The cumulative effect of all risk factors common to the tables is presented simultaneously and transparently.

The systems used are automated tools that perform mathematical calculations based on manually entered risk factor parameter values. In this study, the scenarios were designed using combinations of risk factor values, and each parameter value was manually entered into the systems individually. For women and men separately, 720 scenarios were generated for each system, and considering all 3 systems together, a total of 4320 scenarios were obtained.

The 10-year CVD risk score results obtained by comparing the Reynolds, PREVENT, and Framingham systems (ASCVD - atherosclerotic CVD for PREVENT) are interpreted differently by each system. To avoid confusion in the tables, these interpretations are shown in different colors. In the Framingham system, patients with a risk score <10% are classified as low risk, those between 10% and 20% as moderate risk, and those above 20% as high risk. This classification is presented in Framingham tables with low risk in blue, moderate risk in yellow, and high risk in red. The Reynolds system classifies risk scores as normal (<10%) or abnormal (>10%). This classification is presented in the Reynolds system tables with normal scores in blue and abnormal scores in red. The PREVENT system uses percentage ranges to classify risk: <5% is low risk, 5%-7.4% is borderline risk, 7.5%-19.9% is moderate risk, and ≥20% is high risk. In this classification, low risk is blue, borderline risk is yellow, moderate risk is orange, and high risk is red in the PREVENT tables.

Statistical Analysis

This study has a simulation-based comparative design and does not rely on empirical data analysis. Therefore, inferential statistical methods and hypothesis testing were not applied. Scores for the Framingham, Reynolds, and PREVENT risk models were calculated using standardized input parameters, and the results were evaluated descriptively. Differences between the models were compared using absolute values and relative changes, and discrepancies between risk classifications were analyzed. All calculations were performed using the official web-based tools of the respective models; no additional statistical software was used. Data organization and comparative evaluation were carried out using Microsoft Excel 365, version 2602 (Microsoft Corp., Redmond, WA, USA). This approach is consistent with simulation-based comparative studies focusing on model output evaluation rather than statistical inference.

RESULTS

Examination of Risk Scores in Women

Results of the Framingham Risk Scoring System

According to the Framingham CVD risk calculation system, low risk is represented by blue, moderate risk by yellow, and high risk by red (Table 1). Based on the obtained data, moderate- and high-risk levels were detected at certain ages in women who smoke. In smoking women, a moderate risk (10%) was observed at age 35 years and a high risk (21.5%) at age 50 years, given specific HDL-C, TC, and SBP values. Similarly, in non-smoking women, a 45-year-old with an HDL-C value of 100 mg/dL, TC value of 280 mg/dL, and SBP of 160 mm Hg, her risk score is 10.0%, indicating moderate risk. Additionally, a 65-year-old woman who does not smoke, with the same biochemical values, was observed to have a high-risk situation, with a risk score of 21.5%.

Results of the Reynolds Risk Scoring System

In the Reynolds CVD risk calculation system, blue represents normal values, and red represents abnormal values (Table 2). According to the obtained data, among women who smoke, a 60-year-old with an HDL-C value of 35 mg/dL, a TC of 320 mg/dL, and SBP of 120 mmHg showed abnormal biochemical values. In this case, the risk score was calculated as 10.1%.

Similarly, among non-smoking women, a 70-year-old with an HDL-C value of 50 mg/dL, TC of 320 mg/dL, and SBP of 150 mmHg also showed abnormal biochemical values. In this case, the risk score was calculated as 10.6%.

Results of the PREVENT Risk Scoring System

In the PREVENT ASCVD risk calculation system, low risk is represented by blue, borderline risk by yellow, and moderate risk by orange (Table 3).

According to the results obtained, among women who smoke, the PREVENT ASCVD risk calculation system first showed borderline risk at age 50. At this age, the woman with an HDL-C value of 20 mg/dL, a TC value of 320 mg/dL, and an SBP value of 90 mm Hg had a risk score of 5.0%. Later, at the age of 65, moderate risk was encountered, with a woman having an HDL-C value of 35 mg/dL, a TC value of 280 mg/dL, and an SBP value of 120 mm Hg, resulting in a risk score of 7.5%.

Among non-smoking women, borderline risk was observed at age 65. At this age, the woman with an HDL-C value of 60 mg/dL, TC of 200 mg/dL, and SBP of 150 mm Hg had a risk score of 5.0%. Additionally, at the age of 70, another woman with an HDL-C value of 20 mg/dL, TC of 280 mg/dL, and SBP of 90 mm Hg showed moderate risk, with a calculated risk score of 7.6% (Table 3).

Table 1. Effect of Smoking on Framingham Risk Score Outcomes in Women

Female													
HDL-C (mg/dL)	Smoking (%) Framingham						Age (years)	No Smoking (%) Framingham						SBP (mm Hg)
100	21.5	24.8	>30	>30	>30	>30	75	13.7	15.9	21.5	24.8	28.5	28.5	160
60	18.5	21.5	28.5	>30	>30	>30		11.7	13.7	18.5	21.5	24.8	24.8	150
50	15.9	18.5	24.8	28.5	>30	>30		10.0	11.7	15.9	18.5	21.5	21.5	140
45	15.9	18.5	24.8	28.5	>30	>30		10.0	11.7	15.9	18.5	21.5	21.5	130
35	15.9	18.5	24.8	28.5	>30	>30		10.0	11.7	15.9	18.5	21.5	21.5	120
20	11.7	13.7	18.5	21.5	24.8	24.8		7.3	8.6	11.7	13.7	15.9	15.9	90
100	18.5	21.5	28.5	>30	>30	>30	70	11.7	13.7	18.5	21.5	24.8	24.8	160
60	15.9	18.5	24.8	28.5	>30	>30		10.0	11.7	15.9	18.5	21.5	21.5	150
50	13.7	15.9	21.5	24.8	28.5	28.5		8.6	10.0	13.7	15.9	18.5	18.5	140
45	13.7	15.9	21.5	24.8	28.5	28.5		8.6	10.0	13.7	15.9	18.5	18.5	130
35	13.7	15.9	21.5	24.8	28.5	28.5		8.6	10.0	13.7	15.9	18.5	18.5	120
20	10.0	11.7	15.9	18.5	21.5	21.5		6.3	7.3	10.0	11.7	13.7	13.7	90
100	15.9	18.5	24.8	28.5	>30	>30	65	10.0	11.7	15.9	18.5	21.5	21.5	160
60	13.7	15.9	21.5	24.8	28.5	28.5		8.6	10.0	13.7	15.9	18.5	18.5	150
50	11.7	13.7	18.5	21.5	24.8	24.8		7.3	8.6	11.7	13.7	15.9	15.9	140
45	11.7	13.7	18.5	21.5	24.8	24.8		7.3	8.6	11.7	13.7	15.9	15.9	130
35	11.7	13.7	18.5	21.5	24.8	24.8		7.3	8.6	11.7	13.7	15.9	15.9	120
20	8.6	10.0	13.7	15.9	18.5	18.5		5.3	6.3	8.6	10.0	11.7	11.7	90
100	13.7	15.9	21.5	24.8	28.5	28.5	60	8.6	10.0	13.7	15.9	18.5	18.5	160
60	11.7	13.7	18.5	21.5	24.8	24.8		7.3	8.6	11.7	13.7	15.9	15.9	150
50	10.0	11.7	15.9	18.5	21.5	21.5		6.3	7.3	10.0	11.7	13.7	13.7	140
45	10.0	11.7	15.9	18.5	21.5	21.5		6.3	7.3	10.0	11.7	13.7	13.7	130
35	10.0	11.7	15.9	18.5	21.5	21.5		6.3	7.3	10.0	11.7	13.7	13.7	120
20	7.3	8.6	11.7	13.7	15.9	15.9		4.5	5.3	7.3	8.6	10.0	10.0	90
100	11.7	13.7	18.5	21.5	24.8	24.8	55	7.3	8.6	11.7	13.7	15.9	15.9	160
60	10.0	11.7	15.9	18.5	21.5	21.5		6.3	7.3	10.0	11.7	13.7	13.7	150
50	8.6	10.0	13.7	15.9	18.5	18.5		5.3	6.3	8.6	10.0	11.7	11.7	140
45	8.6	10.0	13.7	15.9	18.5	18.5		5.3	6.3	8.6	10.0	11.7	11.7	130
35	8.6	10.0	13.7	15.9	18.5	18.5		5.3	6.3	8.6	10.0	11.7	11.7	120
20	6.3	7.3	10.0	11.7	13.7	13.7		3.9	4.5	6.3	7.3	8.6	8.6	90
100	10.0	11.7	15.9	18.5	21.5	21.5	50	6.3	7.3	10.0	11.7	13.7	13.7	160
60	8.6	10.0	13.7	15.9	18.5	18.5		5.3	6.3	8.6	10.0	11.7	11.7	150
50	7.3	8.6	11.7	13.7	15.9	15.9		4.5	5.3	7.3	8.6	10.0	10.0	140
45	7.3	8.6	11.7	13.7	15.9	15.9		4.5	5.3	7.3	8.6	10.0	10.0	130
35	7.3	8.6	11.7	13.7	15.9	15.9		4.5	5.3	7.3	8.6	10.0	10.0	120
20	5.3	6.3	8.6	10.0	11.7	11.7		3.3	3.9	5.3	6.3	7.3	7.3	90
100	7.3	8.6	11.7	13.7	15.9	15.9	45	4.5	5.3	7.3	8.6	10.0	10.0	160
60	6.3	7.3	10.0	11.7	13.7	13.7		3.9	4.5	6.3	7.3	8.6	8.6	150
50	5.3	6.3	8.6	10.0	11.7	11.7		3.3	3.9	5.3	6.3	7.3	7.3	140
45	5.3	6.3	8.6	10.0	11.7	11.7		3.3	3.9	5.3	6.3	7.3	7.3	130
35	5.3	6.3	8.6	10.0	11.7	11.7		3.3	3.9	5.3	6.3	7.3	7.3	120
20	3.9	4.5	6.3	7.3	8.6	8.6		2.4	2.8	3.9	4.5	5.3	5.3	90

(*Continued*)

Table 1. Effect of Smoking on Framingham Risk Score Outcomes in Women (*Continued*)

	Female												
HDL-C (mg/dL)	Smoking (%) Framingham						Age (years)	No Smoking (%) Framingham						SBP (mm Hg)
100	6.3	7.3	10.0	11.7	13.7	13.7	40	3.9	4.5	6.3	7.3	8.6	8.6	160
60	5.3	6.3	8.6	10.0	11.7	11.7		3.3	3.9	5.3	6.3	7.3	7.3	150
50	4.5	5.3	7.3	8.6	10.0	10.0		2.8	3.3	4.5	5.3	6.3	6.3	140
45	4.5	5.3	7.3	8.6	10.0	10.0		2.8	3.3	4.5	5.3	6.3	6.3	130
35	4.5	5.3	7.3	8.6	10.0	10.0		2.8	3.3	4.5	5.3	6.3	6.3	120
20	3.3	3.9	5.3	6.3	7.3	7.3		2.0	2.4	3.3	3.9	4.5	4.5	90
100	4.5	5.3	7.3	8.6	10.0	10.0	35	2.8	3.3	4.5	5.3	6.3	6.3	160
60	3.9	4.5	6.3	7.3	8.6	8.6		2.4	2.8	3.9	4.5	5.3	5.3	150
50	3.3	3.9	5.3	6.3	7.3	7.3		2.0	2.4	3.3	3.9	4.5	4.5	140
45	3.3	3.9	5.3	6.3	7.3	7.3		2.0	2.4	3.3	3.9	4.5	4.5	130
35	3.3	3.9	5.3	6.3	7.3	7.3		2.0	2.4	3.3	3.9	4.5	4.5	120
20	2.4	2.8	3.9	4.5	5.3	5.3		1.5	1.7	2.4	2.8	3.3	3.3	90
100	3.3	3.9	5.3	6.3	7.3	7.3	30	2.0	2.4	3.3	3.9	4.5	4.5	160
60	2.8	3.3	4.5	5.3	6.3	6.3		1.7	2.0	2.8	3.3	3.9	3.9	150
50	2.4	2.8	3.9	4.5	5.3	5.3		1.5	1.7	2.4	2.8	3.3	3.3	140
45	2.4	2.8	3.9	4.5	5.3	5.3		1.5	1.7	2.4	2.8	3.3	3.3	130
35	2.4	2.8	3.9	4.5	5.3	5.3		1.5	1.7	2.4	2.8	3.3	3.3	120
20	1.7	2.0	2.8	3.3	3.9	3.9		1.0	1.2	1.7	2.0	2.4	2.4	90
	130	160	200	240	280	320		130	160	200	240	280	320	
	Total cholesterol (mg/dL)							Total cholesterol (mg/dL)						

According to the Framingham system, in women aged 30-75 years, smoking (left) and no smoking (right), HDL-C (100, 60, 50, 45, 35, 20 mg/dL), TC (130, 160, 200, 240, 280, 320 mg/dL), and SBP (160, 150, 140, 130, 120, 90) parameters for women who smoke between the ages of 30 and 75 are presented. In the Framingham system, those with a risk score <10% are classified as low risk (blue color in the table), those with a score of 10%-20% are classified as moderate risk (yellow color in the table), and those with a score >20% are classified as high risk (red color in the table).
HDL-C, high-density lipoprotein cholesterol; SBP, systolic blood pressure; TC, total cholesterol.

Examination of Risk Scores in Men

Results of the Framingham Risk Scoring System

According to the Framingham CVD risk calculation system, moderate risk was first encountered at the age of 35 in men who smoke. At this age, individuals with an HDL-C value of 35 mg/dL, TC of 280 mg/dL, and SBP of 120 mm Hg had a risk score of 11.2%. High risk was first encountered at age 45, with the same biochemical parameters, and the individual's risk score was 21.6%.

Among men who do not smoke, moderate risk was first encountered at the age of 45. At this age, individuals with an HDL-C value of 35 mg/dL, a TC value of 280 mg/dL, and an SBP value of 120 mm Hg had a risk score of 11.2%. High risk was first encountered at the age of 55, with the same biochemical parameters, and the risk score was 21.6% (Table 4).

Results of the Reynolds Risk Scoring System

According to the Reynolds CVD risk calculation system, in men who smoke, abnormal biochemical values were first encountered at age 55. At this age, individuals with an HDL-C value of 35 mg/dL, TC of 280 mg/dL, and SBP of 120 mm Hg had a risk score of 10.2% (Table 5).

Among men who do not smoke, abnormal values were first encountered at the age of 60. At this age, individuals with an HDL-C of 45 mg/dL, TC of 280 mg/dL, and SBP of 130 mm Hg had a risk score of 10.1% (Table 5).

Results of the PREVENT Risk Scoring System

According to the PREVENT ASCVD risk calculation system, in men who smoke, borderline risk was first encountered at age 40. At this age, the individual with an HDL-C of 20 mg/dL, TC of 320 mg/dL, and SBP of 90 mm Hg had a risk score of 5.1%. Moderate risk was first encountered at age 50 with the same biochemical parameters, and the risk score was 8.3%. High risk was first encountered at age 70, with a risk score of 20.2%.

Among those who do not smoke, borderline risk was first encountered at age 50. At this age, the individual with an HDL-C of 20 mg/dL, TC of 320 mg/dL, and SBP of 90 mm Hg had a risk score of 5.5%. Moderate risk was first encountered at age 60, with an HDL-C of 50 mg/dL, TC of 320 mg/dL, and SBP of 140 mm Hg, resulting in a risk score of 7.7%. High risk was encountered at age 70, with a risk score of 21.2% (Table 6).

Table 2. Effect of Smoking on Reynolds Risk Score Outcomes in Women

	Female												
HDL-C (mg/dL)	Smoking (%) Reynolds						Age (years)	No Smoking (%) Reynolds						SBP (mm Hg)
100	7.8	9.3	12.4	15.7	19.1	22.4	75	3.5	4.2	5.7	7.3	8.9	10.6	160
60	11.4	13.5	17.9	22.4	27	31.5		5.2	6.2	8.3	10.6	12.9	15.4	150
50	11.3	13.5	17.9	22.4	26.9	31.4		5.2	6.2	8.3	10.6	12.9	15.3	140
45	10.2	12.2	16.2	20.3	24.5	28.7		4.6	5.6	7.5	9.5	11.7	13.9	130
35	10.6	12.7	16.8	21.1	25.4	29.7		4.8	5.8	7.8	9.9	12.1	14.4	120
20	8.5	10.1	13.5	17.0	20.6	24.3		3.8	4.6	6.2	7.9	9.7	11.5	90
100	5.3	6.3	8.5	10.8	13.2	15.7	70	2.4	2.8	3.9	4.9	6.1	7.2	160
60	7.8	9.3	12.4	15.7	0.19	22.4		3.5	4.2	5.7	7.2	8.9	10.6	150
50	7.7	9.2	12.4	15.6	18.9	22.3		3.5	4.2	5.7	7.2	8.9	10.6	140
45	7.0	8.3	11.2	14.1	17.2	20.3		3.1	3.8	5.1	6.5	8.0	9.5	130
35	7.3	8.7	11.6	14.7	17.9	21.1		3.3	3.9	5.3	6.8	8.3	9.9	120
20	5.8	6.9	9.3	11.8	14.4	17		2.6	3.1	4.2	5.4	6.6	7.9	90
100	3.6	4.3	5.8	7.4	9.1	10.8	65	1.6	1.9	2.6	3.3	4.1	4.9	160
60	5.3	6.3	8.5	10.8	13.2	15.6		2.4	2.8	3.8	4.9	6.0	7.2	150
50	5.3	6.3	8.5	10.8	13.1	15.6		2.4	2.8	3.8	4.9	6.0	7.2	140
45	4.7	5.7	7.6	9.7	11.9	14.1		2.1	2.5	3.4	4.4	5.4	6.5	130
35	4.9	5.9	8.0	10.1	12.4	14.7		2.2	2.7	3.6	4.6	5.7	6.8	120
20	3.9	4.7	6.3	8.1	9.9	11.8		1.7	2.1	2.8	3.6	4.5	5.4	90
100	2.4	2.9	3.9	5.0	6.2	7.4	60	1.1	1.3	1.8	2.2	2.8	3.3	160
60	3.6	4.3	5.8	7.4	9.0	10.8		1.6	1.9	2.6	3.3	4.1	4.9	150
50	3.6	4.3	5.8	7.4	9.0	10.7		1.6	1.9	2.6	3.3	4.1	4.9	140
45	3.2	3.8	5.2	6.6	8.1	9.7		1.4	1.7	2.3	3.0	3.7	4.4	130
35	3.3	4.0	5.4	6.9	8.5	10.1		1.5	1.8	2.4	3.1	3.8	4.6	120
20	2.6	3.2	4.3	5.5	6.7	8.0		1.2	1.4	1.9	2.5	3.0	3.6	90
100	1.6	2.0	2.6	3.4	4.2	5.0	55	0.7	0.9	1.2	1.5	1.9	2.2	160
60	2.4	2.9	3.9	5.0	6.2	7.4		1.1	1.3	1.7	2.2	2.8	3.3	150
50	2.4	2.9	3.9	5.0	6.1	7.3		1.1	1.3	1.7	2.2	2.8	3.3	140
45	2.2	2.6	3.5	4.5	5.5	6.6		1.0	1.2	1.6	2.0	2.5	3.0	130
35	2.3	2.7	3.7	4.7	5.8	6.9		1.0	1.2	1.6	2.1	2.6	3.1	120
20	1.8	2.1	2.9	3.7	4.6	5.5		0.8	0.9	1.3	1.7	2.0	2.5	90
100	1.1	1.3	1.8	2.3	2.8	3.4	50	0.5	0.6	0.8	1.0	1.3	1.5	160
60	1.6	1.9	2.6	3.4	4.2	5.0		0.7	0.9	1.2	1.5	1.9	2.2	150
50	1.6	1.9	2.6	3.4	4.2	5.0		0.7	0.9	1.2	1.5	1.9	2.2	140
45	1.5	1.7	2.4	3.0	3.7	4.5		0.6	0.8	1.1	1.3	1.7	2.0	130
35	1.5	1.8	2.5	3.2	3.9	4.7		0.7	0.8	1.1	1.4	1.7	2.1	120
20	1.2	1.4	2.0	2.5	3.1	3.7		0.5	0.6	0.9	1.1	1.4	1.7	90
100	0.7	0.9	1.2	1.5	1.9	2.3	45	0.3	0.4	0.5	0.7	0.8	1.0	160
60	1.1	1.3	1.8	2.3	2.8	3.4		0.5	0.6	0.8	1.0	1.3	1.5	150
50	1.1	1.3	1.8	2.3	2.8	3.4		0.5	0.6	0.8	1.0	1.2	1.5	140
45	1.0	1.2	1.6	2.0	2.5	3.0		0.4	0.5	0.7	0.9	1.1	1.3	130
35	1.0	1.2	1.7	2.1	2.6	3.2		0.5	0.5	0.7	0.9	1.2	1.4	120
20	0.8	1.0	1.3	1.7	2.1	2.5		0.4	0.4	0.6	0.7	0.9	1.1	90

(*Continued*)

Table 2. Effect of Smoking on Reynolds Risk Score Outcomes in Women (*Continued*)

	Female													
HDL-C (mg/dL)	Smoking (%) Reynolds						Age (years)	No Smoking (%) Reynolds						SBP (mm Hg)
100	0.7	0.9	1.2	1.5	1.9	2.3	40	0.3	0.4	0.5	0.7	0.8	1.0	160
60	1.1	1.3	1.8	2.3	2.8	3.4		0.5	0.6	0.8	1.0	1.3	1.5	150
50	1.1	1.3	1.8	2.3	2.8	3.4		0.5	0.6	0.8	1.0	1.2	1.5	140
45	1.0	1.2	1.6	2.0	2.5	3.0		0.4	0.5	0.7	0.9	1.1	1.3	130
35	1.0	1.2	1.7	2.1	2.6	3.2		0.5	0.5	0.7	0.9	1.2	1.4	120
20	0.8	1.0	1.3	1.7	2.1	2.5		0.4	0.4	0.6	0.7	0.9	1.1	90
100	0.7	0.9	1.2	1.5	1.9	2.3	35	0.3	0.4	0.5	0.7	0.8	1.0	160
60	1.1	1.3	1.8	2.3	2.8	3.4		0.5	0.6	0.8	1.0	1.3	1.5	150
50	1.1	1.3	1.8	2.3	2.8	3.4		0.5	0.6	0.8	1.0	1.2	1.5	140
45	1.0	1.2	1.6	2.0	2.5	3.0		0.4	0.5	0.7	0.9	1.1	1.3	130
35	1.0	1.2	1.7	2.1	2.6	3.2		0.5	0.5	0.7	0.9	1.2	1.4	120
20	0.8	1.0	1.3	1.7	2.1	2.5		0.4	0.4	0.6	0.7	0.9	1.1	90
100	0.7	0.9	1.2	1.5	1.9	2.3	30	0.3	0.4	0.5	0.7	0.8	1.0	160
60	1.1	1.3	1.8	2.3	2.8	3.4		0.5	0.6	0.8	1.0	1.3	1.5	150
50	1.1	1.3	1.8	2.3	2.8	3.4		0.5	0.6	0.8	1.0	1.2	1.5	140
45	1.0	1.2	1.6	2.0	2.5	3.0		0.4	0.5	0.7	0.9	1.1	1.3	130
35	1.0	1.2	1.7	2.1	2.6	3.2		0.5	0.5	0.7	0.9	1.2	1.4	120
20	0.8	1.0	1.3	1.7	2.1	2.5		0.4	0.4	0.6	0.7	0.9	1.1	90
	130	160	200	240	280	320		130	160	200	240	280	320	
	Total cholesterol (mg/dL)							Total cholesterol (mg/dL)						

According to the Reynolds system, in women, smoking (left) and no smoking (right), between the ages of 30 and 75, HDL-C (100, 60, 50, 45, 35, 20 mg/dL), TC (130, 160, 200, 240, 280, 320 mg/dL), and SBP (160, 150, 140, 130, 120, 90) parameters for women aged 30-75 are presented. The Reynolds system classifies risk scores as normal (blue color in the table) if <10% and abnormal (red color in the table) if >10%.
HDL-C, high-density lipoprotein cholesterol; SBP, systolic blood pressure; TC, total cholesterol.

DISCUSSION

In this study, a simulation was performed to compare CVD risk scores using the widely applied Framingham and Reynolds systems, as well as more recently developed PREVENT system. The effects of age, gender, smoking status, HDL-C, TC, and SBP on CVD risk were examined. The findings indicated that advancing age, male gender, smoking, low HDL-C, high TC, and elevated SBP all increased risk. When comparing the systems, it was observed that the Framingham system limits detailed risk differentiation because all values above 30% are grouped into a single "high-risk" category. The Reynolds system classifies risk only as "normal" or "abnormal" and generally produces the same risk score for individuals under 50 years of age. In contrast, the PREVENT system offers both 10- and 30-year risk estimates and calculates an individual's "risk age," allowing for a more detailed assessment.

This study, conducted using systems that estimate the 10-year CVD-ASCVD risk, presents the impact of these identified risk factors on CVD from a broad perspective.

The findings demonstrate that the effects of risk factors on CVD can vary according to different age groups and genders, emphasizing the importance of developing personalized approaches in risk calculation systems. For instance, the impact of smoking varies depending on gender and age, indicating that risk assessments should be made more precise by considering individual health histories.

The data indicated that within the Framingham CVD risk calculation system, when the same biochemical parameters are considered, the levels of moderate and high CVD risk are greater in men than in women across all age groups. Among both smokers and non-smokers with identical parameter values, although the age at which moderate risk first appears is similar between men and women, the risk scores are observed to be higher in men. Many age and parameter values that are classified as low or moderate risk for women fall into the moderate or high-risk categories for men. These findings indicate that gender is a significant factor affecting CVD risk and that men encounter high-risk levels at earlier ages.

In the Reynolds CVD risk calculation system, similar to the Framingham system, abnormal risk scores are higher in men than in women. Abnormal CVD risk is observed at younger ages in men compared to women. Age and parameter values that are considered low/moderate risk for women may fall into the moderate/high-risk categories for men. This finding suggests that men begin to experience CVD risk at earlier ages, indicating that earlier intervention may be required.

Table 3. Effect of Smoking on PREVENT Risk Score Results in Women

	Female												
HDL-C (mg/dL)	Smoking (%) PREVENT						Age (years)	No Smoking (%) PREVENT						SBP (mm Hg)
100	9.8	9.8	9.9	9.9	9.9	10.0	75	7.3	7.3	7.3	7.4	7.4	7.4	160
60	12.0	12.0	12.0	12.1	12.1	12.2		8.9	9.0	9.0	9.0	9.1	9.1	150
50	12.0	12.0	12.0	12.1	12.1	12.2		8.9	9.0	9.0	9.0	9.1	9.1	140
45	11.6	11.6	11.6	11.7	11.7	11.8		8.6	8.7	8.7	8.7	8.8	8.8	130
35	11.6	11.6	11.6	11.7	11.7	11.8		8.6	8.6	8.7	8.7	8.8	8.8	120
20	12.8	12.9	12.9	13.0	13.0	13.1		9.6	9.6	9.7	9.7	9.8	9.8	90
100	6.8	7.0	7.2	7.5	7.7	7.9	70	4.9	5.0	5.1	5.3	5.5	5.7	160
60	8.9	9.1	9.4	9.7	10.0	10.3		6.4	6.5	6.7	6.9	7.1	7.4	150
50	8.9	9.1	9.3	9.6	9.9	10.2		6.3	6.5	6.7	6.9	7.1	7.3	140
45	8.4	8.6	8.9	9.2	9.5	9.8		6.0	6.2	6.4	6.6	6.8	7.0	130
35	8.4	8.6	8.9	9.1	9.4	9.7		6.0	6.1	6.3	6.5	6.7	6.9	120
20	9.4	9.6	9.9	10.2	10.6	10.9		6.7	6.9	7.1	7.3	7.6	7.8	90
100	4.7	5.0	5.3	5.6	5.9	6.3	65	3.2	3.4	3.6	3.8	4.0	4.3	160
60	6.6	6.9	7.3	7.7	8.2	8.7		4.5	4.7	5.0	5.3	5.6	5.9	150
50	6.5	6.8	7.2	7.6	8.1	8.6		4.4	4.6	4.9	5.2	5.6	5.9	140
45	6.1	6.4	6.8	7.2	7.6	8.1		4.2	4.3	4.6	4.9	5.2	5.5	130
35	6.0	6.3	6.7	7.1	7.5	8.0		4.1	4.3	4.6	4.9	5.2	5.5	120
20	6.8	7.1	7.6	8.0	8.5	9.0		4.7	4.9	5.2	5.5	5.8	6.2	90
100	3.3	3.5	3.8	4.2	4.5	5.0	60	2.1	2.3	2.5	2.7	3.0	3.2	160
60	4.8	5.1	5.6	6.1	6.7	7.3		3.1	3.4	3.7	4.0	4.4	4.8	150
50	4.7	5.1	5.5	6.0	6.6	7.2		3.1	3.3	3.6	4.0	4.3	4.7	140
45	4.4	4.7	5.1	5.6	6.1	6.6		2.9	3.1	3.3	3.6	4.0	4.4	130
35	4.3	4.6	5.0	5.5	6.0	6.5		2.8	3.0	3.3	3.6	3.9	4.3	120
20	4.9	5.3	5.7	6.3	6.8	7.4		3.2	3.4	3.8	4.1	4.5	4.9	90
100	2.2	2.4	2.7	3.1	3.5	3.9	55	1.4	1.5	1.7	1.9	2.2	2.4	160
60	3.5	3.8	4.3	4.8	5.4	6.1		2.2	2.4	2.7	3.0	3.4	3.8	150
50	3.4	3.8	4.2	4.7	5.3	6.0		2.1	2.3	2.6	3.0	3.4	3.8	140
45	3.1	3.4	3.8	4.3	4.8	5.4		1.9	2.1	2.4	2.7	3.0	3.4	130
35	3.1	3.3	3.8	4.2	4.8	5.3		1.9	2.1	2.4	2.7	3.0	3.4	120
20	3.5	3.9	4.3	4.9	5.5	6.1		2.2	2.4	2.7	3.1	3.4	3.9	90
100	1.5	1.7	2.0	2.3	2.7	3.1	50	0.9	1.0	1.2	1.4	1.6	1.8	160
60	2.5	2.8	3.3	3.8	4.4	5.1		1.5	1.7	2.0	2.3	2.7	3.1	150
50	2.5	2.8	3.2	3.7	4.3	5.0		1.5	1.7	1.9	2.2	2.6	3.0	140
45	2.2	2.5	2.9	3.3	3.8	4.4		1.3	1.5	1.7	2.0	2.3	2.7	130
35	2.2	2.4	2.8	3.3	3.8	4.4		1.3	1.5	1.7	2.0	2.3	2.6	120
20	2.5	2.8	3.3	3.8	4.4	5.0		1.5	1.7	2.0	2.3	2.6	3.0	90
100	1.0	1.2	1.4	1.7	2.0	2.4	45	0.6	0.7	0.8	1.0	1.2	1.4	160
60	1.8	2.1	2.5	3.0	3.6	4.2		1.1	1.2	1.4	1.7	2.1	2.5	150
50	1.8	2.0	2.4	2.9	3.5	4.1		1.0	1.2	1.4	1.7	2.0	2.4	140
45	1.6	1.8	2.1	2.6	3.1	3.6		0.9	1.0	1.2	1.5	1.8	2.1	130
35	1.5	1.8	2.1	2.5	3.0	3.5		0.9	1.0	1.2	1.4	1.7	2.0	120
20	1.8	2.0	2.4	2.9	3.5	4.1		1.0	1.2	1.4	1.7	2.0	2.4	90

(*Continued*)

Table 3. Effect of Smoking on PREVENT Risk Score Results in Women (*Continued*)

Female														
HDL-C (mg/dL)	Smoking (%) PREVENT						Age (years)	No Smoking (%) PREVENT						SBP (mm Hg)
100	0.7	0.8	1.0	1.2	1.5	1.9	40	0.4	0.5	0.6	0.7	0.8	1.0	160
60	1.3	1.6	1.9	2.3	2.9	3.5		0.7	0.9	1.1	1.3	1.6	2.0	150
50	1.3	1.5	1.8	2.3	2.8	3.4		0.7	0.8	1.0	1.3	1.5	1.9	140
45	1.1	1.3	1.6	2.0	2.4	3.0		0.6	0.7	0.9	1.1	1.3	1.6	130
35	1.1	1.3	1.6	1.9	2.3	2.9		0.6	0.7	0.9	1.1	1.3	1.6	120
20	1.3	1.5	1.8	2.2	2.7	3.4		0.7	0.8	1.0	1.2	1.5	1.9	90
100	0.5	0.6	0.7	0.9	1.2	1.5	35	0.3	0.3	0.4	0.5	0.6	0.8	160
60	1.0	1.1	1.5	1.8	2.3	2.9		0.5	0.6	0.8	1.0	1.2	1.6	150
50	0.9	1.1	1.4	1.8	2.2	2.8		0.5	0.6	0.7	0.9	1.2	1.5	140
45	0.8	0.9	1.2	1.5	1.9	2.4		0.4	0.5	0.6	0.8	1.0	1.3	130
35	0.8	0.9	1.2	1.5	1.8	2.3		0.4	0.5	0.6	0.8	1.0	1.2	120
20	0.9	1.1	1.4	1.7	2.2	2.8		0.5	0.6	0.7	0.9	1.2	1.5	90
100	0.3	0.4	0.5	0.7	0.9	1.2	30	0.2	0.2	0.3	0.3	0.4	0.6	160
60	0.7	0.8	1.1	1.4	1.9	2.4		0.4	0.4	0.6	0.7	1.0	1.2	150
50	0.7	0.8	1.1	1.4	1.8	2.3		0.3	0.4	0.5	0.7	0.9	1.2	140
45	0.6	0.7	0.9	1.2	1.5	2.0		0.3	0.3	0.5	0.6	0.8	1.0	130
35	0.5	0.7	0.9	1.1	1.5	1.9		0.3	0.3	0.4	0.6	0.7	1.0	120
20	0.6	0.8	1.0	1.3	1.7	2.2		0.3	0.4	0.5	0.7	0.9	1.1	90
	130	160	200	240	280	320		130	160	200	240	280	320	
	Total cholesterol (mg/dL)							Total cholesterol (mg/dL)						

According to the PREVENT system, in women aged 30-75, smoking (left) and no smoking (right), HDL-C (100, 60, 50, 45, 35, 20 mg/dL), TC (130, 160, 200, 240, 280, 320 mg/dL), and SBP (160, 150, 140, 130, 120, 90) parameters for women aged 30-75 are presented. The PREVENT system classifies risk scores into percentile ranges as follows: <5% low risk (blue color in the table), 5%-7.4% borderline risk (yellow color in the table), 7.5%-19.9% moderate risk (orange color in the table), and ≥20% high risk (red color in the table).
HDL-C, high-density lipoprotein cholesterol; SBP, systolic blood pressure; TC, total cholesterol.

According to the results of the PREVENT ASCVD risk calculation system, the age at which CVD risk first appears is lower in men than in women. Furthermore, when considering all risk factors, tables created for men show a higher risk score, while high-risk status is not observed in the tables created for women. These findings suggest that men display a higher and more intense risk profile in the CVD risk chart. Many of the values seen as borderline and moderate risk in women fall into the moderate and, in some cases, high-risk categories in men.

According to the findings, all 3 different CVD risk calculation systems used in the study show a linear relationship between age and risk. Specifically, the Framingham system demonstrates that, independent of smoking, CVD risk increases with age when HDL-C, TC, and SBP values remain constant in both men and women. However, the Framingham system does not calculate a risk score above 30%; therefore, individuals with a risk score of 30% or higher are classified into the same high-risk category.

Similarly, in the Reynolds system, an increase in CVD risk was observed in both women and men after the age of 50. However, in groups younger than 50, individuals with the same biochemical parameters showed the same CVD risk score. This indicates that the Reynolds system makes the effect of age on CVD risk more pronounced at a certain age threshold.

The PREVENT ASCVD risk calculation system can more clearly calculate age-related CVD risk scores compared to other systems. Independent of smoking, it has been found that CVD risk increases with age in both men and women with the same parameter values. This feature allows PREVENT to assess the effect of age on CVD risk within scenarios designed with specified simulation parameters.

These findings demonstrate that age is an important factor in increasing CVD risk, and that this relationship can vary depending on gender and the risk calculation system used. Systems in which the effect of age is more pronounced can offer personalized approaches in risk assessments. Understanding the role of age in CVD risk is essential for planning individualized health interventions and for accurately performing age-based risk calculations. The findings obtained in the study also show that smoking increases CVD risk in both women and men across all 3 CVD risk calculation systems. A significant increase in risk was observed in individuals who smoke compared to those who do not.

In the CVD risk tables, created using the Framingham, Reynolds, and PREVENT calculation systems, risk scores

Table 4. Effect of Smoking on Framingham Risk Score Outcomes in Men

	Male												
HDL-C (mg/dL)	Smoking (%) Framingham						Age (years)	No Smoking (%) Framingham						SBP (mm Hg)
100	>30	>30	>30	>30	>30	>30	75	25.3	29.4	>30	>30	>30	>30	160
60	>30	>30	>30	>30	>30	>30		21.6	25.3	29.4	>30	>30	>30	150
50	>30	>30	>30	>30	>30	>30		25.3	29.4	>30	>30	>30	>30	140
45	>30	>30	>30	>30	>30	>30		25.3	29.4	>30	>30	>30	>30	130
35	>30	30	>30	>30	>30	>30		25.3	29.4	>30	>30	>30	>30	120
20	>30	>30	>30	>30	>30	>30		21.6	25.3	29.4	>30	>30	>30	90
100	>30	30	>30	>30	>30	>30	70	21.6	25.3	29.4	>30	>30	>30	160
60	>30	>30	>30	>30	>30	>30		18.4	21.6	25.3	29.4	>30	>30	150
50	>30	>30	>30	>30	>30	>30		21.6	25.3	29.4	>30	>30	>30	140
45	>30	>30	>30	>30	>30	>30		21.6	25.3	29.4	>30	>30	>30	130
35	>30	>30	>30	>30	>30	>30		21.6	25.3	29.4	>30	>30	>30	120
20	>30	>30	>30	>30	>30	>30		18.4	21.6	25.3	29.4	>30	>30	90
100	29.4	>30	>30	>30	>30	>30	65	15.6	18.4	21.6	25.3	29.4	29.4	160
60	25.3	29.4	>30	>30	>30	>30		13.2	15.6	18.4	21.6	25.3	25.3	150
50	29.4	>30	>30	>30	>30	>30		15.6	18.4	21.6	25.3	29.4	29.4	140
45	29.4	>30	>30	>30	>30	>30		15.6	18.4	21.6	25.3	29.4	29.4	130
35	29.4	>30	>30	>30	>30	>30		15.6	18.4	21.6	25.3	29.4	29.4	120
20	25.3	29.4	>30	>30	>30	>30		13.2	15.6	18.4	21.6	25.3	25.3	90
100	25.3	29.4	>30	>30	>30	>30	60	13.2	15.6	18.4	21.6	25.3	25.3	160
60	21.6	25.3	29.4	>30	>30	>30		11.2	13.2	15.6	18.4	21.6	21.6	150
50	25.3	29.4	>30	>30	>30	>30		13.2	15.6	18.4	21.6	25.3	25.3	140
45	25.3	29.4	>30	>30	>30	>30		13.2	15.6	18.4	21.6	25.3	25.3	130
35	25.3	29.4	>30	>30	>30	>30		13.2	15.6	18.4	21.6	25.3	25.3	120
20	21.6	25.3	29.4	>30	>30	>30		11.2	13.2	15.6	18.4	21.6	21.6	90
100	21.6	25.3	29.4	>30	>30	>30	55	11.2	13.2	15.6	18.4	21.6	21.6	160
60	18.4	21.6	25.3	29.4	>30	>30		9.4	11.2	13.2	15.6	18.4	18.4	150
50	21.6	25.3	29.4	>30	>30	>30		11.2	13.2	15.6	18.4	21.6	21.6	140
45	21.6	25.3	29.4	>30	>30	>30		11.2	13.2	15.6	18.4	21.6	21.6	130
35	21.6	25.3	29.4	>30	>30	>30		11.2	13.2	15.6	18.4	21.6	21.6	120
20	18.4	21.6	25.3	29.4	>30	>30		9.4	11.2	13.2	15.6	18.4	18.4	90
100	15.6	18.4	21.6	25.3	29.4	29.4	50	7.9	9.4	11.2	13.2	15.6	15.6	160
60	13.2	15.6	18.4	21.6	25.3	25.3		6.7	7.9	9.4	11.2	13.2	13.2	150
50	15.6	18.4	21.6	25.3	29.4	29.4		7.9	9.4	11.2	13.2	15.6	15.6	140
45	15.6	18.4	21.6	25.3	29.4	29.4		7.9	9.4	11.2	13.2	15.6	15.6	130
35	15.6	18.4	21.6	25.3	29.4	29.4		7.9	9.4	11.2	13.2	15.6	15.6	120
20	13.2	15.6	18.4	21.6	25.3	25.3		6.7	7.9	9.4	11.2	13.2	13.2	90
100	11.2	13.2	15.6	18.4	21.6	21.6	45	5.6	6.7	7.9	9.4	11.2	11.2	160
60	9.4	11.2	13.2	15.6	18.4	18.4		4.7	5.6	6.7	7.9	9.4	9.4	150
50	11.2	13.2	15.6	18.4	21.6	21.6		5.6	6.7	7.9	9.4	11.2	11.2	140
45	11.2	13.2	15.6	18.4	21.6	21.6		5.6	6.7	7.9	9.4	11.2	11.2	130
35	11.2	13.2	15.6	18.4	21.6	21.6		5.6	6.7	7.9	9.4	11.2	11.2	120
20	9.4	11.2	13.2	15.6	18.4	18.4		4.7	5.6	6.7	7.9	9.4	9.4	90

(*Continued*)

Table 4. Effect of Smoking on Framingham Risk Score Outcomes in Men (*Continued*)

	Male												
HDL-C (mg/dL)	**Smoking (%) Framingham**						**Age (years)**	**No Smoking (%) Framingham**						**SBP (mm Hg)**
100	9.4	11.2	13.2	15.6	18.4	18.4	**40**	4.7	5.6	6.7	7.9	9.4	9.4	**160**
60	7.9	9.4	11.2	13.2	15.6	15.6		3.9	4.7	5.6	6.7	7.9	7.9	**150**
50	9.4	11.2	13.2	15.6	18.4	18.4		4.7	5.6	6.7	7.9	9.4	9.4	**140**
45	9.4	11.2	13.2	15.6	18.4	18.4		4.7	5.6	6.7	7.9	9.4	9.4	**130**
35	9.4	11.2	13.2	15.6	18.4	18.4		4.7	5.6	6.7	7.9	9.4	9.4	**120**
20	7.9	9.4	11.2	13.2	15.6	15.6		3.9	4.7	5.6	6.7	7.9	7.9	**90**
100	5.6	6.7	7.9	9.4	11.2	11.2	**35**	2.8	3.3	3.9	4.7	5.6	5.6	**160**
60	4.7	5.6	6.7	7.9	9.4	9.4		2.3	2.8	3.3	3.9	4.7	4.7	**150**
50	5.6	6.7	7.9	9.4	11.2	11.2		2.8	3.3	3.9	4.7	5.6	5.6	**140**
45	5.6	6.7	7.9	9.4	11.2	11.2		2.8	3.3	3.9	4.7	5.6	5.6	**130**
35	5.6	6.7	7.9	9.4	11.2	11.2		2.8	3.3	3.9	4.7	5.6	5.6	**120**
20	4.7	5.6	6.7	7.9	9.4	9.4		2.3	2.8	3.3	3.9	4.7	4.7	**90**
100	3.9	4.7	5.6	6.7	7.9	7.9	**30**	1.9	2.3	2.8	3.3	3.9	3.9	**160**
60	3.3	3.9	4.7	5.6	6.7	6.7		1.6	1.9	2.3	2.8	3.3	3.3	**150**
50	3.9	4.7	5.6	6.7	7.9	7.9		1.9	2.3	2.8	3.3	3.9	3.9	**140**
45	3.9	4.7	5.6	6.7	7.9	7.9		1.9	2.3	2.8	3.3	3.9	3.9	**130**
35	3.9	4.7	5.6	6.7	7.9	7.9		1.9	2.3	2.8	3.3	3.9	3.9	**120**
20	3.3	3.9	4.7	5.6	6.7	6.7		1.6	1.9	2.3	2.8	3.3	3.3	**90**
	130	**160**	**200**	**240**	**280**	**320**		**130**	**160**	**200**	**240**	**280**	**320**	
	Total cholesterol (mg/dL)							**Total cholesterol (mg/dL)**						

According to the Framingham system, in men aged 30-75 who smoking (left) and no smoking (right), HDL-C (100, 60, 50, 45, 35, 20 mg/dL), TC (130, 160, 200, 240, 280, 320 mg/dL), and SBP (160, 150, 140, 130, 120, 90) parameters for women who smoke between the ages of 30 and 75 are presented. In the Framingham system, those with a risk score <10% are classified as low risk (blue color in the table), those with a score of 10%-20% are classified as moderate risk (yellow color in the table), and those with a score >20% are classified as high risk (red color in the table).
HDL-C, high-density lipoprotein cholesterol; SBP, systolic blood pressure; TC, total cholesterol.

were calculated by evaluating HDL-C and SBP values. The results indicate that low HDL-C levels significantly increase CVD risk, and this increase becomes more pronounced when combined with elevated SBP. The interaction between HDL-C and SBP provides an important parameter for more accurate and comprehensive CVD risk assessments. These findings suggest that increasing HDL-C levels and controlling SBP could be important strategies for the prevention and management of CVD.

The results of the study indicate that, among individuals with the same gender, age, HDL-C, and SBP values, analyses performed using the Framingham CVD risk calculation system show that increases in TC levels generally lead to an elevated CVD risk. However, it was observed that when TC levels rise from 280 mg/dL to 320 mg/dL, the risk does not change. This finding suggests that in the Framingham system, TC levels may stabilize at a certain point in risk assessment, and beyond this level, the risk does not further increase.

Similarly, in the Reynolds system, it was found that increases in TC levels elevated CVD risk. The system appears to confirm that as TC levels rise, the risk continues to increase. However, it was observed that the Reynolds system provides a broader risk range, and the increase in risk becomes more pronounced with higher TC levels.

According to evaluations specific to the PREVENT system, it was observed that in both smoking and non-smoking women aged 75, increases in TC levels raised CVD risk, although the risk ratios were close to each other and sometimes even identical. In other age groups as well, it was concluded that increases in TC levels generally elevated CVD risk. The PREVENT system appears to offer more specific risk score calculations based on age and highlights TC level as a key factor influencing risk. In men, it was determined that CVD risk increased with rising TC levels among individuals with the same values. This finding indicates that the PREVENT system systematically associates increases in TC levels with elevated CVD risk in men.

Overall, these findings demonstrate that TC levels are an important parameter in the assessment of CVD risk, and that all 3 systems show a significant impact of TC increases on risk. However, since each system has different risk calculation mechanisms, the effect of changes in TC levels varied across the systems. These differences arise from the specific characteristics of how each system calculates CVD risk.

Table 5. Effect of Smoking on Reynolds Risk Score Results in Men

	Male												
HDL-C (mg/dL)	Smoking (%) Reynolds						Age (years)	No Smoking (%) Reynolds						SBP (mm Hg)
100	18.3	20.5	24.7	28.7	32.5	0.36	75	12.6	14.2	17.3	20.2	23.1	25.8	160
60	22.3	25	30	34.6	38.9	42.9		15.5	17.4	21.2	24.7	28.0	31.2	150
50	21.6	24.1	0.29	33.5	37.7	41.7		15.0	16.8	20.4	23.8	27.1	30.2	140
45	19.5	21.9	26.4	30.6	34.5	38.2		13.5	15.2	18.5	21.6	24.6	27.5	130
35	19.3	21.6	26.1	30.2	34.1	37.8		13.3	15.0	18.2	21.3	24.3	27.1	120
20	15.7	17.6	21.3	24.9	28.3	31.4		10.7	12.1	14.8	17.4	19.9	22.3	90
100	13.8	15.6	18.9	22.1	25.2	28.1	70	9.5	10.7	13.1	15.4	17.6	19.8	160
60	17.0	19.1	23.1	26.9	30.5	33.9		11.7	13.2	16.1	18.9	21.6	24.1	150
50	16.4	18.5	22.4	26.1	29.5	32.8		11.3	12.7	15.5	18.2	20.8	23.3	140
45	14.8	16.7	20.3	23.7	26.9	30.0		10.2	11.5	14.0	16.5	18.8	21.1	130
35	14.6	16.5	20.0	23.4	26.5	29.6		10.0	11.3	13.8	16.3	18.6	20.9	120
20	11.8	13.3	16.3	19.1	21.8	24.3		8.1	9.1	11.2	13.2	15.1	17.0	90
100	10.2	11.5	14.1	16.5	18.9	21.2	65	6.9	7.8	9.6	11.4	13.1	14.7	160
60	12.6	14.2	17.3	20.3	23.1	25.9		8.6	9.7	11.9	14.0	16.1	18.1	150
50	12.2	13.7	16.7	19.6	22.4	25.0		8.3	9.4	11.5	13.5	15.5	17.5	140
45	11.0	12.4	15.1	17.7	20.2	22.7		7.4	8.4	10.3	12.2	14.0	15.8	130
35	10.8	12.2	14.9	17.5	20.0	22.4		7.3	8.3	10.2	12.0	13.8	15.6	120
20	8.7	9.8	12.0	14.2	16.2	18.3		5.9	6.7	8.2	9.7	11.2	12.6	90
100	7.3	8.3	10.1	12.0	13.7	15.5	60	4.9	5.6	6.9	8.1	9.4	10.6	160
60	9.1	10.2	12.5	14.8	16.9	19.0		6.1	7.0	8.5	10.1	11.6	13.1	150
50	8.7	9.9	12.1	14.2	16.3	18.3		5.9	6.7	8.2	9.7	11.2	12.6	140
45	7.8	8.9	10.9	12.8	14.7	16.6		5.3	6.0	7.4	8.7	10.1	11.4	130
35	7.7	8.7	10.7	12.7	14.5	16.3		5.2	5.9	7.3	8.6	9.9	11.2	120
20	6.2	7.0	8.6	10.2	11.7	13.2		4.2	4.7	5.8	6.9	8.0	9.0	90
100	5.0	5.7	7.0	8.3	9.6	10.8	55	3.4	3.8	4.7	5.6	6.5	7.4	160
60	6.3	7.1	8.7	10.3	11.9	13.4		4.2	4.8	5.9	7.0	8.1	9.1	150
50	6.0	6.8	8.4	10.0	11.4	12.9		4.1	4.6	5.7	6.8	7.8	8.8	140
45	5.4	6.1	7.6	8.9	10.3	11.6		3.7	4.1	5.1	6.1	7.0	7.9	130
35	5.3	6.1	7.5	8.8	10.2	11.5		3.6	4.1	5.0	6.0	6.9	7.8	120
20	4.3	4.8	6.0	7.1	8.2	9.2		2.9	3.3	4.0	4.8	5.5	6.3	90
100	3.3	3.8	4.7	5.6	6.4	7.3	50	2.2	2.6	3.2	3.7	4.3	4.9	160
60	4.2	4.7	5.8	6.9	8.0	9.0		2.8	3.2	3.9	4.7	5.4	6.1	150
50	4.0	4.6	5.6	6.7	7.7	8.7		2.7	3.1	3.8	4.5	5.2	5.9	140
45	3.6	4.1	5.0	6.0	6.9	7.8		2.4	2.7	3.4	4.0	4.7	5.3	130
35	3.6	4.0	5.0	5.9	6.8	7.7		2.4	2.7	3.3	4.0	4.6	5.2	120
20	2.8	3.2	4.0	4.7	5.5	6.2		1.9	2.2	2.7	3.2	3.7	4.2	90
100	2.1	2.4	3.0	3.5	4.1	4.6	45	1.4	1.6	2.0	2.4	2.8	3.1	160
60	2.7	3.0	3.7	4.4	5.1	5.8		1.8	2.0	2.5	3.0	3.4	3.9	150
50	2.6	2.9	3.6	4.3	4.9	5.6		1.7	1.9	2.4	2.9	3.3	3.8	140
45	2.3	2.6	3.2	3.8	4.4	5.0		1.5	1.7	2.2	2.6	3.0	3.4	130
35	2.3	2.6	3.2	3.8	4.3	4.9		1.5	1.7	2.1	2.5	2.9	3.3	120
20	1.8	2.0	2.5	3.0	3.5	3.9		1.2	1.4	1.7	2.0	2.3	2.6	90

(*Continued*)

Table 5. Effect of Smoking on Reynolds Risk Score Results in Men (*Continued*)

	Male												
HDL-C (mg/dL)	**Smoking (%) Reynolds**						**Age (years)**	**No Smoking (%) Reynolds**						**SBP (mm Hg)**
100	2.1	2.4	3.0	3.5	4.1	4.6	**40**	1.4	1.6	2.0	2.4	2.8	3.1	**160**
60	2.7	3.0	3.7	4.4	5.1	5.8		1.8	2.0	2.5	3.0	3.4	3.9	**150**
50	2.6	2.9	3.6	4.3	4.9	5.6		1.7	1.9	2.4	2.9	3.3	3.8	**140**
45	2.3	2.6	3.2	3.8	4.4	5.0		1.5	1.7	2.2	2.6	3.0	3.4	**130**
35	2.3	2.6	3.2	3.8	4.3	4.9		1.5	1.7	2.1	2.5	2.9	3.3	**120**
20	1.8	2.0	2.5	3.0	3.5	3.9		1.2	1.4	1.7	2.0	2.3	2.6	**90**
100	2.1	2.4	3.0	3.5	4.1	4.6	**35**	1.4	1.6	2.0	2.4	2.8	3.1	**160**
60	2.7	3.0	3.7	4.4	5.1	5.8		1.8	2.0	2.5	3.0	3.4	3.9	**150**
50	2.6	2.9	3.6	4.3	4.9	5.6		1.7	1.9	2.4	2.9	3.3	3.8	**140**
45	2.3	2.6	3.2	3.8	4.4	5.0		1.5	1.7	2.2	2.6	3.0	3.4	**130**
35	2.3	2.6	3.2	3.8	4.3	4.9		1.5	1.7	2.1	2.5	2.9	3.3	**120**
20	1.8	2.0	2.5	3.0	3.5	3.9		1.2	1.4	1.7	2.0	2.3	2.6	**90**
100	2.1	2.4	3.0	3.5	4.1	4.6	**30**	1.4	1.6	2.0	2.4	2.8	3.1	**160**
60	2.7	3.0	3.7	4.4	5.1	5.8		1.8	2.0	2.5	3.0	3.4	3.9	**150**
50	2.6	2.9	3.6	4.3	4.9	5.6		1.7	1.9	2.4	2.9	3.3	3.8	**140**
45	2.3	2.6	3.2	3.8	4.4	5.0		1.5	1.7	2.2	2.6	3.0	3.4	**130**
35	2.3	2.6	3.2	3.8	4.3	4.9		1.5	1.7	2.1	2.5	2.9	3.3	**120**
20	1.8	2.0	2.5	3.0	3.5	3.9		1.2	1.4	1.7	2.0	2.3	2.6	**90**
	130	**160**	**200**	**240**	**280**	**320**		**130**	**160**	**200**	**240**	**280**	**320**	
	Total cholesterol (mg/dL)							**Total cholesterol (mg/dL)**						

According to the Reynolds system, in men who smoking (left) and no smoking (right), between the ages of 30 and 75, HDL-C (100, 60, 50, 45, 35, 20 mg/dL), TC (130, 160, 200, 240, 280, 320 mg/dL), and SBP (160, 150, 140, 130, 120, 90) parameters for women aged 30-75 are presented. The Reynolds system classifies risk scores as normal (blue color in the table) if <10% and abnormal (red color in the table) if >10%.
HDL-C, high-density lipoprotein cholesterol; SBP, systolic blood pressure; TC, total cholesterol.

The results of the study indicate that TC is an effective risk factor for CVD and stands out as a key parameter across all risk calculation systems. It was observed that high TC levels increase CVD risk, and that this increase is evident in both men and women. Additionally, it was found that the impact of rising TC levels becomes more pronounced with age, with the effect increasing as age advances. These findings further emphasize how critical TC is as a parameter in CVD risk assessment.

In this study, the CVD risks of individuals with specified parameters were compared using the Framingham, Reynolds, and PREVENT systems. While all 3 systems share several common parameters, each also includes unique parameters of its own. The Framingham system, unlike the other 2, produces higher numerical risk scores. Risk scores in the Framingham system are categorized into low, intermediate, and high-risk levels.

In the Reynolds system, CVD risk scores for individuals under 50 years of age were found to be the same. Moreover, in the Reynolds system, risk outcomes are classified as either normal or abnormal. Although the Framingham system generates higher numerical risk scores, some values considered normal according to the Framingham system were evaluated as abnormal by the Reynolds system.

The PREVENT system, unlike the other 2 systems, calculates CVD and ASCVD risks using a broader range of risk factors. This system provides separate risk calculations for 10-year and 30-year periods, allowing for a more detailed assessment. Risk scores are categorized into low risk, borderline risk, intermediate risk, and high risk, with clearly defined value ranges for each category.

The PREVENT system generally produces lower risk scores compared to the other 2 systems for individuals with the same conditions. This difference may be attributed to the fact that PREVENT was developed using more recent data, a contemporary population, and a more updated methodology.

In addition to traditional risk factors, the PREVENT system also considers additional factors such as HbA1c, BMI, uACR, Social Deprivation Index (SDI), and eGFR. This enables risk assessment for a broader patient population, including those with cardiovascular, kidney, and metabolic diseases. Furthermore, factors such as the SDI are included to provide a more comprehensive analysis. The risk score outcomes calculated through simulation by PREVENT can provide information on treatment options for patients, assist healthcare professionals in disease management, and thus offer an important opportunity to potentially alter the course of high-mortality diseases such as CVD. This holistic approach

Table 6. Effect of Smoking on PREVENT Risk Score Results in Men

	Male												
HDL-C (mg/dL)	Smoking (%) PREVENT						Age (years)	No Smoking (%) PREVENT						SBP (mm Hg)
100	9.5	10.2	11.2	12.4	13.6	15.0	75	7.9	8.5	9.4	10.4	11.4	12.6	160
60	12.1	13.0	14.3	15.7	17.2	18.8		10.1	10.9	12.0	13.2	14.5	15.9	150
50	12.3	13.2	14.5	15.9	17.4	19.1		10.3	11.0	12.2	13.4	14.7	16.1	140
45	12.0	12.9	14.2	15.6	17.0	18.7		10.0	10.8	11.9	13.1	14.4	15.8	130
35	12.2	13.1	14.4	15.8	17.3	18.9		10.2	11.0	12.1	13.3	14.6	16.0	120
20	16.3	17.5	19.1	20.9	22.8	24.7		13.8	14.8	16.2	17.7	19.4	21.2	90
100	7.0	7.6	8.6	9.6	10.8	12.0	70	5.5	6.1	6.8	7.6	8.6	9.6	160
60	9.3	10.1	11.3	12.6	14.1	15.7		7.4	8.1	9.0	10.1	11.3	12.6	150
50	9.4	10.2	11.4	12.7	14.2	15.7		7.4	8.1	9.1	10.2	11.4	12.7	140
45	9.0	9.8	11.0	12.2	13.6	15.2		7.2	7.8	8.7	9.8	11.0	12.2	130
35	9.1	9.9	11.0	12.3	13.7	15.3		7.2	7.9	8.8	9.9	11.0	12.3	120
20	12.3	13.3	14.8	16.5	18.3	20.2		9.8	10.7	12.0	13.3	14.8	16.5	90
100	5.2	5.7	6.5	7.4	8.4	9.6	65	3.9	4.3	4.9	5.6	6.4	7.3	160
60	7.1	7.8	8.9	10.1	11.4	12.9		5.4	5.9	6.7	7.7	8.7	9.9	150
50	7.1	7.8	8.9	10.1	11.4	12.9		5.3	5.9	6.7	7.7	8.7	9.9	140
45	6.7	7.4	8.4	9.6	10.8	12.3		5.1	5.6	6.4	7.3	8.3	9.4	130
35	6.7	7.4	8.4	9.5	10.8	12.3		5.0	5.6	6.4	7.3	8.3	9.4	120
20	9.1	10.0	11.4	12.9	14.5	16.4		6.9	7.7	8.7	9.9	11.2	12.7	90
100	3.8	4.2	4.9	5.7	6.6	7.6	60	2.7	3.0	3.5	4.1	4.7	5.5	160
60	5.4	6.0	6.9	8.0	9.2	10.6		3.9	4.3	5.0	5.8	6.7	7.8	150
50	5.3	5.9	6.9	7.9	9.2	10.5		3.8	4.3	5.0	5.7	6.6	7.7	140
45	5.0	5.5	6.4	7.4	8.6	9.9		3.5	4.0	4.6	5.4	6.2	7.2	130
35	4.9	5.5	6.3	7.3	8.5	9.8		3.5	3.9	4.6	5.3	6.1	7.1	120
20	6.7	7.5	8.7	10.0	11.5	13.1		4.8	5.4	6.3	7.3	8.4	9.7	90
100	2.7	3.1	3.7	4.3	5.1	6.0	55	1.9	2.1	2.5	3.0	3.5	4.1	160
60	4.1	4.6	5.4	6.3	7.4	8.7		2.8	3.1	3.7	4.4	5.1	6.0	150
50	4.0	4.5	5.3	6.2	7.3	8.6		2.7	3.1	3.6	4.3	5.0	5.9	140
45	3.6	4.1	4.9	5.7	6.7	7.9		2.5	2.8	3.3	3.9	4.6	5.4	130
35	3.6	4.0	4.8	5.6	6.6	7.7		2.4	2.8	3.3	3.8	4.5	5.3	120
20	4.9	5.6	6.5	7.7	9.0	10.5		3.4	3.8	4.5	5.3	6.2	7.3	90
100	2.0	2.3	2.7	3.3	3.9	4.7	50	1.3	1.5	1.8	2.1	2.6	3.1	160
60	3.0	3.5	4.2	5.0	6.0	7.1		2.0	2.3	2.7	3.3	3.9	4.7	150
50	3.0	3.4	4.1	4.9	5.8	6.9		1.9	2.2	2.6	3.2	3.8	4.5	140
45	2.7	3.1	3.7	4.4	5.2	6.3		1.7	2.0	2.4	2.9	3.4	4.1	130
35	2.6	3.0	3.6	4.3	5.1	6.1		1.7	1.9	2.3	2.8	3.3	4.0	120
20	3.6	4.1	4.9	5.8	7.0	8.3		2.3	2.7	3.2	3.8	4.6	5.5	90
100	1.4	1.7	2.0	2.5	3.0	3.7	45	0.9	1.0	1.3	1.5	1.9	2.3	160
60	2.3	2.7	3.2	3.9	4.8	5.8		1.4	1.6	2.0	2.4	3.0	3.6	150
50	2.2	2.6	3.1	3.8	4.6	5.6		1.4	1.6	1.9	2.3	2.9	3.5	140
45	2.0	2.3	2.8	3.4	4.1	5.0		1.2	1.4	1.7	2.1	2.5	3.1	130
35	1.9	2.2	2.7	3.2	3.9	4.8		1.2	1.3	1.6	2.0	2.4	3.0	120
20	2.6	3.0	3.7	4.4	5.4	6.5		1.6	1.9	2.3	2.8	3.4	4.1	90

(*Continued*)

Table 6. Effect of Smoking on PREVENT Risk Score Results in Men (*Continued*)

	Male												
HDL-C (mg/dL)	Smoking (%) PREVENT						Age (years)	No Smoking (%) PREVENT						SBP (mm Hg)
100	1.0	1.2	1.5	1.9	2.3	2.9	40	0.6	0.7	0.9	1.1	1.4	1.7	160
60	1.7	2.0	2.5	3.1	3.8	4.7		1.0	1.2	1.5	1.8	2.2	2.8	150
50	1.6	1.9	2.4	2.9	3.6	4.5		1.0	1.1	1.4	1.7	2.1	2.7	140
45	1.4	1.7	2.1	2.6	3.2	3.9		0.8	1.0	1.2	1.5	1.9	2.3	130
35	1.4	1.6	2.0	2.4	3.0	3.7		0.8	0.9	1.2	1.4	1.8	2.2	120
20	1.9	2.2	2.7	3.4	4.1	5.1		1.1	1.3	1.6	2.0	2.5	3.0	90
100	0.8	0.9	1.1	1.4	1.8	2.3	35	0.4	0.5	0.6	0.8	1.0	1.3	160
60	1.3	1.5	1.9	2.4	3.0	3.8		0.7	0.8	1.1	1.3	1.7	2.1	150
50	1.2	1.4	1.8	2.3	2.9	3.6		0.7	0.8	1.0	1.3	1.6	2.0	140
45	1.0	1.2	1.6	2.0	2.5	3.1		0.6	0.7	0.9	1.1	1.4	1.7	130
35	1.0	1.2	1.5	1.8	2.3	2.9		0.5	0.6	0.8	1.0	1.3	1.6	120
20	1.4	1.6	2.0	2.5	3.2	4.0		0.8	0.9	1.1	1.4	1.8	2.3	90
100	0.5	0.7	0.8	1.1	1.4	1.8	30	0.3	0.3	0.4	0.6	0.7	0.9	160
60	1.0	1.2	1.5	1.9	2.4	3.1		0.5	0.6	0.8	1.0	1.3	1.6	150
50	0.9	1.1	1.4	1.8	2.2	2.9		0.5	0.6	0.7	0.9	1.2	1.5	140
45	0.8	0.9	1.2	1.5	1.9	2.4		0.4	0.5	0.6	0.8	1.0	1.3	130
35	0.7	0.8	1.1	1.4	1.8	2.3		0.4	0.5	0.6	0.7	0.9	1.2	120
20	1.0	1.2	1.5	1.9	2.4	3.1		0.5	0.6	0.8	1.0	1.3	1.7	90
	130	160	200	240	280	320		130	160	200	240	280	320	
	Total cholesterol (mg/dL)							Total cholesterol (mg/dL)						

According to the PREVENT system, in men aged 30-75 who smoking (left) and no smoking (right), HDL-C (100, 60, 50, 45, 35, 20 mg/dL), TC (130, 160, 200, 240, 280, 320 mg/dL), and SBP (160, 150, 140, 130, 120, 90) parameters for women aged 30-75 are presented. The PREVENT system classifies risk scores into percentile ranges as follows: <5% low risk (blue color in the table), 5%-7.4% borderline risk (yellow color in the table), 7.5%-19.9% moderate risk (orange color in the table), and ≥20% high risk (red color in the table).
HDL-C, high-density lipoprotein cholesterol; SBP, systolic blood pressure; TC, total cholesterol.

enables healthcare systems to assess and conduct risk management within risk scenarios based on simulations.[13,19]

Krishnan et al developed an online calculation tool that also allows the estimation of individuals' PREVENT risk age. This system enables the assessment of concordance between chronological age and risk age (i.e., whether one's risk age exceeds their actual chronological age). The study found that discordance was more pronounced among middle-aged adults, individuals with adverse social factors, those with lower educational attainment, and members of racial and ethnic minority groups. Notably, among individuals with lower education levels, 22.8% of women and 32.5% of men had a PREVENT risk age exceeding their chronological age by more than 10 years. Considering individuals' risk age may provide a clearer understanding of risk factors and their consequences. The online calculation tool can be accessed at: https://nwkhanlab.shinyapps.io/riskage/.[20] Recently, steps have also been taken through artificial intelligence–based research to identify individuals with CVD, diagnose CVD as a predictable disease, examine the impact of risk factors on the disease, and ensure that treatment interventions for patients can be carried out transparently.[21]

Study Limitations

This study is a simulation study in which no real patient data were used. The common risk factors included in the 3 cardiovascular risk assessment systems were identified, and the shared value ranges they cover were used to generate the reported risk scores. The absence of real patient data may be considered a limitation of this study. The point emphasized in the study is that different risk calculation systems yield numerically different scores and different classifications when dealing with the same risk profiles. However, this study does not provide any output regarding accuracy and reliability. This is a significant limitation of the study.

In the PREVENT system, ASCVD risk is calculated instead of CVD risk, and the results of this risk score are presented in tables. During the study, while calculating CVD risk in the PREVENT system, the common risk factors of age, gender, HDL-C, and SBP values were kept constant; when TC values were increased, contrary to expectations, CVD risk decreased rather than increased. This is a point that requires further investigation. Therefore, to provide a clear result, the 10-year ASCVD risk was calculated. This is a limitation of the study.

The different risk scoring systems examined in this study have different parameters. However, it is not possible to obtain the output of the whole system by including each parameter and comparing all parameters. Each system has different parameter values, but when the systems are considered as a whole in a comparison-based study, it is not possible to equalize

them. In this study, there is no other option but to obtain and compare the scoring output. However, since the comparison cannot be addressed as a whole, this is a limitation.

CONCLUSION

The aim of this study is to highlight the output differences and classification discordance for individuals when the same parameter values are considered using different risk scoring systems. Considering all these assessments, the newly developed PREVENT system enables a clearer distinction between low-risk and high-risk patients. This allows healthcare professionals to evaluate patients within clearer boundaries and intervene more appropriately. These interventions, including lifestyle changes and the development of accurate treatment protocols, can alter the course of CVD. This, in turn, will contribute to reducing mortality and morbidity rates associated with CVD worldwide. In terms of the prevention, delay, and clinical management of CVDs, the development and validation of risk prediction systems are crucial steps.

Ethics Committee Approval: This study was conducted exclusively using simulation-based methods and did not involve human participants, animals, biological specimens, or identifiable personal data. Therefore, in accordance with institutional regulations and internationally accepted research ethics guidelines, ethical approval and informed consent were not required for this study.

Peer-review: Externally peer-reviewed.

Acknowledgments: This study was made possible through the valuable support and facilities provided by Lokman Hekim University, to which the authors express their sincere gratitude. They used ChatGPT to improve the language and readability of this manuscript.

Author Contributions: Conceptualization - Y.A., M.B.Ş., D.Y.; Design – Y.A., M.B.Ş., D.Y.; Supervision – Y.A., M.B.Ş., D.Y.; Analysis and interpretation - Y.A., M.B.Ş., D.Y.; Literature review - Y.A., M.B.Ş.; Writer - Y.A., M.B.Ş.; Critical review - Y.A., D.Y.

Declaration of Interests: The authors have no conflict of interest to declare.

Funding: The authors declared that this study has received no financial support.

REFERENCES

1. Proportional mortality. https://ncdportal.org/CountryProfile/GHE110/Global. Accessed 12 January 2025
2. Vaduganathan M, Mensah GA, Turco JV, Fuster V, Roth GA. The global burden of cardiovascular diseases and risk: A compass for future health. *J Am Coll Cardiol*. 2022;80(25):2361-2371. [CrossRef]
3. Cardiovascular diseases. https://www.who.int/health-topics/cardiovascular-diseases#tab=tab_1. Accessed 12 January 2025
4. Kaminsky LA, German C, Imboden M, Ozemek C, Peterman JE, Brubaker PH. The importance of healthy lifestyle behaviors in the prevention of cardiovascular disease. *Prog Cardiovasc Dis*. 2022;70:8-15. [CrossRef]
5. Stewart J, Manmathan G, Wilkinson P. Primary prevention of cardiovascular disease: a review of contemporary guidance and literature. *JRSM Cardiovasc Dis*. 2017;6:2048004016687211. [CrossRef]
6. Reamy BV, Williams PM, Kuckel DP. Prevention of cardiovascular disease. *Prim Care*. 2018;45(1):25-44. [CrossRef]
7. Perk J, De Backer G, Gohlke H, et al. European Guidelines on cardiovascular disease prevention in clinical practice (version 2012): the Fifth Joint Task Force of the European Society of Cardiology and Other Societies on Cardiovascular Disease Prevention in Clinical Practice (constituted by representatives of nine societies and by invited experts). *Atherosclerosis*. 2012;223(1):1-68. [CrossRef]
8. Conroy RM, Pyörälä K, Fitzgerald AP, et al. Estimation of ten-year risk of fatal cardiovascular disease in Europe: the SCORE project. *Eur Heart J*. 2003;24(11):987-1003. [CrossRef]
9. Woodward M, Brindle P, Tunstall-Pedoe H. Adding social deprivation and family history to cardiovascular risk assessment: the ASSIGN score from the Scottish Heart Health Extended Cohort (SHHEC). *Heart*. 2005;93(2):172-176.
10. Ridker PM, Buring JE, Rifai N, Cook NR. Development and validation of improved algorithms for the assessment of global cardiovascular risk in women: the Reynolds Risk Score. *JAMA*. 2007;297(6):611-619. [CrossRef]
11. Ridker PM, Paynter NP, Rifai N, Gaziano JM, Cook NR. C-reactive protein and parental history improve global cardiovascular risk prediction: the Reynolds Risk Score for men. *Circulation*. 2008;118(22):2243-2251. [CrossRef]
12. Hippisley-Cox J, Coupland C, Vinogradova Y, Robson J, May M, Brindle P. Derivation and validation of QRISK, a new cardiovascular disease risk score for the United Kingdom: prospective open cohort study. *BMJ*. 2007;335(7611):136. [CrossRef]
13. Khan SS, Matsushita K, Sang Y, et al. Development and validation of the American Heart Association's PREVENT equations. *Circulation*. 2024;149(6):430-449. [CrossRef]
14. Talha I, Elkhoudri N, Hilali A. Major limitations of cardiovascular risk scores. *Cardiovasc Ther*. 2024;2024(1):4133365. [CrossRef]
15. Berger JS, Jordan CO, Lloyd-Jones D, Blumenthal RS. Screening for cardiovascular risk in asymptomatic patients. *J Am Coll Cardiol*. 2010;55(12):1169-1177. [CrossRef]
16. About the Framingham Heart study. https://www.framinghamheartstudy.org/fhs-about/. Accessed 06 February 2025
17. O'Donnell CJ, Elosua R. Cardiovascular risk factors. Insights from Framingham Heart study. *Rev Esp Cardiol (Engl Ed)*. 2008;61(3):299-310.
18. Andersson C, Johnson AD, Benjamin EJ, Levy D, Vasan RS. 70-year legacy of the Framingham Heart Study. *Nat Rev Cardiol*. 2019;16(11):687-698. [CrossRef]
19. Khan SS, Lloyd-Jones DM. Statins for primary prevention of cardiovascular disease—with PREVENT, what's a clinician to do? *JAMA*. 2024;332(12):961-962. [CrossRef]
20. Krishnan V, Huang X, Perak AM, et al. PREVENT risk age equations and population distribution in US adults. *JAMA Cardiol*. 2025;10(9):962-964. [CrossRef]
21. Kırboğa KK, Küçüksille EU. Identifying cardiovascular disease risk factors in adults with explainable artificial intelligence. *Anatol J Cardiol*. 2023;27(11):657-663. [CrossRef]

THE ANATOLIAN JOURNAL OF CARDIOLOGY

Official journal of the TURKISH SOCIETY OF CARDIOLOGY

Circulating Protein Biomarkers for Primary Cardiomyopathy: Evidence from Mendelian Randomization and Clinical Validation

ABSTRACT

Background: Primary (non-ischemic) cardiomyopathy poses diagnostic challenges due to phenotypic heterogeneity and non-specific clinical presentation, and commonly used circulating biomarkers have limited disease specificity. The aim was to prioritize mechanism-informed plasma biomarkers and evaluate their diagnostic discrimination in a clinical cohort.

Methods: pQTL data from 8 proteomic studies covering 5,034 proteins were integrated, and Mendelian randomization was performed across 3 cardiomyopathy GWAS datasets. Top MR candidates were clinically validated by enzyme-linked immunosorbent assays quantification in a prospective case–control cohort of 81 subjects (48 cardiomyopathy patients and 33 healthy controls). Echocardiography evaluated cardiac function and remodeling, correlating with plasma biomarker levels.

Results: Proteome-wide MR prioritized 27 proteins linked to cardiomyopathy risk. Clinical validation confirmed significant differences in plasma levels of 5 selected biomarkers (CD163, LGALS3BP, FABP5, FSTL3, VCAM1). CD163 (odds ratio (OR) = 1.019, $P < .0001$) was positively associated with CM, while LGALS3BP (OR = 0.390, $P < .0001$), FABP5, FSTL3, and VCAM1 showed inverse associations. Multivariate analysis revealed CD163 and LGALS3BP as independent CM predictors, strongly correlating with echocardiographic indices of cardiac dysfunction. Receiver operating characteristic analyses showed individual area under the curve (AUC) ranging from 0.632 (VCAM1) to 0.917 (CD163). Given the modest discrimination of VCAM1, 5- versus 4-protein combined models were compared, and a parsimonious 4-protein panel was selected (CD163, LGALS3BP, FABP5, FSTL3). The 4-protein panel achieved an apparent AUC of 0.993, with optimism-corrected and repeated cross-validated AUCs of 0.988 and 0.980.

Conclusion: This integrative genetic-to-clinical approach supports a 4-protein plasma panel with promising diagnostic discrimination for primary cardiomyopathy, warranting external validation. CD163 and LGALS3BP emerged as particularly informative markers for further evaluation.

Keywords: CD163, clinical validation, ELISA, LGALS3BP, mendelian randomization, plasma biomarkers, primary cardiomyopathy

INTRODUCTION

Cardiomyopathy is a major contributor to heart failure, arrhythmias, and sudden cardiac death worldwide, with increasing prevalence and substantial clinical and socioeconomic impact.[1,2] Although echocardiography and cardiac MRI can detect structural and functional abnormalities, diagnostic evaluation can be challenging in routine practice because phenotypic presentations are heterogeneous and symptoms are often non-specific, particularly in earlier or milder stages. In addition, commonly used circulating biomarkers reflect myocardial injury or hemodynamic stress but have limited disease specificity. These gaps highlight the need for complementary circulating markers that can support diagnostic discrimination and patient characterization in primary cardiomyopathy.[3-5]

Mounting evidence suggests that chronic inflammation, myocardial fibrosis, metabolic dysregulation, and extracellular matrix remodeling play central roles in the pathogenesis and progression of cardiomyopathy—even before overt systolic

Copyright@Author(s) - Available online at anatoljcardiol.com.
Content of this journal is licensed under a Creative Commons Attribution-NonCommercial 4.0 International License.

ORIGINAL INVESTIGATION

Jie He[1]
Xiaoyan Liu[2]
Jianhui Tang[1]
Chunrong Tang[1]
Xiaofen Liu[1]
Zhuoyuan Yu[3]

[1]*Department of Cardiology, Jintang County Second People's Hospital, Chengdu, Sichuan, People's Republic of China*
[2]*Department of Military Traffic Injury Prevention and Control, Daping Hospital, Army Medical University, Chongqing, China*
[3]*Department of Urology, The First Affiliated Hospital of Chongqing Medical University, Chongqing, People's Republic of China*

Corresponding author:
Zhuoyuan Yu
✉ dryzy@stu.cqmu.edu.cn

Received: October 23, 2025
Accepted: May 13, 2026
Available Online Date: August 4, 2026

Cite this article as: He J, Liu X, Tang J, Tang C, Liu X, Yu Z. Circulating protein biomarkers for primary cardiomyopathy: evidence from mendelian randomization and clinical validation. *Anatol J Cardiol.* 2026;30(10):684-692.

DOI: 10.14744/AnatolJCardiol.2026.5927

dysfunction develops.[6-8] However, sensitive and mechanism-specific plasma biomarkers that reflect these key processes are lacking in routine clinical practice. Most currently used blood-based markers predominantly reflect end-stage damage rather than upstream, actionable pathophysiology.[9] Recent studies reported oxidative stress and neurohumoral biomarkers associated with heart failure phenotypes, underscoring the need for mechanism-informed plasma markers.[10,11]

Large-scale genetic studies have now cataloged thousands of protein quantitative trait loci (pQTLs), providing a unique opportunity to systematically prioritize circulating proteins with potential causal relevance to disease.[12,13] Mendelian randomization (MR) can leverage these genetic instruments to identify proteins that may not only signal increased risk but could serve as future therapeutic targets. Nonetheless, few studies have moved beyond genetic discovery to real-world clinical translation—prospectively validating MR-nominated candidates in contemporary patient cohorts. Recent reports highlight genetic heterogeneity within primary cardiomyopathies, including β1-adrenergic receptor polymorphisms in hypertrophic cardiomyopathy, supporting precision, genetics-anchored approaches.[14]

In this study, proteome-wide pQTL data were integrated with large-scale cardiomyopathy GWAS, using MR to identify candidate plasma biomarkers, and then validating their diagnostic utility in a prospectively recruited clinical cohort. The clinical validation focused on primary cardiomyopathy as an overall entity: although subtype heterogeneity exists, these phenotypes commonly converge on shared pathways of inflammation, fibrosis, and myocardial remodeling in real-world diagnostic pathways. Therefore, the subtype distribution and key echocardiographic measurements are reported, while standardized echocardiographic assessment and targeted enzyme-linked immunosorbent assays (ELISA) quantification to develop a clinically relevant plasma biomarker panel for primary cardiomyopathy.

METHODS

Study Design

This study followed an integrative design beginning with proteome-wide genetic analyses and culminating in clinical validation (Figure 1). First, summary statistics from large-scale plasma proteomic genome-wide association studies were assembled (pQTL GWAS). Protein quantitative trait loci (pQTLs) across the human proteome were identified and then applied 2-sample MR to test for causal effects of circulating proteins on cardiomyopathy risk. Finally, top MR candidates were examined in a prospective clinical cohort using ELISAs for biomarker validation. The overall workflow from pQTL data integration and MR screening to clinical validation is illustrated schematically in Figure 1.

Proteomic Protein Quantitative Trait Loci Datasets

pQTL findings from 8 published proteomic studies, encompassing a total of 5 034 unique plasma proteins and 13 636 independent pQTL instruments, were aggregated (2 157 cis-pQTLs and 11 479 trans-pQTLs). The data sources and cohort details are as follows: Fenland study (UK), N = 10 708 participants, 4 775 proteins assayed by SomaScan v4.[15] Iceland study, N = 35 559 Icelanders, 4 719 proteins (Somalogic aptamers).[16,17] INTERVAL study (UK), N = 3 301 blood donors, 2,995 proteins (SomaScan assay).[18] The UK Biobank Pharma Proteomics Project (UKB-PPP), N = 34 557 UK Biobank participants, 2 922 unique proteins (Olink Explore 3072 panels).[19] This is the largest pQTL resource, with ~14,287 significant protein–variant associations (81% novel) reported. The published primary pQTL hits from the full UKB-PPP release were used.[19] Additionally, pQTL data from the initial UKB-PPP Pilot/Phase I (≈35 571 participants) for cross-validation was included.[20] KORA F4 study (Germany), N = 1 000 adults, 1 124 proteins (Somalogic v1).[21] SCALLOP consortium (Europe), N = 30 931, 90 cardiovascular-related proteins (Olink panels).[22] FHS Offspring study (USA), N = 6 861 Framingham Heart Study participants, 71 selected CVD proteins (multiplex immunoassays).[23]

All pQTL coordinates were aligned to the human hg19 reference genome. Uniform quality control and instrument selection criteria were applied across datasets. Only pQTL variants reaching genome-wide significance ($P < 5 \times 10^{-8}$) in their original study were considered. The extended major histocompatibility complex (MHC) region on chr6 (positions 25-34 Mb) were excluded to avoid complex LD. Within each protein's locus, if multiple significant SNPs were in linkage disequilibrium, LD clumping ($r^2 < .001$) were performed to retain a single sentinel SNP per locus. For each protein, one or more independent pQTL instruments were selected that were sufficiently strong (F-statistic > 10, corresponding to an approximate $r^2 > 1\%$ in the discovery cohort). When a protein was measured in multiple studies, the dataset with the highest variance explained (e.g. the pQTL with highest r^2 for that protein) was retained to represent that protein's genetic instrument. Cis-pQTLs were defined as variants located within or near the encoding gene (within ±500 kb of the gene locus), while trans-pQTLs were those mapping outside this cis window. In total, 13 636 SNP–protein instruments were curated (2 157 cis and 11 479 trans) for the MR analysis. Each instrument was oriented to the allele associated with higher protein level, and palindromic SNPs were aligned by effect allele frequency to ensure consistency between exposure and outcome data.

Cardiomyopathy GWAS Datasets

Three complementary genome-wide association datasets for cardiomyopathy outcomes were obtained to serve

HIGHLIGHTS

- Proteome-wide MR screens 5,034 proteins for cardiomyopathy risk.
- Prospective enzyme-linked immunosorbent assays validation confirms 4 plasma biomarkers.
- CD163 predicts higher risk; LGALS3BP is protective; both are independent.
- Four-protein panel shows strong discrimination after internal validation.
- Biomarker levels track echocardiographic dysfunction.

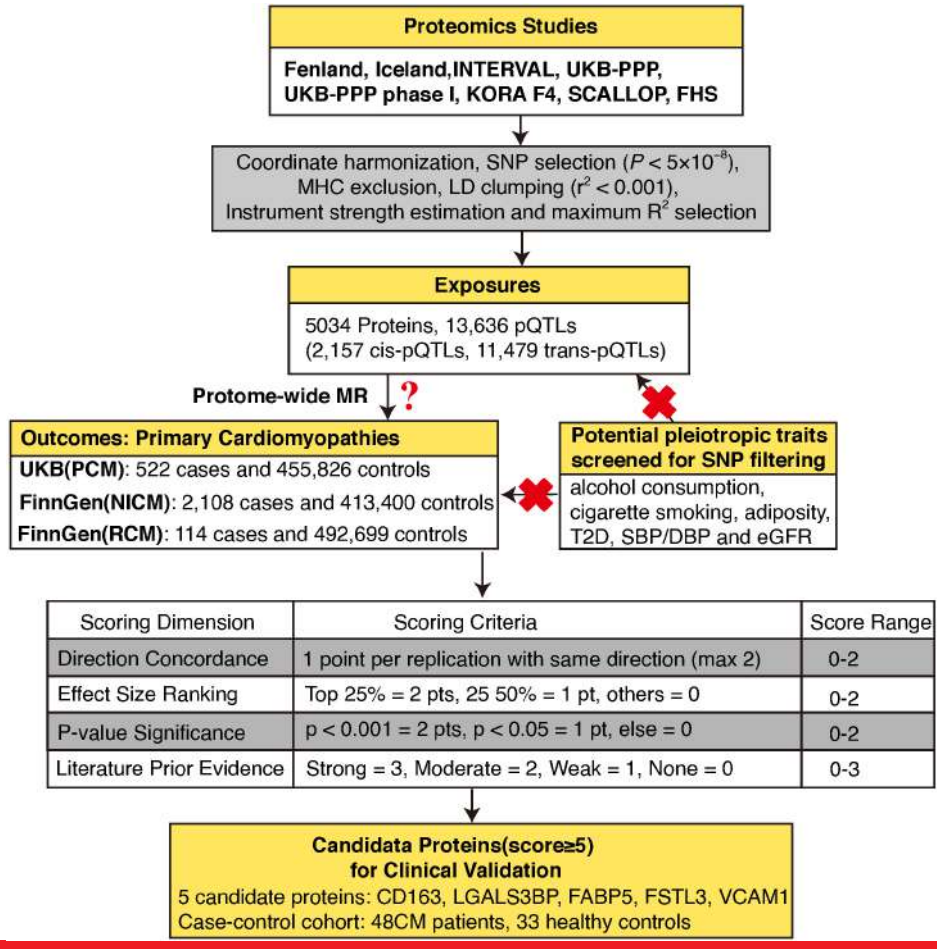

Figure 1. Study design and workflow for biomarker discovery and validation. An overview of the integrative pipeline combining proteome-wide pQTL data from 8 large-scale proteomic studies with 3 cardiomyopathy GWAS datasets (UKB–PCM, FinnGen–NICM, and FinnGen–RCM) using Mendelian randomization (MR). After harmonization, filtering, and instrument selection, 13,636 pQTLs (2,157 cis and 11,479 trans) across 5,034 proteins were evaluated. A multi-dimensional scoring system based on replication consistency, effect size, *P*-value, and literature evidence was used to prioritize candidate proteins for clinical validation. Five proteins (CD163, LGALS3BP, FABP5, FSTL3, and VCAM1) were selected for ELISA testing (48 CM patients, 33 healthy controls); subsequent panel refinement yielded a parsimonious 4-protein panel as the primary combined model. The pleiotropy-screening traits were used for instrument screening to mitigate horizontal pleiotropy, rather than representing a comprehensive list of clinical differential diagnoses.

as MR outcome data. (1) UK Biobank primary cardiomyopathy: Cases of primary (non-ischemic) cardiomyopathy in UK Biobank were defined as participants with any cardiomyopathy diagnosis (e.g. dilated or hypertrophic cardiomyopathy, ICD-10 I42/I43) not attributable to ischemic heart disease. There were 522 cases and 455 826 controls of European ancestry in this analysis. (2) FinnGen Non-ischemic Cardiomyopathy: FinnGen Release 11 results were used for the endpoint "Non-ischemic cardiomyopathy," which had 2 108 cases and 413 400 controls of Finnish ancestry. FinnGen cases were identified via ICD codes (e.g. I42.x excluding ischemic causes); summary statistics were obtained from the FinnGen open data portal. (3) FinnGen restrictive cardiomyopathy: This analysis from FinnGen R11 included 114 cases of restrictive cardiomyopathy (a rare phenotype) and 492 699 controls. In both FinnGen GWAS, logistic models were adjusted for age, sex, genotype batch, and population structure, and individuals with confounding conditions (such as ischemic heart disease, chronic heavy alcohol use, uncontrolled diabetes, obesity, severe hypertension, or chronic kidney disease) were excluded by FinnGen's endpoint definitions to isolate idiopathic cardiomyopathy.

For each protein, its causal effect on cardiomyopathy were estimated in each GWAS dataset using appropriate MR methods: the Wald ratio for single-instrument proteins and inverse-variance weighted (IVW) meta-analysis for proteins with multiple independent pQTLs. Heterogeneity among instruments was evaluated using Cochran's Q test, and a random-effects IVW model was used for sensitivity analysis when significant heterogeneity was detected; however, fixed-effects IVW was used for primary results due to typically small instrument numbers.

In ther analysis, most MR *P*-values were relatively large, and after FDR correction, no protein reached statistical significance. Therefore, the MR results were treated

as hypothesis-generating signals for prioritization rather than definitive discovery. Nominal MR evidence together with a pre-specified multi-dimensional scoring framework were used to select candidates for prospective clinical testing. This approach enables the identification of potentially meaningful biomarkers that might otherwise be overlooked due to statistical conservatism. Finally, MR results across the 3 cardiomyopathy GWAS datasets were synthesized using fixed-effect meta-analysis (inverse-variance weighted) to generate overall estimates and assess consistency.

Protein Prioritization Scoring Scheme

To prioritize candidates for clinical testing, a pre-specified composite scoring framework (Supplementary Table 1) intended as a heuristic ranking tool rather than formal inference. The component weights and cutoffs were chosen pragmatically a priori to reflect translational considerations, and were not derived from an optimized statistical model. The score combines 4 domains capturing direction concordance across datasets, magnitude of MR effects, nominal statistical support, and prior literature evidence. Proteins above a predefined score threshold were shortlisted, and final selection for ELISA testing further considered assay availability and clinical feasibility. This composite scoring framework was defined for the present study and has not been externally validated.

After performing 2-sample MR separately in 3 cardiomyopathy GWAS datasets (UK Biobank primary cardiomyopathy, FinnGen non-ischemic cardiomyopathy, and FinnGen restrictive cardiomyopathy), each protein was prioritized using a 4-dimension composite score (range 0-9):

1. Direction concordance (0–2 points): Proteins received higher scores when the direction of association was consistent across the three cardiomyopathy GWAS datasets.
2. Effect magnitude (0–2 points): Proteins were ranked according to the relative magnitude of the observed MR effect estimates, with larger effects receiving higher scores.
3. Nominal statistical support (0–2 points): Proteins with stronger nominal statistical evidence in the broader cardiomyopathy GWAS analyses received higher scores.
4. Prior literature evidence (0–3 points): Prior evidence was evaluated according to the extent of human, genetic, clinical, or experimental support linking each protein to cardiomyopathy, heart failure, myocardial remodeling, fibrosis, inflammation, or related cardiac phenotypes.

Proteins with a total score ≥5 were shortlisted for potential clinical validation. Ties were broken by smaller meta-analytic *P*-values. This composite scoring framework was defined for the present study and has not been externally validated.

Clinical Cohort

This was a prospective case–control, exploratory clinical validation study. A total of 81 individuals were prospectively recruited for clinical validation of identified biomarkers, including 48 patients with cardiomyopathy (cases) and 33 healthy controls. Cardiomyopathy subtypes (dilated, hypertrophic, and restrictive) were adjudicated by cardiologists based on comprehensive clinical records and echocardiographic findings, in accordance with contemporary diagnostic criteria. Secondary causes were excluded based on documented clinical assessments and available investigations. Baseline assessment and blood sampling were completed at enrollment (morning phlebotomy prior to any cardiac-specific treatment); no longitudinal follow-up was conducted, and therefore no loss to follow-up occurred. The sample size was feasibility-based; no a priori calculation was performed. Effect sizes (odds ratios) with 95% confidence intervals are reported, and findings require external validation in independent cohorts. Patients were enrolled from December 2022 to May 2025 at a single tertiary center. All participants provided written informed consent, and the study protocol was approved by the Institutional Review Board (approval No. 2022-KY-003; April 2022). Inclusion criteria for cases were a diagnosis of cardiomyopathy (predominantly non-ischemic etiologies, confirmed by imaging and clinical evaluation) prior to initiation of therapy. Controls were volunteers with no history of heart failure or structural heart disease, frequency-matched to cases by age and sex. At enrollment, a detailed medical history and physical examination were obtained. Laboratory personnel were blinded to case–control status. Whole blood (5 mL in EDTA) was processed within 30 minutes of collection; plasma was aliquoted and stored at −80 °F until assays.

All participants underwent standard transthoracic echocardiography using a Sonoscape ultrasound system, performed by experienced sonographers. Key echocardiographic parameters included left ventricular end-diastolic diameter (LVEDD), left atrial diameter (LA), interventricular septal thickness (IVS), ejection fraction (LVEF), fractional shortening (FS), and mitral inflow velocities (E, A) for calculation of the E/A ratio. These measurements were used to assess left ventricular size and systolic function (LVEDD, LVEF, FS), wall thickness (IVS), atrial enlargement (LA), and diastolic filling patterns (E/A ratio). All procedures were conducted in accordance with the Declaration of Helsinki and applicable regulations.

All plasma samples were analyzed using commercially available sandwich ELISA kits for 8 proteins: CD163 (Proteintech, KE00190), LGALS3BP (Proteintech, KE00155), FABP5 (CUSABIO, CSB-EL007946HU), FSTL3 (Thermo Fisher, EHFSTL3), VCAM1 (CUSABIO, CSB-E04753h), PICP (Cloud-Clone, SEA573Hu), Galectin-3 (Proteintech, KE00126), and PIIINP (Cloud-Clone, SEA570Hu). All assays were performed in accordance with the manufacturers' protocols. Briefly, samples and standards were loaded in duplicate into 96-well plates pre-coated with target antibodies, incubated, washed, and then treated with detection antibodies and colorimetric substrate according to the kit instructions. Optical density was read at the specified wavelength, and concentrations were calculated using standard curves generated for each assay. All samples were measured blinded to clinical group.

Receiver Operating Characteristic Analysis and Multivariable Biomarker Model

For the single-center case–control cohort (48 cardiomyopathy cases and 33 controls), plasma concentrations of 5

biomarkers (CD163, LGALS3BP, FABP5, FSTL3, VCAM1) were analyzed. Participants with missing biomarker values were excluded from Receiver operating characteristic (ROC) analyses (complete-case analysis). Each biomarker was standardized to z-scores before modeling.

For individual ROC curves, a univariable logistic regression with case/control status as the outcome was fitted for each biomarker, and the model-based predicted probabilities were used to derive the ROC curve and area under the curve (AUC).

For combined prediction, the 4-protein panel (CD163, LGALS3BP, FABP5, and FSTL3) was selected as the primary combined model, given the modest individual discrimination of VCAM1. To quantify the incremental value of VCAM1, a 5-protein model including VCAM1 was additionally fitted, and compared the discrimination of the 4- and 5-protein models using DeLong's test (Supplementary Table 2). As VCAM1 provided negligible incremental contribution, the 4-protein panel was retained as the primary combined model. Predicted probabilities from the multivariable biomarker model were used to construct the combined ROC curve and AUC; this multivariable analysis reflects mutual adjustment among biomarkers rather than adjustment for clinical covariates.

Internal validation was performed using bootstrap optimism correction (2000 resamples) and repeated 10-fold cross-validation (50 repeats); corresponding performance metrics are reported in Supplementary Table 2. To assess incremental value beyond routinely available information, sensitivity analyses were conducted by adding the 4-protein panel to base models including age, sex, systolic blood pressure, and either LVEF or LVEDD (Supplementary Table 3).

Statistical Analysis

Clinical analyses were performed in R (v4.x) and/or Python (standard glm/scikit-learn routines for logistic regression and ROC computation) and GraphPad Prism 9 (for descriptive statistics, graphics, and correlation analysis). Associations between plasma biomarkers and echocardiographic parameters were assessed using Spearman correlation. Diagnostic performance was evaluated as described above. For the clinical validation analyses only, a 2-sided $P < .05$ was considered statistically significant.

RESULTS

Proteome-Wide Data Integration and Mendelian Randomization Screening

First, pQTL data from 8 large proteomics cohorts were harmonized z(Supplementary Table 4): Fenland (4775 proteins in 10708 participants),[15] Iceland (4719 proteins in 35559 participants),[16,17] UKB-PPP (2922 proteins in 34557 participants),[19] INTERVAL (2995 proteins in 3301 participants),[18] KORA F4 (1124 proteins in 1000 participants),[21] UKB-PPP Phase I (1463 proteins in 35571 participants),[20] SCALLOP (90 proteins in 30931 participants),[22] and FHS (71 proteins in 6861 participants)[23] (Figure 1). Altogether, 5034 proteins (13636 pQTLs: 2157 cis, 11479 trans) were available for downstream MR (Figure 1).

Cardiomyopathy GWAS and Confounder Filtering

Proteome-wide MR was carried out in 3 cardiomyopathy GWAS datasets: primary cardiomyopathy (PCM) in UK Biobank (522 cases, 455826 controls), Non-Ischemic Cardiomyopathy (NICM) in FinnGen R11 (2108 cases, 413400 controls), and restrictive cardiomyopathy (RCM) in FinnGen R11 (114 cases, 492699 controls). Prior to MR, all pQTLs were filtered to remove any variants ($P < 5 \times 10^{-8}$) associated with key confounders—alcohol consumption, smoking status, measures of adiposity, type 2 diabetes, systolic/diastolic blood pressure, and eGFR—thereby minimizing horizontal pleiotropy.

Mendelian Randomization-Derived Protein Associations

Inverse-variance weighted MR (or Wald ratio when only 1 instrument was available) was then performed in each GWAS, and the 3 sets of estimates were combined by fixed-effects meta-analysis.

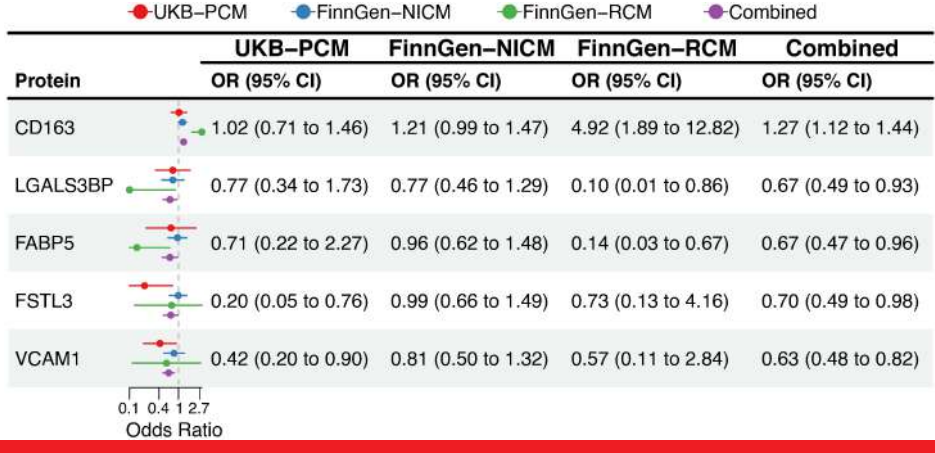

Protein	UKB–PCM OR (95% CI)	FinnGen–NICM OR (95% CI)	FinnGen–RCM OR (95% CI)	Combined OR (95% CI)
CD163	1.02 (0.71 to 1.46)	1.21 (0.99 to 1.47)	4.92 (1.89 to 12.82)	1.27 (1.12 to 1.44)
LGALS3BP	0.77 (0.34 to 1.73)	0.77 (0.46 to 1.29)	0.10 (0.01 to 0.86)	0.67 (0.49 to 0.93)
FABP5	0.71 (0.22 to 2.27)	0.96 (0.62 to 1.48)	0.14 (0.03 to 0.67)	0.67 (0.47 to 0.96)
FSTL3	0.20 (0.05 to 0.76)	0.99 (0.66 to 1.49)	0.73 (0.13 to 4.16)	0.70 (0.49 to 0.98)
VCAM1	0.42 (0.20 to 0.90)	0.81 (0.50 to 1.32)	0.57 (0.11 to 2.84)	0.63 (0.48 to 0.82)

Figure 2. Forest plots of odds ratios for candidate proteins across 3 cardiomyopathy GWAS datasets. Forest plots showing mendelian randomization-derived odds ratios (ORs) and 95% confidence intervals (CIs) for each candidate protein (CD163, LGALS3BP, FABP5, FSTL3, VCAM1) across UKB–Primary Cardiomyopathy (PCM), FinnGen Non-ischemic Cardiomyopathy (NICM), FinnGen Restrictive Cardiomyopathy (RCM), and the combined meta-analysis. Directionally consistent associations and pooled effects support the potential causal relevance of these proteins to cardiomyopathy risk.

Overall, proteome-wide MR prioritized 27 proteins with scores ≥5 (Supplementary Table 1). From this set, 5 proteins were selected for further validation—CD163, LGALS3BP, FABP5, FSTL3, and VCAM1—based on prior evidence implicating them in cardiomyopathy biology. In fixed-effects meta-analysis of MR estimates across primary cardiomyopathy, non-ischemic cardiomyopathy, and restrictive cardiomyopathy GWAS, the pooled odds ratios per 1-SD increase in genetically predicted protein level were as follows: CD163, 1.27 (95% CI, 1.12-1.44); LGALS3BP, 0.67 (95% CI, 0.49-0.93); FABP5, 0.67 (95% CI, 0.47-0.96); FSTL3, 0.70 (95% CI, 0.49-0.98); and VCAM1, 0.63 (95% CI, 0.48-0.82) (Figure 2).

Clinical Enzyme-Linked Immunosorbent Assays Validation Cohort Characteristics

From December 2022 to May 2025, 81 participants were prospectively recruited at a single tertiary care hospital. All participants provided written informed consent prior to enrollment, and the study protocol was approved by the institutional ethics committee (IRB no. 2022-KY-003). A total of 48 patients diagnosed with primary cardiomyopathy (CM) and 33 age- and sex-matched healthy controls were included. Demographic characteristics such as age, sex, BMI, blood pressure, smoking and drinking status, diabetes prevalence, and eGFR did not significantly differ between groups (Table 1).

Among cardiomyopathy patients (n = 48), 28 were diagnosed with dilated cardiomyopathy, 14 with restrictive cardiomyopathy, and 6 with hypertrophic cardiomyopathy. Key echocardiographic measurements by subtype are summarized in Supplementary Table 5.

All participants underwent transthoracic echocardiography using a Sonoscape system. The following echocardiographic parameters were recorded: LVEDD, LA, IVS, LVEF, FS, and mitral inflow velocities (E and A) for E/A ratio calculation. Compared with controls, CM patients exhibited markedly impaired cardiac structure and function, including increased LVEDD (58.4 ± 10.7 mm vs. 49.6 ± 2.8 mm, $P < .0001$), enlarged LA (42.0 ± 3.6 mm vs. 34.5 ± 2.7 mm, $P < .0001$), thickened IVS (10.6 ± 2.4 mm vs. 9.0 ± 0.9 mm, $P = .0001$), reduced LVEF (50.3 ± 13.1% vs. 64.1 ± 4.5%, $P < .0001$), decreased FS (23.2 ± 7.7% vs. 34.3 ± 3.6%, $P < .0001$), and a non-significant trend toward higher E/A ratio (1.5 ± 1.1 vs. 1.2 ± 0.2, $P = .0553$).

Plasma concentrations of 8 biomarkers were quantified by sandwich ELISA (Table 1). CM patients exhibited significantly higher levels of inflammatory and fibrotic markers—CD163 (339.7 ± 122.2 ng/mL vs. 143.4 ± 77.7 ng/mL; $P < .0001$), PICP (5.4 ± 1.0 ng/mL vs. 3.9 ± 1.0 ng/mL; $P < .0001$), PIIINP (71.6 ± 12.4 ng/mL vs. 41.4 ± 5.5 ng/mL; $P < .0001$), and Gal-3 (1.9 ± 0.4 ng/mL vs. 1.2 ± 0.4 ng/mL; $P < .0001$)—and significantly lower levels of candidate proteins LGALS3BP (3.1 ± 0.5 μg/mL vs. 6.4 ± 1.0 μg/mL; $P < .0001$), FABP5 (3.8 ± 2.0 ng/mL vs. 5.1 ± 2.0

Table 1. Baseline Characteristics, Plasma Biomarkers, and Echocardiographic Parameters of Study Participants

Characteristics	Subjects [Mean ± SD or n (%)] Healthy Controls (n = 33) (%)	Cardiomyopathy Patients (n = 48) (%)	*P*
Age (years)	50.2 ± 7.7	53.0 ± 11.0	.218
Male (%)	18/33 (54.6)	25/48 (52.1)	>.9999
BMI (kg/m^2)	24.6 ± 2.7	26.0 ± 3.6	.0613
SBP (mm Hg)	123.3 ± 9.8	126.9 ± 11.2	.1385
DBP (mm Hg)	79.3 ± 6.7	81.3 ± 8.0	.234
Smoking (%)	9 (27.27)	20 (41.67)	.2402
Drinking (%)	12 (36.36)	16 (33.33)	.8153
Diabetes (%)	2 (6.06)	6 (12.50)	.462
eGFR (mL/min)	92.0 ± 7.7	90.0 ± 13.5	.442
Plasma markers			
CD163 (ng/mL)	143.4 ± 77.7	339.7 ± 122.2	<.0001
LGALS3BP (μg/mL)	6.4 ± 1.0	3.1 ± 0.5	<.0001
FABP5 (ng/mL)	5.1 ± 2.0	3.8 ± 2.0	.0022
FSTL3 (ng/mL)	9.4 ± 1.9	8.0 ± 1.8	.0007
VCAM1 (ng/mL)	649.1 ± 131.7	558.2 ± 232.9	.046
PICP (ng/mL)	3.9 ± 1.0	5.4 ± 1.0	<.0001
PIIINP (ng/mL)	41.4 ± 5.5	71.6 ± 12.4	<.0001
Gal-3 (ng/mL)	1.2 ± 0.4	1.9 ± 0.4	<.0001
Echocardiographic parameters			
LVEF (%)	64.1 ± 4.5	50.3 ± 13.1	<.0001
FS (%)	34.3 ± 3.6	23.2 ± 7.7	<.0001
LVEDD (mm)	49.6 ± 2.8	58.4 ± 10.7	<.0001
LA (mm)	34.5 ± 2.7	42.0 ± 3.6	<.0001
IVS (mm)	9.0 ± 0.9	10.6 ± 2.4	.0001
E/A ratio	1.2 ± 0.2	1.5 ± 1.1	.0553

BMI, body mass index; DBP, diastolic blood pressure; E/A, ratio of early to late mitral inflow velocity; eGFR, estimated glomerular filtration rate; FS, fractional shortening; IVS, interventricular septal thickness at end-diastole measured on routine transthoracic echocardiography; LA, left atrial diameter; LVEDD, left ventricular end-diastolic diameter; LVEF, left ventricular ejection fraction; SBP, systolic blood pressure.

Table 2. Association of Plasma Protein Levels with Cardiomyopathy Risk: Univariate and Multivariate Logistic Regression <.001

Protein	Univariate OR	Univariate 95% CI	Univariate *P*	Multivariate OR	Multivariate 95% CI	Multivariate *P*
CD163	1.019	1.01–1.03	<.001	1.044	1.01–1.08	.012
LGALS3BP	0.390	0.27–0.56	<.001	0.161	0.04–0.63	.009
FABP5	0.716	0.56–0.92	.008	0.488	0.22–1.10	.083
FSTL3	0.645	0.49–0.85	.002	1.700	0.72–4.00	.224
VCAM1	0.998	1.00–1.00	.050	0.994	0.99–1.00	.131

CI, confidence interval; OR, odds ratio.

ng/mL; $P = .0022$), FSTL3 (8.0 ± 1.8 ng/mL vs. 9.4 ± 1.9 ng/mL; $P = .0007$), and VCAM1 (558.2 ± 232.9 ng/mL vs. 649.1 ± 131.7 ng/mL; $P = .0460$).

Clinical Validation of Protein Biomarkers

In the ELISA-validated cohort, univariate logistic regression showed that higher CD163 levels were associated with increased odds of cardiomyopathy [OR (odds ratio) 1.019; 95% CI, 1.010-1.030; $P = 1.49 \times 10^{-6}$], whereas higher LGALS3BP (OR 0.390; 95% CI, 0.270-0.560; $P = 3.92 \times 10^{-7}$), FABP5 (OR 0.716; 95% CI, 0.560-0.920; $P = .0077$), FSTL3 (OR 0.645; 95% CI, 0.490-0.850; $P = .0018$), and VCAM1 (OR 0.998; 95% CI, 1.000-1.000; $P = .0504$) levels were protective (Table 2). When CD163, LGALS3BP, FABP5, FSTL3, and VCAM1 were entered together in a multivariate model, only CD163 (OR 1.044, 95% CI 1.010-1.078; $P = .0116$) and LGALS3BP (OR 0.161, 95% CI 0.040-0.625; $P = .0087$) remained independent predictors of cardiomyopathy (Table 2). Spearman correlation analysis showed that CD163 and LGALS3BP were associated with several echocardiographic indices of cardiac structure and function, whereas FABP5 and VCAM1 showed weaker or limited correlations (Figure 3A). Receiver-operating characteristic analysis further confirmed CD163's superior discrimination (AUC = 0.917) and LGALS3BP's strong performance (AUC = 0.870), with FSTL3 (AUC = 0.716) and FABP5 (AUC = 0.681) showing moderate accuracy and VCAM1 being less discriminative (AUC = 0.632). Figure 3B shows the ROC curves for CD163, LGALS3BP, FABP5, FSTL3, and the combined four-protein panel, which achieved an apparent AUC of 0.993. Given the limited incremental value of VCAM1, the primary 4-protein combined panel (CD163, LGALS3BP, FABP5, FSTL3) were compared with the 5-protein model including VCAM1; the apparent AUCs were similar (0.993 vs 0.991; $P = .523$). Internal validation indicated optimism-corrected and repeated cross-validated AUCs of 0.988 and 0.980 for the 4-protein panel (Supplementary Table 2). In pre-specified sensitivity analyses adjusting for age, sex, systolic blood pressure, and either LVEF or LVEDD, addition of the 4-protein panel improved discrimination compared with covariates alone (Supplementary Table 3).

DISCUSSION

In this study, large-scale proteomic data from 8 cohorts including more than 120 000 participants and 5 034 circulating proteins were harmonized and integrated, followed by rigorous MR analyses across 3 cardiomyopathy GWAS datasets totaling over 460 000 individuals. After stringent filtering of confounding variants, MHC region exclusion, and LD clumping, 27 proteins with genetically informed associations with cardiomyopathy risk were informed. Five proteins (CD163, LGALS3BP, FABP5, FSTL3, VCAM1), selected based on robust biological plausibility and assay availability, underwent detailed clinical validation in the prospectively enrolled cohort of 81 subjects. In panel refinement analyses with internal validation, VCAM1 provided negligible incremental discrimination; therefore, a parsimonious 4-protein panel was adopted as the primary model. The 4-protein panel showed high apparent discrimination (AUC = 0.993), and bootstrap optimism correction and repeated cross-validation

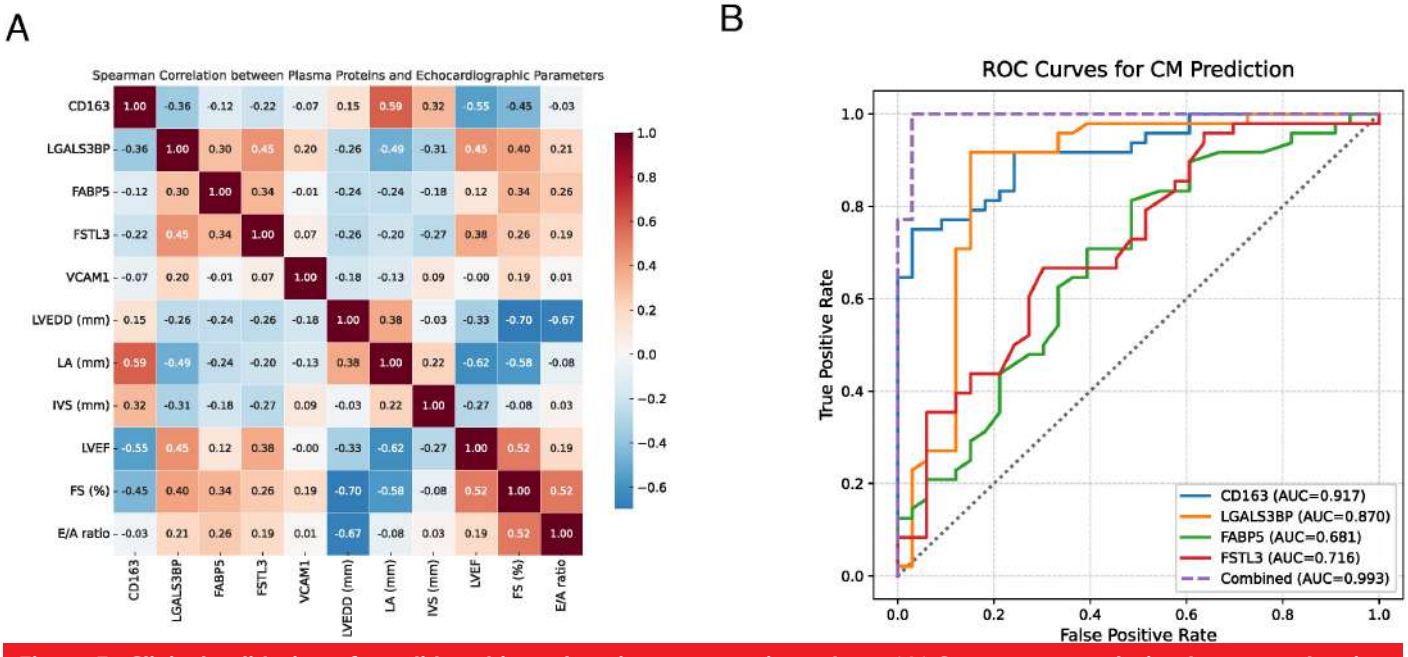

Figure 3. Clinical validation of candidate biomarkers in a prospective cohort. (A) Spearman correlation heatmap showing associations between plasma biomarker levels (CD163, LGALS3BP, FABP5, FSTL3, VCAM1) and echocardiographic parameters (LVEDD, LA, IVS, LVEF, FS, E/A ratio). Red indicates positive correlations; blue indicates negative correlations. (B) Receiver operating characteristic (ROC) curves for the 4 individual proteins (CD163, LGALS3BP, FABP5, and FSTL3) and the combined 4-protein panel. The combined model achieved an apparent (in-sample) AUC of 0.993; given the modest sample size and case–control design, apparent performance may be optimistic. Optimism-corrected and repeated cross-validated AUCs are reported in Supplementary Table 2, and external validation is warranted.

supported its internal performance. However, given the modest sample size and lack of external validation, this result should still be interpreted cautiously.

The study emphasizes CD163 and LGALS3BP as particularly promising biomarkers. CD163, a macrophage-specific scavenger receptor, is widely recognized as a marker of macrophage activation and inflammation, playing a significant role in myocardial remodeling and fibrosis in various cardiovascular conditions.[24] The data, consistent with previous clinical findings, indicate elevated CD163 levels in cardiomyopathy patients correlating strongly with echocardiographic markers of cardiac dysfunction, such as reduced LVEF. Conversely, LGALS3BP has primarily been studied in oncology as a regulator of immune response and extracellular matrix remodeling, but its cardioprotective role in the results, demonstrated by reduced plasma levels and a protective MR effect, suggests an intriguing and previously unrecognized mechanism potentially opposing myocardial fibrosis and remodeling.[25,26]

FABP5 and FSTL3 showed moderate associations with cardiomyopathy in the analyses. FABP5, involved in fatty acid transport and metabolism within cardiomyocytes, has been implicated in metabolic dysregulation contributing to cardiac hypertrophy and dysfunction.[2728] Similarly, FSTL3, known to modulate TGF-β signaling, has been associated with cardiac hypertrophic responses and fibrosis, supporting its relevance as a potential biomarker in cardiac remodeling.[29,30] Although their associations were relatively moderate, both proteins likely reflect distinct but complementary pathogenic pathways contributing to cardiomyopathy. VCAM1 exhibited the weakest association in the study. This adhesion molecule, previously linked with endothelial dysfunction and inflammation in cardiovascular diseases, may reflect broader vascular and inflammatory processes rather than specific myocardial pathology, explaining its relatively lower discriminative capacity.[31-33] Further research in larger and diverse cohorts is warranted to clarify VCAM1's clinical utility and precise role in cardiomyopathy.

Beyond these biological insights, the findings also carry potential clinical implications. In routine practice, establishing an accurate diagnosis of cardiomyopathy can be challenging, and commonly used markers such as NT-proBNP and cardiac troponins are not specific for cardiomyopathy.[34,35] The 4-protein panel—particularly CD163 and LGALS3BP—showed strong discrimination between cardiomyopathy patients and healthy controls in the cohort, supporting its potential as an adjunct to standard diagnostic evaluation. Further validation in larger, independent cohorts will be essential to confirm generalizability and to define its incremental value over routinely available clinical and echocardiographic information.

The MR-driven identification process, integrating extensive proteomic and genetic data with targeted clinical validation, significantly reduces biases and enhances translational potential compared to previous biomarker studies lacking genetic causality support.

Several limitations should be acknowledged. First, the clinical validation was conducted in a relatively small, single-center case–control cohort with a feasibility-based sample size, and no a priori power calculation was performed. Although internal validation using bootstrap optimism correction and repeated cross-validation was performed, the very high apparent AUC of the 4-protein panel should be interpreted with caution, as some degree of model optimism or overfitting cannot be fully excluded in the absence of external validation. Therefore, validation in an independent cohort will be essential to confirm the reproducibility and real-world clinical utility of this biomarker panel. Second, the cohort reflects real-world referrals and may include mild or borderline phenotypes, and cardiomyopathy subtyping relied on clinical records and echocardiography without systematic CMR or genetic testing, introducing potential phenotype misclassification. Third, while extensive instrument filtering was applied, residual horizontal pleiotropy and other sources of bias cannot be fully excluded in MR analyses. In addition, no MR association survived FDR correction, and therefore the proteome-wide MR results should be interpreted as hypothesis-generating, with an increased risk of false-positive prioritization that requires independent replication. Fourth, candidate selection and panel construction were constrained by assay availability, and the cross-sectional design and sample size precluded prognostic assessment and reliable subtype-stratified modeling; therefore, subtype-specific and longitudinal inferences require future studies.

In conclusion, the integrated MR-to-clinical pipeline prioritized circulating protein candidates and identified a 4-protein biomarker panel with promising diagnostic discrimination for primary cardiomyopathy in this exploratory cohort. Given the very high apparent AUC and the lack of external validation, these findings should be considered preliminary and require confirmation in larger, independent cohorts.

AI Disclosure: Large Language Models (ChatGPT) were used only for language polishing of non-substantive text. No AI was used for data analysis or figure generation. All content was verified by the authors.

Ethics Committee Approval: This study was approved by the Ethics Committee of Second People's Hospital of Jintang County, Chengdu, China, (Approval No: 2022-KY-003; Date: April 6, 2022).

Informed Consent: Written informed consent was obtained from all participants before enrollment.

Peer-review: Externally peer-reviewed.

Acknowledgments: The authors thank the Fenland, Iceland, INTERVAL, UKB-PPP, KORA, SCALLOP, and FHS studies for providing proteomics data. Gratitude is extended to all participants, institutions, and staff involved in these studies for their contributions to this research. Appreciation is also extended to all cited studies for sharing data, software, and platforms.

Author Contributions: Concept – Z.Y., J.H.; Design – Z.Y., J.H.; Supervision – Z.Y., J.H.; Resources – J.H., X.Y.L., J.T., C.T., X.F.L.; Materials – J.H., X.Y.L., J.T., C.T., X.F.L.; Data Collection and/or Processing – Z.Y., J.H., X.Y.L., J.T., C.T., X.F.L.; Analysis and/or

Interpretation – J.H., Z.Y., X.Y.L.; Literature Search – J.H., Z.Y., X.Y.L.; Writing – J.H., Z.Y.; Critical Review – J.H., X.Y.L., Z.Y.

Declaration of Interests: None of the authors has any conflicts of interest or serves as a member of the journal's Editorial Board or Advisory Board.

Funding: This work was supported by the Chengdu Municipal Health Commission (Grant No. 2022629).

REFERENCES

1. Kaski JP, Arbelo E. The 2023 ESC guidelines for the management of cardiomyopathies: the 10 commandments. *Eur Heart J*. 2024;45(13):1101. [CrossRef]
2. Karuna N, Tonry C, Ledwidge M, et al. Proteomic-based biomarker discovery reveals panels of diagnostic biomarkers for early identification of heart failure subtypes. *J Transl Med*. 2025;23(1):546. [CrossRef]
3. Nazir A, Nazir A, Afzaal U, et al. Advancements in biomarkers for early detection and risk stratification of cardiovascular diseases-A literature review. *Health Sci Rep*. 2025;8(5):e70878. [CrossRef]
4. Wang Y, Jia H, Song J. Accurate classification of non-ischemic cardiomyopathy. *Curr Cardiol Rep*. 2023;25(10):1299-1317. [CrossRef]
5. Ciarambino T, Menna G, Sansone G, et al. Cardiomyopathies: an overview. *Int J Mol Sci*. 2021;22(14):7722. [CrossRef]
6. Maruyama K, Imanaka-Yoshida K. The pathogenesis of cardiac fibrosis: a review of recent progress. *Int J Mol Sci*. 2022;23(5):2617. [CrossRef]
7. Kong P, Christia P, Frangogiannis NG. The pathogenesis of cardiac fibrosis. *Cell Mol Life Sci*. 2014;71(4):549-574. [CrossRef]
8. Pan K-L, Hsu Y-C, Chang S-T, et al. The role of cardiac fibrosis in diabetic cardiomyopathy: from pathophysiology to clinical diagnostic tools. *Int J Mol Sci*. 2023;24(10):8604. [CrossRef]
9. Stege NM, de Boer RA, van den Berg MP, et al. The time has come to explore plasma biomarkers in genetic cardiomyopathies. *Int J Mol Sci*. 2021;22(6):2955. [CrossRef]
10. Turinay Ertop ZŞ, Aslan AN, Neşelioğlu S, et al. Thiol/disulfide homeostasis: A new oxidative marker in heart failure patients with preserved ejection fraction. *Anatol J Cardiol*. 2024;28(8):406-412. [CrossRef]
11. Örsçelik Ö, Yeşil E, Uyar H, et al. Relationship between urinary angiotensinogen and mortality in patients with heart failure with reduced ejection fraction. *Anatol J Cardiol*. 2023;27(7):417-422. [CrossRef]
12. Si S, Liu H, Xu L, et al. Identification of novel therapeutic targets for chronic kidney disease and kidney function by integrating multi-omics proteome with transcriptome. *Genome Med*. 2024;16(1):84. [CrossRef]
13. Sun J, Zhao J, Jiang F, et al. Identification of novel protein biomarkers and drug targets for colorectal cancer by integrating human plasma proteome with genome. *Genome Med*. 2023;15(1):75. [CrossRef]
14. Raimoglou D, İzgi C, Enar R, et al. Structural and functional impact of Adrenoceptor Beta-1 gene polymorphism in patients with hypertrophic cardiomyopathy and response to beta-blocker therapy. *Anatol J Cardiol*. 2024;28(3):150-157. [CrossRef]
15. Pietzner M, Wheeler E, Carrasco-Zanini J, et al. Mapping the proteo-genomic convergence of human diseases. *Science*. 2021;374(6569):eabj1541. [CrossRef]
16. Eldjarn GH, Ferkingstad E, Lund SH, et al. Large-scale plasma proteomics comparisons through genetics and disease associations. *Nature*. 2023;622(7982):348-358. [CrossRef]
17. Ferkingstad E, Sulem P, Atlason BA, et al. Large-scale integration of the plasma proteome with genetics and disease. *Nat Genet*. 2021;53(12):1712-1721. [CrossRef]
18. Sun BB, Maranville JC, Peters JE, et al. Genomic atlas of the human plasma proteome. *Nature*. 2018;558(7708):73-79. [CrossRef]
19. Sun BB, Chiou J, Traylor M, et al. Plasma proteomic associations with genetics and health in the UK Biobank. *Nature*. 2023;622(7982):329-338. [CrossRef]
20. Sun BB, Chiou J, Traylor M, et al. Genetic regulation of the human plasma proteome in 54,306 UK Biobank participants. *bioRxiv*. 2022:2022.06.17.496443. [CrossRef]
21. Suhre K, Arnold M, Bhagwat AM, et al. Connecting genetic risk to disease end points through the human blood plasma proteome. *Nat Commun*. 2017;8:14357. [CrossRef]
22. Folkersen L, Gustafsson S, Wang Q, et al. Genomic and drug target evaluation of 90 cardiovascular proteins in 30,931 individuals. *Nat Metab*. 2020;2(10):1135-1148. [CrossRef]
23. Yao C, Chen G, Song C, et al. Genome-wide mapping of plasma protein QTLs identifies putatively causal genes and pathways for cardiovascular disease. *Nat Commun*. 2018;9(1):3268. [CrossRef]
24. Skytthe MK, Graversen JH, Moestrup SK. Targeting of CD163+ macrophages in inflammatory and malignant diseases. *Int J Mol Sci*. 2020;21(15):5497. [CrossRef]
25. Capone E, Iacobelli S, Sala G. Role of galectin 3 binding protein in cancer progression: a potential novel therapeutic target. *J Transl Med*. 2021;19(1):405. [CrossRef]
26. Kim D-H, Sung M, Park M-S, et al. Galectin 3-binding protein (LGALS3BP) depletion attenuates hepatic fibrosis by reducing transforming growth factor-β1 (TGF-β1) availability and inhibits hepatocarcinogenesis. *Cancer Commun (Lond)*. 2024;44(10):1106-1129. [CrossRef]
27. Hotamisligil GS, Bernlohr DA. Metabolic functions of FABPs--mechanisms and therapeutic implications. *Nat Rev Endocrinol*. 2015;11(10):592-605. [CrossRef]
28. Storch J, Corsico B. The multifunctional family of mammalian fatty acid-binding proteins. *Annu Rev Nutr*. 2023;43:25-54. [CrossRef]
29. Tian S, Xu X, Yang X, et al. Roles of follistatin-like protein 3 in human non-tumor pathophysiologies and cancers. *Front Cell Dev Biol*. 2022;10:953551. [CrossRef]
30. Ghazal R, Wang M, Liu D, et al. Cardiac fibrosis in the multiomics era: implications for heart failure. *Circ Res*. 2025;136(7):773-802. [CrossRef]
31. Kaur R, Singh V, Kumari P, et al. Novel insights on the role of VCAM-1 and ICAM-1: potential biomarkers for cardiovascular diseases. *Ann Med Surg (Lond)*. 2022;84:104802. [CrossRef]
32. Jager A, van Hinsbergh VW, Kostense PJ, et al. Increased levels of soluble vascular cell adhesion molecule 1 are associated with risk of cardiovascular mortality in type 2 diabetes: the Hoorn study. *Diabetes*. 2000;49(3):485-491. [CrossRef]
33. Gustavsson C, Agardh C-D, Zetterqvist AV, et al. Vascular cellular adhesion molecule-1 (VCAM-1) expression in mice retinal vessels is affected by both hyperglycemia and hyperlipidemia. *PLoS One*. 2010;5(9):e12699. [CrossRef]
34. Spadotto A, Morabito D, Carecci A, et al. The Challenges of Diagnosis and Treatment of arrhythmogenic cardiomyopathy: are We there yet? *Rev Cardiovasc Med*. 2022;23(8):283. [CrossRef]
35. Samanidis G. Current challenges in diagnosis and treatment of cardiovascular disease. *J Pers Med*. 2024;14(8):786. [CrossRef]

Supplementary Table 1. Candidate Protein Prioritization

Protein	Direction-concordance score	Effect-magnitude score	Nominal-evidence score	Prior-evidence score	Total priority score	Selected for ELISA evaluation
CD163	2	2	0	3	7	Yes
LGALS3BP	2	2	0	3	7	Yes
FABP5	2	2	0	2	6	Yes
PTPRR	2	2	2	0	6	No
METTL1	2	2	1	0	5	No
GNRH1	2	2	1	0	5	No
ANXA2	2	0	0	3	5	No
PSAP	2	1	0	2	5	No
SDCBP2	2	2	1	0	5	No
DOS	2	2	1	0	5	No
RCOR1	2	2	1	0	5	No
KRT20	2	2	1	0	5	No
HMBS	2	2	1	0	5	No
HAGH	2	2	1	0	5	No
IL18BP	2	2	1	0	5	No
SH2D1B	2	2	1	0	5	No
PFDN2	2	2	1	0	5	No
DNAJB12	2	2	1	0	5	No
SERPINB4	2	2	1	0	5	No
CCL20	2	2	1	0	5	No
CADM3	2	2	1	0	5	No
CD33	2	2	1	0	5	No
VCAM1	2	2	1	0	5	Yes
ZNF275	1	2	2	0	5	No
FSTL3	2	2	1	0	5	Yes
DDHD2	2	2	1	0	5	No
DNAJB8	2	2	1	0	5	No

Note: The composite score was used as an exploratory heuristic tool for candidate prioritization and not for formal statistical inference. Among the 27 proteins meeting the score threshold, five proteins were selected for ELISA evaluation after additional consideration of biological relevance, complementary pathway representation, commercial assay availability, and clinical feasibility.

Supplementary Table 2. Internal validation of the biomarker panel models

Model	Predictors	Apparent AUC	Optimism-corrected AUC	95% CI	Repeated 10-fold CV AUC	95% range
Four-protein panel (primary)	CD163, LGALS3BP, FABP5, FSTL3	0.993	0.988	0.973–1.000	0.98	0.975–0.985
Five-protein panel (sensitivity)	CD163, LGALS3BP, FABP5, FSTL3, VCAM1	0.991	0.985	0.972–1.000	0.98	0.973–0.985

AUCs were estimated using logistic regression. Internal validation was performed using bootstrap optimism correction (B = 2000 resamples) and repeated stratified 10-fold cross-validation (50 repeats). DeLong test comparing the four- vs five-protein panels: ΔAUC = 0.002, $P = .523$.

Supplementary Table 3. Sensitivity analyses adjusting for age, sex, systolic blood pressure, LVEF and LVEDD

Model	Predictors	Apparent AUC	Optimism-corrected AUC	95% CI	Repeated 10-fold CV AUC	95% range	ΔAUC vs covariates-only	DeLong *P*-value
(A) Sensitivity analyses adjusting for age, sex, systolic blood pressure, and LVEF								
Covariates-only	age, sex, SBP, LVEF	0.878	0.855	0.783–0.934	0.843	0.827–0.855		
Covariates + four-protein panel	age, sex, SBP, LVEF + (CD163, LGALS3BP, FABP5, FSTL3)	0.997	0.993	0.984–1.000	0.988	0.983–0.991	0.119	0.002
(B) Sensitivity analyses adjusting for age, sex, systolic blood pressure, and LVEDD								
Covariates-only	age, sex, SBP, LVEDD	0.826	0.797	0.714–0.889	0.788	0.769–0.803		
Covariates + four-protein panel	age, sex, SBP, LVEDD + (CD163, LGALS3BP, FABP5, FSTL3)	0.996	0.99	0.979–1.000	0.985	0.978–0.990	0.169	0

Models were fitted using logistic regression. Bootstrap optimism correction used B=2000 resamples. Repeated cross-validation used stratified 10-fold CV with 50 repeats; the reported range corresponds to the 2.5th and 97.5th percentiles across repeats. ΔAUC and p-values are based on DeLong tests comparing apparent AUCs.

Supplementary Table 4. Summary Information of Included Proteomics Studies

Study	Platform	Ancestries	Number of proteins	Number of pQTLs	Sample size
Fenland	SomaLogic	European	4,775	8,328	10,708
Iceland	SomaLogic	European	4,719	18,084	35,559
INTERVAL	SomaLogic	European	2,995	1,927	3,301
UKB-PPP	Olink	European	2,922	14,287	34,557
UKB-PPP phase I	Olink	European	1,463	10,248	35,571
KORA F4	SomaLogic	European	1,124	539	1,000
SCALLOP	Olink	European	90	451	30,931
FHS	xMAP	European	71	16,602	6,861

Supplementary Table 5. Key echocardiographic measurements by cardiomyopathy subtype

Subtype	n	LVEF	LVEDD	IVS	LA	E/A
DCM	28	42.4 ± 9.4	66.3 ± 6.0	9.8 ± 1.1	42.2 ± 3.1	0.75 ± 0.16
RCM	14	58.7 ± 9.3	48.4 ± 2.9	9.9 ± 1.0	43.6 ± 3.4	3.02 ± 0.82
HCM	6	67.7 ± 3.0	44.5 ± 2.3	16.2 ± 1.1	37.6 ± 3.4	1.49 ± 0.33

IVS denotes interventricular septal thickness at end-diastole, obtained from routine transthoracic echocardiography.

THE ANATOLIAN JOURNAL OF CARDIOLOGY

Official journal of the TURKISH SOCIETY OF CARDIOLOGY

Composite Uric Acid Index for Prediction of Significant Coronary Stenosis on Computed Tomography Angiography

ABSTRACT

Background: A recently proposed uric acid index combining fasting glucose, triglycerides, and uric acid has shown promise in cardiovascular risk stratification. It was assessed whether the index could predict significant coronary artery stenosis (≥50%) on coronary computed tomography (CT) angiography and compared its diagnostic performance with serum uric acid.

Methods: In this retrospective, single-center study, 258 adults who underwent coronary CT angiography between January 2023 and December 2024 were included. Coronary calcification was scored using the Agatston method by 2 cardiologists. Clinical, demographic, and laboratory data were collected. The uric acid index was calculated as Ln [triglycerides × uric acid × glucose/2]. Univariable and hierarchical multiple logistic regression analyses were performed.

Results: Seventy-one patients (27.5%) showed ≥50% stenosis. Those with stenosis were older and had higher Agatston scores, creatinine, uric acid, glucose, HbA1c, and lower high-density lipoprotein cholestrol (HDL-C). In the final multiple models adjusted for age, sex, creatinine and Agatston score, the uric acid index remained a strong independent predictor of ≥50% stenosis (odds ratio [OR] = 1.988, $P = .019$, 95% confidence interval [CI] = 1.117-3.538). The index demonstrated significant incremental predictive value over the base model, with a Net Reclassification Improvement (NRI) of 0.500 ($P < .05$) and an Integrated Discrimination Improvement (IDI) of 0.029. The area under the curve for the uric acid index (0.688) exceeded that of uric acid (0.664).

Conclusion: In a real-world coronary CT angiography cohort, the composite uric acid index independently predicted significant coronary stenosis. Its incremental predictive value requires validation in larger, prospective studies.

Keywords: Biomarkers, coronary stenosis, CT angiography, uric acid

INTRODUCTION

Ischemic heart disease remains a leading global cause of mortality, posing a substantial public health challenge. Obesity, diabetes, and hypertension—interconnected metabolic and genetic trends—are progressively driving the rise in prevalence.[1] As these upstream risk factors continue to grow, future trends in ischemic disease may worsen, emphasizing the necessity for more accurate predictive metabolic biomarkers.[2] Recent global data indicate an increasing prevalence of cardiovascular disease in individuals who appear healthy and asymptomatic and may harbor risk, thereby emphasizing the necessity for early risk assessment.[3]

Serum levels of triglycerides, glucose, and uric acid, which are interlinked through shared metabolic pathways, have been shown to predict cardiovascular risk more accurately when integrated into composite indices rather than assessed individually.[4,5] A novel uric acid index incorporating glucose, triglycerides, and uric acid demonstrates enhanced predictive capability for cardiovascular risk, exceeding the predictive value of its individual components.[6] However, it remains unclear whether this combined index offers superior predictive value over serum uric acid alone in identifying clinically significant coronary artery lesions. The present study therefore aims to assess the independent predictive power of the

Copyright@Author(s) - Available online at anatoljcardiol.com.
Content of this journal is licensed under a Creative Commons Attribution-NonCommercial 4.0 International License.

ORIGINAL INVESTIGATION

Volkan Çamkıran[1]
Gediz Doğay Us[2,3]
Eray Aksoy[4]
Şahhan Kılıç[5]
Gülsüm Bingöl[6]
Leyla Bulut[7]
Haşim Tüner[8]
Elif Ayduk Gövdeli[9]
Ümit Acar[10]
Batool Achmar[11]
Barış Ökçün[10]
Melih Us[3]

[1]Department of Cardiology, Faculty of Medicine, İstinye University, İstanbul, Türkiye
[2]Department of Cardiovascular Disease, School of Nutrition and Translational Research in Metabolism, Maastricht University, Maastricht, The Netherlands
[3]Department of Cardiovascular Disease, Pax Clinic, İstanbul, Türkiye
[4]Department of Cardiovascular Surgery, Vehbi Koç Foundation American Hospital, İstanbul, Türkiye
[5]Department of Cardiology, Ministry of Health Çorlu State Hospital, Çorlu, Türkiye
[6]Department of Cardiology, Faculty of Medicine, Arel University, İstanbul, Türkiye
[7]Department of Biochemistry, Prof. Dr. Süleyman Yalçın City Hospital, İstanbul, Türkiye
[8]Department of Cardiology, İstanbul Arel University, Memorial Bahçelievler Hospital, İstanbul, Türkiye
[9]Department of Cardiology, Royal Brompton Hospital, Chelsea, London, United Kingdom
[10]Department of Cardiology, İstanbul Üniversitesi – Cerrahpaşa Faculty of Medicine, İstanbul, Türkiye
[11]Bahçeşehir University Faculty of Medicine, İstanbul, Türkiye

Corresponding author:
Volkan Çamkıran
✉ wolfkan36@gmail.com

Received: February 2, 2026
Accepted: June 2, 2026
Available Online Date: July 21, 2026

Cite this article as: Çamkıran V, Us GD, Aksoy E, *et al*. Composite uric acid index for prediction of significant coronary stenosis on computed tomography angiography. *Anatol J Cardiol*. 2026;30(10):693-699.

DOI: 10.14744/AnatolJCardiol.2026.6279

uric acid index for detecting ≥50% coronary artery stenosis as determined by coronary computed tomography (CT) angiography.

METHODS

This retrospective observational study was conducted in the Department of Cardiology of a tertiary-care center. The study protocol was approved by a Local Institutional Ethics Committee at its meeting on January 5, 2023, with decision number 86. All participants provided informed consent. The study was carried out in accordance with the principles of the Declaration of Helsinki.

All consecutive adult patients (≥18 years) who underwent coronary computed tomography (CT) angiography between January 2023 and December 2024 were screened for eligibility. The cohort included both outpatients and inpatients referred for diverse indications, such as routine health check-ups of asymptomatic individuals, evaluation of atypical or typical angina (including intermittent or persistent chest pain), assessment of dyspnea or reduced exercise tolerance, and preoperative cardiac evaluation before noncardiac surgery. Patients with complete demographic and laboratory data were included. Patients were excluded if they had pregnancy, incomplete or missing digital records, known coronary artery disease or prior coronary revascularization (PCI or coronary artery bypass grafting (CABG)), active infection or inflammatory disease, chronic kidney disease (eGFR < 60 mL/min/1.73 m^2), hepatic dysfunction (ALT or AST > 3× upper limit of normal), gout or urate-lowering therapy, malignancy, or use of lipid-lowering or antidiabetic drugs that could influence metabolic parameters.

Coronary calcium scoring was performed using the standard Agatston method[7] by 2 independent cardiologists, and results were recorded in a computerized database. Coronary stenosis severity was graded according to the Coronary Artery Disease—Reporting and Data System (CAD-RADS) classification, and significant stenosis was defined as CAD-RADS ≥3 (≥50% luminal narrowing). Baseline demographic, clinical, and laboratory variables were retrieved from the hospital's electronic medical records and entered into a dedicated study dataset. The uric acid index was calculated as previously described[6] using the formula Ln [fasting triglycerides (mg/dL) × fasting uric acid (mg/dL) × fasting glucose (mg/dL)/2].

HIGHLIGHTS

- A composite uric acid score that combines fasting glucose, triglycerides, and uric acid was tested for predicting substantial coronary stenosis on coronary computed tomography angiography.
- In a retrospective real-world cohort, patients with ≥50% coronary artery stenosis had significantly higher uric acid levels.
- These results provide credence to the possible use of a metabolic composite score in coronary risk assessment, which calls for further investigation.

The normality of continuous variables was tested with the Kolmogorov–Smirnov test. Normally distributed data are presented as mean ± SD and compared using the Student's *t*-test, whereas non-normally distributed data are presented as median [interquartile range] and compared using the Mann–Whitney *U*-test. Categorical variables are expressed as counts and percentages and compared with the chi-square test. Correlations between the uric acid index and metabolic or imaging parameters were assessed using Pearson's (for normally distributed continuous data) or Spearman's (for non-normally distributed continuous data) correlation coefficients as appropriate. To assess the independent predictive value of the uric acid index, a hierarchical multiple logistic regression analysis that is strongly correlated with HbA1c were performed. To avoid multicollinearity, HbA1c was strictly excluded from the multiple models, as the uric acid index formula inherently incorporates fasting glucose levels. The incremental value of the uric acid index was assessed by adding it to a baseline model (containing age, sex, creatinine and Agatston score) and calculating the Net Reclassification Improvement (NRI) and Integrated Discrimination Improvement (IDI). Receiver-operating characteristic (ROC) curves were compared using DeLong's test to evaluate the superiority of the index over serum uric acid alone. Hierarchical logistic regression models were constructed: Model 1 (unadjusted), Model 2 (adjusted for age, sex), and Model 3 (adjusted for age, sex, creatinine, and Agatston score). Receiver-operating characteristic curves were constructed to compare the discriminatory performance of the uric acid index versus uric acid alone, and area under the curve (AUC) values, sensitivities, and specificities were reported. A 2-sided $P < .05$ was considered statistically significant. All statistical analyses were performed using IBM SPSS Statistics, version 19 (IBM Corp., Armonk, NY, USA).

RESULTS

Among the 258 participants, 71 (27.5%) exhibited ≥ 50% stenosis at coronary CT angiography, while 187 (72.5%) had < 50% stenosis. Patients with significant stenosis were older (median 61 [50-70] vs. 51 [43-60] years, $P < .001$), had higher Agatston scores (54 [3-325] vs. 0 [0-13], $P < .001$), and larger ascending aortic diameters (34 [32-38] vs. 33 [29-35] mm, $P = .002$) compared with those without stenosis. Sex distribution did not differ significantly between groups (male 69% vs. 58.3%, $P = .114$) (Table 1).

Laboratory analysis revealed that the ≥ 50% stenosis group had higher serum creatinine (1.0 ± 0.7 vs. 0.8 ± 0.2 mg/dL, $P = .003$), higher uric acid (6.2 [5.1-6.8] vs. 5.1 [3.8-6.2] mg/dL, $P < .001$), higher fasting glucose (97 [84-111] vs. 91 [83-100] mg/dL, $P = .030$), higher HbA1c (6.1 ± 1.4 vs. 5.6 ± 0.7 %, $P = .006$), and lower HDL-C (43 [35-59] vs. 53 [41-64] mg/dL, $P = .012$). The uric acid index was also significantly higher among the participants with ≥ 50% stenosis (10.8 ± 0.7 vs. 10.3 ± 0.8, $P < .001$) (Table 2).

In univariable logistic regression analyses (Table 3), age (OR = 1.056, $P < .001$, 95% CI: 1.025-1.088), creatinine (OR = 11.710; $P = .005$, 95% CI: 2.132-64.302), HbA1c (OR = 1.776; $P = .003$, 95%

Table 1. Comparison of Clinical Data and Demographics Between Patients and Controls

Demographic and Clinical Variables	Patients CAD–RADS ≥III ≥50% Stenosis (n = 71) (%)	Controls CAD–RADS <III <50% Stenosis (n = 187) (%)	*P*
Male gender, n (%)	49 (69)	109 (58.3)	.114
Age (years)	61 (50-70)	51 (43-60)	<.001
Agatston score*	54 (3-325)	0 (0-13)	<.001
Ascending aorta (mm)*	34 (32-38)	33 (29-35)	.002

Expressed as median (interquartile range).

CI: 1.217-2.591), and the uric acid index (OR = 2.176; *P* = .001, 95% CI: 1.392-3.401) were all significantly associated with the presence of ≥ 50% stenosis. Additionally, Agatston score and ascending aorta diameter were also significant predictors.

A hierarchical multiple logistic regression analysis were performed to assess the robustness of the uric acid index as a predictor of ≥50% coronary stenosis (Table 3). In the unadjusted model (Model 1), the uric acid index was strongly associated with significant stenosis (OR = 2.176, *P* = .001, 95% CI: 1.392-3.401). When adjusted for demographic factors including age and male sex (Model 2), the association remained significant (OR = 1.861, *P* = .018, 95% CI: 1.112-3.114). Finally, in the fully adjusted model (Model 3), which further included renal function (creatinine) and Agatston score, the uric acid index retained its independent association with significant stenosis (OR = 1.988, *P*p = .019, 95% CI: 1.117-3.538). The addition of UAI to the base model (age, sex, creatinine, and Agatston score) significantly improved the model's performance (NRI: 0.500; IDI: 0.029). In this final model (Model 3), the Agatston score (OR = 1.005, *P* = .011, 95% CI: 1.001-1.009) and age (OR = 1.057, *P* = .021, 95% CI: 1.008-1.107) were identified as independent predictors, while male sex (*P* = .132) and creatinine (*P* = .297) did not reach statistical significance. HbA1c was excluded from this final model to avoid multicollinearity. This stepwise analysis demonstrates that the predictive value of the uric acid index is robust and independent of key demographic and metabolic confounders.

Receiver-operating characteristic analysis demonstrated that the uric acid index provided slightly superior discrimination for ≥50% stenosis compared with serum uric acid alone (AUC 0.688 vs. 0.664; sensitivity 67% vs. 63%; specificity 70% vs. 65%). According to the DeLong test, this difference in diagnostic performance was statistically significant (*P* = .032) (Table 4).

Table 2. Comparison of Laboratory Characteristics Between Patients and Controls

Laboratory Variables	CT Coronary Angiography ≥50% Stenosis (n = 71)	CT Coronary Angiography <50% Stenosis (n = 187)	*P*
WBC (10^3/μL)	8.1 (6.9-9.5)	7.9 (6.8-9.4)	.422
Hemoglobin (g/dL)	12.9±2.7	13.3±3.1	.224
Creatinine (mg/dL)	1±0.7	0.8±0.2	.003
Urea (mg/dL)	33±13	30±7.6	.387
Sodium (mmol/L)	142±3.9	140±3.4	.651
Potassium (mmol/L)	4.4±0.4	4.3±0.4	.239
Calcium (mg/dL)	9.6±0.5	9.4±1.2	.913
Uric acid (mg/dL)	6.2 (5.1-6.8)	5.1 (3.8-6.2)	<.001
Glucose(mg/dL)	97 (84-111)	91 (83-100)	.030
Albumin (g/L)	4.5±0.4	4.5±0.3	.233
AST (U/L)	20 (16-269)	19 (16-24)	.798
ALT (U/L)	22 (17-30)	21 (16-31)	.473
Total cholesterol (mg/dL)	206 (188-239)	212 (174-246)	.832
LDL-C (mg/dL)	133 (105-155)	127 (90-158)	.447
HDL-C (mg/dL)	43 (35-59)	53 (41-64)	.012
Triglyceride (mg/dL)	161 (108-215)	134 (85-203)	.062
Hb A1c (%)	6.1±1.4	5.6±0.7	.006
Homocysteine (μmol/L)	12 (9.5-15.3)	11.3 (9.7-14.5)	.533
NT-pro BNP (pg/mL)	55 (29-339)	51 (33-74)	.711
Uric acid index	10.8±0.7	10.3±0.8	<.001

Values are presented as mean ± SD or median (interquartile range) depending on normal distribution.
ALT, alanine aminotransferase; AST, aspartate aminotransferase; HBA1c, glycated hemoglobin; HDL-C, high-density lipoprotein cholesterol; LDL-C, low-density lipoprotein cholesterol; NT-pro BNP, N-terminal natriuretic peptide; WBC, white blood cell.

Table 3. Univariate and Multiple Predictors of 50% Stenosis on Coronary CT Angiography

	Univariate Predictors			Multiple Predictors		
	OR	95% CI	*P*	OR	95% CI	*P*
Age (years)	1.056	1.025-1.088	<.001	1.057	1.008-1.107	.021
Male sex	1.583	0.887-2.825	.114	0.417	0.133-1.302	.132
Agatston score	1.007	1.003-1.011	.001	1.005	1.001-1.009	.011
Ascending aorta	1.158	1.063-1.261	.001			
Creatinine	11.710	2.132-64.302	.005	1.755	0.610-5.047	.297
Uric acid	1.503	1.177-1.918	.001			
Glucose	1.013	1.002-1.023	.016			
HDL-C	0.974	0.952-0.996	.023			
Triglyceride	1.002	0.999-1.004	.165			
Hb A1c	1.776	1.217-2.591	.003			
Uric acid index	2.176	1.392-3.401	.001	1.988	1.117-3.538	.019
Hierarchical Models						
Model 1				2.176	1.392-3.401	.001
Model 2				1.861	1.112-3.114	.018
Model 3				1.988	1.117-3.538	.019

Model 1: Unadjusted Uric Acid Model.
Model 2: Model 1 adjusted for Age and Male Sex.
Model 3: Model 2 adjusted for Creatinine and Agatston Score (Fully Adjusted Final Model).
CI, confidence interval; CT, computed tomography; HbA1C, glycated hemoglobin; HDL-C, high-density lipoprotein cholestrol; OR, odds ratio.

Scatter plots illustrating the relationships between the uric acid index and key metabolic and imaging parameters are presented in Figure 1. The uric acid index showed a significant negative correlation with HDL-C (panel a: $r = -.477$, $P < .001$, $r^2 = .228$) and significant positive correlations with ascending aortic diameter (panel b: $r = .365$, $P < .001$, $r^2 = .133$), non-HDL-C (panel c: $r = 0.477$, $P < .001$, $r^2 = 0.228$), triglycerides (panel d: $r = .795$, $P < .001$, $r^2 = .632$), serum uric acid (panel e: $r = .463$, $P < .001$, $r^2 = .214$), and glucose (panel f: $r = .499$, $P < .001$, $r^2 = .249$).

DISCUSSION

This single-center study evaluated whether a composite uric acid index combining fasting triglyceride, glucose, and uric acid values could predict the presence of significant coronary artery stenosis detected by CT angiography. The index was significantly elevated in individuals with ≥50% stenosis and remained an independent predictor even after adjustment for conventional cardiovascular risk factors. Although its discriminatory capacity was modest, it slightly exceeded that of serum uric acid alone. To the best of the knowledge, this study is the first to examine the standalone predictive performance of the uric acid index in cardiovascular risk stratification.

Table 4. ROC Analysis for Prediction of 50% Stenosis in Coronary CT Angiography

	Threshold	Specificity	Sensitivity	AUC (95% CI)
Uric acid	>5.6	65	63	0.664
UA index	>10.7	70	67	0.688

AUC, area under the curve; CT, computed tomography; ROC, receiver operating characteristic; UA, uric acid.

While many studies have examined serum uric acid levels in relation to coronary atherosclerosis, compelling evidence in asymptomatic populations supports its value as a screening biomarker. In a community cohort, Kiss et al[8] found that higher serum uric acid was independently associated with coronary artery calcium after adjusting for conventional risk factors. More recently, a CT angiography study showed elevated uric acid to be linked with greater plaque burden and stenosis severity,[9] while another work demonstrated associations with noncalcified plaque beyond calcified lesions.[10] Interestingly, in patients undergoing CABG, Wu et al[11] reported that adding serum uric acid to the TyG index produced a significant improvement in prognostic prediction—change in C-statistic 0.038, continuous NRI 0.336, IDI 0.031 ($P < .001$)—indicating a synergistic effect in patients undergoing surgical revascularization. The findings are consistent with this, showing that in a CT angiography–based cohort, a composite uric acid index retains independent predictive power for ≥50% stenosis, suggesting that integrating uric acid into metabolic indices might modestly improve discrimination compared to uric acid alone. Taken together, these findings support the rationale for further evaluating simple, routinely available metabolic parameters in combination as potential tools for early risk stratification, particularly in populations undergoing noninvasive coronary imaging.

The diagnostic superiority of the uric acid index over serum uric acid alone has been rarely investigated in the literature. Most longitudinal cohorts have focused exclusively on serum uric acid. A large Korean cohort of approximately 92,000 adults without gout reported that each 1 mg/dL increment in uric acid was associated with a 6% higher risk of incident cardiovascular disease or mortality (HR ~1.06).[12] Similarly, the

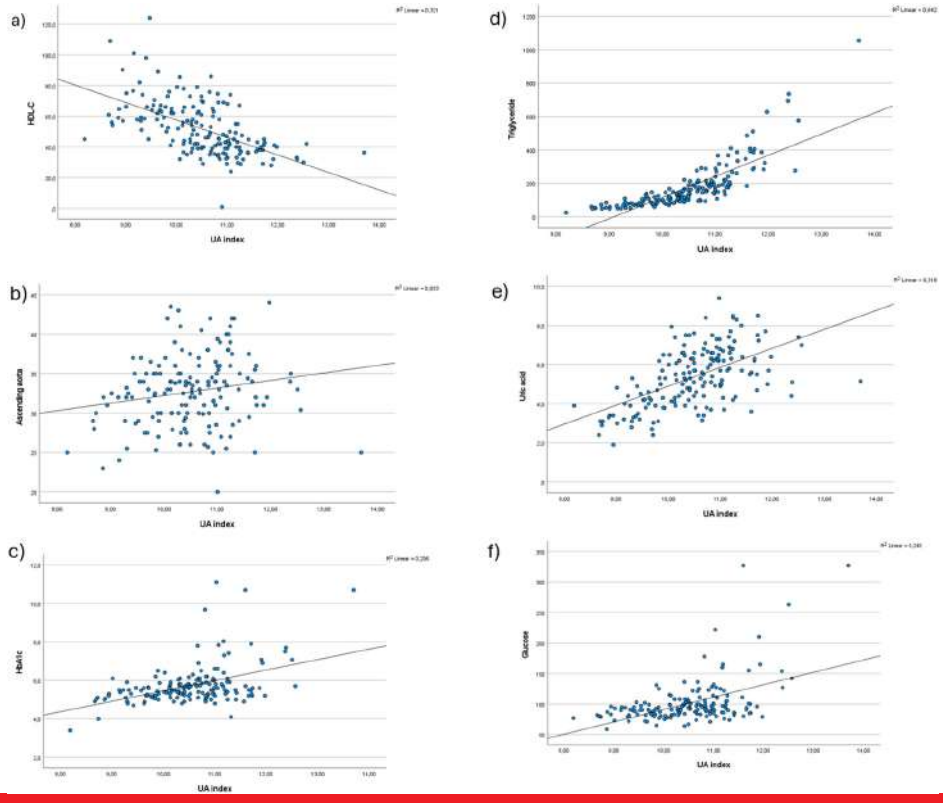

Figure 1. Scatter plots demonstrating linear correlations between the uric acid index and cardiometabolic/imaging parameters. (A) HDL-C ($r = -.477$, $P < .001$, $r^2 = .228$); (B) ascending aortic diameter ($r = .365$, $P < .001$, $r^2 = .133$); (C) non-HDL-C ($r = .477$, $P < .001$, $r^2 = .228$); (D) triglycerides ($r = .795$, $P < .001$, $r^2 = .632$); (E) serum uric acid ($r = .463$, $P < .001$, $r^2 = .214$); (F) fasting glucose ($r = .499$, $P < .001$, $r^2 = .249$). *r*, correlation coefficient; r^2, coefficient of determination; HDL-C, high-density lipoprotein cholesterol; non-HDL-C, non-high-density lipoprotein cholesterol.

URRAH study demonstrated a graded association between uric acid levels and all-cause or cardiovascular mortality, independent of triglyceride levels (adjusted HR 1.53 for all-cause, 2.08 for CVD per 1 mg/dL increase).[13] These studies highlight the prognostic relevance of uric acid as a cardiometabolic biomarker, yet they do not address whether its predictive value improves when incorporated into composite indices.[14] In another study, however, uric acid index showed a stronger correlation with cardiovascular risk ($R^2 = .31$) than uric acid alone ($R^2 = .19$), and remained independently associated with high cardiovascular risk after adjustment (PRa = 1.58, 95% CI 1.11-2.24).[10] The results align with these findings, demonstrating that a composite uric acid index is elevated among individuals with significant coronary stenosis and retains independent predictive value after controlling for conventional risk factors.

The hierarchical analysis showed that the uric acid index remained a significant predictor even after adjusting for age, sex, renal function and Agatston score. Although the odds ratio decreased slightly from 2.176 to 1.988 after adjustments, the persistence of statistical significance suggests that the index captures a metabolic risk profile not fully explained by traditional risk factors alone. This supports its potential utility as a practical, low-cost screening marker in asymptomatic individuals.

Few studies explored combinations of uric acid with other biomarkers to improve cardiovascular risk prediction. Yi et al[15] showed that the uric acid-to-HDL cholesterol ratio (UHR) was strongly associated with cardiovascular disease incidence, with participants in higher UHR quartiles showing markedly greater CVD rates (quartile 4: 11%) and a non-linear relationship between UHR and cardiovascular risk.[15] Similarly, Zhang et al[16] demonstrated that the uric acid-to-albumin ratio predicted coronary slow flow even among individuals without significant stenosis, suggesting its potential utility in detecting early vascular dysfunction.[16] These observations parallel the findings in a CT angiography cohort, in which a composite uric acid index independently predicted ≥ 50% stenosis. Collectively, the evidence indicates that integrating uric acid with metabolic parameters may modestly enhance cardiovascular risk discrimination compared with single-marker approaches.

The strengths of this study include the use of coronary CT angiography, which allows direct visualization and quantification of coronary artery stenosis, providing a more accurate assessment of subclinical atherosclerosis compared with serum biomarkers or clinical scores alone. In addition, the relatively large sample size enhances the statistical robustness and generalizability of the findings. The study also utilized routinely available biochemical parameters,

making the uric acid index a practical and easily applicable tool in clinical settings.

Limitations of the Study

The study was conducted in a single tertiary-care center and relied on a retrospective review of consecutive cases, which may introduce selection bias and limit the generalizability of the findings. Although all available data were extracted from the digital archive, some potentially relevant variables could not be captured. Laboratory values were obtained in routine clinical practice rather than within a standardized research protocol, introducing the possibility of measurement variability. Due to the retrospective nature of the study, complete laboratory data (specifically HbA1c and creatinine) were not available for all patients, which necessitated the exclusion of some participants from the multiple analysis. Furthermore, to prevent multicollinearity with the glucose component of the index, HbA1c was not included in the final regression model. Additionally, while the Agatston score is a potent predictor of stenosis, its inclusion in the fully adjusted hierarchical model (Model 3) did not attenuate the independent predictive power of the uric acid index. This confirms that the index provides significant incremental value beyond traditional risk factors and coronary calcification. However, larger prospective studies are still warranted to further validate its long-term prognostic utility across diverse populations. Finally, as an observational study, causality between the uric acid index and the presence of significant coronary artery stenosis on CT angiography cannot be established. Larger, prospective studies in different settings are warranted to validate the findings and to define practical cut-off values for the uric acid index in cardiovascular risk assessment.

CONCLUSION

In a real-life cardiology practice, the composite uric acid index—combining triglyceride, glucose, and uric acid—was independently associated with the presence of ≥ 50% stenosis on coronary CT angiography, even after hierarchical adjustment for age, sex, renal function and Agatston score. Although its discriminatory performance was only modestly superior to that of uric acid alone, the findings suggest that combining simple metabolic biomarkers may provide incremental value in cardiovascular risk evaluation. Prospective validation in larger, multi-center, and ethnically diverse cohorts is warranted before considering the routine clinical implementation of this index.

Ethics Committee Approval: This study was approved by the Ethics Committee of Memorial Bahcelievler Hospital (Approval No: 86, Date: 05.01.2023).

Informed Consent: All participants provided informed consent.

Peer-review: Internally peer-reviewed.

Author Contributions: Concept – V.Ç.; Design – V.Ç., M.U.; Supervision – V.Ç., E.Ö., B.Ö.; Resources – E.A., H.T., B.A.; Materials – V.Ç., L.B.; Data Collection and/or Processing – G.D.U., G.B., E.A.G.; Analysis and/or Interpretation – G.D.U., G.B., E.A.G.; Literature Search – Ş.K., M.U.; Writing – V.Ç., G.D.U., E.A., G.B., L.B., Ü.A., B.A.; Critical Review – V.Ç., E.Ö., B.Ö.

Declaration of Interests: The authors have no conflict of interest to declare.

Funding: The authors declared that this study has received no financial support.

REFERENCES

1. Nowbar AN, Gitto M, Howard JP, et al. Mortality from ischemic heart disease. *Circ Cardiovasc Qual Outcomes*. 2019;12(6):e005375. [CrossRef]
2. Wang Y, Li Q, Bi L, et al. Global trends in the burden of ischemic heart disease based on the global burden of disease study 2021: the role of metabolic risk factors. *BMC Public Health*. 2025;25(1):310. [CrossRef]
3. Sun J, Qiao Y, Zhao M, et al. Global, regional, and national burden of cardiovascular diseases in youths and young adults aged 15-39 years in 204 countries/territories, 1990-2019: a systematic analysis of Global Burden of Disease Study 2019. *BMC Med*. 2023;21(1):222. [CrossRef]
4. Ma X, Dong L, Shao Q, et al. Triglyceride glucose index for predicting cardiovascular outcomes after percutaneous coronary intervention in patients with type 2 diabetes mellitus and acute coronary syndrome. *Cardiovasc Diabetol*. 2020;19(1):31. [CrossRef]
5. Hong S, Han K, Park CY. The triglyceride glucose index is a simple and low-cost marker associated with atherosclerotic cardiovascular disease: a population-based study. *BMC Med*. 2020;18(1):361. [CrossRef]
6. Rojas-Humpire R, Jáuregui-Rodríguez K, Albornoz S, et al. Association and diagnostic value of a novel uric acid index to cardiovascular risk. *Pract Lab Med*. 2021;26:e00247. [CrossRef]
7. Agatston AS, Janowitz WR, Hildner FJ, et al. Quantification of coronary artery calcium using ultrafast computed tomography. *J Am Coll Cardiol*. 1990;15(4):827-832. [CrossRef]
8. Kiss LZ, Bagyura Z, Csobay-Novák C, et al. Serum uric acid is independently associated with coronary calcification in an asymptomatic population. *J Cardiovasc Transl Res*. 2018;12(3):204-210. [CrossRef]
9. Lacaita PG, Schoegl S, Barbieri F, et al. The influence of serum uric acid on coronary atherosclerosis plaque phenotypes by computed tomography angiography: the missing link? *Nutr Metab Cardiovasc Dis*. 2024;35(4):103828. [CrossRef]
10. Mello FM, Bensenor IM, Santos IS, et al. Serum uric acid levels and subclinical atherosclerosis: results from the Brazilian Longitudinal Study of Adult Health (ELSA-Brasil). *Curr Probl Cardiol*. 2022;48(3):101525. [CrossRef]
11. Wu Z, Cheng C, Sun X, et al. The synergistic effect of the triglyceride-glucose index and serum uric acid on the prediction of major adverse cardiovascular events after coronary artery bypass grafting: a multicenter retrospective cohort study. *Cardiovasc Diabetol*. 2023;22(1):103. [CrossRef]
12. Kim JY, Seo C, Pak H, et al. Uric acid and risk of cardiovascular disease and mortality: a longitudinal cohort study. *J Korean Med Sci*. 2023;38(38):e302. [CrossRef]
13. Mengozzi A, Pugliese NR, Desideri G, et al. Serum uric acid Predicts All-Cause and cardiovascular Mortality Independently of hypertriglyceridemia in cardiometabolic Patients without Established CV Disease: a Sub-Analysis of the uric acid Right for heArt Health (URRAH) Study. *Metabolites. PubMed*. 2023;13(2):244. [CrossRef]

14. Ndrepepa G. Uric acid and cardiovascular disease—recent evidence on the association and underlying mechanisms. *J Lab Precis Med*. 2025;10:8. [CrossRef]
15. Yi Y, Luo Q, Chen J, et al. Association between the uric acid-to-HDL-cholesterol ratio (UHR) and the risk of cardiovascular disease and dyslipidemia: a population-based study. *Lipids Health Dis*. 2025;24(1):143. [CrossRef]
16. Zhang XJ, Hou AJ, Luan B, et al. Uric acid to albumin ratio as a novel predictor for coronary slow flow phenomenon in patients with chronic coronary syndrome and non-obstructive coronary arteries. *BMC Cardiovasc Disord*. 2024;24(1):358. [CrossRef]

THE ANATOLIAN JOURNAL OF CARDIOLOGY

Official journal of the TURKISH SOCIETY OF CARDIOLOGY

Longitudinal Assessment of Diastolic Function and Myocardial Strain in Type 2 Diabetes: A Comparison of Empagliflozin and Linagliptin

ORIGINAL INVESTIGATION

ABSTRACT

Background: The cardiovascular effects of sodium–glucose cotransporter-2 inhibitors and dipeptidyl peptidase-4 inhibitors have attracted increasing interest in patients with type 2 diabetes mellitus. This study aimed to compare the time-dependent effects of empagliflozin and linagliptin on left ventricular diastolic function and global longitudinal strain (GLS).

Methods: This prospective longitudinal study included 350 patients with type 2 diabetes mellitus treated with empagliflozin (n = 200) or linagliptin (n = 150). Transthoracic echocardiography and speckle-tracking strain analysis were performed at baseline, 1 month, and 6 months. Diastolic function was evaluated using septal e′ velocity, E/e′ ratio, isovolumetric relaxation time (IVRT), and mitral E-wave deceleration time. Longitudinal changes were analyzed using linear mixed-effects models including treatment group, time, and group × time interaction.

Results: Diastolic function parameters improved significantly over time in both groups (all $P < .001$). At follow-up, HbA1c levels decreased in both groups, with comparable glycemic control achieved at 6 months. Significant group × time interactions were observed for septal e′ velocity, E/e′ ratio, and IVRT (all $P < .001$). These findings remained consistent after adjustment for baseline differences. At 6 months, empagliflozin was associated with greater improvement in septal e′ velocity and IVRT, whereas linagliptin resulted in a more pronounced reduction in the E/e′ ratio. Although GLS improved in both groups, its temporal pattern differed significantly between treatments ($P < .001$).

Conclusion: Empagliflozin and linagliptin exert distinct effects on left ventricular diastolic function and myocardial deformation in type 2 diabetes mellitus. Empagliflozin appears to provide earlier improvement in diastolic relaxation and GLS, whereas linagliptin may have a greater effect on filling pressures. These findings should be interpreted cautiously and considered hypothesis-generating; confirmation in randomized controlled trials is required to determine their clinical relevance.

Keywords: Diastolic dysfunction, diabetes mellitus, echocardiography

INTRODUCTION

Type 2 diabetes (T2D) is strongly associated with heart failure (HF), subclinical myocardial dysfunction, and diastolic dysfunction, beyond microvascular complications.[1] In diabetes, early-stage left ventricular relaxation disorders, increased filling pressures, and myocardial deformation anomalies can occur; this phenotype is defined within the concept of "diabetic cardiomyopathy" and predisposes to the development of clinical HF.[2]

Sodium–glucose cotransporter-2 inhibitors (SGLT2i) have become one of the most potent classes of drugs for improving cardiovascular (CV) endpoints in T2D. Empagliflozin has demonstrated significant benefits on HF and renal endpoints; its efficacy has been demonstrated in randomized studies reporting positive effects on clinical endpoints, particularly in the Heart Failure with Reduced Ejection Fraction (HFrEF) population.[3] The fact that empagliflozin also reduces HF hospitalizations in the Heart Failure with Preserved Ejection Fraction (HFpEF) population has supported its inclusion among the essential therapies

Copyright@Author(s) - Available online at anatoljcardiol.com.
Content of this journal is licensed under a Creative Commons Attribution-NonCommercial 4.0 International License.

Oğuz Kaan Kaya[1]
Gökhan Köker[2]

[1]*Department of Cardiology, Antalya Training and Research Hospital, University of Health Sciences, Antalya, Türkiye*
[2]*Department of Internal Medicine, Antalya Training and Research Hospital, University of Health Sciences, Antalya, Türkiye*

Corresponding author:
Oğuz Kaan Kaya
✉ oguzkaankaya@hotmail.com

Received: February 21, 2026
Accepted: June 10, 2026
Available Online Date: July 21, 2026

Cite this article as: Kaya OK, Köker G. Longitudinal assessment of diastolic function and myocardial strain in type 2 diabetes: a comparison of empagliflozin and linagliptin. *Anatol J Cardiol.* 2026;30(10):700-707.

DOI: 10.14744/AnatolJCardiol.2026.6348

in the SGLT2i class of HF spectrum in current guidelines.[4,5] It is suggested that this clinical benefit is due to multiple mechanisms, including osmotic diuresis/natriuresis, reduced preload/afterload, reprogramming of cardiac energy metabolism, reduction of inflammation and oxidative stress, improved endothelial function, and effects at the microvascular level.[6,7]

In the class of dipeptidyl peptidase-4 inhibitors (DPP-4i), cardiovascular safety is generally considered neutral, although interdrug heterogeneity and different effects depending on patient phenotype are discussed.[8] Linagliptin has demonstrated a non-inferior safety profile in large-scale studies, particularly with regard to renal safety and cardiovascular endpoints.[9] However, prospective longitudinal data directly comparing the effects of DPP-4i on diastolic function and myocardial deformation with SGLT2i are limited.[10]

Classic ejection fraction (EF) measurements may be insufficient for detecting early myocardial involvement due to diabetes. Global longitudinal strain (GLS) obtained by speckle-tracking echocardiography is a sensitive indicator of subclinical systolic dysfunction and contributes to early risk stratification in the diabetic population.[11] In diastolic function assessment, parameters such as septal e′, E/e′ ratio, isovolumetric relaxation time (IVRT), and deceleration time (DT) provide complementary information about both relaxation and filling pressures.[12] Furthermore, the potential effects of different systemic stress conditions on diastolic function have been previously highlighted; for example, the potential effects of acute allergic reactions on diastolic function have been reported at the clinical level.[13]

In this context, the aim of the study is to compare the time-dependent effects of empagliflozin and linagliptin on diastolic function parameters (septal e′, E/e′, IVRT, DT) and absolute GLS in patients with T2D in a prospective longitudinal design and to reveal treatment-specific differentiating patterns through group × time interaction.[14]

HIGHLIGHTS

- Empagliflozin and linagliptin demonstrate distinct time-dependent effects on left ventricular diastolic function in type 2 diabetes.
- Empagliflozin treatment is associated with earlier and more sustained improvement in diastolic relaxation parameters and global longitudinal strain.
- Linagliptin shows a more pronounced effect on parameters reflecting left ventricular filling pressures.
- Longitudinal strain imaging enables detection of subclinical myocardial dysfunction despite preserved ejection fraction.
- Findings highlight differential cardiac response patterns between antidiabetic therapies.
- These findings are hypothesis-generating and require confirmation in randomized controlled studies.

METHODS

Study Design and Patient Population

This prospective longitudinal study included a total of 350 patients diagnosed with T2D and scheduled to begin treatment with empagliflozin or linagliptin between January 2020 and June 2024. Patients were divided into empagliflozin (n=200) or linagliptin (n=150) treatment groups according to clinical indications.

Treatment allocation was not randomized and was based on clinical indication and physician discretion, reflecting real-world clinical practice.

Baseline concomitant medications, particularly those potentially affecting diastolic function, were recorded and analyzed.

Ethics Statement

The study was conducted in accordance with the principles of the Declaration of Helsinki. The study protocol was approved by an institutional Clinical Research Ethics Committee on 12 September 2019 (Decision No: 2019-272). Written informed consent was obtained from all participants prior to enrollment.

Inclusion and Exclusion Criteria

The study included patients over 18 years of age with T2D who were in sinus rhythm, had preserved left ventricular EF, and completed scheduled follow-up visits.

Patients meeting any of the following criteria were excluded from the study:

- Recent acute coronary syndrome (within the past 6 months) or clinically unstable coronary artery disease,
- Clinically significant valvular disease,
- Heart failure (LVEF <50%),
- Atrial fibrillation or other persistent arrhythmias,
- Chronic renal failure (eGFR <30 mL/min/1.73 m^2),
- Active infection, systemic inflammatory, or malignant disease,
- Changes in dosage or discontinuation of existing antihypertensive or antidiabetic treatments (other than empagliflozin or linagliptin) during the study period,
- Inadequate image quality that may impair the reliability of echocardiographic measurements.

Patients with stable coronary artery disease were not excluded from the study.

Echocardiographic Evaluation

All patients underwent transthoracic echocardiography using a commercially available ultrasonography system (Philips EPIQ 7, Philips Medical Systems, Andover, MA, USA). Echocardiographic assessments were performed by experienced cardiologists, unaware of the treatment groups. The examinations were performed with the patients in the left lateral decubitus position; parasternal long and short axis and apical 2, 3, and 4-chamber views were obtained in accordance with the guidelines of the American Society of Echocardiography and the European Association of Cardiovascular Imaging.

Left ventricular diameters, wall thicknesses, and systolic function parameters were measured using 2-dimensional and M-mode echocardiography. Left ventricular EF was calculated using the biplane Simpson method. Pulsatile wave Doppler and tissue Doppler imaging techniques were used to evaluate diastolic function; septal early diastolic mitral annulus velocity (e′), transmitral E-wave velocity, E/e′ ratio, IVRT, and mitral E-wave deceleration time (DT) were measured.

Speckle-Tracking and Global Longitudinal Strain Analysis

Global longitudinal strain analysis was performed using the speckle-tracking method obtained from apical 4, 2, and 3-cavity images. Global longitudinal strain measurements were calculated by averaging the values obtained from 3 apical planes. The analyses were performed blindly by an experienced observer. In the study, GLS values were reported as absolute values (absolute GLS) in accordance with clinical interpretation. Echocardiographic and strain assessments were repeated at baseline, at 1 month, and at 6 months of treatment.

Laboratory Evaluation

Fasting venous blood samples were taken from all patients and subjected to biochemical and hematological evaluations. Serum urea and creatinine levels, as well as total cholesterol, LDL cholesterol, HDL cholesterol, and triglyceride levels, were measured using automated biochemistry analyzers.

Complete blood count parameters (hemoglobin, hematocrit, leukocyte, and platelet counts) were evaluated using standard hematology analyzers. All laboratory measurements were performed in the hospital's central laboratory and in accordance with international quality control standards.

Statistical Analysis

Statistical analyses were performed using R software (R Foundation for Statistical Computing, Vienna, Austria). Continuous variables are expressed as mean ± SD, and categorical variables are expressed as number and percentage. For baseline comparisons between groups, the independent samples *t*-test was used for continuous variables, and the chi-square or Fisher exact test was used for categorical variables.

Linear mixed-effects models were used to evaluate time-dependent group differences, including treatment group, time, and their interaction (group × time) as fixed effects and a random intercept for each individual. Additionally, to account for potential confounding due to baseline differences, the models were further adjusted for clinically relevant covariates including age, baseline HbA1c, smoking status, and coronary artery disease. These covariates were selected based on their clinical relevance and potential confounding effects on diastolic function. The group × time interaction term was considered the primary parameter for assessing differential temporal effects between treatment groups.

Given the non-randomized design, covariate-adjusted analyses and within-patient longitudinal comparisons were performed to mitigate the potential impact of baseline differences and selection bias.

In addition, the consistency of the findings was evaluated by comparing adjusted and unadjusted models, which yielded similar results, supporting the robustness of the analysis.

As a sensitivity analysis, repeated-measures analysis of variance (RM-ANOVA) was additionally performed for GLS, septal e′ velocity, E/e′ ratio, and IVRT. Normality was assessed using the Shapiro–Wilk test. Outliers were assessed by visual inspection of boxplots and standardized residuals. Post-hoc pairwise comparisons were adjusted using the Holm method. The consistency of RM-ANOVA findings with the primary linear mixed-effects models was evaluated to assess the robustness of the results.

RESULTS

Initial Clinical and Echocardiographic Features

The study included a total of 350 patients with T2D: 200 who started treatment with empagliflozin and 150 who started treatment with linagliptin.

The groups were similar in terms of age and gender distribution (age: 55.9 ± 6.8 vs. 54.7 ± 7.1 years; male proportion: 46% vs. 44%; $P > .05$ for both). The prevalence of hypertension and coronary artery disease did not differ significantly between the groups ($P > .05$); however, smoking was more frequent in the empagliflozin group ($P < .01$). Baseline HbA1c levels were significantly higher in the linagliptin group (7.71 ± 1.02 vs. 7.11 ± 0.97; $P < .001$).

At baseline echocardiographic evaluation, left ventricular EF was preserved in both groups but was statistically significantly higher in the empagliflozin group (61.9 ± 2.4 vs. 61.1 ± 2.5; $P = .001$). Among diastolic function parameters, IVRT and DT were longer in the empagliflozin group, whereas the E/e′ ratio was higher in the linagliptin group ($P < .01$ for all). Absolute GLS values were similar between groups at baseline (16.0 ± 1.0 vs. 16.3 ± 1.3; $P > .05$). Baseline clinical and echocardiographic characteristics are summarized in Table 1.

Changes Over Time and Intergroup Comparisons

During the follow-up period, significant changes were observed in diastolic function parameters and myocardial deformation measurements in both groups ($P < .001$ for all parameters for time effect). Overall longitudinal changes in myocardial deformation during follow-up are summarized in Figure 1. In linear mixed-effects models, the group × time interaction was significant for septal e′, E/e′ ratio, IVRT, and absolute GLS ($P < .001$ for all).

At follow-up, HbA1c levels decreased in both groups, and comparable glycemic control was achieved at 6 months, suggesting that differences in cardiac parameters were not solely attributable to glycemic effects.

In covariate-adjusted analyses including age, baseline HbA1c, smoking status, and coronary artery disease, the main findings remained robust. Detailed model outputs are provided in the Supplementary Material (Supplementary Table 1). Significant group × time interactions persisted for

Table 1. Baseline Clinical and Echocardiographic Characteristics

Variables	Empagliflozin (n = 200)	Linagliptin (n = 150)	*P*
Age (years)	55.9 ± 8.1	54.7 ± 7.9	.047
Male, n (%)	92 (46)	66 (44)	.792
Hypertension, n (%)	110 (55)	82 (55)	1.000
Smoking, n (%)	38 (19)	53 (35)	.0046
Coronary artery disease, n (%)	20 (10)	28 (19)	<.001
HbA1c (%)	7.11 ± 0.62	7.71 ± 0.68	<.001
LVEF (%)	61.9 ± 3.4	61.1 ± 3.2	.001
IVS (mm)	11.0 ± 1.2	10.8 ± 1.1	.096
LVEDD (mm)	47.6 ± 3.8	48.0 ± 3.6	.242
LVESD (mm)	28.0 ± 3.1	27.6 ± 3.0	.059
IVRT (ms)	108 ± 14	104 ± 13	.002
DT (ms)	225 ± 28	200 ± 26	<.001
Septal e′ (cm/s)	6.14 ± 1.02	6.06 ± 1.01	.616
E/e′	0.97 ± 0.21	1.18 ± 0.24	<.001
|GLS| (%)	16.0 ± 2.1	16.3 ± 2.0	.088

Data are presented as mean ± SD or number (percentage).
P values were calculated using the independent samples *t*-test for continuous variables and the chi-square test or Fisher's exact test, as appropriate, for categorical variables.
DT, deceleration time; GLS, global longitudinal strain; IVRT, isovolumetric relaxation time; HbA1c, glycated hemoglobin; LVEF, left ventricular ejection fraction; IVS, interventricular septum; LVEDD, left ventricular end-diastolic diameter; LVESD, left ventricular end-systolic diameter; IVRT, isovolumetric relaxation time; DT, deceleration time; septal e′, septal early diastolic mitral annular velocity; E/e′, ratio of early transmitral inflow velocity to early diastolic mitral annular velocity; GLS, global longitudinal strain.

GLS ($P < .001$), septal e′ ($P < .001$), E/e′ ratio ($P < .001$), and IVRT ($P < .001$), indicating that the observed differential temporal patterns between empagliflozin and linagliptin were independent of baseline differences.

As a sensitivity analysis, RM-ANOVA was additionally performed. The results were fully consistent with the primary linear mixed-effects models. Significant group × time interactions were observed for GLS ($F = 70.327$, $P < .001$), septal e′ velocity ($F = 84.649$, $P < .001$), E/e′ ratio ($F = 16.101$, $P < .001$), and IVRT ($F = 70.889$, $P < .001$) (Supplementary Table 2).

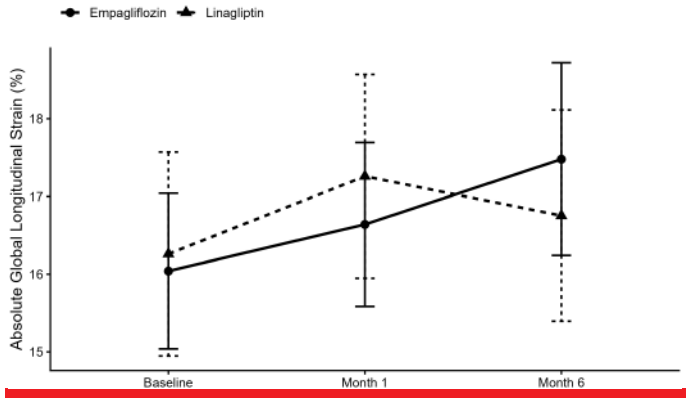

Figure 1. Temporal changes in absolute global longitudinal strain (GLS) during follow-up in patients treated with empagliflozin or linagliptin. Data are presented as mean ± SD at baseline, 1 month, and 6 months. A significant time × treatment interaction was observed, indicating differential longitudinal GLS responses between treatment groups. This interaction remained significant after adjustment for baseline differences. Higher absolute GLS values indicate better left ventricular systolic deformation.

Septal e′

In the empagliflozin group, septal e′ values increased by 0.96 ± 0.11 cm/s at 1 month and by 1.98 ± 0.11 cm/s at 6 months compared with baseline ($P < .001$ for both).

In the linagliptin group, a more limited increase was observed at month 1 (0.76 ± 0.12 cm/s; $P < .001$), while no significant change from baseline was detected at month 6 ($P > .05$). At 6 months, the difference between groups was statistically significant in favor of empagliflozin (–1.99 cm/s; $P < .001$) (Table 2, Table 3). The longitudinal changes in septal e′ velocity according to treatment group are illustrated in Figure 2A.

E/e′ Ratio

In both groups, the E/e′ ratio decreased significantly over time. This decrease was more pronounced in the linagliptin group; a reduction of –0.21 ± 0.02 was observed at 6 months compared with baseline ($P < .001$), whereas a decrease of –0.07 ± 0.02 was observed in the empagliflozin group ($P < .001$). In intergroup comparisons, the linagliptin group exhibited significantly lower E/e′ ratios at all time points ($P < .01$ for all) (Table 2). The longitudinal trends of the E/e′ ratio in both treatment groups are shown in Figure 2B.

Table 2. Between-Group Comparison of Baseline and 6-Month Changes in Echocardiographic and Metabolic Parameters

Parameters	Empagliflozin Baseline	Empagliflozin 6 months	Linagliptin Baseline	Linagliptin 6 months	*P* for group × time interaction
|GLS| (%)	16.04 ± 1.00	17.48 ± 1.08	16.26 ± 1.05	16.75 ± 1.10	<.001 *Pinteraction*
Septal e′ (cm/s)	6.14 ± 1.49	8.12 ± 1.52	6.06 ± 1.43	6.13 ± 1.46	<.001 *Pinteraction*
E/e′	0.97 ± 0.18	0.90 ± 0.17	1.18 ± 0.19	0.97 ± 0.18	<.001 *Pinteraction*
IVRT (ms)	108.5 ± 9.1	96.2 ± 10.4	104.4 ± 9.5	101.9 ± 10.1	<.001 *Pinteraction*

Data are presented as mean ± SD.
Between-group differences over time were assessed using linear mixed-effects models including fixed effects for treatment group, time, and group × time interaction, with a random intercept for each subject. *P* values represent the significance of the group × time interaction. Post-hoc pairwise comparisons were adjusted using the Holm method and were derived from estimated marginal means. All analyses were performed in 200 empagliflozin-treated and 150 linagliptin-treated patients with complete follow-up.
GLS, global longitudinal strain; IVRT, isovolumetric relaxation time.

Table 3. Within-Group Changes in Empagliflozin and Linagliptin

Parameters	Baseline	1 month	6 months	*P* (overall)
A (Empagliflozin)				
|GLS| (%)	16.04 ± 1.00	16.64 ± 1.06	17.48 ± 1.08	<.001
Septal e′ (cm/s)	6.14 ± 1.49	7.10 ± 1.38	8.12 ± 1.52	<.001
E/e′	0.97 ± 0.18	0.93 ± 0.18	0.90 ± 0.17	<.001
IVRT (ms)	108.5 ± 9.1	100.3 ± 11.5	96.2 ± 10.4	<.001
B (Linagliptin)				
|GLS| (%)	16.26 ± 1.05	17.26 ± 1.09	16.75 ± 1.10	<.001
Septal e′ (cm/s)	6.06 ± 1.43	6.82 ± 1.40	6.13 ± 1.46	<.001
E/e′	1.18 ± 0.19	1.10 ± 0.18	0.97 ± 0.18	<.001
IVRT (ms)	104.4 ± 9.5	101.0 ± 10.2	101.9 ± 10.1	<.001

Data are presented as mean ± SD.
Within-group changes over time in the empagliflozin group were assessed using linear mixed-effects models, including time as a fixed effect and a random intercept for each subject.
Post-hoc comparisons were performed using estimated marginal means with Holm adjustment for multiple comparisons.
P values represent comparisons of follow-up time points (month 1 and month 6) vs. baseline.
Within-group changes over time in the linagliptin group were evaluated using linear mixed-effects models including time as a fixed effect and a random intercept for each subject.
Post-hoc comparisons were conducted using estimated marginal means with Holm adjustment for multiple comparisons.
P values represent comparisons of follow-up time points (month 1 and month 6) versus baseline.
GLS, global longitudinal strain; IVRT, isovolumetric relaxation time.

Isovolumetric Relaxation Time and Deceleration Time

A significant reduction in IVRT and DT values was observed in the empagliflozin group. Isovolumetric relaxation time decreased by −12.3 ± 0.5 ms at 6 months compared with baseline in the empagliflozin group ($P < .001$), whereas a more limited reduction of −2.5 ± 0.6 ms was observed in the linagliptin group ($P < .01$). At 6 months, the between-group difference in IVRT was statistically significant in favor of empagliflozin ($P < .001$) (Table 2).

Global Longitudinal Strain

Absolute GLS values improved over time in both groups. In the empagliflozin group, absolute GLS increased from 16.0 ± 1.0 at baseline to 17.5 ± 1.2 at 6 months ($P < .001$). In the linagliptin group, although a more pronounced improvement was observed at 1 month (17.3 ± 1.3), this effect was partially attenuated at 6 months (16.8 ± 1.4). The pattern of GLS change over time differed significantly between groups, as reflected by a significant group × time interaction ($P < .001$) (Figure 1).

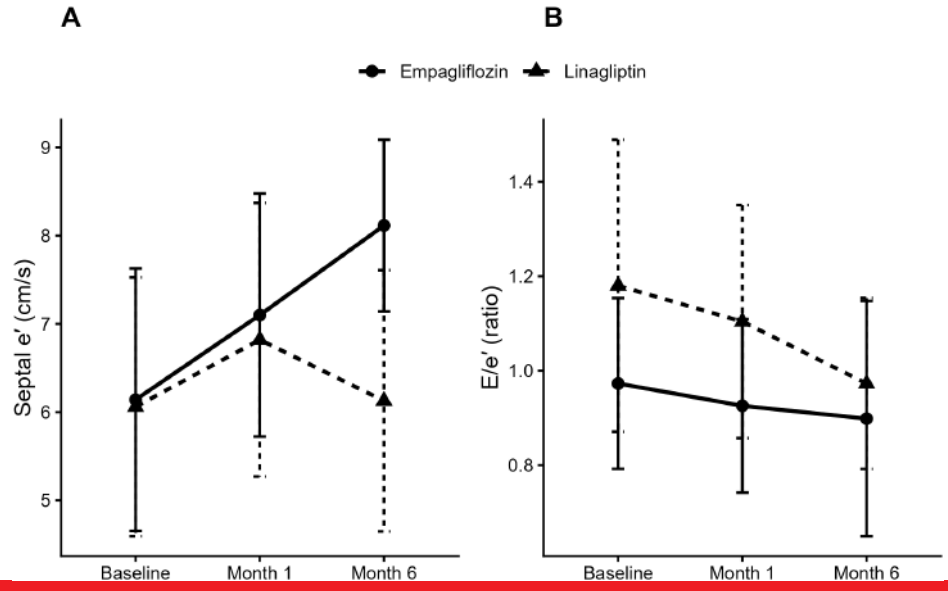

Figure 2. Longitudinal changes in diastolic function parameters during follow-up according to treatment group. (A) Septal early diastolic mitral annular velocity (septal e′). (B) Ratio of early mitral inflow velocity to septal mitral annular velocity (E/e′). Values are presented as mean ± SD at baseline, 1 month, and 6 months. Empagliflozin treatment was associated with greater improvement in septal e′, whereas a more pronounced reduction in E/e′ was observed with linagliptin, reflecting differential effects on left ventricular diastolic function over time. These findings remained consistent in covariate-adjusted analyses. e′, early diastolic mitral annular velocity; E/e′, ratio of early mitral inflow velocity to mitral annular early diastolic velocity.

Summary of Results

In summary, empagliflozin treatment was associated with a more pronounced and sustained improvement in diastolic relaxation parameters (septal e′, IVRT, and DT) and absolute GLS, whereas linagliptin treatment exerted a stronger effect on the E/e′ ratio, reflecting left ventricular filling pressures. These differential response patterns suggest treatment-specific effects on the underlying cardiac phenotype.

DISCUSSION

The findings of this study show that empagliflozin and linagliptin have time-dependent but distinct effects on left ventricular diastolic function and myocardial deformation parameters in patients with T2D. Although improvements in diastolic function parameters and GLS measurements were observed in both treatment arms during the follow-up period, the significant group × time interaction for septal e′, E/e′, IVRT, and absolute GLS suggests that these changes are not solely time-dependent and that the antidiabetic agent used is a determining factor in the direction and magnitude of the cardiac response.

Importantly, these findings remained consistent after adjustment for baseline differences, including age, HbA1c, smoking status, and coronary artery disease, supporting the robustness of the observed treatment-specific temporal patterns.

Baseline differences between groups, particularly in HbA1c levels, smoking status, and coronary artery disease prevalence, should be considered when interpreting the findings, although covariate-adjusted analyses demonstrated consistent results. Importantly, these variables were included in the adjusted mixed-effects models, and the primary findings remained robust after adjustment. Although stable coronary artery disease was included in the study population, it was incorporated as a covariate in the adjusted statistical models and did not materially affect the primary findings. Furthermore, similar results were observed in both adjusted and unadjusted analyses, further supporting the robustness of the findings.

In particular, the empagliflozin group showed a more pronounced and sustained increase in GLS along with early and progressive improvement in diastolic relaxation, while the linagliptin group featured a more significant decrease in the E/e′ ratio, reflecting filling pressures. These differing response profiles may be related to the specific and partially divergent effects of SGLT2 inhibitors and DPP-4 inhibitors on myocardial energy metabolism, preload/afterload balance, interstitial fibrosis, and microvascular function.

However, given the observational and non-randomized nature of the study, these findings should be interpreted with caution, and causal inferences cannot be definitively established.

In this context, the study observed significant changes in both diastolic function and myocardial deformation parameters in T2D patients treated with empagliflozin and linagliptin during a 6-month follow-up period. The most important finding is that the group × time interaction was significant for septal e′, E/e′, and IVRT, and the improvement pattern in absolute GLS diverged between the 2 treatment arms. These results suggest that antidiabetic treatments may affect cardiac phenotype through different mechanisms.[15]

The strong effect of SGLT2i on HF endpoints has been demonstrated with empagliflozin in the HFrEF population; one of the key explanations is that this class reduces hemodynamic overload and modulates congestion via the cardiac-renal axis.[3] The clinical benefits reported with empagliflozin in HFpEF have also made the mechanisms that may affect diastolic function and filling pressures more visible.4 In line with this clinical framework, the data showed a more pronounced increase in septal e′, particularly in the early phase, and shortening of IVRT in the empagliflozin arm, which presented a pattern consistent with improvement in the relaxation phase and an increase in relaxation rate.[16] It is suggested that SGLT2i's effects on microvascular function, intracellular sodium–calcium balance, and mitochondrial efficiency may improve diastolic relaxation and deformation parameters.[6,17]

In the linagliptin group, a more significant decrease in the E/e′ ratio was observed, which may indicate a potential advantage in terms of filling pressures. While cardiovascular safety has been well established,[9] the extent to which these echocardiographic improvements translate into meaningful clinical outcomes remains uncertain, particularly in the absence of hard clinical endpoints in the present study.

When evaluated in terms of GLS, the improvement observed in absolute GLS values in both groups is consistent with the early and modifiable nature of diabetic myocardial dysfunction.[11] However, the divergence of the change pattern over time into 2 groups suggests that the effects of empagliflozin and linagliptin on myocardial deformation cannot be reduced to the same biological pathway.

There are observational/medium-scale studies reporting improvements in deformation parameters in the short-to-medium term in SGLT2i through reduction in preload/afterload and regression of interstitial edema.[18,19] On the DPP-4i side, the data are more heterogeneous, with some studies reporting limited or neutral changes in strain parameters.[20]

In the study, the significant change in DT throughout the follow-up period and the significant signal it gave in terms of group × time interaction emphasize that diastolic filling dynamics should be considered dynamically, not only with relaxation/filling pressure indicators but also with the time components of the transmitral flow pattern.[12] This concept is consistent with recent insights highlighting that the interpretation of left ventricular diastolic function may substantially vary depending on the specific diastolic indices used, underscoring the importance of a comprehensive and methodologically nuanced echocardiographic assessment.[21] This finding is clinically significant because symptom burden and exertional dyspnea in diabetic patients may sometimes be associated with decreased diastolic reserve while EF is preserved.[22]

From a clinical perspective, these findings may suggest that different antidiabetic agents could exert heterogeneous

effects on cardiac functional profiles; however, such interpretations should be considered hypothesis-generating and require confirmation in randomized controlled trials.

In conclusion, this prospective longitudinal study demonstrated that empagliflozin and linagliptin exert time-dependent but significantly different effects on left ventricular diastolic function and myocardial deformation parameters in patients with T2D.

While empagliflozin was associated with a more pronounced and sustained improvement in markers of diastolic relaxation and myocardial deformation, and linagliptin showed a greater effect on parameters reflecting filling pressures, these observations should be interpreted within the limitations of an observational design.

Further randomized and outcome-driven studies are needed to determine the clinical relevance of these differential effects, ideally incorporating clinical endpoints and multimodal imaging approaches to better define their translational significance.

Study Limitations

This study has some limitations. First, the non-randomized design of the study introduces the possibility of selection bias and limits causal inference. Second, a single-center design can limit the generalizability of the results. Third, no invasive hemodynamic measurements were performed; diastolic function was assessed using echocardiographic parameters. Fourth, the study's primary endpoints did not include clinical events (such as hospitalization or mortality due to HF) but focused primarily on echocardiographic phenotyping.

During the follow-up period, dose adjustments or discontinuation of concomitant treatments were minimized using exclusion criteria, but could not be completely ruled out. However, the prospective longitudinal design, the evaluation with serial speckle-tracking echocardiography in the same patients, and the linear mixed-effects model approach based on group × time interaction enhance the methodological power of the study in revealing treatment-specific cardiac response patterns. Finally, although covariate-adjusted analyses were performed, residual confounding related to non-randomized treatment allocation cannot be completely excluded.

CONCLUSION

This prospective longitudinal study demonstrated that empagliflozin and linagliptin exert time-dependent but distinct effects on left ventricular diastolic function and myocardial deformation parameters in patients with T2D. Although improvements in diastolic function parameters and absolute GLS values were observed in both treatment arms, the significant group × time interaction detected for septal e′, E/e′, IVRT, and GLS suggests that this improvement is related to the specific cardiac response profiles of the antidiabetic agents used. Empagliflozin treatment was associated with a more pronounced and sustained improvement pattern, particularly in indicators of diastolic relaxation and myocardial deformation, while linagliptin treatment showed a more significant effect on parameters reflecting filling pressures.

These findings should be considered hypothesis-generating, and further randomized controlled trials with clinical endpoints are required to determine their clinical relevance.

Ethics Committee Approval: This study was approved by the Ethics Committee of Antalya Training and Research Hospital (Approval No: 2019-272, Date: 12 September 2019).

Informed Consent: Written informed consent was obtained from all participants.

Peer-review: Externally peer-reviewed.

Author Contributions: Concept – O.K.K., G.K.; Design – O.K.K., G.K.; Supervision – O.K.K.; Resources – O.K.K., G.K.; Materials – O.K.K., G.K.; Data Collection and/or Processing – O.K.K., G.K.; Analysis and/or Interpretation – O.K.K., G.K.; Literature Search – O.K.K., G.K.; Writing – O.K.K.; Critical Review – G.K.

Declaration of Interests: The authors have no conflict of interest to declare.

Funding: The authors declared that this study has received no financial support.

REFERENCES

1. Cosentino F, Grant PJ, Aboyans V, et al. 2019 ESC Guidelines on diabetes, pre-diabetes, and cardiovascular diseases developed in collaboration with the EASD. *Eur Heart J*. 2020;41(2):255-323. [CrossRef]
2. Dillmann WH. Diabetic cardiomyopathy. *Circ Res*. 2019;124(8):1160-1162. [CrossRef]
3. Packer M, Anker SD, Butler J, et al. Cardiovascular and renal outcomes with empagliflozin in heart failure. *N Engl J Med*. 2020;383(15):1413-1424. [CrossRef]
4. McDonagh TA, Metra M, Adamo M, et al. 2021 ESC Guidelines for the diagnosis and treatment of acute and chronic heart failure. *Eur Heart J*. 2021;42(36):3599-3726. [CrossRef]
5. Anker SD, Butler J, Filippatos G, et al. Empagliflozin in heart failure with a preserved ejection fraction. *N Engl J Med*. 2021;385(16):1451-1461. [CrossRef]
6. Verma S, McMurray JJV. SGLT2 inhibitors and mechanisms of cardiovascular benefit: a state-of-the-art review. *Diabetologia*. 2018;61(10):2108-2117. [CrossRef]
7. Heerspink HJL, Stefánsson BV, Correa-Rotter R, et al. Dapagliflozin in patients with chronic kidney disease. *N Engl J Med*. 2020;383(15):1436-1446. [CrossRef]
8. Scheen AJ. Could metformin modulate cardiovascular outcomes differently with DPP-4 inhibitors compared with SGLT2 inhibitors? *Diabetes Metab*. 2021;47(4):101209. [CrossRef]
9. Rosenstock J, Perkovic V, Johansen OE, et al. Effect of linagliptin vs placebo on major cardiovascular events in adults with type 2 diabetes and high cardiovascular and renal risk: The CARMELINA randomized clinical trial. *JAMA*. 2019;321(1):69-79. [CrossRef]
10. Seferović PM, Coats AJS, Ponikowski P, et al. European Society of Cardiology/Heart Failure Association position paper on the role and safety of new glucose-lowering drugs in patients with heart failure. *Eur J Heart Fail*. 2020;22(2):196-213. [CrossRef]
11. Ernande L, Bergerot C, Rietzschel ER, et al. Diastolic dysfunction in patients with type 2 diabetes mellitus: is it really the first

marker of diabetic cardiomyopathy? *J Am Soc Echocardiogr*. 2011;24(11):1268-1275.e1. [CrossRef]
12. Nagueh SF, Smiseth OA, Appleton CP, et al. Recommendations for the evaluation of left ventricular diastolic function by echocardiography: an update from the American Society of Echocardiography and the European Association of Cardiovascular Imaging. *J Am Soc Echocardiogr*. 2016;29(4):277-314. [CrossRef]
13. Kaya OK, Dagli N, Yildiz M, et al. The effect of acute allergic reactions on diastolic heart function. *Clin Invest Med*. 2014;37(2):E70-E76. [CrossRef]
14. Twisk JWR, de Vente W. Hybrid models were found to be very elegant to disentangle longitudinal within- and between-subject relationships. *J Clin Epidemiol*. 2019;107:66-70. [CrossRef]
15. Zinman B, Wanner C, Lachin JM, et al. Empagliflozin, cardiovascular outcomes, and mortality in type 2 diabetes. *N Engl J Med*. 2015;373(22):2117-2128. [CrossRef]
16. Fitchett D, Zinman B, Wanner C, et al. Heart failure outcomes with empagliflozin in patients with type 2 diabetes at high cardiovascular risk: results of the EMPA-REG OUTCOME® trial. *Eur Heart J*. 2016;37(19):1526-1534. [CrossRef]
17. Cowie MR, Fisher M. SGLT2 inhibitors: Mechanisms of cardiovascular benefit beyond glycaemic control. *Nat Rev Cardiol*. 2020;17(12):761-772. [CrossRef]
18. Santos-Gallego CG, Requena-Ibanez JA, San Antonio R, et al. Empagliflozin ameliorates diastolic dysfunction and left ventricular fibrosis/stiffness in nondiabetic heart failure: A multimodality study. *JACC Cardiovasc Imaging*. 2021;14(2):393-407. [CrossRef]
19. Pabel S, Hamdani N, Luedde M, et al. SGLT2 inhibitors and their mode of action in heart failure-has the mystery been unravelled? *Curr Heart Fail Rep*. 2021;18(5):315-328. [CrossRef]
20. Epelde F. Impact of DPP-4 inhibitors in patients with diabetes mellitus and heart failure: an in-depth review. *Medicina (Kaunas)*. 2024;60(12):1986. [CrossRef]
21. Aslanger E, Yıldırımtürk Ö, Akaslan D, et al. Which diastolic pressure should be used to assess diastolic function? *Anatol J Cardiol*. 2024;28(3):158-164. [CrossRef]
22. Dunlay SM, Givertz MM, Aguilar D, et al. Type 2 diabetes mellitus and Heart Failure: a Scientific Statement from the American Heart Association and the Heart Failure Society of America: this statement does not represent an update of the 2017 ACC/AHA/HFSA heart failure guideline update. *Circulation*. 2019;140(7). [CrossRef].

Supplementary Table 1. Group × Time Interaction Results from Linear Mixed-Effects Models

Outcome	Model	F value	*P*
GLS	Adjusted	70.33	<0.001
Septal e′	Adjusted	84.65	<0.001
E/e′	Adjusted	16.10	<0.001
IVRT	Adjusted	70.89	<0.001

Group × time interaction terms derived from linear mixed-effects models adjusted for age, baseline HbA1c, smoking status, and coronary artery disease. Results were consistent across adjusted and unadjusted models, supporting the robustness of the findings

Supplementary Table 2. Group × Time Interaction Results from Repeated-Measures ANOVA (Sensitivity Analysis)

Outcome	Group × Time Interaction F value	*P*
GLS	70.327	<0.001
Septal e′	84.649	<0.001
E/e′	16.101	<0.001
IVRT	70.889	<0.001

Group × time interaction terms derived from repeated-measures ANOVA models. Results were fully consistent with the primary linear mixed-effects models, supporting the robustness of the findings.

THE ANATOLIAN JOURNAL OF CARDIOLOGY

Official journal of the TURKISH SOCIETY OF CARDIOLOGY

Percutaneous Treatment of Ascending Aortic Pseudoaneurysms: A Case Series

CASE REPORT

Fatma Can[1]
Muhsin Melik[1]
Gönül Zeren[1]
İlhan İlker Avcı[2]
Mustafa Azmi Sungur[1]
Melih Öz[3]
Utku Uluköksal[1]
Barış Şimşek[1]
Mehmet Fatih Yılmaz[4]
Can Yücel Karabay[1]

[1]*Department of Cardiology, University of Health Sciences, Dr. Siyami Ersek Thoracic and Cardiovascular Surgery Training and Research Hospital, İstanbul, Türkiye*
[2]*Department of Cardiology, Bayındır İçerenköy Hospital, İstanbul, Türkiye*
[3]*Department of Cardiology, Ümraniye Training and Research Hospital, İstanbul, Türkiye*
[4]*Department of Cardiology, Faculty of Medicine, Yeditepe University, İstanbul, Türkiye*

Corresponding author:
Muhsin Melik
✉ drmuhsinmelik@gmail.com

Available Online Date: August 11, 2026

Cite this article as: Can F, Melik M, Zeren G, et al. Percutaneous treatment of ascending aortic pseudoaneurysms: a case series. *Anatol J Cardiol.* 2026;30(10):708-712.

DOI: 10.14744/AnatolJCardiol.2026.6424

INTRODUCTION

Ascending aortic pseudoaneurysm is a rare clinical entity associated with a high mortality potential and most commonly occurs as a late complication of prior cardiac or aortic surgery. These lesions typically originate from areas where aortic wall integrity has been disrupted during surgical manipulation and are most frequently observed along suture lines, cannulation sites, and aortotomy regions. Nevertheless, cases related to traumatic, infectious, or inflammatory etiologies have also been reported, and in a small proportion of patients, no identifiable precipitating factor can be demonstrated.[1,2]

The clinical presentation spans a wide spectrum; depending on the size and anatomical location of the pseudoaneurysm, patients may remain asymptomatic or may present with symptoms such as chest pain, dysphagia, or hoarseness secondary to compression of adjacent mediastinal structures. However, the clinical course of ascending aortic pseudoaneurysms is often unpredictable and may culminate in life-threatening catastrophic complications, including rupture, fistulization to neighboring structures, embolic events, or the development of a chronic infectious focus. This potentially devastating natural history necessitates early diagnosis and an active treatment approach in most cases.[3]

Through this case series, 3 ascending aortic pseudoaneurysm cases with distinct clinical courses and outcomes are presented to contribute to the existing literature.

CASE REPORTS

Clinical, anatomical, and procedural characteristics of the patients are summarized in Tables 1 and 2.

Case 1

A 76-year-old female patient with a history of aortic valve replacement (AVR) 20 years earlier presented to the emergency department with a pulsatile mass on the chest wall (Video 1). Computed tomographic angiography (CTA) revealed a 10 × 7 cm pseudoaneurysm originating from the proximal portion of the aortic arch and extending into the anterior mediastinum, with active contrast enhancement (Figure 1A).

Given the patient's high surgical risk and the anatomical suitability of the lesion, percutaneous closure was planned. The procedure was performed via the right femoral artery. Initial aortography was performed using a pigtail catheter to assess the relationship between the pseudoaneurysm sac and the ascending aorta, as well as the location of the neck. A 7F ASD delivery system was positioned in the ascending aorta. A 6F right Judkins catheter was then advanced through the delivery system to provide telescopic coaxial support, and the pseudoaneurysm sac was selectively cannulated. After a 0.014-inch ChoICE Extra Support Guide Wire was advanced into the pseudoaneurysm sac to provide stable intraluminal support, the delivery system was advanced to the pseudoaneurysm neck (Figure 1B). The position of the delivery system was confirmed by controlled contrast injection.

Copyright@Author(s) - Available online at anatoljcardiol.com.
Content of this journal is licensed under a Creative Commons Attribution-NonCommercial 4.0 International License.

Table 1. Clinical and Anatomical Characteristics of the Patients

	Case 1	Case 2	Case 3
Age (years)	76	60	66
Sex	Female	Male	Male
Previous cardiac surgery	AVR + MVR (20 years prior)	CABG ×4 + septal myectomy + AML plication + neochordae (11 months prior)	AVR (2 years prior)
Time from index surgery	20 years	8 months (symptom onset)	2 years
Presentation	Pulsatile chest wall mass	Incidental	Chest pain
Infection present	No	Yes (sternal osteomyelitis)	No
Pseudoaneurysm location	Ascending aorta	Ascending aorta	Ascending aorta
Sac diameter	100 × 70 mm	49 × 41.5 mm	76 × 71 mm
Neck diameter	6 mm	7 mm	Not specified
Associated hematoma	No	Yes (~20 mm)	Rupture present
Hemodynamic instability	No	No	Yes

AVR, aortic valve replacement. MVR, mitral valve replacement. AML, anterior mitral leaflet. CABG, coronary artery bypass grafting

Because the pseudoaneurysm neck measured 6 mm, an 8-mm Amplatzer Septal Occluder device (Abbott) was selected to achieve adequate oversizing and stable anchoring. The device was deployed under fluoroscopic guidance to cover the pseudoaneurysm neck (Figure 1C). Before release, control aortography confirmed stable device positioning and the absence of residual leakage. The device was then released, and final aortography demonstrated complete exclusion of the pseudoaneurysm. Follow-up imaging confirmed sustained complete occlusion throughout the 2-year follow-up period (Figure 1D, 1E).

Case 2

Eight months after the index surgery, the patient developed sternal discharge and was treated with antibiotic therapy. During follow-up, the patient underwent reoperation, and 2 infected sternal wires were removed. While the patient was receiving treatment for sternal osteomyelitis, imaging revealed an ascending aortic pseudoaneurysm measuring 49 × 41.5 mm, with a neck diameter of 7 mm (Figure 1F). Owing to the high surgical risk, the case was evaluated by the Heart Team, and percutaneous closure was planned because the pseudoaneurysm anatomy was considered suitable.

Under fluoroscopic and transesophageal echocardiographic (TEE) guidance, vascular access was obtained via the right femoral artery. A 7F ASD delivery system was advanced over Amplatz Super Stiff guidewire into the ascending aorta and positioned close to the pseudoaneurysm neck (Video 2). After removal of the dilator, a 6F right Judkins catheter was advanced through the lumen of the parked delivery system using a telescopic coaxial technique. The pseudoaneurysm sac was selectively cannulated under fluoroscopic guidance, and the position of the catheter tip within the sac was confirmed by controlled contrast injection.

Following successful cannulation, a 0.014-inch ChoICE Extra Support Guide Wire (Boston Scientific) was advanced through the 6F right Judkins catheter into the pseudoaneurysm sac, where a loop was formed to ensure adequate wire stability. After sufficient intraluminal support had been achieved, the 7F ASD delivery system was advanced in a controlled manner over the 6F right Judkins catheter to the level of the pseudoaneurysm neck while maintaining coaxial alignment (Video 3).

Because the pseudoaneurysm neck measured approximately 7 mm on preprocedural imaging, an 8-mm Amplatzer Septal Occluder device (Abbott) was selected to achieve adequate oversizing and secure anchoring. After confirmation of the delivery system position by contrast injection (Video 4), the device was successfully deployed across the pseudoaneurysm neck under combined fluoroscopic and TEE guidance (Video 5). Final angiography and TEE demonstrated complete exclusion of the pseudoaneurysm, with no residual flow or device-related complications (Video 6).

Follow-up computed tomography performed 1 week after the intervention showed no evidence of active contrast extravasation and demonstrated thrombosis of the pseudoaneurysm sac. At the 3-month follow-up, computed tomography confirmed complete closure of the pseudoaneurysm sac, with a reduction in its size (Figure 1G). However,

Table 2. Procedural Results and Follow-up

	Case 1	Case 2	Case 3
Device used	8 mm ASD occluder	8 mm ASD occluder	—
Technical success (angiography)	Complete exclusion	Complete exclusion	—
Early CT (≤1 week)	Mild residual leak	No extravasation	—
Mid-term CT	Complete thrombosis (2 years follow-up)	Complete occlusion (3 months)	—
Late recurrence	No	Yes (14 months)	—
Clinical status at last follow-up	Alive	Died following redo surgical repair	Death before intervention

ASD, Atrial septal defect; CT, computed tomography.

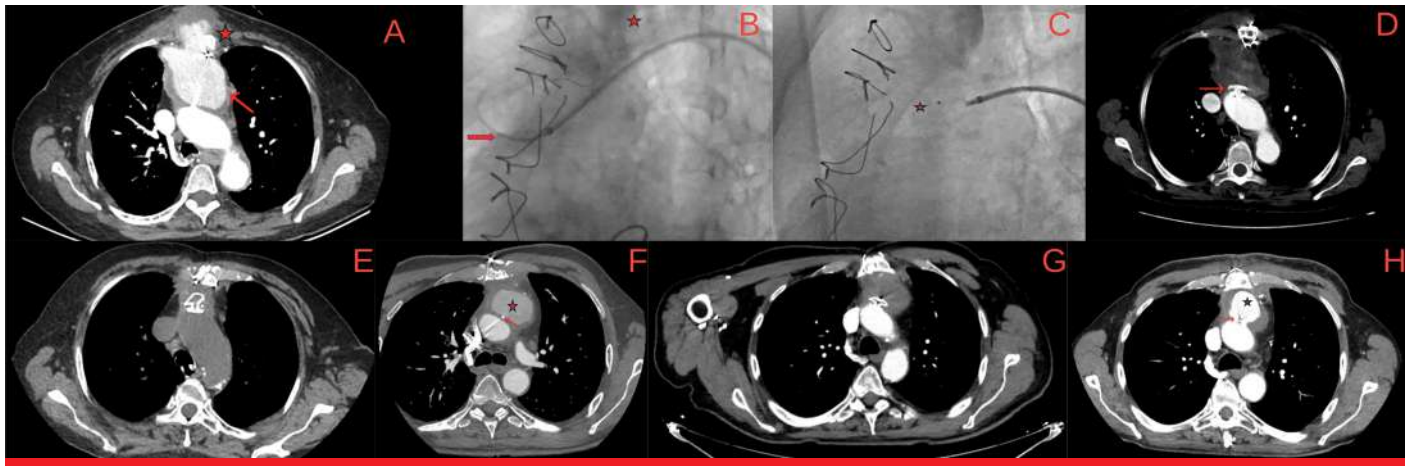

Figure 1. (A) Pre-procedural computed tomography angiography (CTA) demonstrating a 10 × 7 cm pseudoaneurysm arising from the ascending aorta and extending into the anterior mediastinum toward the chest wall with active contrast opacification, with the pseudoaneurysm sac indicated by an arrow and the pulsatile anterior chest wall mass marked with an asterisk. (B) Fluoroscopic image obtained after selective cannulation of the pseudoaneurysm neck with a 6F right Judkins catheter advanced through the 7F ASD delivery system. The 6F right Judkins catheter is indicated by the arrow, and the looped 0.014-inch ChoICE Extra Support guidewire positioned within the pseudoaneurysm sac for stable intraluminal support is indicated by the asterisk. The 7F ASD delivery system was advanced over the wire toward the pseudoaneurysm neck. (C) Fluoroscopic image showing deployment of the 8-mm Amplatzer Septal Occluder device across the pseudoaneurysm neck. The device is indicated by the asterisk. (D) Early post-procedural CTA showing appropriate positioning of the septal occluder device at the pseudoaneurysm neck (arrow) with minimal residual contrast opacification within the sac. (E) Non-contrast CT obtained at 2-year follow-up demonstrating marked reduction in pseudoaneurysm size with complete thrombosis and the occluder device remaining in situ. (F) Pre-procedural CTA demonstrating a 49 × 41.5 mm ascending aortic pseudoaneurysm located at the 2 o'clock position adjacent to the ascending aorta, with the pseudoaneurysm neck indicated by an arrow and the pseudoaneurysm sac marked with an asterisk. An associated hematoma measuring approximately 20 mm is also observed. (G) Early post-procedural CTA demonstrating appropriate device positioning with complete thrombosis of the pseudoaneurysm sac. (H) Fourteen-month follow-up CTA demonstrating recurrent contrast opacification of the pseudoaneurysm sac, with the septal occluder device indicated by an arrow and the recurrent pseudoaneurysm sac marked with an asterisk.

14 months later, the patient re-presented with recurrent discharge from the sternal incision site. Although computed tomography showed that the device remained in a stable position, a recurrent pseudoaneurysm with a maximum diameter of 37 mm, associated with an aortocutaneous fistula, was detected adjacent to the device (Figure 1H). After re-evaluation by the Heart Team, redo surgery was performed; however, the patient died in the early postoperative period.

Case 3

A ruptured ascending aortic pseudoaneurysm followed a catastrophic clinical course. Rapid hemodynamic deterioration occurred shortly after diagnostic imaging, precluding definitive intervention and resulting in cardiovascular collapse.

DISCUSSION

The management of postoperative ascending aortic pseudoaneurysm remains clinically challenging due to its unpredictable course and the absence of a standardized treatment algorithm. In clinical practice, most cases require an invasive approach, and the treatment strategy is primarily determined by surgical risk, the anatomical characteristics of the pseudoaneurysm, and the patient's overall clinical condition. Although surgical repair has long been established as an effective and definitive treatment modality, the need for redo sternotomy and cardiopulmonary bypass significantly complicates decision-making, particularly in high-risk patients.

The case series illustrates the heterogeneous clinical spectrum of postoperative ascending aortic pseudoaneurysms and the variability in treatment response. In the first case, percutaneous closure was both technically and clinically successful, and the patient remained stable during follow-up with a marked reduction in pseudoaneurysm size on serial imaging. In the second case, despite initial technical success and early radiological improvement, recurrence was observed at 14-month follow-up. In the third case, although intervention was planned, the patient experienced rapid hemodynamic deterioration and died, underscoring the potentially fulminant nature of this condition.

Percutaneous closure of ascending aortic pseudoaneurysms has emerged as an important alternative therapeutic option in carefully selected patients with suitable anatomical characteristics and prohibitively high surgical risk. The success of this approach depends on meticulous pre-procedural imaging, appropriate device sizing according to pseudoaneurysm neck diameter, and careful assessment of device stability during the procedure.

In these cases, procedural planning was primarily guided by CTA. Computed tomographic angiography enabled

comprehensive evaluation of critical anatomical details, including pseudoaneurysm neck diameter, neck length, sac morphology, and the relationship of the orifice to the surrounding aortic tissue and adjacent vital structures. During the procedure, fluoroscopy and TEE played complementary roles in real-time device guidance and procedural assessment. The contribution of TEE was multifaceted, allowing confirmation of entry into the pseudoaneurysm sac, assessment of device position and stability, detection of residual flow, and evaluation of the relationship between the device, the aortic wall, and adjacent cardiac structures. In particular, TEE served a complementary and critical role in confirming CTA-based neck measurements and assessing residual shunting after device deployment. This multimodal imaging approach facilitated accurate decision-making regarding device selection and sizing.[4]

During the device sizing process, a mildly oversized occluder device was selected relative to the measured neck diameter in order to ensure stable anchoring and minimize residual flow. Avoiding excessive protrusion of the device into the aortic lumen was considered a fundamental principle during device selection.[5]

Optimal device selection in ascending aortic pseudoaneurysms is not standardized; therefore, the decision-making process should be individualized according to pseudoaneurysm neck diameter, morphology, sac configuration, localization, relationship with adjacent anatomical structures, landing zone suitability, and the ability to safely advance and stabilize the selected device and its delivery system within the ascending aorta.[6] Various endovascular treatment modalities, including septal occluders, vascular plugs, coil embolization, and covered stent-grafts, have been described in the literature. Previous systematic data have demonstrated that Amplatzer septal occluder devices were the most frequently used devices in endovascularly treated cases, followed by vascular plugs and muscular ventricular septal defect (VSD) occluders.[1]

In the treated cases, the presence of a discrete pseudoaneurysm neck with a relatively large sac favored the use of a double-disc occluder system. Atrial septal defect (ASD) occluders were preferred because their broad and symmetric discs allow stable apposition on both sides of the neck, thereby enabling effective sac exclusion while minimizing the risk of device migration in the high-flow, pulsatile environment of the ascending aorta.[6] In contrast, vascular plugs rely primarily on cylindrical intraluminal apposition, which may represent a theoretical disadvantage in short-necked, high-flow pseudoaneurysms because of the potential risk of incomplete sealing, device migration, or late recanalization. Similarly, the bulkier waist configuration of muscular VSD occluders and the asymmetric/tubular design of patent ductus arteriosus (PDA) occluders were considered less suitable for fragile postoperative ascending aortic tissue and wide-sac, short-neck anatomy.

Although covered stent-graft implantation may represent another potential treatment option, it was not preferred in the patients because of ascending aortic localization, inadequate proximal and distal landing zones, aortic curvature, and proximity to the coronary ostia and/or graft anastomoses. These anatomical limitations may complicate safe stent-graft deployment and preservation of adjacent structures; therefore, in patients with favorable neck morphology, an off-label occluder-based closure strategy was considered more appropriate.[6,7]

In this context, procedural technique and system stability represent critical determinants of procedural safety. In the cases, aggressive manipulation within the pseudoaneurysm sac was avoided; stiff guidewires were not used within the sac, and soft-tipped extra-support guidewires were preferred to provide controlled support. This strategy was adopted to minimize the risk of perforation, dissection, or sac rupture in the high-flow and structurally fragile environment of the ascending aorta. In cases of inadequate support, microcatheter use may provide additional coaxial stability and facilitate more controlled and safer advancement, particularly during selective cannulation of the pseudoaneurysm neck.

Nevertheless, despite initially successful closure in the second patient, recurrence developed during 1-year follow-up. Similarly, the recurrence experience reported by Tang et al[4] in a postoperative ascending aortic pseudoaneurysm case and the clinical course described by Gormley et al[8] in a patient with ascending aortic pseudoaneurysm secondary to sternal osteomyelitis suggest that, in pseudoaneurysms with an infectious etiology, a percutaneous approach should often be considered a bridge to surgery rather than definitive therapy. Therefore, dynamic reassessment of treatment strategies remains essential in this subgroup of patients.

CONCLUSION

The management of postoperative ascending aortic pseudoaneurysms requires comprehensive evaluation of etiology, anatomical morphology, and clinical stability. Within a Heart Team–based, individualized treatment framework, percutaneous therapy may offer a safe and feasible alternative in patients with favorable anatomy and high surgical risk when performed with careful technical execution.

Artificial Intelligence Usage Statement: The authors declare that no artificial intelligence (AI)–assisted technologies were used in the preparation of this manuscript.

Informed Consent: Written informed consent was obtained from the patients.

Declaration of Interests: Can Yücel Karabay is an Associate Editor of The Anatolian Journal of Cardiology. The other authors have no conflicts of interest to declare.

Funding: The authors declare that this study received no financial support.

Video 1: Pulsatile anterior chest wall mass in Case 1 due to ascending aortic pseudoaneurysm.

Video 2: Advancement of the 7F ASD delivery system with dilator from the right femoral artery.

Video 3: Advancement of the 7F delivery system over a coaxially stabilized guidewire–catheter rail to the pseudoaneurysm neck.

Video 4: Contrast injection through the delivery system confirming intrapseudoaneurysmal position.

Video 5: Unsheathing and deployment of the septal occluder device through the delivery system.

Video 6: Contrast injection demonstrating final device position and assessment for residual leak.

REFERENCES

1. Quevedo HC, Santiago-Trinidad R, Castellanos J, et al. Systematic review of interventions to repair ascending aortic pseudoaneurysms. *Ochsner J*. 2014;14(4):576-585. https://pmc.ncbi.nlm.nih.gov/articles/PMC4295735/.
2. Kpodonu J, Wheatley GH 3rd, Ramaiah VG, et al. Endovascular repair of an ascending aortic pseudoaneurysm with a septal occluder device: mid-term follow-up. *Ann Thorac Surg*. 2008;85(1):349-351. [CrossRef]
3. Mazzolai L, Teixido-Tura G, Lanzi S, et al. 2024 ESC Guidelines for the management of peripheral arterial and aortic diseases. *Eur Heart J*. 2024;45(36):3538-3700. [CrossRef]
4. Tang L, Lesser JR, Gössl M, et al. Transcatheter closure of complex ascending aortic pseudoaneurysms after cardiac surgery. *Circ Cardiovasc Interv*. 2018;11(9):e007052. [CrossRef]
5. Stehli J, Alie-Cusson FS, Panneton JM, et al. Percutaneous closure of iatrogenic ascending aortic pseudoaneurysms following surgical aortic repair. *JACC Case Rep*. 2021;3(2):327-333. [CrossRef]
6. Hussain J, Strumpf R, Wheatley G, et al. Percutaneous closure of aortic pseudoaneurysm by Amplatzer occluder device-case series of six patients. *Catheter Cardiovasc Interv*. 2009;73(4):521-529. [CrossRef]
7. Abed M, Fukui M, Goessl M, et al. Minimally invasive aortic pseudoaneurysm repair with atrial septal defect occluder. Ann Thorac Surg Short Rep. *Ann Thorac Surg Short Rep*. 2025;3(4):997-999. [CrossRef]
8. Gormley S, Zaman Z, Mani K, et al. Aorto-cutaneous fistula of the ascending aorta-case report and a literature review of endovascular management. *J Vasc Surg Cases Innov Tech*. 2022;9(1):100971. [CrossRef]

THE ANATOLIAN JOURNAL OF CARDIOLOGY

Official journal of the TURKISH SOCIETY OF CARDIOLOGY

Interpreting Early Reticulocyte Response After Intravenous Iron Therapy in Heart Failure

LETTER TO THE EDITOR

To the Editor,

Kumral et al[1] evaluated whether an early reticulocyte rise after intravenous ferric carboxymaltose identifies short-term hematologic response in hospitalized heart failure with left ventricular ejection fraction below 50%.[1] The topic is clinically relevant because intravenous iron is recommended in symptomatic heart failure with iron deficiency, but treatment monitoring still relies on ferritin and transferrin saturation measured weeks after administration.[2]

However, the present data support early biological signal detection rather than a definitive treatment-response marker. First, 183 of 251 screened patients were excluded, mainly because baseline or follow-up laboratory data and clinical follow-up were unavailable.[1] This degree of post-screen exclusion can introduce substantial selection bias. The final analysis included only 68 patients, and the non-responder group was particularly small. Long-term comparisons based on such imbalanced subgroups are vulnerable to unstable event estimates.

Second, the 1-month hemoglobin increase is a post-baseline classification. Associations between this responder status and 2-year emergency visits or mortality should therefore be interpreted as prognostic associations, not as evidence that the early reticulocyte rise mediates later clinical benefit. In the same study, responders already had higher baseline reticulocyte values.[1] This pattern suggests that baseline marrow activity may identify a biologically fitter subgroup with greater erythropoietic reserve, independent of the treatment effect itself.

Third, the manuscript alternates between describing reticulocytes as a percentage of circulating red cells and reporting them in 10^9/L.[1] Clarification of whether the primary analyses used relative reticulocyte percentage, absolute reticulocyte count, or both would improve reproducibility. This distinction is relevant because anemia severity can alter percentage-based interpretation, whereas absolute reticulocyte indices are generally preferred for response assessment.[3]

The current findings justify prospective validation of early reticulocyte kinetics after intravenous iron. They do not yet establish reticulocyte rise as a surrogate for long-term clinical benefit in heart failure, particularly when larger trials of intravenous iron have shown more consistent effects on hospitalization than on mortality.[4,5]

Declaration of Interests: The authors have no conflict of interest to declare.

Funding: The authors declared that this study has received no financial support.

REFERENCES

1. Kumral Z, Uysal H, Yılmaz MB. Perennial parameter for intravenous iron therapy in heart failure: reticulocyte crisis. *Anatol J Cardiol*. 2025;30(2):109-115. [CrossRef]
2. McDonagh TA, Metra M, Adamo M, et al. 2023 Focused update of the 2021 ESC guidelines for the diagnosis and treatment of acute and chronic heart failure. *Eur Heart J*. 2023;44(37):3627-3639. [CrossRef]

Copyright@Author(s) - Available online at anatoljcardiol.com.
Content of this journal is licensed under a Creative Commons Attribution-NonCommercial 4.0 International License.

Hasan Burak İşleyen[1]
Sercan Bulut[2]
Fatih Kızkapan[2]
Cevahir Alioğlu[3]

[1]*Department of Cardiology, Faculty of Medicine, Nişantaşı University, İstanbul, Türkiye*
[2]*Department of Cardiology, Bağcılar Training and Research Hospital, İstanbul, Türkiye*
[3]*Department of Cardiology, Bezmialem Vakıf University, İstanbul, Türkiye*

Corresponding author:
Hasan Burak İşleyen
✉hasanburak.isleyen@nisantasi.edu.tr

Available Online Date: June 5, 2026

Cite this article as: İşleyen HB, Bulut S, Kızkapan F, Alioğlu C. Interpreting early reticulocyte response after intravenous iron therapy in heart failure. *Anatol J Cardiol*. 2026;30(10):713-714.

DOI: 10.14744/AnatolJCardiol.2026.6518

3. Buttarello M. Laboratory diagnosis of anemia: are the old and new red cell parameters useful in classification and treatment, how? *Int J Lab Hematol*. 2016;38(suppl 1):123-132. [CrossRef].
4. Ponikowski P, Kirwan BA, Anker SD, et al. Ferric carboxymaltose for iron deficiency at discharge after acute heart failure: a multicentre, double-blind, randomised, controlled trial. *Lancet*. 2020;396(10266):1895-1904. [CrossRef]
5. Kalra PR, Cleland JGF, Petrie MC, et al. Intravenous ferric derisomaltose in patients with heart failure and iron deficiency in the UK (IRONMAN): an investigator-initiated, prospective, randomised, open-label, blinded-endpoint trial. *Lancet*. 2022; 400(10369):2199-2209. [CrossRef]

THE ANATOLIAN JOURNAL OF CARDIOLOGY

Official journal of the TURKISH SOCIETY OF CARDIOLOGY

Reply to the Letter to the Editor: "Interpreting Early Reticulocyte Response After Intravenous Iron Therapy in Heart Failure"

LETTER TO THE EDITOR
REPLY

To the Editor,

We thank the authors[1] for their interest in our study[2] and for their constructive comments regarding the interpretation of early reticulocyte dynamics following intravenous iron therapy in patients with heart failure.

First, the authors note the high number of excluded patients. As stated in our manuscript, most exclusions were due to the absence of paired laboratory measurements within the predefined 72- to 120-hour window or incomplete follow-up data. Because early reticulocyte assessment is not routinely performed in clinical practice, requiring both baseline and early post-treatment measurements inevitably reduced the analyzable cohort. Nevertheless, this approach was necessary to evaluate early hematologic kinetics following intravenous iron therapy in a real-world clinical setting.

Second, we agree that classification based on a ≥1 g/dL hemoglobin increase at 1 month represents a post-baseline categorization and therefore associations with long-term outcomes should be interpreted cautiously. Our primary aim was to assess whether early reticulocyte dynamics could identify patients demonstrating an active erythropoietic response after intravenous iron therapy. Although responders had higher baseline reticulocyte levels, the predictive signal was not limited to baseline measurements. Importantly, the early dynamic change in reticulocyte levels (delta reticulocyte) was also significantly associated with subsequent hemoglobin increase.

Third, our analyses focused on the change in reticulocyte levels between baseline and 72-120 hours (delta reticulocyte). Receiver operating characteristic analysis identified a >9% increase in delta reticulocyte as the optimal threshold predicting a ≥1 g/dL hemoglobin increase at 1 month, and patients were categorized accordingly.

These findings suggest that early reticulocyte kinetics may represent a practical indicator of early hematologic responsiveness to intravenous iron therapy. While hypothesis generating, they highlight the potential value of early erythropoietic markers for treatment monitoring in patients with heart failure.

Declaration of Interests: The authors have no conflict of interest to declare.

Funding: The authors declared that this study has received no financial support.

REFERENCES

1. İşleyen HB, Bulut S, Kızkapan F, Alioğlu C. Interpreting early reticulocyte response after intravenous iron therapy in heart failure. *Anatol J Cardiol*. 2026;30(10):713-714.
2. Kumral Z, Uysal H, Yılmaz MB. Perennial parameter for intravenous iron therapy in heart failure: reticulocyte crisis. *Anatol J Cardiol*. 2025;30(2):109-115. [CrossRef]

Copyright@Author(s) - Available online at anatoljcardiol.com.
Content of this journal is licensed under a Creative Commons Attribution-NonCommercial 4.0 International License.

Zeynep Kumral
Hacer Uysal
Mehmet Birhan Yılmaz

Department of Cardiology, Dokuz Eylül University, Faculty of Medicine, İzmir, Türkiye

Corresponding author:
Zeynep Kumral
✉ zeynepkumral@gmail.com

Available Online Date: June 5, 2026

Cite this article as: Kumral Z, Uysal H, Yılmaz MB. Reply to the letter to the editor: "interpreting early reticulocyte response after intravenous iron therapy in heart failure". *Anatol J Cardiol*. 2026;30(10):715.

DOI: 10.14744/AnatolJCardiol.2026.6560

THE ANATOLIAN JOURNAL OF CARDIOLOGY

Official journal of the TURKISH SOCIETY OF CARDIOLOGY

Ambiguity of Medina 0.0.1 Bifurcation Disease Without Intravascular Imaging

LETTER TO THE EDITOR

To the Editor,

We have recently read with great interest the article by Akın et al[1] entitled "Safety Profile of Drug-Coated Balloon Angioplasty for Isolated Side Branch Lesions: A Single-Center Experience."[1] This study highlights that drug-coated balloon (DCB) angioplasty offers a significant clinical benefit in optimizing Medina 0.0.1 bifurcation disease. However, we believe there are several key points that need to be addressed.

Coronary lesions affecting only the side branch (SB) ostium, classified as Medina 0.0.1, are exceedingly rare, comprising roughly 3-5% of total bifurcation lesions. From the perspective of most interventional cardiologists, they have been considered "non-true" bifurcations, assuming they possess diminished clinical relevance due to their infrequency, lack of main vessel (MV) involvement, and the restricted myocardial region supplied by the afflicted SB.[2,3] Consequently, they are generally considered less clinically relevant and routinely omitted from key trials and guidelines. Recent registry-based analysis indicates that this assumption may be erroneous. Isolated SB lesions have been linked to unfavorable clinical outcomes that are equivalent to or exceed those of genuine bifurcation lesions following percutaneous coronary intervention (PCI), despite their seemingly straightforward angiographic presentation.[3] In isolated Medina 0.0.1 bifurcation lesions, angiography-based diagnostic and treatment strategies raise some concerns, especially in the current era of intravascular imaging: 1) an angiographically "simple" appearance leads to underestimation of disease severity; 2) foreshortening, an eccentric plaque, and an elliptical ostium can lead to an inaccurate severity assessment; 3) subclinical plaque extensions into the proximal MV are often missed without intravascular imaging. In the present study, although the authors acknowledge the lack of intravascular imaging in the limitations section, we believe that concluding the current analysis of isolated ostial SB disease without performing intravascular evaluation in any patient may mislead clinicians. Additionally, in the present study, 27.1% of patients had isolated ostial left circumflex artery (LCX) lesions.[1] Ostial LCX disease (left main 0, 0, 1 lesion) has traditionally been viewed as undesirable for PCI due to its technical complexity and the potential for severe complications. A recent study indicated that 66% of patients presented with continuous plaques extending from the left main to the LCX, and 62% had plaques involving both the left main and the LCX.[4] In the present study,[1] we suggest that in some patients, DCB angioplasty might have been conducted without addressing the diseased section of the MV. Moreover, ostial SB disease is marked by significant calcification, elastic fibrils, and fibrous components. As a result, these lesions require the use of adjuvant lesion preparation tools, such as cutting/scoring balloons and rotoablation. This study does not provide details about the lesion preparation methods used.

Ezgi Gültekin Güner

Ahmet Güner

Department of Cardiology, Mehmet Akif Ersoy Thoracic and Cardiovascular Surgery Training and Research Hospital, İstanbul, Türkiye

Corresponding author:
Ahmet Güner
✉ ahmetguner488@gmail.com

Available Online Date: August 3, 2026

Cite this article as: Güner EG, Güner A. Ambiguity of Medina 0.0.1 Bifurcation Disease Without Intravascular Imaging. *Anatol J Cardiol.* 2026;30(10):716-717.

DOI: 10.14744/AnatolJCardiol.2026.6745

Declaration of Interests: The authors have no conflict of interest to declare.

Funding: The authors declared that this study has received no financial support.

Copyright@Author(s) - Available online at anatoljcardiol.com.
Content of this journal is licensed under a Creative Commons Attribution-NonCommercial 4.0 International License.

REFERENCES

1. Akın H, Bilge Ö, Işık F, et al. Safety profile of drug-coated balloon angioplasty for isolated side branch lesions: A single-center experience. *Anatol J Cardiol*. 2026;30(7):465-470. [CrossRef]
2. Lee CH, Nam CW. Contemporary approaches to isolated ostial side branch diseases: a comprehensive review of Medina 0.0.1 bifurcation lesions. *Korean Circ J*. 2026 [CrossRef]
3. Mohamed MO, Lamellas P, Roguin A, et al. Clinical outcomes of percutaneous coronary intervention for bifurcation lesions according to Medina classification. *J Am Heart Assoc*. 2022;11(17):e025459. [CrossRef]
4. Pan L, Lu WJ, Han ZY, et al. Drug-coated balloons for the treatment of ostial left anterior descending or ostial left circumflex artery lesions: a patient-level propensity score-matched analysis. *J Geriatr Cardiol*. 2023;20(10):716-727. [CrossRef]

THE ANATOLIAN JOURNAL OF CARDIOLOGY

Official journal of the TURKISH SOCIETY OF CARDIOLOGY

Reply to the Letter to the Editor: "Ambiguity of Medina 0.0.1 Bifurcation Disease Without Intravascular Imaging"

LETTER TO THE EDITOR
REPLY

To the Editor,

We thank the authors[1] for their interest in our study[2] and for their thoughtful comments.

First, we fully agree that intravascular imaging provides valuable information in the assessment of bifurcation lesions, particularly in Medina 0.0.1 disease. As the authors correctly emphasized, angiography may underestimate lesion extent because of vessel overlap, foreshortening, eccentric plaque distribution, and the presence of subclinical plaque extension into the main vessel. For this reason, the absence of intravascular imaging was explicitly acknowledged as one of the major limitations of our study. However, our investigation was designed to reflect real-world practice in a retrospective cohort and to evaluate the procedural safety and feasibility of a DCB-only strategy rather than to establish definitive anatomical characterization. Therefore, our conclusions were intentionally limited to safety and feasibility and should be interpreted within this context.

Second, regarding ostial LCX lesions, we acknowledge the possibility of plaque extension from the left main coronary artery into the LCX. Nevertheless, all angiograms were reviewed by experienced interventional cardiologists, and lesions were classified according to angiographic Medina criteria. Furthermore, the primary objective of the present study was not to determine plaque distribution but to evaluate clinical and procedural outcomes following DCB treatment in lesions considered suitable for a DCB strategy in routine clinical practice. We agree that future studies incorporating systematic IVUS or OCT assessment would provide a more accurate understanding of plaque extension and lesion morphology.

Third, regarding lesion preparation, all lesions underwent mandatory predilatation before DCB application. Drug-coated balloon treatment was performed only when accepted angiographic criteria were achieved, including TIMI 3 flow, residual stenosis ≤30%, and absence of severe dissection. Because of the retrospective nature of the study and the relatively small sample size, detailed data regarding the use of adjunctive lesion preparation devices, such as cutting balloons, scoring balloons, or atherectomy systems, were not consistently available and therefore were not included in the analysis. We agree that these devices may be particularly valuable in selected calcified ostial lesions and require further investigation in future prospective studies.

In conclusion, we appreciate the authors' comments, which highlight important considerations regarding lesion assessment and preparation in Medina 0.0.1 bifurcation disease. We believe our findings should be viewed as hypothesis-generating

Halil Akın[1]
Önder Bilge[2]
Ferhat Işık[2]
Abdurrahman Akyüz[2]
Emre Kıvrak[1]
Esra Yılmaz[1]
İlke Çelikkale[1]
Özcan Özdemir[3]
İbrahim Halil Tanboğa[4]

[1]Department of Cardiology, Faculty of Medicine, Lokman Hekim University, Ankara, Türkiye
[2]Department of Cardiology, University of Health Sciences Diyarbakır Gazi Yaşargil Education and Research Hospital, Diyarbakır, Türkiye
[3]Department of Cardiology, Etlik City Hospital, Ankara, Türkiye
[4]Department of Cardiology, University of Nişantaşı, İstanbul, Türkiye

Corresponding author:
Halil Akın
✉ halilakin@yandex.com

Available Online Date: August 3, 2026

Cite this article as: Akın H, Bilge Ö, Işık F, *et al*. Reply to the Letter to the Editor: "Ambiguity of Medina 0.0.1 Bifurcation Disease Without Intravascular Imaging." *Anatol J Cardiol*. 2026;30(10):718-719.

DOI: 10.14744/AnatolJCardiol.2026.6760

Copyright@Author(s) - Available online at anatoljcardiol.com.
Content of this journal is licensed under a Creative Commons Attribution-NonCommercial 4.0 International License.

and supportive of further prospective studies utilizing routine intravascular imaging and detailed lesion characterization.

Declaration of Interests: The authors have no conflict of interest to declare.

Funding: The authors declared that this study has received no financial support.

REFERENCES

1. Güner EG, Güner A. Ambiguity of medina 0.0.1 bifurcation disease without intravascular imaging. *Anatol J Cardiol*; 2026; 30(10):716-717.
2. Akın H, Bilge Ö, Işık F, et al. Safety profile of drug-coated balloon angioplasty for isolated side branch lesions: a single-center experience. *Anatol J Cardiol*. 2026;30(7):465-470. [CrossRef]

THE ANATOLIAN JOURNAL OF CARDIOLOGY

Official journal of the TURKISH SOCIETY OF CARDIOLOGY

Spontaneous Echo Contrast or Thrombus? Intracardiac Echocardiography and Isoproterenol Infusion Provide the Answer

A 77-year-old man with heart failure and chronic kidney disease presented with dyspnea and palpitations. Atrial fibrillation (AF) was documented, and catheter ablation was planned. Pre-procedural transesophageal echocardiography demonstrated a calcified echogenic structure located within the mid-portion of the left atrial appendage (LAA). The appendage appeared patent up to this level; however, the distal portion could not be clearly delineated. The region beyond the echogenic structure resembled the transverse sinus but did not demonstrate the typical anechoic appearance expected for the transverse sinus and contained SEC-like swirling echoes. Consequently, it remained unclear whether this area represented the distal LAA or the pericardial transverse sinus, rendering TEE inconclusive for reliable assessment of LAA anatomy and thrombus exclusion (Figure 1; Video 1).

Given the inconclusive transesophageal findings, further evaluation with intracardiac echocardiography (ICE) was done. Initial imaging from the pulmonary artery provided improved delineation of the LAA anatomy, demonstrating a relatively shallow appendage surrounded by a prominent transverse sinus space. Despite the clearer anatomical visualization, a large, echogenic, mass-like appearance within the LAA raised persistent concern for thrombus formation (Figure 2A and 2B; Video 2A and 2B). Therefore, additional functional assessment was required to differentiate the true thrombus from the dense spontaneous echo contrast.

Transseptal access was subsequently obtained under ICE guidance using a no-touch technique. The ICE catheter was inserted into the left atrium and positioned in the left superior pulmonary vein to obtain dedicated views of the LAA. From this vantage point, integration of the appendage again demonstrated a large, echogenic, mass-like appearance, maintaining a strong suspicion for thrombus, and

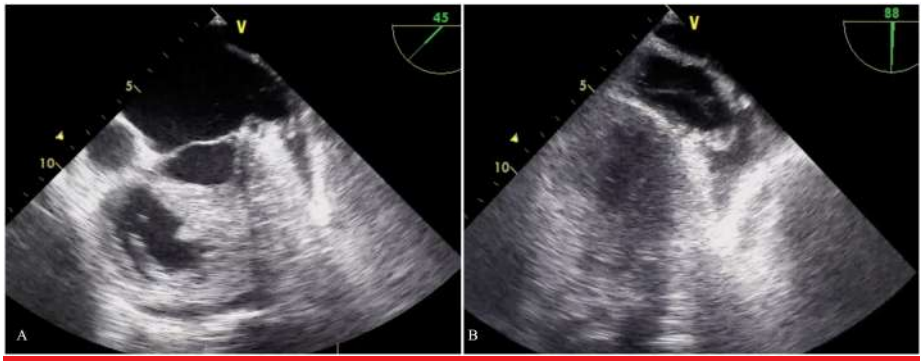

Figure 1. Transesophageal echocardiography of the left atrial appendage. (A) View at 45° demonstrating dense echogenic material within the left atrial appendage. (B) View at 88° confirming persistent echogenic appearance suspicious for spontaneous echo contrast versus thrombus.

Copyright@Author(s) - Available online at anatoljcardiol.com.
Content of this journal is licensed under a Creative Commons Attribution-NonCommercial 4.0 International License.

E-PAGE ORIGINAL IMAGE

Can Sezer
Cem Çöteli
Gül Sinem Kılıç
Uğur Canpolat
Hikmet Yorgun
Kudret Aytemir

Department of Cardiology, Hacettepe University Faculty of Medicine, Ankara, Türkiye

Corresponding author:
Can Sezer
✉ drcansezer97@gmail.com

Available Online Date: August 3, 2026

Cite this article as: Sezer C, Çöteli C, Kılıç GS, Canpolat U, Yorgun H, Aytemir K. Spontaneous Echo Contrast or Thrombus? Intracardiac Echocardiography and Isoproterenol Infusion Provide the Answer. *Anatol J Cardiol.* 2026;30(10):E-24-E-25.

DOI: 10.14744/AnatolJCardiol.2026.6791

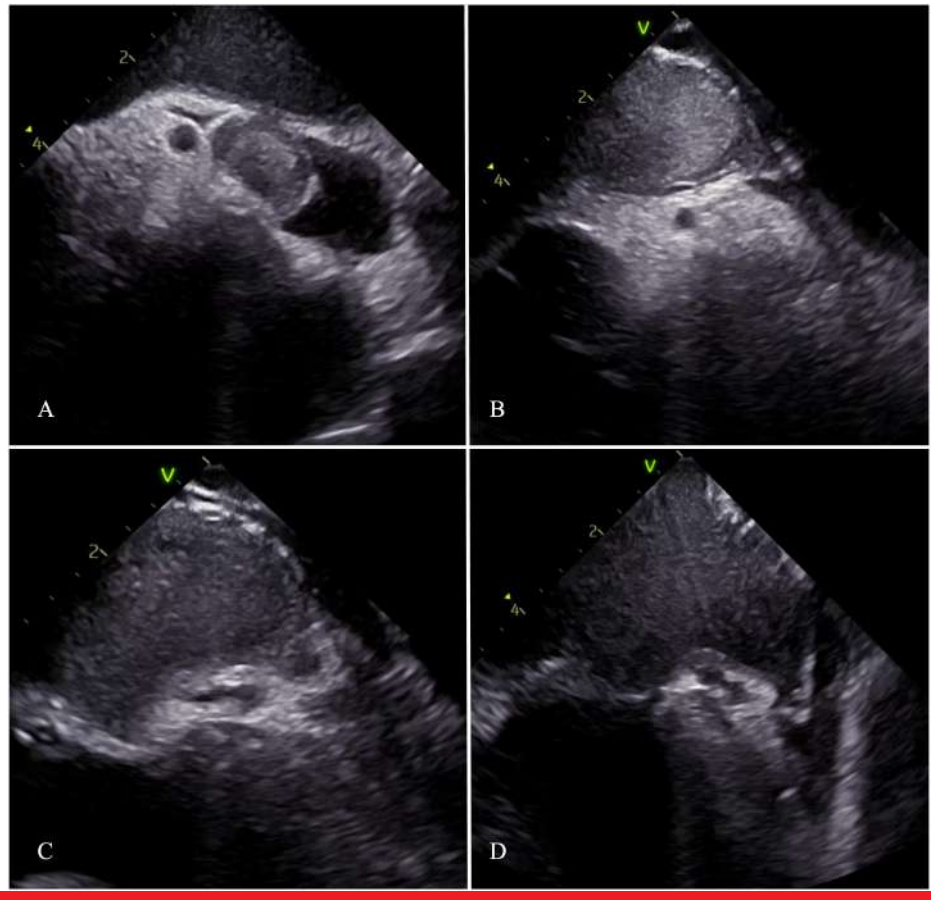

Figure 2. Intracardiac echocardiographic evaluation of the left atrial appendage. (A) Right atrial view demonstrating a globular echogenic structure within the left atrial appendage. (B) Left atrial view after transseptal access providing improved delineation. (C) During isoproterenol infusion, dispersion of spontaneous echo contrast is observed. (D) After isoproterenol infusion, resolution of spontaneous echo contrast.

cancellation of the ablation procedure was initially considered. As a final diagnostic maneuver, isoproterenol infusion was initiated to differentiate thrombus from dense SEC. Following adrenergic stimulation, the echogenic material within the LAA rapidly and completely dispersed, confirming the diagnosis of dense SEC and effectively excluding thrombus (Figure 2C and 2D; Video 2C and 2D). Therefore, catheter ablation was continued safely.

Informed Consent: Written informed consent was obtained from the patient for the publication of this case and the accompanying images.

Declaration of Interests: The authors have no conflict of interest to declare.

Funding: The authors declared that this study has received no financial support.

Video 1: Transesophageal echocardiographic imaging of the left atrial appendage at 65° demonstrating dense echogenic material.

Video 2: Intracardiac Echocardiography With Pharmacologic Provocation. (A) Intracardiac echocardiographic view from the right atrium. (B) Left atrial view after transseptal access. (C) Dispersion of spontaneous echo contrast during isoproterenol infusion. (D) Resolution of spontaneous echo contrast after isoproterenol infusion.